Lehrstuhl für Bodenkunde

Technische Universität München

The soils of Bhutan: Parent materials, soil forming processes, and new insights into the palaeoclimate of the Eastern Himalayas.

Thomas Caspari

Vollständiger Abdruck der von der Fakultät Wissenschaftszentrum Weihenstephan für Ernährung, Landnutzung und Umwelt der Technischen Universität München zur Erlangung des akademischen Grades eines

Doktors der Naturwissenschaften (Dr. rer. nat.)

genehmigten Dissertation.

Vorsitzender: Univ.-Prof. Dr. Jörg Pfadenhauer

Prüfer der Dissertation:

1. Univ.-Prof. Dr. Rupert Bäumler,
   Friedrich-Alexander-Universität Erlangen-Nürnberg
2. Univ.-Prof. Dr. Wolfgang Zech,
   Universität Bayreuth (schriftliche Beurteilung)
3. Univ.-Prof. Dr. Ingrid Kögel-Knabner

Die Dissertation wurde am 05.04.2005 bei der Technischen Universität München eingereicht und durch die Fakultät Wissenschaftszentrum Weihenstephan für Ernährung, Landnutzung und Umwelt am 16.06.2005 angenommen.

"I do not know what I may appear to the world,
but to myself I seem to have been only a boy playing on the seashore,
and diverting myself in now and then finding a smoother pebble or a prettier shell than ordinary, whilst the great ocean of truth lay all undiscovered before me."

Isaac Newton (1642-1727)

Acknowledgements

It is a pleasure to thank the many people who made this thesis possible.

It is difficult to overstate my gratitude to my supervisor Dr. Rupert Bäumler. With his enthusiasm, his inspiration, and his great efforts to explain things clearly and simply, he helped to make the Bhutan project fun for me. Throughout our research, he provided encouragement, sound advice, good teaching, good company, and lots of good ideas.

I am particularly grateful to Dr. Ian Baillie, who has always generously shared his enormous knowledge and field experience in the challenge to solve the mysteries of the Bhutanese soils. His scientific and linguistic input has substantially contributed to the quality of this work. He has also facilitated the trip to southern Bhutan, provided otherwise inaccessible papers and maps – and was the only *chilip* I have seen being adventurous enough to drive a car in Bhutan outside the capital Thimphu.

The collaboration with our Bhutanese partners from the Soil Survey Unit (SSU) within the National Soil Services Centre (NSSC) is the framework behind this dissertation. I especially want to thank Chencho Norbu as the Programme Director for his sympathetic open-mindedness and scientific as well as administrative support. I equally want to thank Tshering Dorji (SSU), Yeshey Dema and Karma Dema from the Soil Fertility Unit (SFU), and Jamyang from the Soil and Plant Analytical Laboratory (SPAL).

The merits for the success of our fieldwork go to Kado Tshering (soil surveyor) and Phub Tshering (driver). I cannot think of better companions to deal with all expected and unexpected situations in rural Bhutan. They have provided considerable technical and logistical support, and generously overlooked our sometimes surely inappropriate Western attitudes and behaviours. Their valuable information on “big” issues (local deities, land use history etc.) as well as advice on “small” things (flees, medicinal plants etc.) decisively helped to make our stay in their “parallel universe” a feasible and memorable experience.

I am indebted to all of my colleagues from the Soil Science Institute of the Technische Universität München under the leadership of Prof. Dr. Ingrid Kögel-Knabner. They have provided a relaxed and stimulating environment in which to learn and grow. My fellow PhD colleagues Ingo Schöning, Steffen Jann, Dirk Hensel, Silke Müller, Markus

Steffens and Nora Tyufekchieva deserve special mention. My associates altruistically shared their knowledge, and of these I want to thank Dr. Peter Schad (soil classification & encouraging words), Dr. Werner Häusler (XRD measurements & interpretation), Dr. Karin Eusterhues (geological support, REM-EDX images) and Dr. Kai-Uwe Totsche (statistics support & column experiments).

During my 3-year laboratory analyses marathon, I would have been lost without the help of supporting hands. Thank you, Ulrike Maul, for your supernatural assistance and the professional sample handling. I also want to thank my student helpers, among them especially Manuela Diethelm, Pascal Hardung, Markus Kreuß, Sabine Munzert, Li Shui, Jan Spalensky and Irene Stenzel.

The Bhutanese-German expedition team in 2001; from left to right: Kado Tshering, the author, Prof. Dr. Rupert Bäumler, Phub Tshering.

In the name of all project participants, I want to thank the German Research Foundation (Deutsche Forschungsgemeinschaft, DFG) for financial support of the Bhutanese-German collaboration (grant no. BA 1637/1-1 to 1-3).

Lastly, and most importantly, I wish to thank my parents, Margret and Bernhard Caspari. They bore me, raised me, supported me, taught me, and loved me. To them I dedicate this thesis.

Summary

The objective of this work is to extend the present knowledge about the soils of temperate Bhutan. The three main parts comprise I.) a comprehensive pedogeochemical characterisation, II.) the analysis of particular soil forming processes, and III.) the use of the soils information to shed light on landscape history and palaeoclimate.

The Kingdom of Bhutan is situated on the southern slopes of the Eastern Himalayas. Monsoonal climate and steep gradients provide unfavourable conditions for undisturbed soil formation. Consequently most soil profiles are polygenetic. In order to examine the connexion of the present soils with the underlying landscape and to identify the main controls during soil weathering, total major, trace and rare earth element (REE) contents are determined for selected saprolites and their associated pedons. Major element results largely reflect the underlying geology and there is no geochemical evidence for allochthonous aeolian materials in Bhutan. The REE patterns are typical for post-Archaean materials. Whereas they appear rather homogenised in topsoils, the influence of the parent materials causes deviations from the general trend with increasing depth. The gneissic, metasedimentary and phyllitic lithologies of Central Bhutan appear to be closely related. Occurrence of marine Tethyan sediments in Central Bhutan at 3,000 m a.s.l. is confirmed. Chemical Indices of Alteration (CIA) of between 71 and 92 indicate advanced weathering even at high altitudes. Above approximately 3,500 m a.s.l., physical weathering causes passive REE enrichment, but no differentiation of their concentrations or patterns within the profile. Below, increased chemical weathering and leaching appears to be sufficient for REE release *and* translocation.

On a more explorative level, a synthesis of field findings and analytical results draws our attention to two particular soil forming processes. The first involves the basin-shaped Phobjikha Valley, which is situated at 2,900-3,200 m a.s.l. in western Central Bhutan. The local environmental setting with strong along-valley winds, frequent freeze-thaw cycles, extensive dry periods and sparse vegetation cover encourages the generation and transport of silt-sized particles. The effects of this process are evidenced in the smooth valley morphology and in the nature of the examined pedons; their involvement in continuous redistribution of local sediments is reflected by a homogeneous silty-clayey, stone-free texture, varying profile depths, buried topsoils and weakly developed recent A horizons. In protected locations, in situ weathering of the metamorphic parent materials results in alu-andic features. In areas of preferred aeolian deposition, argic and ferralic features emerge, with clay contents of up to 60% and surface areas of > 50 m^2 g^{-1}. Under forest, umbric horizons develop. Cluster and factor analyses of soil chemical and physical parameters confirm the redistribution of local sediments as a dominant factor behind the measured variables.

Andic features in non-volcanic environments seem to be widespread in Bhutan at altitudes between 2,200-3,500 m a.s.l. Another part of this study is therefore dedicated to the detailed characterisation of specific properties and processes of formation, using an exemplary non-volcanic Andosol profile from eastern Central Bhutan. The results indicate advanced soil development with high amounts of oxidic Fe and Al compounds, low bulk densities of partly < 0.5 g cm^{-3}, P retention > 85%, and a dominance of Al-hydroxy-interlayered phyllosilicates. SEM of sand fractions indicate micro-aggregates highly resistant to dispersion. Column experiments show podzolisation with mobilisation and translocation of DOM, Fe and Al. NMR spectroscopy and ^{14}C ages of 16 ka BP indicate re-stabilisation of DOM. Applying classification criteria, these soils appear to have andic and podzolic features, but are neither Andosols nor Podzols *sensu stricto*. Because of their widespread occurrence and distinct properties, it is suggested to either simplify the criteria for existing soil types, or clearly define a separation of volcanic and non-volcanic/non-allophanic Andosols.

Regarding the palaeoclimatic indication of the collected soil data, buried topsoils in Phobjikha Valley are dated at about 2,000 ^{14}C years BP, and indicate a weakening or absence of sediment influx under warmer and wetter conditions towards the end of the Holocene climatic optimum. Charcoal on top of palaeosols suggests that man since then contributed to the reactivation of local sediment redistribution. No clear indication of glacial activities is found, and the massive silty sediments, the presence of debris slopes and asymmetric cross sections of the side valleys suggest periglacial conditions. No glacial influence is also detected in the middle reaches of the Chamkhar Chhu river in eastern Central Bhutan, where the properties and development of soils on fluvial deposits are examined. At least 28 river terraces rise to relative heights of nearly 300 meters above the recent riverbed (2,655 m a.s.l.). The largest and well preserved terrace of the system is of Late Pleistocene age. Polygenetic structures and buried topsoils indicate several interruptions of soil development under periglacial conditions. ^{14}C dating suggests discontinuities at approximately 10,175, 8,710, 4,055 and 1,715 years BP. Weighted profile averages of texture, specific surface area, pedogenic iron compounds and weathering indices prove the existence of an uninterrupted chronosequence, in which weathering and soil development continuously become more intense with increasing relative height above the current riverbed. The chronologies established must remain preliminary and fragmentary at present due to the lack of reliable radiocarbon data and the restricted access to Northern Bhutan.

Glossary

AMS	Accelerator Mass Spectrometry
BET	Surface area measurement after Brunauer, Emmett & Teller
BG	Background solution
BP	Before Present
BSSP	Bhutan Soil Survey Project
CIA	Chemical Index of Alteration
CXTFIT	Concentration Distant (X) Time Fit model
DCB	Dithionite-Citrate-Bicarbonate solution
DOM	Dissolved Organic Matter
EDX	Energy-Dispersive X-Ray analysis
ESC	Essential Structural Components
FAO	Food and Agricultural Organisation of the United Nations
GLOF	Glacier Lake Outburst Flood
GNH	Gross National Happiness
GPS	Global Positioning System
HPGe	High-Purity Germanium Detector
HREE	Heavy Rare Earth Elements (Eu-Lu)
ICIMOD	International Centre for Integrated Mountain Development
INAA	Instrumental Neutron Activation Analysis
ISSS	International Society of Soil Science
LGM	Last Glacial Maximum
LIL	Large Ion Lithophile elements
LOI	Loss On Ignition
LREE	Light Rare Earth Elements (La-Sm)
MoA	Ministry of Agriculture, Royal Government of Bhutan
MBT	Main Boundary Thrust
MCT	Main Central Thrust
MREE	Middle Rare Earth Elements
NMR	Nuclear Magnetic Resonance spectroscopy
NSSC	National Soil Services Centre (Semtokha, Bhutan)
ODOE	Optical Density of Oxalate Extract
PAAS	Post-Archaean Australian Shale
PSD	Particle Size Distribution
REE	Rare Earth Elements
REID	Research, Extension and Irrigation Division (REID) at MoA
RGoB	Royal Government of Bhutan
RNR-RC	Renewable Natural Resources Research Centre
SEM	Scanning Electron Microscopy
SPAL	Soil and Plant Analytical Laboratory, Semtokha, Bhutan
TUM	Technical University of Munich
UCC	Upper Continental Crust
UNEP	United Nations Environment Programme
WRB	World Reference Base for Soil Resources
XRA	X-Ray Absorption analysis
XRD	X-Ray Diffraction analysis

List of Tables

List of Figures

List of Figures (continued)

1 Introduction

The present study represents the first detailed soil scientific work conducted in the Eastern Himalayan Kingdom of Bhutan. As the study area is largely unknown for most readers, this introductory section starts with a geographic summary of the long secluded country. It then summarizes the soils information which were available prior to our project. Information will be further given on the scope and framework of our Bhutanese-German collaboration, and some basic conditions of soil scientific work in Bhutan will be highlighted.

1.1 Characterisation of the study area

1.1.1 Geographic location of Bhutan

The Buddhist Kingdom of Bhutan covers about 47,000 square kilometres on the southern slopes of the Eastern Himalayas between latitudes 26°47'N to 28°26'N and longitudes 88°52'E to 92°03'E (*Fig. 1*).

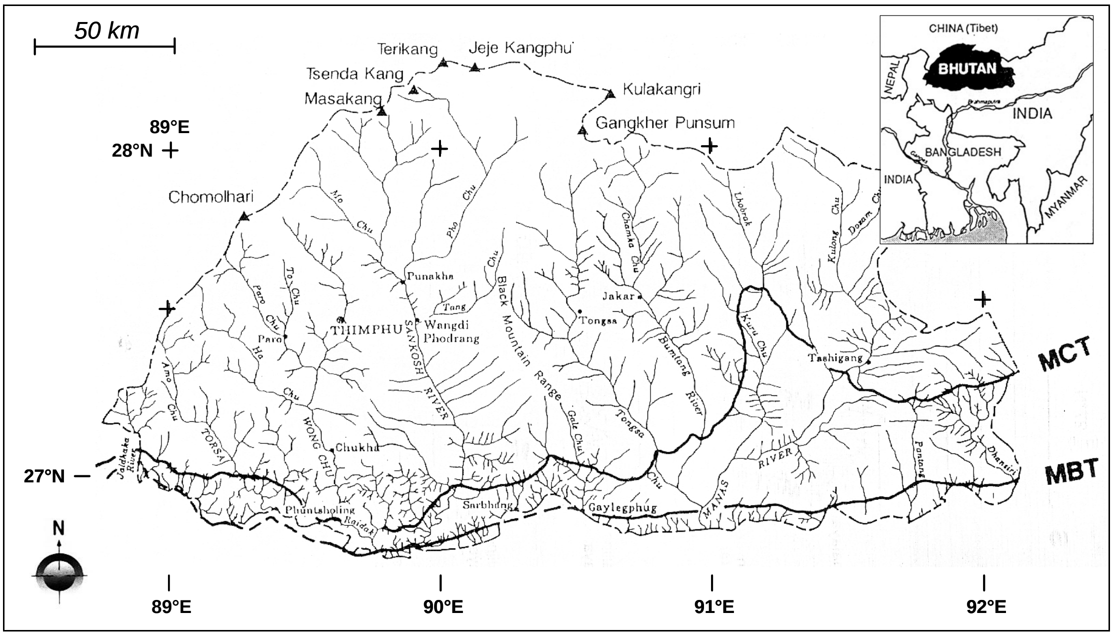

Fig. 1: Country map of Bhutan (after Takada 1991); MCT = Main Central Thrust, MBT = Main Boundary Thrust; Thimphu = capital city; ▲= mountain peaks.

In the south, it borders the floodplains of the Eastern Indian states of West Bengal and Assam at approximately 200 m a.s.l.. From there, the tropical foothills rise with steep slopes until less steep, basin-like terrain is reached in most parts of the country. Located at altitudes between 2,500 up to 4,000 m a.s.l., these inner valleys represent Bhutan's cultural heartland. To the north, the gradient increases again to the east-west aligned main chain of the High Himalaya, which includes peaks of more than 7,500 m a.s.l. and marks the border with neighbouring China (Tibet).

1.1.2 Physiographic zonation and climate

Metaphorically speaking, the extraordinary steepness of large parts of the country evokes the picture of Bhutan as a huge staircase consisting of consecutive E-W oriented altitudinal belts. This is the main concept behind the zonations of Karan (1967), Eguchi (1987, 1991) and Takada (1991). Compared to the Central Himalayas, however, Bhutan is characterised by a predominantly N-S oriented landscape. The most prominent north-south ranges include the Black Mountains, the Dagala, Pelela, Yotongla, Thrumsingla and Korila ranges, which are separated from each other by the main rivers draining the country. Navara (1997) is among those who first recognised this aspect, and Norbu et al. (2003a) have recently suggested a differentiated concept, integrating all of the main components of the natural environment (*Table 1*).

The great range in altitude and topography within Bhutan produces a wide range of climatic conditions. The climate charts of exemplary sites are shown in *Fig. 2*. A dominant factor is the Indian monsoon which blows north from the Bay of Bengal and is most intense between June and September, making Bhutan the wettest country within the Himalayan Range. The general climate can be described as wet and hot in the subtropical southern foothills, where annual precipitation is between 1,200 and 2,000 mm, but can be as high as 5,000 mm along the southern border areas. The inner valleys are dry and warm with approximately 500-1,000 mm a^{-1}, and the N-S mountain ranges being moister and cooler. The northern part of Bhutan can be described as dry and cool, with areas above 4,000 m a.s.l. receiving less than 500 mm annual rainfall (RGoB 1997). For temperature, Eguchi (1991) gives a decrease of 0.5-0.6°C per 100 m of altitude. The Bhutanese winters are generally dry and influenced by outflows from the Tibetan high pressure system (Norbu et al. 2003a).

Table 1: Physiographic zonation of Bhutan according to Norbu et al. (2003a)

Zone		**Altitude range** (m a.s.l.)	**Climate**	**Landforms**	**Soils**	**Natural vegetation**
High Himalaya	Trans-Himalayan plateau	4,000 – 5,500	Alpine-arctic; dry	Wide U–valleys; some with old lake beds; rolling interfluves	Not seen, but probably limited development	Sparse high altitude steppe
	High peaks	5,000 – 7,600	Alpine & arctic; sub-humid	Very high mountains; glaciers & glacial lakes in U-valleys	Stony debris	Mostly bare; some mosses & alpines
	Dissected plateaux	4,000 – 5,500	Alpine; sub-humid	Rolling dissected plateaux with many lakes & wide U-valleys	Stony debris; silty meadow soils & scattered shallow peat	Much bare; alpine grassland; juniper & *Rhododendron* scrub
N-S valleys and ranges	Northern valleys and ranges in W & C	2,000 – 4,500	Temperate-alpine; subhumid	High N–S ranges; deep U- valleys upstream, more V- downstream	Temperate forest soils, stagnogleys, podzols & alpine meadow soils	Mixed conifer and fir forests; alpine meadow & scrub
	Inner valleys and passes in W & C	1,100 – 4,000	Temperate-subalpine; moist on slopes, sub-humid on valley floors	High N–S ranges; wide valleys with river terraces & large side valley fans	Temperate forest soils, stagnogleys, and podzols	Chir pine woodland on lower slopes; temperate broadleaf upslope; temperate & subalpine conifer forests at higher altitudes
	Eastern valleys and ranges	500 – 4,000	Warm temperate-subalpine; moist on slopes, dry-subhumid on valley floors	High N–S ranges; deep, narrow V – valleys; few terraces or fans		
	Southern mountains and gorges	400 – 5,100	Subtropical-alpine; wet-moist	High N–S ranges, with plateau remnants; deep, narrow and steep valleys & gorges	Subtropical and temperate forest soils, stagnogleys, podzols & alpine meadow soils	Subtropical & temperate broadleaf forests; temperate subalpine conifer forests; alpine meadow & scrub
	Merak-Sakten block	1,500 – 4,500	Temperate-subalpine; moist	High E-W block; upstream valleys wide with terraces & fans; valleys downstream deeper & steeper	Temperate forest soils, stagnogleys, podzols & alpine meadow soils	Chir wood-land in lower valleys; temperate & subalpine conifer forests, alpine meadow & scrub
South	Front hills	100 – 2,000	Tropical-temperate; very wet	Alternating E–W & N-S valleys and steep ridges	Deep, stony, and unstable; highly leached & weathered	Tropical, subtropical & warm temperate broadleaf forests
	SE Bhutan	100 – 3,000	Tropical-temperate; wet	Alternating E–W & N-S valleys & steep ridges	Deep, stony, and unstable; highly leached & weathered	Tropical, subtropical & temperate broadleaf forests
	Piedmont (Duars)	100 – 600	Tropical-subtropical; wet-very wet	Low angle piedmont fans & terraces; wide braided river beds	Deep, stony, raw alluvial soils; highly leached	Tropical & subtropical broadleaf forests; riverine scrub

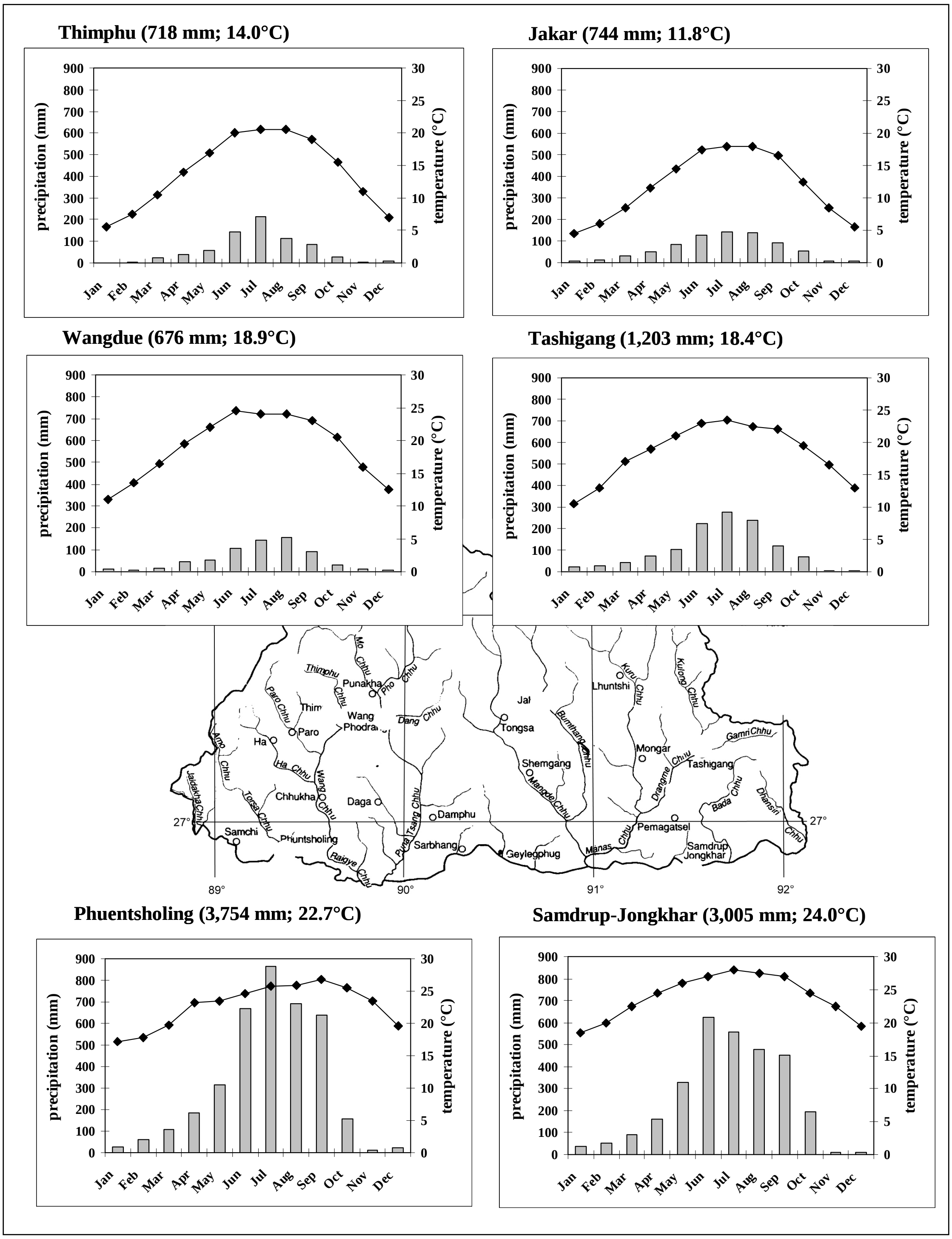

Fig. 2: Climate charts for selected locations in Bhutan; total annual precipitation and mean annual temperature are given in brackets; precipitation data are plotted as grey columns; lines represent mean monthly temperatures; data source: RGoB (2004), except for Phuentsholing (FAO 1995).

1.1.3 Natural vegetation

The flora of Bhutan is among the aspects best reported so far thanks to the encyclopaedic work of Grierson & Long (1983). Bhutan has generally maintained much of its natural vegetation, and official statistics show a forest cover of 72.5% (RGoB 2003). Other sources indicate lower values of 64% (Gupta & Ura 1992), and a possible cover of below 60% is mentioned in the country's most recent Afforestation Master Plan (FAO 1991).

Fig. 3: Exemplary herbs of temperate Bhutan. Scabiosa species below Tango Monastry near Thimphu (left), approx. 2,600 m a.s.l.; Arisaema erubescens, stand of fruit (right), Phobjikha Valley, 3,300 m a.s.l.

Ohsawa (1987) has highlighted the main vegetation zones of the Bhutan Himalaya. The foothills (200-1,000 m a.s.l.) are covered by mesic subtropical forests with *Gmelina arborea* and *Shorea robusta* as the main timber species. Above and until approximately 2,000 m a.s.l., we find warm broadleaf forests with *Schima wallichii*, *Castonopsis indica, Betula alnoides, Alnus nepalensis, Engelhardia spicata, Macaranga pustulata* and a variety of *Lithocarpus* species. In drier areas, the chir pine (*Pinus roxburghii*) occurs and the shrub layer is poorly developed.

Evergreen oak forests with *Quercus semecarpifolia, Q. lanata, Q. lamellosa* are characteristic for the lower part of the temperate zone (2,000-2,700 m). They also frequently contain species of the *Acer*, *Castanopsis* and *Juglans* genera. On moist slopes with annual precipitation above 2,500 mm, cool moist broadleaved forests with *Acer campbellii* and *Betula alnoides* prevail. The upper part of the temperate zone (2,700-3,500 m a.s.l.), corresponding to most inner valleys and also including the N-S ridges, is characterised by conifer forests. The dominant species in drier sites up to 3,100 m is blue pine (*Pinus wallichiana*), being the high altitude equivalent to the chir pine. *Pinus bhutanica* and oak species are also typical for blue pine forests. With increasing altitude, we find spruce and Hemlock forests with *Picea brachytyla*, *P. spinulosa*, Hemlock (*Tsuga dumosa*), *Betula utilis* and *Larix griffithiana*. The understorey may include *Rosa macrophylla, Berberis praecipua*, *Salix daltonia*, *Pieris spp.*, *Taxus baccata* and some rarer species. As ground cover, bamboo species (e.g. *Yushania microphylla*) and a multitude of herbs are commonly found (*Fig. 3*).

The Bhutan fir (*Abies densa* Griff.) dominates the subalpine range from 3,300-3,800 m a.s.l. close to the treeline. The often luxurious understory may include *Rhododendron spp.*, *Betula utilis*, *Skimmia laureola*, *Juniperus pseudosabina*, *Prunus rufa*, *Ribes takare*, *Rubus fragarioides, Sorbus foliolosa* and *Daphne bholua.* Bamboo is still common as ground cover besides the herbs *Primula denticulata* and *Rheum acuminatum* and the grass *Arundinaria maling*.

In the alpine zone, *Rhododendron lepidotum* and *Juniperus (recurva, squamata)* form dense shrubs, preferably on sheltered, leeward slopes between 3,700-4,200 m a.s.l.. In their protective cover, *Morina nepalensis*, *Pedicularis megalantha*, *Phlomis tibetica*, *Potentilla arbuscula*, *Primula sikkimensis*, *Thalictrum chelidonii*, *Trollius pumilus* and other herbs can flourish. Alpine meadows dominate the more exposed, windward sites and stretch up as high as 4,800 m a.s.l.. In this comparatively dry ecosystem, main forbs include *Cyananthus, Delphinium, Gentiana, Potentilla, Primula, Ranunculus, Rhuem* and *Selinum* species, and grasses and sedges of the genera *Festuca*, *Stipa, Poa, Agrostis* and *Danthonia* (Harris 2000).

1.1.4 Geology

The southern slopes of the Eastern Himalayas are among the most complex landscapes in the world. They are located on a section of continental crust that had already undergone early Palaeozoic tectonism (Gehrels et al. 2003) before the India-Eurasia collision, which started 50-55 million years ago. This has been the driving force behind the subsequent step-wise uplift of the Himalayas and the Tibetan plateau during middle and late Tertiary time (Patriat & Achache 1984, Rowley 1996, Hodges 2000). The current rate of uplift is estimated to be around 1.0-1.5 mm a^{-1} (Iwata 1987, Fort 1996).

In his pioneering work, Gansser (1983) has described the main geological units of the Bhutan Himalaya, which are considered to be lateral analogues to those of other Himalayan areas (Motegi 2002). The thick thrust sheets of the Central Crystalline Complex underlie the greater part of the kingdom (*Fig. 4*). They consist of pre-collisional granitoid gneisses and migmatites, including Indian Shield basement materials. Related to these units are high grade metamorphic metasediments, which in a pattern of inverted metamorphism underlie the crystalline in substantial parts of Central and West Bhutan, and e.g. outcrop as Paro Metasediments in the Bumthang area. On top of the gneisses – following a major metamorphic break – the Tethyan Sequence, consisting of partly calcareous materials, has been conserved in several places. Their most prominent appearances are in the north-western Lingshi Basin, the northern Toma La and Lunana Belt, the central Bhutanese Tangchu Basin and the Merak-Sakten Sector in the east. These sediments appear analogous to the Tibetan Sedimentary Series described by Le Fort (1981) from Central Nepal. They represent marine materials from the bed of the Tethys Ocean, which were uplifted and partly metamorphosed during the intercontinental collision. At their base, a schistose and phyllitic lithology has been identified and termed Chekha Formation by several authors (Jangpangi 1978, Gansser 1983, Tangri & Pande 1995). Within this formation, the metamorphic grade rapidly decreases upward (Grujic et al. 2002). Depending on regional variation, the upper contact of the Chekha Formation is with magmatic materials (Singhi Volcanics) or with the fossiliferous Deshichiling and Maneting formation, all of which belong to the Pele La Group (Tangri & Pande 1995; formerly named Black Mountain Group by Chaturvedi et al. 1983, and recently Dangchu Group by Chhetri & Gurung 2001). Fossil ages range from Ordovician to Carboniferous (Singh 1973, Jangpangi 1978, Chaturvedi

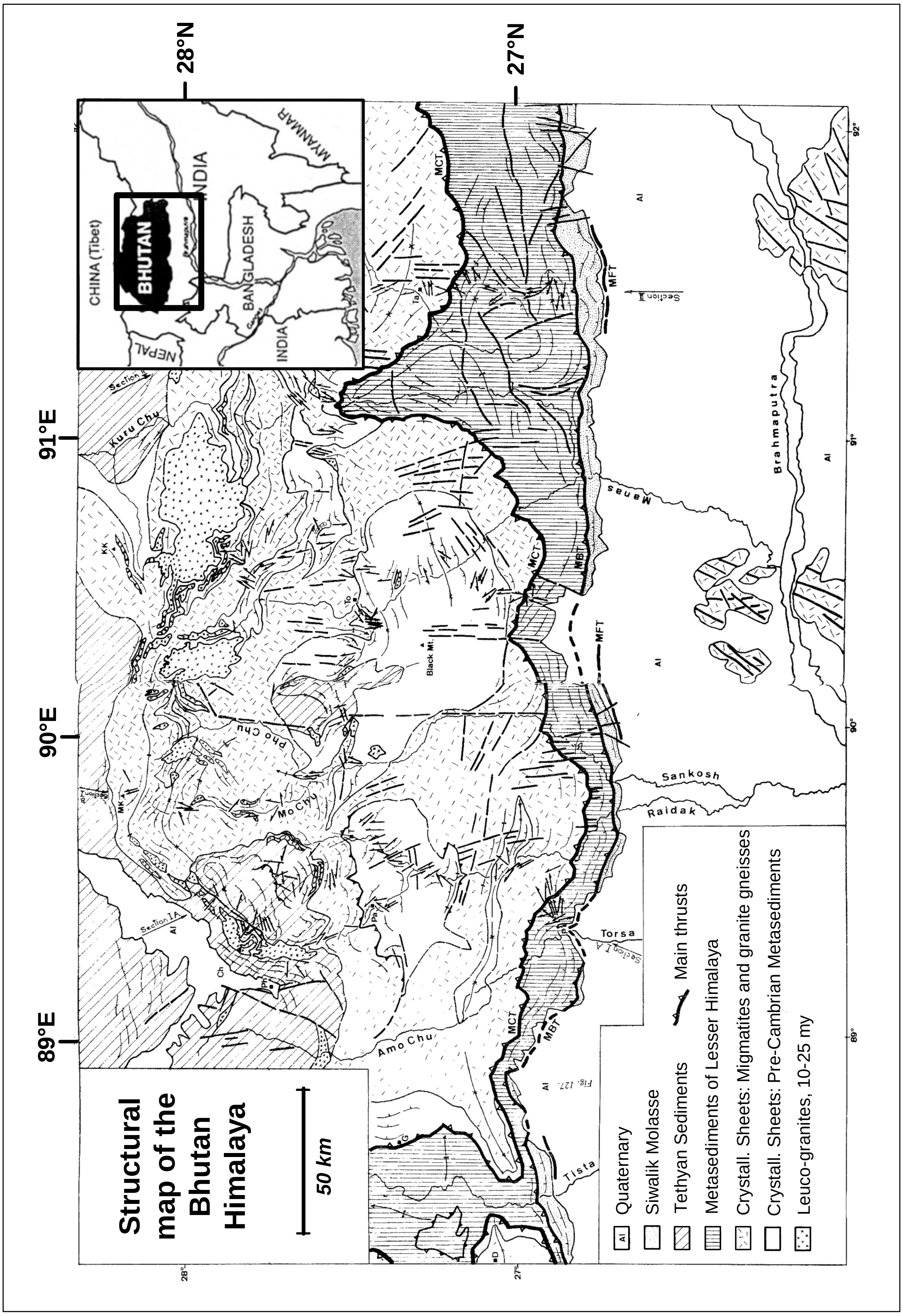

Fig. 4: Geology of Bhutan as mapped by Gansser (1983, modified). The coverage of the map is indicated by the framed part of the inset in the upper right corner.

et al. 1983, Koike 2001), or Late Precambrian to early Cambrian (Tangri et al. 2003). In the south of Bhutan, the Main Central Thrust (MCT) divides the main crystalline complex from the late Precambrian metasediments of the Lesser Himalaya. These contain a wide range of low grade metamorphic and sedimentary rocks. In the foothills bordering India, there are the discretely developed, molasse-like sediments of the Siwalik Group. Miocene leucogranites frequently occur in North Bhutan along the border with Tibet, and also outcrop as dykes within the Tethyan units (Castelli & Lombardo 1988, Copeland et al. 1990). Although this general outline is widely accepted, there are ongoing debates, as to which of the contacts between the litho-units are gradational or tectonic. Motegi (2002) gives an overview of the controversial issues, and Koike et al. (2002) discuss the stratigraphy and correlation of the Tethyan sediments in particular.

1.2 Previous soils information

1.2.1 Indigenous knowledge

There are no reports about famines on regional and/or national scale in Bhutan (Gupta & Ura 1992), and one can assume that the small-scale subsistence agriculture which dominates large parts of the country was and still is based on excellent indigenous soils knowledge. As a result of the general steepness of the terrain, only 8% of the country's total area are currently under use, and it is unlikely to exceed 10% in the future (Baillie et al. 2004). Indigenous sustainable land use strategies e.g. include *tseri* (shifting) cultivation, crop rotation, intercropping, contour ploughing, preparation of manure and its regular application, and low plant population densities. Roder et al. (1993) describe *pangshing* (gras fallow) cultivation, a labour-intensive procedure of burning heaped dry topsoil, using plant biomass or manure and soil organic matter as "fuel". Besides beneficial effects of pH increase, improved K availability and reduced C/N ratio, major disadvantage of this practices are the substantial gaseous losses of N and C, and full exposure to erosion in the initial period after burning. Fallow periods of 15-20 years are required to maintain the sustainability of this land use type.

The level of land degradation is low. Karan (1967) noted a minimal level of soil erosion, and Young (1994) estimated 10% of Bhutan's arable land being subjected to some degradation. Norbu et al. (2003b) provide the first reliable account of the different types of land degradation within the country with special attention to their occurrence, causes and interactions. In situ degradation due to soil organic matter depletion is identified as the main degradation process.

1.2.2 Soil survey and classification

Karan (1967) was the first to give some general remarks on colour, texture and depth of soils in different parts of the country, and suggested their zonal distribution from north to south equivalent to the climatic and vegetation zones. This concept was taken up and expanded by Okazaki (1987), who suggested five major soil groups that are vertically distributed according to the altitude (*Fig. 5*).

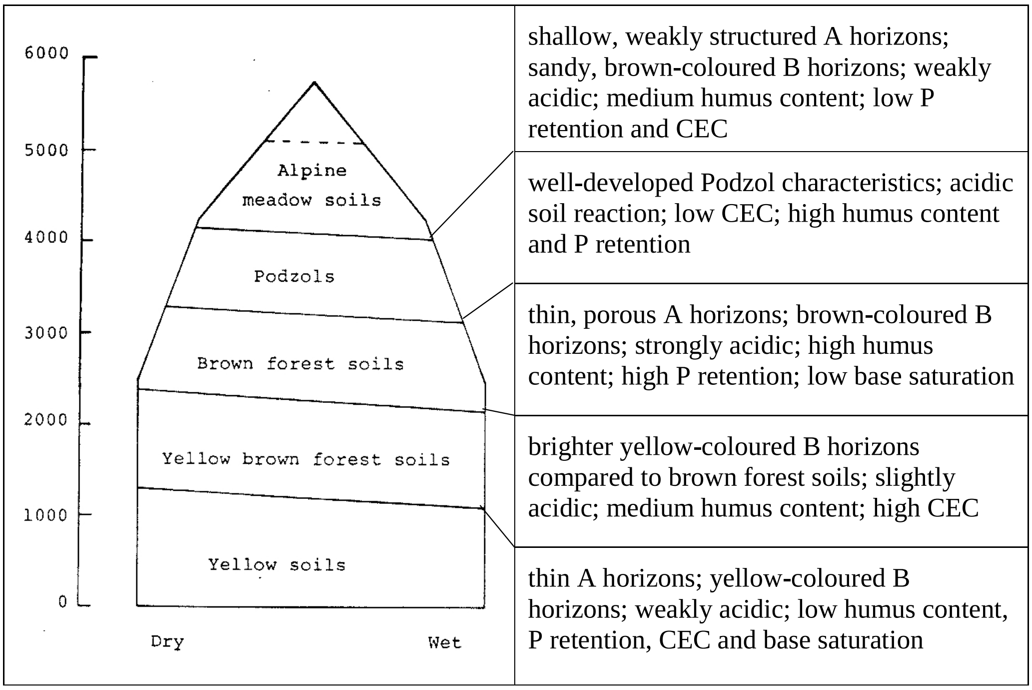

Fig. 5: Vertical distribution of Bhutan's soils according to Okazaki (1987)

Following the perceived need for systematic information about the nature and distribution of the soils of Bhutan and in order to build its own soil scientific expertise, the Royal Government of Bhutan established the Bhutanese Soil Survey Project (BSSP) in 1996 with assistance from Denmark, the Netherlands and the European Union. The project is part of the National Soil Services Centre (NSSC) of the Research, Extension and Irrigation Division (REID) in the Ministry of Agriculture (MoA). It began field activities in June 1997. The emphasis in the initial stages of the project was on training of Bhutanese nationals as soil surveyors, and the establishment of a functioning soil survey organisation. By now, about 15 soil surveys have been completed for a wide range of mostly agriculturally used sites in Bhutan. The findings are summarised by Baillie et al. (2004). In their review, the authors stress that the Bhutanese soils tend to be deep and well-developed in many places, which would not have been necessarily expected in face of the steep and rugged terrain in combination with monsoonal rains and frequent earthquakes. Only the soils on the southern foothills are less weathered and leached as could be expected under humid subtropical conditions. Soil development in the temperate, inner valleys between 2,200 and 3,500 m is characterised by moderate to advanced weathering and leaching. Soils of this zone often qualify as Cambisols according to the WRB classification (ISSS 1998), however, orange-coloured non-volcanic Andosols also frequently occur (Bäumler et al. 2005). Leaching, acidification and podzolisation increase with altitude, and podzolised soils are most frequent in the subalpine zone from 3,500 m to the tree line at about 4,000 m. Above that, we find alpine turf soils and unweathered glacial deposits (Baillie et al. 2004), which mostly qualify as Regosols. Occurrence of permafrost has been estimated from about 5,000 m a.s.l. or higher (Takada 1991).

An overall typical feature of Bhutanese soils is their short-range variability and regolith heterogeneity. Interruptions of soil formation are the exception rather than the rule, masking pedogenetic differences and complicating classification.

1.3 Bhutanese-German collaboration

To clarify aspects of soil genesis of high altitude and alluvial soils in Bhutan, a collaborative research was initiated in 1999 between the BSSP and the Soil Science Institute of the Technical University of Munich (TUM), Germany. The collaboration was scheduled for a period of 4 years, and supported by a grant from the German Research Foundation (Deutsche Forschungsgemeinschaft, DFG). The soils of Bajo RNR-RC and soils developed on fluvial terraces in the Chamkhar Chhu valley north of

Jakar were subject of the first joint research trip in autumn 2000. In 2001, the second excursion lead to the Phobji-Gangtey valley system in Central Bhutan (Caspari 2003). A final expedition in 2002 revolved around the landslides of the eastern Bhutanese Tshogoempa Village in Tashigang District, where we discussed possible causes and mitigation measures (Wangchuck et al. 2003). The presentation on the importance and implementation of the sustainable management of Bhutan's soil resources during the international conference on "Operationalising the Concept of Gross National Happiness" in the Bhutanese capital Thimphu (Caspari et al. 2004a) has been the last major activity and marks the preliminary end of the collaboration.

1.4 Basic conditions of soil scientific work in Bhutan

1.4.1 Technical aspects

In spite of – or rather because of? – the general lack of information on its soils, Bhutan is a tempting and yet challenging landscape for soil scientists. Travel is only possible in spring (March-May) and autumn (September-November), because the only trans-national road is partially blocked during summer monsoon and by snow in winter time. Access to rural areas is generally slow, and remote areas can only be reached by foot. This means that heavy equipment cannot be used in the field, and also that the fieldwork needs careful planning, as a return to the study area may not be feasible. Maps and other basic fieldwork documents are hardly available. This is for geological maps as well as for satellite imagery.

1.4.2 Cultural and religious aspects

On a national scale, the access to certain parts of Bhutan is restricted, either to avoid "cultural contamination" as foreseen in the concept of Gross National Happiness (GNH), or – in case of the northernmost territories – for military reasons. On a local scale, it is important to understand that for most people soil is more than a mere production factor and represents a medium through which to get in contact with local deities and spirits (Ura 2001). Locations for our fieldwork have always been carefully chosen, and had to be at a certain distance from the next religious building (*dzong* or *lhakang*) or other "holy places", which were not as visually obvious, at least not to us

European visitors. While digging a profile, the plant cover and topsoil were carefully removed (and put on top again afterwards) and all macroscopic animals were brought to safety. When we wanted to dig a soil profile close to Rukubji Village in Central Bhutan, we would have only been allowed to do so if we could have promised not to cause a future crop failure. At that time we did not know about the local crop failure in 1984 which was seen as a consequence of annoying the protecting deity *dramar pelzang* by moving his dwelling (*tsenkhang*) to another place following road construction in 1981 (Schicklgruber & Pommaret 1997). Nevertheless, we were most heartedly welcome in most places, and our fieldwork was eyed with interest and curiosity (*Fig. 6*).

Fig. 6: Locals watching the soil scientific field work near Tshogoempa Village, East Bhutan.

2 State of the art and objectives

From the multitude of possible questions involving the soils of Bhutan, three major research topics have been identified in the scope of the present study: (i) the thorough geochemical investigation of Bhutanese soils from different geological backgrounds, (ii) the examination of two particular, largely unknown soil forming processes in Central Bhutan, and (iii) the use of the collected data for highlighting aspects of landscape history and palaeoclimate at the southern slopes of the Eastern Himalayas. In this chapter, the state of knowledge is outlined for each of these three areas. The associated aims and objectives constitute the last paragraph of each section.

2.1 REE-based geochemical investigation of soils

In order to geochemically identify and differentiate rocks, soils and sediments, rare earth element (REE) data in the form of chondrite-normalised plots have been widely used (Xing & Dudas 1993, Ramesh & Ramasamy 1997, Gallet et al. 1998, Chang et al. 2000, Nath et al. 2000, Xiong et al. 2002, Das & Haake 2003, Egashira et al. 2004, Honda et al. 2004). The rare earth elements comprise the 15 lanthanide elements with atomic numbers 57 (La) through 71 (Lu), and are classified in a light (LREE: 57-62) and heavy (HREE: 63-71) subgroup. As members of the Group IIIA of the Periodic Table, they naturally occur as trivalent cations and in this state are geochemically similar. Exceptions are Eu^{2+} forming in case of strong reducing conditions within the earth’s mantle or lower crust, and Ce^{4+} resulting from oxidation in marine environments.

What renders rare earths particularly interesting in soil genetic research is that they are among the least soluble and most resilient elements, making them suitable for provenance studies, especially in polygenetic soils. The nature of REE distribution during mineralogical reactions associated with weathering is poorly understood (McLennan 1989). In spite of their general immobility, mobilisation and fractionation of the lanthanides do occur in some soils during transportation, sedimentation and weathering of minerals (e.g. Balashov et al. 1964, Roaldset 1973, Cullers et al. 1975, Nesbitt 1979, Duddy 1980, Sharma & Rajamani 2000). REE mobilisation is thought to be caused by rainwater and organic acids penetrating the soil, transforming feldspars and biotite into clay minerals. The consequent increase in pH results in the precipitation and adsorption of rare earths onto the clay minerals. Attached to these, and also as free and hydrated REE^{3+} ions or as carbonate complexes, they may be transported to lower, less weathered soil horizons (Nesbitt 1979). However, there is general agreement that they do not travel far and are mostly recycled within the solum. Soils and regoliths therefore act as large, long-term storage reservoirs for REEs (Nesbitt & Markovics 1997). REE fractionation is thought to be controlled mainly by the abundances of primary and secondary minerals (Nesbitt 1979).

There are few geochemical data available for Bhutan. It is therefore the objective of Chapter 4 to provide a first systematic account of major, trace and rare earth element data of soils which have developed on Bhutanese regoliths from lithologically different sources. Special attention is focussed on (i) in how far the geochemical soil data reflect the underlying geology, (ii) the differences within and between soil profiles from different parts of Bhutan, and (iii) in how far these differences can be attributed to weathering, sediment transport and/or polygenesis.

2.2 Selected aspects of soil formation

2.2.1 Redistribution of local sediments and its influence on soil formation

Most pedons found in Bhutan are polygenetic reflecting the repeated interruptions during pedogenesis, but are nevertheless surprisingly deep and well-developed in many sites (Baillie et al. 2004). Among the various parent materials for soil formation, loess-like aeolian sediments are known to play an important role on the southern slopes of the Himalayas. They are reported by Gardner & Rendell (1994) from the Kashmir Basin (NW-India) and Pakistan, by Guggenberger et al. (1998) and Bäumler (2001a) from the Solu-Khumbu area, East Nepal, by Saijo & Tanaka (2002) from Central Nepal’s Thakkhola Basin, and by Caspari et al. (2004b) from the Bumthang area, Central Bhutan.

Loess-like sediments are generally thought to have originated in cooler and drier climates, when vegetation cover was sparse. The deposits are often punctuated by palaeosols, which are assumed to have developed during stable phases with moister climates and denser vegetation (Gerasimov 1973). Loess-palaeosol sequences can therefore act as local signals of past environmental changes (Kukla 1987, Bronger & Heinkele 1989, Kemp & Derbyshire 1998, Kemp 1999), and correlations with other proxies have been successfully established (Kemp 2001). To avoid an over-simplistic view, it has to be considered that: (i) instead of a clear, absolute alternation between loess accumulation on the one hand and soil formation on the other hand, we rather look at dynamic pedosedimentary environments in which there is a changing balance between these two processes (Kemp 2001); and (ii) besides climate, other soil forming factors like organisms, parent material(s) and topography contribute to the formation of loess-palaeosol sequences; Catt (1991) pointed out that loess is especially suitable in terms of palaeoclimate research because two variables (parent material and topography) are removed from the soil forming equation.

In the Himalayan context, Gardner & Rendell (1994) have rejected the notion that loess-like sediments are only associated with cooler climates and mainly formed by means of glacial grinding and frost weathering, as too simple in mountain environments. From soils of the Middle Hills of Nepal, Gardner (1994) described the substantial silt-generating capacity of metamorphic lithologies. She considers the Himalayas to be one of the world's major silt sources since the Later Tertiary, and identified granular disintegration (physical weathering) and particularly chemical decomposition as the main mechanisms for the production of silt-sized particles under subtropical monsoonal climate. Besides metamorphic parent materials, Gardner & Rendell (1994) mention tectonics, local controls – e.g. topography and wind flow intensities – and human activity as important variables in the loess-palaeosol equation. They further hypothesize that "the production of silts, their deposition to form loess, and their subsequent reworking is merely a highly specialised cycle within the sedimentary geology system" (p. 177). They named this cycle the "loess cycle".

The objectives of this section are (i) to elucidate the soil forming processes under cool temperate conditions in central Bhutan on the basis of field observations and laboratory measurements, and (ii) to use explorative statistical methods to show that the redistribution of sediments is a decisive factor behind the different observed variables. Results and discussion around this complex of topics are presented in Chapter 5.1.

2.2.2 Andic features in non-volcanic soils

In 1978 the suborder of andic Inceptisols (Andepts) was revised to introduce the new order of Andisols in the US Soil Taxonomy (Parfitt & Clayden 1991) for soils developed from volcanic materials. Since then, andic and associated podzolic soil properties in many cases have been described in a range of non-volcanic areas all over the world (*Table 2*).

Table 2: Selected literature references of site conditions of non-volcanic Andosols and Cryptopodzols.

Location / altitude a.s.l.	Parent material	Climate	Soil types	Author
NW Spain	Gabbro, schist, amphibolite	humid-temperate (12-14°C); mesic, udic (1,010-1,860 mm)	Dystrandepts, Hapludands; humic Andosols	Garcia-Rodeja et al. 1987
SW Washington (WA, USA) 140-270 m	Marine sediments (siltstones) and loess	cool maritime (10°C); rainy season in winter; mesic (1,500-3,500 mm)	Andic Haplumbrept, Typic Dystrandept	Hunter et al. 1987
SE Alaska / 10 m	Beach gravels (phyllite, sandstone, schist, granite)	cool, perhumid	Andic Humicryods and Haplocryods	Alexander et al. 1993
E Nepal / 2,800 m	Mica schist	8.5-9.0°C; monsoon climate, dry winter season; ustic, mesic (2,000-2,500 mm)	Dystric Haplustands	Bäumler & Zech 1994a
S Switzerland / 515 and 1,000 m	Gneiss	11°C and 6°C; dry winters; rainfall maximum in summer (1,800 mm)	Cryptopodzols, Haplic Podzols	Blaser et al. 1997
E France / 835-1,110 m	Granite, plutonites, porphyrite	7.0-7.5°; humid; udic, mesic – cryic (1,200 – 2,000 mm)	Alic Fulvudands, Andic Haplumbrepts	Aran et al. 1998
S India / 2,000-2,500 m	Regoliths (lateritic); precambrian charnockites	cool (15°C), humid (monsoonal, 2,500 mm); 2-3 month dry season	non-allophanic Andisols	Caner et al. 2000

These soils have developed in various parent materials and under different temperature and moisture regimes. Their properties seem to be related to metal-organic complexes rather than to the formation or presence of short-range order minerals like allophanes and (proto-) imogolites. However, for a long time their geographical extent and importance were deemed to be restricted to small areas. Therefore, they were assigned to Andisols/Andosols in Soil Taxonomy (Soil Survey Staff 1999) and World Reference Base for Soil Resources (ISSS 1998), respectively. However they are not good matches for these taxa, and were called non-volcanic and non-allophanic Andosols/Andisols (*Table 2*), whilst others were assigned to Podzols/Spodosols, and named Cryptopodzols, as they generally lack the visible eluvial and illuvial horizons of true Podzols (Blaser et al. 1997). Parfitt & Clayden (1991) discussed these soils as having intermediate properties "that fell into a black hole" of classification. Soils having andic properties but not restricted to volcanic parent materials (pyroclastites) are generally characterised by short-range order minerals (imogolite or proto-imogolite, and allophane) or Al-humus complexes. They must have a low bulk density or the presence of volcanic glass within a specified horizon thickness, and a high P retention (Soil Survey Staff 1999). They should not have a spodic horizon (ISSS 1998) or, if they do, an albic horizon should also be present (Soil Survey Staff 1999). Typical Andosols/Andisols seem to be more common in regions without a distinct dry season, although Soil Taxonomy does allow for Torrands. In general, they are more characterised by in situ weathering and mineral trans- or neo-formations than by translocation. Al and Fe are released by in-situ silicate weathering, and poorly crystallised oxidic compounds develop. These may interact with water soluble organic compounds to form metal-organic complexes and polymers, which are then immobilised against further translocation and stabilised against biodegradation. In contrast to Andosols/Andisols, Podzols should form distinct eluvial and illuvial horizons under strong leaching environments and acid conditions (Gustafsson et al. 1995).

On the southern slopes of the Eastern Himalayas, these soils are common, extending at least from East Nepal to the eastern border of Bhutan. They occur within the altitude range between 2,500 and about 3,300 m a.s.l., and vertically cover several bioclimatic zones from temperate broad-leafed forests to the upper mixed conifer and silver fir forests. The area is characterised by a climate with strong daily freeze-thaw alternation from late autumn to early spring. This zone is dominated by bright reddish yellow, almost orange coloured deeply weathered soils. They have crumb structures, friable consistence, thixotropic properties, extremely high porosities and surface areas, extremely low bulk densities, and high amounts of organic carbon throughout the solum (Baillie et al. 2004).

Chapter 5.2 of this work will focus on this group of apparently anomalous non-volcanic andic soils with special reference to the specific processes of their formation and the origin of their composite/transitional andic and podzolic properties. It will be discussed in how far we look at a separate soil forming process, which is clearly different from those leading to Andisols/Andosols and Spodosols/Podzols *sensu stricto*.

2.3 Soils as indicators for landscape history and palaeoclimate

It has been one of the findings of the Himalayan Interdisciplinary Paleoclimate Project (HIPP) that in spite of the diversity of natural archives in the highlands of Central Asia there is a paucity of terrestrial based records (Wake & Mayewski 1995). This holds especially for Bhutan, where little Quaternary research has been conducted so far, also because access to the northern parts of the country has been largely restricted. Following the “Glacier and glacial lake inventory within the Glacier Lake Outburst Floods Monitoring Programme (GLOF)” which has been undertaken as a joint venture by the International Centre for Integrated Mountain Development (ICIMOD) and the United Nations Environment Programme (UNEP) in 2002, there is good knowledge on the present state of glaciers and glacial lakes. According to their findings, glaciers in the Bhutan Himalayas generally occur above the elevation of 4,000 m a.s.l.. There are 677 glaciers and 2674 glacial lakes altogether, making up approximately 127 km^3 of ice reserves and covering an area of 1,317 km^2 (ICIMOD et al. 2002). More detailed findings of a Joint Bhutan-Japan Project on hazard risk assessment of GLOF have been published by Ageta et al. (2000), Iwata et al. (2002a) and Karma et al. (2003). Recent estimates for the present glacial equilibrium-line altitude in North Bhutan are around 5,300 m a.s.l. (Iwata et al. 2003, Meyer et al. 2003).

Regarding past glacial fluctuations, Gansser (1983) has been the first to report terminal moraine stages in the Mo Chhu valley (NW Bhutan) at about 3,300 m a.s.l.. He also claimed remnants of a covered terminal moraine at 2,900 m elevation, and noted striations and other possibly glacial features down to altitudes of about 2,600 m a.s.l. in the Khoma Chhu valley, NE Bhutan. From their examination of moraines in the Linghsi area (NW Bhutan) and Lunana region (N Bhutan), Iwata et al. (2002b) inferred three distinct glacial stages. On the basis of a two ^{14}C dates and a comparison with the chronology established for the Khumbu region (E Nepal), they suggested major glacial advances for the Last Glacial (18-25 ka BP), Early Holocene (10 ka BP) and the Little Ice Age (0.1-3 ka BP). The most recent findings indicate that glaciers in NW Bhutan "only" extended as far down valley as 3,550 m a.s.l. during previous glaciations (Meyer et al. 2003). Iwata et al. (2003) observed fossil cirque glaciers along the Snowman Trekking Route down to 4,400 m. Laskar (1995) stated that true glacial sediments in Bhutan only exist along the present day glaciers, and Gansser (1983) argued that the intense summer monsoon on Bhutan's southern slopes makes it difficult to recognise early glacial stages below 3,000 m a.s.l..

Besides moraines and other glacial features, terrace sediments along the middle reaches of the main Bhutanese rivers may allow insights into past environmental fluctuations and the connected landscape history. However, fluvial terraces and deposits in the intramontane basins of Bhutan are rather less developed compared to Nepal, India and Pakistan. There are definitely no features as substantial as the sediments and terraces around Pokhara and Kathmandu in Nepal (Yamanaka et al. 1982, Yoshida & Igarashi 1984), the Karewa sediments in Kashmir Valley (Pal & Srivastava 1982), or the sediments in-filling the dun valleys of the Lesser Himalayas (Prasad & Verma 1974, Zöller 2000). Takada (1991) surveyed the Quaternary sediments and fluvial terraces along the Sunkosh (Puna Tsang Chhu) river near Wangdue-Phodrang in West Bhutan. He identified several terrace levels of up to 110 m above the current river level, and classified them into Higher (H), Middle (M) and Lower (L) (*Fig. 7*). From the reddish colour of the soils of terraces H, M1, M2, M3 and M4, the author deduces that these terraces originated prior to the LGM. This is corroborated by the observation that the pebbles constituting the M2 terrace are strongly weathered and friable. Large boulders of several meters in diameter found below the M2 terrace near the Wangdue-Phodrang *dzong* (castle fort) are interpreted as stemming from a glacier lake outburst flood (GLOF). The comparatively wide distribution of the L2 surface may have been caused by the increase in sediment load due to the advance of glaciers in the upper reaches during the Little Ice Age.

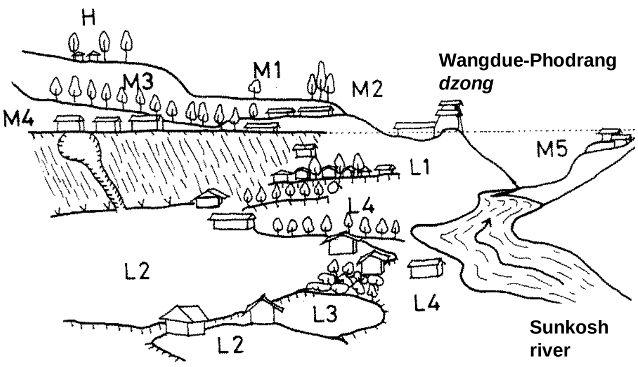

ter-race	relative height [m]	thickness of deposits [m]	age BP
L4	4.5	?	?
L3	4.5< <15	?	?
L2	15	15+	<350±50
L1	29	14+	?
M5	29< < 61	?	?
M4	61	?	>LGM
M3	68	?	ditto
M2	70	ca. 30	ditto
M1	80	?, 80+	ditto
H	110	4+, 80+	ditto

Fig. 7: Sketch and characteristics of fluvial terraces along the Sunkosh River near Wangdue-Phodrang; the view is from N to S (after: Takada 1991).

In the Central Bhutanese valley of the Chamkhar Chhu river, Gurung (2001) has identified a suite of five (I-V) “glacio-fluvial” terraces by geomorphological examination and ^{14}C dating. According to his findings, the lower terraces (I-III) are of Holocene age, and peat material covered by debris flow deposits on top of the highest terrace (V) approximately 70 m above the current river level, are dated to 29,940 ± 180 years BP (Beta-151897). Driftwood in the alluvium of the most prominent terrace of the system, terrace IV at approximately 40 m above the current river level, is dated to 27,340 ± 180 years BP (Beta-151895). Both conventional radiocarbon ages indicate that the sediments were deposited during Late Pleistocene, and corroborate the idea that maximum glaciation stages and the end of the Last Glacial Maximum (LGM) in Asia might have pre-dated the same events in Europe (Gillespie & Molnar 1995, Zech et al. 1996, Benn & Owen 1998, Zech et al. 2000, Bäumler 2004).

The use of soils as indicators for palaeoclimatic changes and landscape history in High Asia is less common compared to the geomorphological approach, especially because in many places, the information contained in soils got lost or overprinted by erosion, solifluction and/or tectonic activities. In combination with morphostratigraphic findings and radiocarbon data, however, it has become a powerful tool in Quaternary research of the Himalayas (e.g. Agrawal et al. 1989, Shiraiwa & Watanabe 1991, Bäumler & Zech 1994b, Bronger et al. 1998, Bäumler 2001b, Zech et al. 2001, Saijo & Tanaka 2002).

Chapter 6 will focus on the palaeoclimatic implications of the Bhutanese-German soil scientific research. The objectives of the first part are to use the findings of the soil survey in the western-central Bhutanese Phobjikha Valley to clarify aspects of landscape history, and to formulate a tentative Quaternary chronology for this study area. The second part elucidates the examination of a large river terrace system along the Chamkhar Chhu river near the village of Thangbi, Central Bhutan, which a German-Bhutanese expedition discovered in 2000. Geomorphological field observations and associated pedochemical analyses are combined to shed light on the Quaternary history of the present soil types and landforms.

3 Materials and Methods

This chapter gives an overview of the locations which were sampled during the joint Bhutanese-German expeditions. For each of the Chapters 4-6, a number of profiles has been selected out of the overall pool, and their particular locations and associated site properties will be given in the referring chapters. Colour photographs for some of the profiles are available in Appendix 3 (page 156ff.).

The soil sampling techniques and parameters surveyed in the field are explained in Section 3.2, and the subsequent section describes the applied laboratory analytical procedures. Finally, some data analyses and the statistical approach are specified.

3.1 Sampling locations

The location of the sampling sites is shown in *Fig. 8*. The sites were visited during two expeditions in 2000 and 2001.

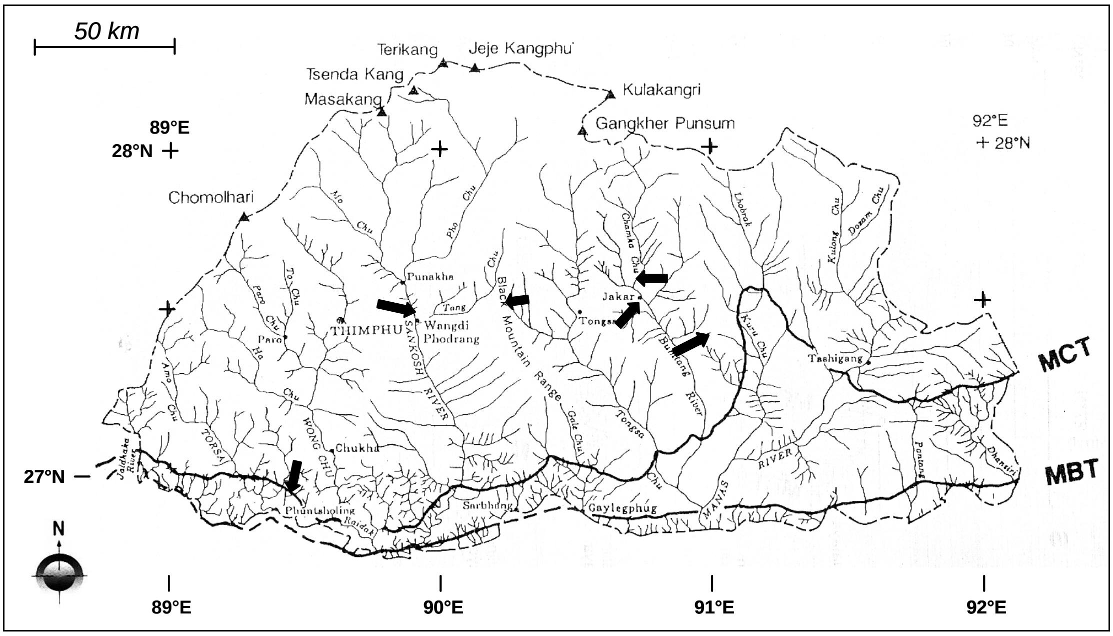

Fig. 8: Soil sampling locations and profile IDs: River terrace system near Thangbi, Bumthang District; PT 034-052 Phobjikha Valley, Wangdue-Phodrang District; PK 135-152, PK 154-155 Thrumsing-La Pass; PT 053 Lame Goempa Research Forest; PT 056 Roadcut north of Phuentsholing; PK 158 Rukubji Village, Wangdue-Phodrang District; PK 156. Bajo RNR-RC; PT 57-62. Map source: Takada (1991).

Most samples during the 2000 expedition were taken from the terrace system along the Chamkhar Chhu River near Thangbi in central Bumthang District. 19 profile pits were sited so as to cover the whole range of the terrace system (PT 034-PT 052). Their location within the study area is shown in *Fig. 9*.

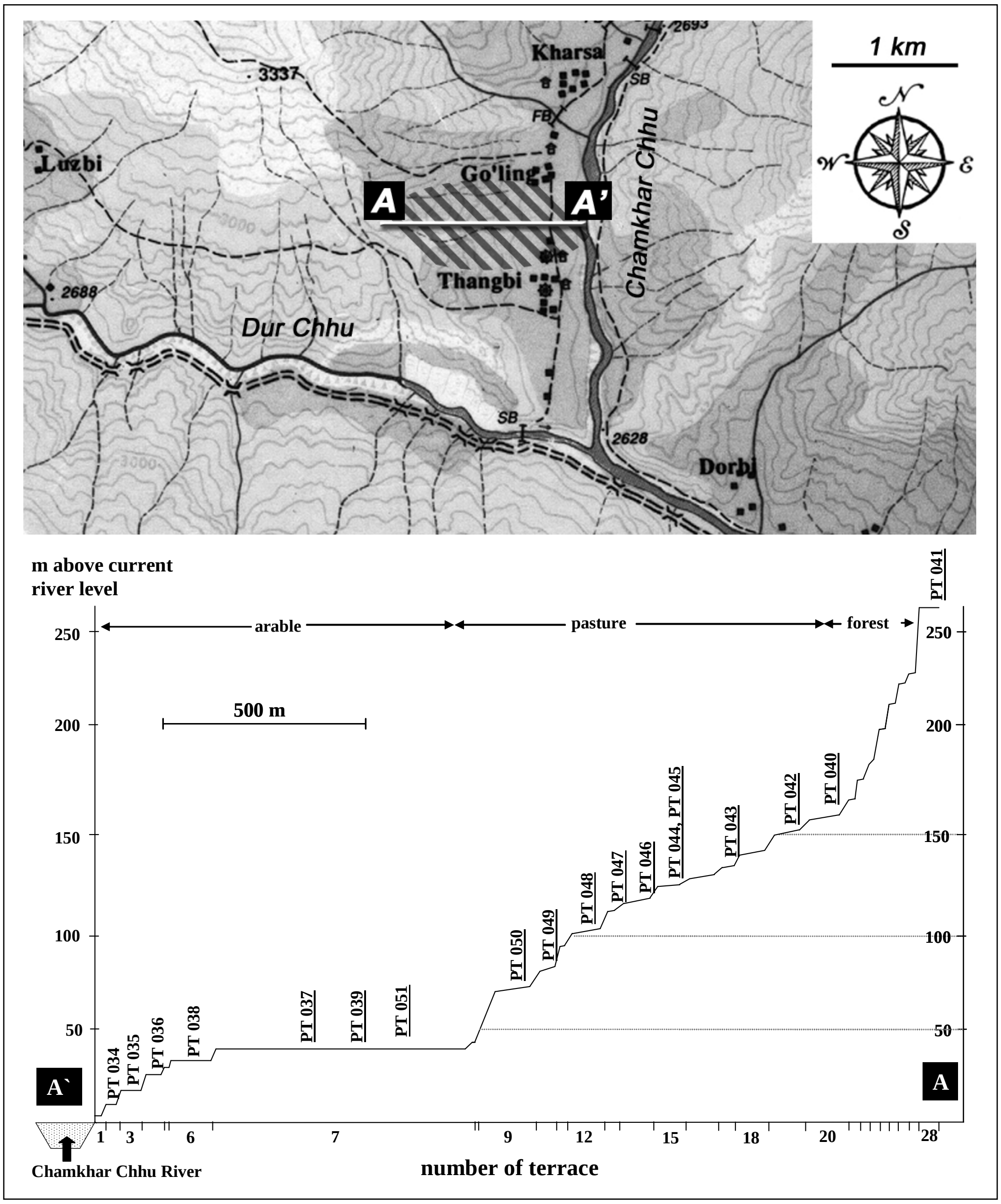

Fig. 9: Location of the Thangbi river terrace system (hatched area in upper part); map source: Survey of Bhutan (1999); the cross section from east (A') to west (A) is shown in the lower part; the profile IDs show the approximate location of the soil pits; underlined profiles are covered by loess.

In the same year, 6 profiles were sampled along the river terraces of the Sunkosh (Puna Tsang Chhu) River on the premises of the Bajo Renewable Natural Resources Research Centre (RNR-RC) (PT 057-PT 062). Three profiles were further established in the Lame Goempa Research Forest south of Jakar, central Bumthang District (PT 054-PT 056), and near the Thrumsing-La Pass (PT 053), eastern Bumthang District.

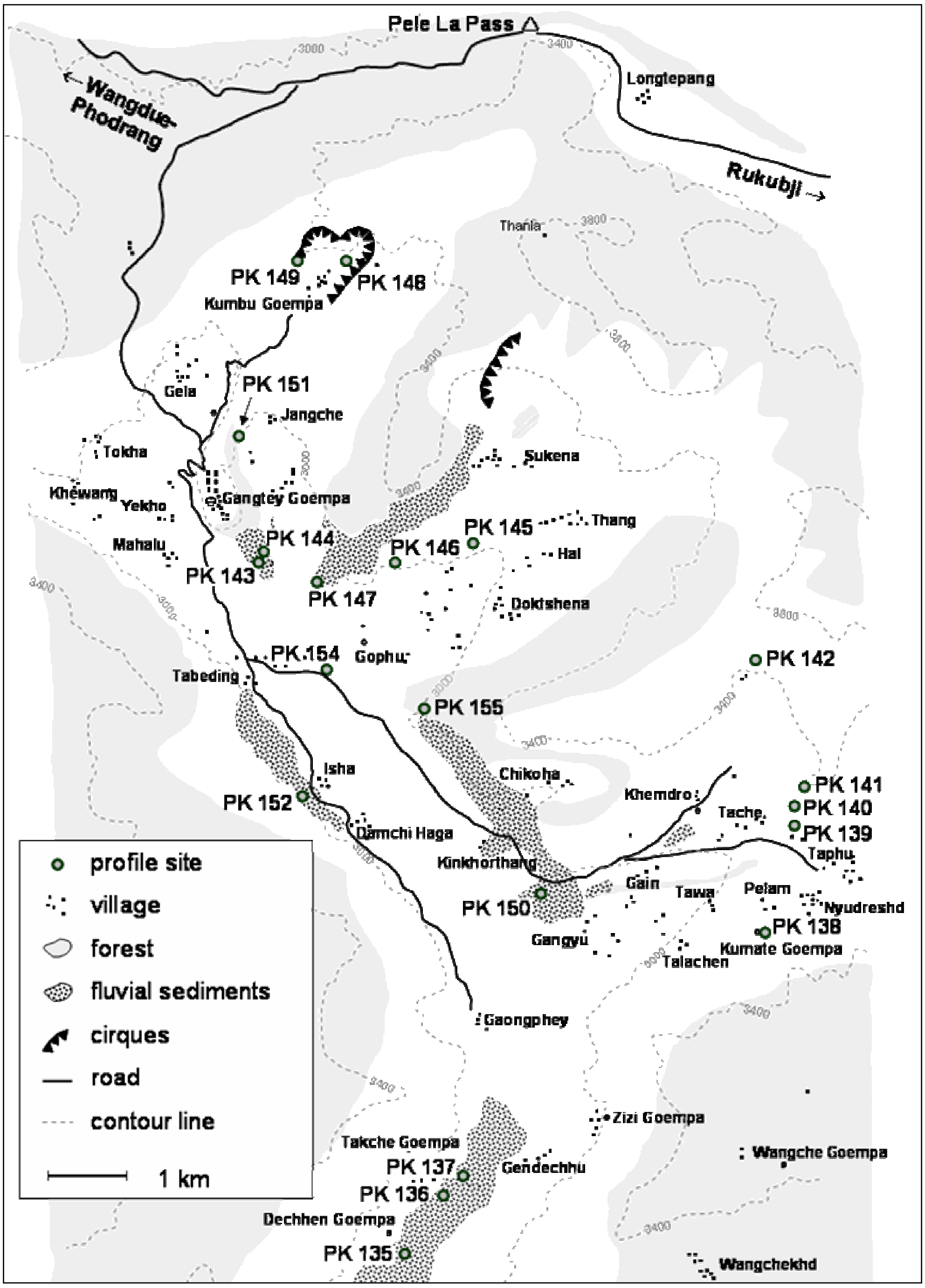

Fig. 10: Location of the soil profiles in Phobjikha Valley, Wangdue-Phodrang District.

In 2001, the major focus has been on the soils of the Phobjikha Valley, eastern Wangdue-Phodrang District, which lies west of the Black Mountains separating West from Central Bhutan. 21 soil profiles were sited to cover the Phobjikha main valley and the two lateral valleys (PK 135-PK 152, PK 154-PK 155) (*Fig. 10*). Two additional profiles (PK 153, PK 156) were established southwest of Rukubji Village, which lies at the eastern slopes of the Black Mountain Range, approximately 10 km east of the Pele La Pass along the East-West highway.

A separate excursion lead to the South Bhutanese foothill region along the border to the Indian state of West Bengal. Three profiles were established along the Thimphu-Phuentsholing Highway (PK 157-PK 159).

3.2 Soil sampling techniques and field parameters

For each sampling site, the geographical coordinates, height above sea level, inclination and exposition of the site, relief data, land use, vegetation, weather and signs of anthropogenic influence were gathered. A Garmin GPS (Garmin International Inc., Olathe, KS, USA) was used to confirm the locations of the soil profiles.

Most soil profiles were in pits, but roadcuts and landslide sites have also been used where appropriate. Digging continued down to the parent material. When no changes could be detected at about 2 m depth, the soil below was examined by augering.

The profiles were described and sampled according to FAO-ISRIC (1990) and horizon designations were made according to the World Reference Base (ISSS 1998). The soil colours were determined in field-moist state using the Munsell Soil Colour Charts (Munsell 1994). Further field parameters included the determination of soil texture, structure of the aggregates, mottles and concretions, coatings, pores and cracks, distribution and frequency of stones and roots, and estimates of humus and carbonate content.

From each distinguishable horizon, one bulk sample (approx. 1 kg) was collected, hand-crushed, air-dried and sieved to 2 mm. Triplicate core samples ($n = 3$, $V = 100\ cm^3$) were also taken. In a few cases, core samples could not be taken due to high stone contents.

3.3 Soil analytical methods

All analyses were performed on air-dried < 2 mm samples. The core samples were analysed for bulk density by the Soil and Plant Analytical Laboratory (SPAL), Semtokha, Bhutan. The bulk samples were transferred to the Soil Science Institute of the Technische Universität München (TUM), Germany, where most geochemical analyses were conducted. Except for the non-replicated XRD, INAA and ^{14}C-AMS determinations, all laboratory measurements were performed in duplicate.

3.3.1 Soil physical characteristics

Bulk density

For the measurement of bulk density, the core samples were dried at 105°C and subsequently weighed.

Surface area (BET)

The surface area of the air-dried fine earth was determined by the N_2-adsorption BET approach (Brunauer et al. 1938), using a Quantachrome Autosorb 1 surface area analyser (Quantachrome Corp., Boynton Beach, FL, USA). Prior to the measurements the samples were outgassed under vacuum (40 mbar) at 70°C for 24 hours, and analysed by multiple-step adsorption of N_2 at 77°K in the relative pressure (p/p_o) range of 0.05 to 0.30.

Particle size distribution

For particle size distribution, the samples were pre-treated with H_2O_2 to destroy organic matter. After dispersion by shaking with tetrasodium pyrophosphate ($Na_4P_2O_7$) and ammonium oxalate solution for 16 hours, the sand fractions were separated by wet sieving (coarse sand, cS: 2000-630 µm; medium sand, mS: 630-200 µm; fine sand, fS: 200-63 µm). For determining the amounts of silt (cSi: 63-20 µm; mSi: 20-6.3 µm; fSi: 6.3-2 µm) and clay (C: < 2 µm), the fractions < 63 µm were freeze-dried, re-suspended in water and subjected to X-ray attenuation (XRA) measurement by using a Sedigraph 5100 (Micromeritics GmbH, Mönchengladbach, Germany). The minimum determinable particle size with this method is 0.5 µm.

Clay mineralogy

Clay fractions (< 2 µm) were separated by sedimentation. The clay mineralogical composition was examined by X-ray diffraction (XRD) analysis (Moore & Reynolds 1989), using oriented samples after saturation with magnesium (air-dried, 25°C), magnesium + glycerol (110°C), and potassium (air-dried and stepwise heated to 560°C). The samples were irradiated between 2° and 18° at a scanning rate of 0.02° and intervals of 5 s, using a Philips PW 1830 diffractometer (Philips, Hamburg, Germany) with Co-Kα radiation and operating at 35 kV and 35 mA.

3.3.2 Column experiments

To study the release and transport of dissolved organic matter (DOM), aluminium and iron, column experiments were performed with two samples of non-volcanic Andosols (see Section 5.2). The main parameters of these experiments are shown in *Table 3*.

Table 3: Main parameters of the column experiments.

parameter	symbol	unit	horizon	
			PT 056/2 (AB)	PT 056/4 (B2)
column length	L	[mm]	1.00E+02	1.00E+02
column diameter	d	[mm]	3.97E+01	3.97E+01
bulk density	db	[g mm^{-3}]	7.33E-04	8.17E-04
pore volume	PV	[mm^3]	7.79E+04	7.54E+04
theta	θ	[-]	6.29E-01	6.09E-01
volumetric flow	Q	[mm^3 s^{-1}]	2.67E+00	2.67E+00
mean pore water velocity	v	[mm s^{-1}]	3.48E-03	3.61E-03
tracer concentration	C_0	[mmol mm^{-3}]	1.23E-05	1.23E-05

The columns were packed with air-dried < 2 mm fraction of the particular horizons and saturated with a background solution (BG) from bottom to top at a low flow rate of one pore volume per week to prevent entrapment of air. The background solution contained 10^{-5} Mol m^{-3} $NaClO_4$ to adjust the ionic strength, and 10^{-6} Mol m^{-3} NaN_3 to prevent microbial activity. A monovalent cation was chosen to adjust to the natural rainwater chemistry at the southern slopes of the Himalayas with a dominance of marine aerosols from the Bay of Bengal during the predominant monsoonal rains and to prevent artificial DOM immobilisation by polyvalent cations (Münch et al. 2002). Flow interruptions were conducted to detect possible kinetic limitations within a mobilisation process. A pulse of deionised water should reveal effects of very low ionic strength on the release of soil borne DOM and metal cations matching the actual conditions during the monsoon season. Chloride (1.2 mol m^{-3}) was used as a conservative tracer to evaluate the transport regime. Column dispersivities were estimated by fitting the advection-dispersion equation to the chloride breakthrough curve using CXTFIT (Parker & van Genuchten 1984). More details on the design and performance of the column experiments are given in Weigand & Totsche (1998) and in Münch et al. (2002).

3.3.3 Soil chemical characteristics

Soil pH

Soil pH was measured in deionised water and 1M KCl at a soil-solution ratio of 1:2.5.

Cation exchange capacity (CEC)

For the determination of the cation exchange capacity (CEC), unbuffered 0.5 M NH_4Cl solution was used to extract exchangeable cations from 2.5 g air-dried soil (Trüby & Aldinger 1989) at a soil-solution ratio of 1:20. Concentrations of extracted H^+, Na^+, K^+, Ca^{2+}, Mg^{2+}, Mn^{2+} and Al^{3+} were measured by ICP-OES (Perkin Elmer Optima 3000, PerkinElmer Inc., Boston, MA, USA).

Soil organic matter

Total carbon (C_{tot}) and total nitrogen (N_{tot}) were measured by dry combustion (975°C), using a Vario EL analyser (Elementar Analysensysteme GmbH, Hanau, Germany). Since all samples were carbonate-free, the total carbon contents are taken as equivalent to organic carbon contents (C_{org}).

^{14}C-AMS (accelerator mass spectrometry) measurements of subsoil organic matter were performed at the Leibniz laboratory for radiometric dating and isotope research (Kiel, Germany). Pre-treatments of the samples included extraction by 1% HCl, 1% NaOH and 1% NaOH at 60°C, combustion at 900°C and reduction of the generated CO_2 to graphite.

Solid state CPMAS ^{13}C nuclear magnetic resonance (NMR) spectroscopy was conducted to provide information about the SOM composition in comparison to Podzols (Bruker DSX 200 spectrometer).

Phosphorus

For total P contents, 130-150 mg samples were digested in a mixture of $HClO_4$, HNO_3 and HF at 300°C in platinum containers. In the resulting solutions, P was measured with a Milton Roy Spectronic 601 spectrophotometer at 882 nm.

Phosphate retention was determined according to Blakemore et al. (1987) in acidic potassium dihydrogen phosphate (KH_2PO_4) solution, adjusted to pH 4.6 by sodium acetate.

Extractable Fe and Al compounds

Free iron compounds (Fe_d), including poor and well crystalline forms, were extracted with dithionite-citrate-bicarbonate (DCB) solution (Mehra & Jackson 1960). Non- or poorly crystallised Fe-oxides, hydroxides and associated gels (Fe_o) were leached by acid ammonium oxalate solution (Van Reeuwijk 2002). DCB- and oxalate-soluble Al (Al_d, Al_o) were determined in the same extracts. The optical density index of the oxalate extract (ODOE) was determined photometrically at 430 nm. For estimating the Fe and Al associated with organic matter, pyrophosphate extractions (Fe_p, Al_p) have been performed with ultra-centrifugation at 18,000 g and “Superfloc” as flocculating agent (Aleksandrova 1960). Silicate-bond iron was calculated from Fe_{t-d}, and well-crystallised iron oxides as Fe_{d-o}. The quotient of well-crystallised iron oxides and total iron content (Fe_{d-o}/Fe_t) was used as a relative measure for weathering intensity (Arduino et al. 1984, 1986).

Element mapping

Scanning electron microscopy and element mapping (SEM-EDX) were done by using a JSM-5900LV (JEOL-USA Inc., Peabody, MA, USA).

3.3.4 Neutron Activation Analysis

Total contents of major, trace and rare earth elements were measured by instrumental neutron activation analysis (INAA) at the Missouri University Research Reactor (MURR), Columbia, MO, USA. A principal advantage of INAA is that it is nearly free of matrix interference effects, as the vast majority of samples are completely transparent to both the probe (the neutron) and the analytical signal (the gamma ray). Moreover, there is little if any reagent or laboratory contamination, because the samples do not have to be digested or dissolved prior to the measurements. INAA only estimates total contents, however gives no indication of the locations or configurations of the detected elements.

Pre-treatments included grinding of the samples to dust size and heating at 900°C to remove organic matter. For analysis, 150-200 mg of powder are weighed into cleaned high-density polyvials, irradiated in pairs using a neutron flux of $8 \cdot 10^{13}$ n cm^{-2} s^{-1} for five seconds, and allowed to decay for 25 minutes. The resulting radioactive isotopes are identified and the element concentrations are determined by the gamma-rays they emit, using a high-resolution, high-purity germanium detector (HPGe). This short irradiation procedure allows the determination of Al, Ca, Dy, K, Mn, Na and Ti. For long irradiations, 24 hour treatments in a neutron flux of $5 \cdot 10^{13}$ n cm^{-2} s^{-1} are performed. After a decay period of 7-8 days, the sample vials are counted for 2,000 seconds (mid count) each, using an HPGe detector coupled to automatic sample changers. After an additional decay of 4-5 weeks, the samples are counted a final time for three hours each (long count). Elements detectable from the mid count include As, La, Lu, Nd, Sm, U, and Yb, and those from the long count include Ce, Co, Eu, Fe, Hf, Sc, Tb and Zr.

As Si could not be determined with INAA, total SiO_2 contents were assumed to be the difference between 100% and the sum of all other major element oxides.

3.4 Data analysis and statistics

3.4.1 Data handling

Within the scope of this study, a multitude of data has been generated. It has neither been sensible nor feasible to discuss all of the gathered results in the light of the identified objectives. Therefore, a number of soil profiles has been selected for each question, which was considered suitable for its solution. Nevertheless, as the collection and provision of soils data has been one of the main objectives of this work, the Appendix starting from page 137 contains all measurement results, as well as colour photographs of all profiles which have been selected for closer description.

3.4.2 Explorative data analyses

Among the data reducing methods, cluster and factor analyses were performed with Statistica 6.1 (StatSoft Inc., Tulsa, OK, USA). For the agglomerative cluster analysis, Euclidean distances were chosen as distance measure, and Ward’s method, which is based on the square of the distances among the points, as the clustering algorithm. A factor analysis was used to group the 24 variables into factors. A scree plot was applied to extract an adequate number of factors. A standardised varimax rotation helped to improve the loadings of the respective factors.

The one-tailed Student’s *t*-test has been used to detect if correlations were significant at the 0.05 (*), 0.01 (**) or 0.001 (***) probability levels.

3.4.3 Weathering indices

In the course of physical and chemical processes of mineral weathering some elements are depleted, while more recalcitrant ones become passively enriched with time. Balance equations can be calculated to examine the degree of alteration compared to the unweathered parent material. This not only allows to detect the weathering maxima within single soil profiles, but also provides a relative dating method for soils within a chronosequence. Two separate approaches have been selected. Firstly, the index after Parker (1970) was applied:

$$\text{Parker index, PI} = \left(\frac{\mathrm{Na_a}}{0.35} + \frac{\mathrm{Mg_a}}{0.9} + \frac{\mathrm{K_a}}{0.25} + \frac{\mathrm{Ca_a}}{0.7} \right) \cdot 100$$

where X_a represents the atomic portion of ion X, measured by INAA ($0 \leq PI \leq 100$).

It calculates the loss and subsequent leaching of the main alkali and alkaline earth cations by mineral hydrolysis. The numbers in the denominator represent factors to allow for the strength of the element-oxygen bond in the primary minerals. The index *de*creases with *in*creasing soil development.

Secondly, the Chemical Index of Weathering (CIA) has been calculated, following Nesbitt & Young (1982):

$$\mathrm{CIA} = \frac{\mathrm{Al_2O_3}}{\mathrm{Al_2O_3} + \mathrm{CaO^*} + \mathrm{Na_2O} + \mathrm{K_2O}} \cdot 100$$

Oxides are expressed as molar proportions, where CaO^* is CaO in silicate minerals only. The index represents the degree of alteration of feldspars to clay minerals in the course of hydrolytic weathering, and indicates the relative contents of clay minerals. Values for unweathered igneous rocks are about 50, whereas intensely weathered residual rocks forming kaolinite and gibbsite can approach 100.

To take into account the varying horizon thicknesses, weighted means of analytical parameters and indices were calculated for each profile as:

$$x_m = \frac{\sum (x_i \cdot d_i)}{\sum d_i}$$

with x_m = profile-weighted mean, x_i = parameter x of horizon i, and d_i = depth of horizon i.

To account for the greatly varying depth of the C horizons, 20 cm have been taken as a standard depth for the lowest soil horizon of each profile.

4 Comparative geochemical investigation of Bhutanese soils

Total major, trace and rare earth element contents of selected Bhutanese soils form the basis of this chapter. Each of the examined sites is within a distinct geological background. Besides providing a systematic account of pedogeochemical data, the following pages include insights into weathering intensities and the connexion of the soils with the underlying geology and landscape.

4.1 Samples and site characteristics

The six soil profiles selected for this purpose are PT 053, PT 056, PK 138, PK 139, PK 156 and PK 158. Their location within Bhutan is shown in *Fig. 8* (page 23), and *Table 4* summarises their associated site properties.

Table 4: Overview of soil profiles and associated site properties. Precipitation values are estimated from RGoB (1997); Systematic rainfall and temperature measurements are only available for the Lame Goempa site (RGoB 2000a).

Profile ID	Location	Geograph. coord.	Altitude a.s.l. [m]	Formation/group	Lithology	Precipitation [mm a^{-1}]	Vegetation
PT 053	Thrumsing La	27°24'N 90°59'E	3,768	Takhtsang Formation, Thimphu Group	Granite gneiss	600	*Abies sp.*, *Rhododendron spp.*
PT 056	Lame Goempa	27°32'N 90°43'E	3,025	Naspe Formation (Paro Metasediments)	Mica schist	1,100 (8°C)	*Pinus sp.*, *Bambus sp.*
PK 158	North of Phuentsholing	26°53'N 89°27'E	1,520	(Intrusions into) Shumar Formation	Restitic melt, migmatite	1,550	Subtropical shrubs and trees
PK 138	Phobjikha Valley	27°25'N 90°14'E	3,185	Deshichiling Formation, Pele La Group (Teth. Sequence)	Quartzitic phyllite	700	Grass, ferns (pasture)
PK 139	Phobjikha Valley	27°26'N 90°14'E	3,095	Maneting Formation, Pele La Group (Teth. Sequence)	Phyllite, marine (Tethyan) sediments	725	Grass, ferns (pasture)
PK 156	Rukubji Village	27°30'N 90°16'E	2,866	Intrusions into Paro Metasediments	Leucogranite	800	Grass and shrubs

Profile PT 053 was established in a Bhutan fir (*Abies densa* Griff.) forest, 100 m below the Thrumsing La pass, which divides Central from East Bhutan and is the highest point of the Bhutanese East-West Highway. The solum is wholly derived from deeply and in-situ weathered granitic gneiss, and no aeolian or fluvial additions have been detected throughout the profile. Podzolisation with associated Bhs and Bs horizons is clearly visible, but an albic horizon is missing. The soil is therefore classified as an Entic Podzol (ISSS 1998). The unexpected depth of weathering is shown by sample PT 053/6 which was taken from friable saprolite at about 4 m. Gansser (1983) designates this lithology as the Takhtsang type gneisses, consisting of muscovite-biotite-granite gneisses (higher amphibolite facies), which are characterised especially by abundant muscovite and paucity of garnets.

Profile PT 056 was situated at 3,025 m a.s.l. in the Lame Goempa Research Forest near Jakar in Bumthang District, Central Bhutan. The Bumthang Basin was mapped as highly metamorphosed Paro Metasediments by Gansser (1983). However, Golani (1995) puts these materials into the Naspe Formation which – together with the conformably underlying Sure Formation and the unconformably overlying Takhtsang Formation – constitutes the Thimphu Group in the Central Crystalline Complex. The soil parent material is dominated by two-mica schists. Garnet amphibolites, which are described by Gansser (1983), have not been detected in PT 056. The profile keys out as Veti-Acroxic Andosol (Dystric). The occurrence and origins of andic features in non-volcanic soils in Bhutan are discussed in detail in Chapter 5.2 (page 81ff.).

Profiles PK 138 and PK 139 (Appendix 3, page 156f.) are located in the basin-shaped Phobjikha valley system, which lies at about 3,000 m a.s.l. in western Central Bhutan (*Fig. 8*, *Fig. 10*). It is on a small outcrop of Palaeozoic extremely low-grade metamorphic rocks of the Tethyan Sequence, which Chaturvedi et al. (1983) designated as a possible southern extension of the Tang Chu Basin. The properties and genesis of the soils of this area are described in Section 5.1. Although the two sites are only a few hundred meters apart, they show marked differences in the field. PK 138 is a silt-rich solum over green-greyish coloured, weathered quartzitic phyllite, starting at 115 cm in the 2C horizon (PK 138/6). The XRD diagram confirms the dominance of muscovite and quartz (*Fig. 11*). Tangri & Pande (1995) point out that the volcanic materials of the Singhi Formation are absent in this sector, and that the Chekha Formation is directly overlain by the Deshichiling and Maneting Formations (*Fig. 13*). According to the detailed mapping of Chaturvedi et al. (1983), the site belongs to the Deshichiling (= Nake Chu) Formation, and following our observations resembles the greenish-grey phyllites in its basal part as described by Tangri & Pande (1995). The profile has a distorted, patchy fossil A horizon, which indicates slope movements under periglacial and/or heavy monsoonal conditions. The profile has been classified as Dystric Andosol (Caspari et al. 2005).

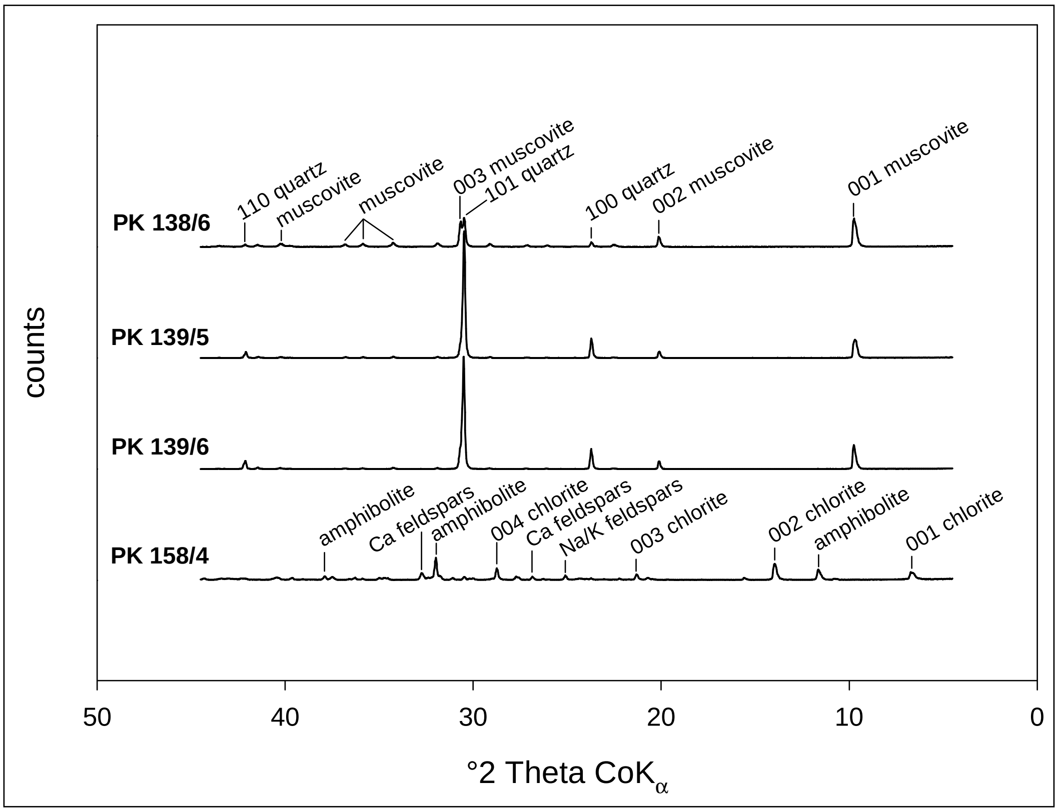

Fig. 11: X-ray diffraction patterns for selected saprolite samples

The XRD diagram of profile PK 139 is nearly identical with that of PK 138 (*Fig. 11*), and shows quartz and – to a lesser extent – muscovite as the main mineral constituents of the 3C horizon (PK 139/6). During fieldwork, however, we noted a strikingly dark colour of the subsoil (10YR 2/2), and found Mn nodules of several cm in diameter (*Fig. 12*). At the base of this profile, we appear to have touched a part of the “richly fossiliferous, dominantly brown, sporadically greenish grey arenite beds”, which Tangri & Pande (1995, p.125) describe in the Maneting Formation. Based on fossil evidence, a mid to late Ordovician age had originally been assigned to the Maneting Formation (Chaturvedi et al. 1983), which after lingulellid (Brachiopod) fossil finds has been

Fig. 12: Mn nodule from the subsoil of profile PK 139.

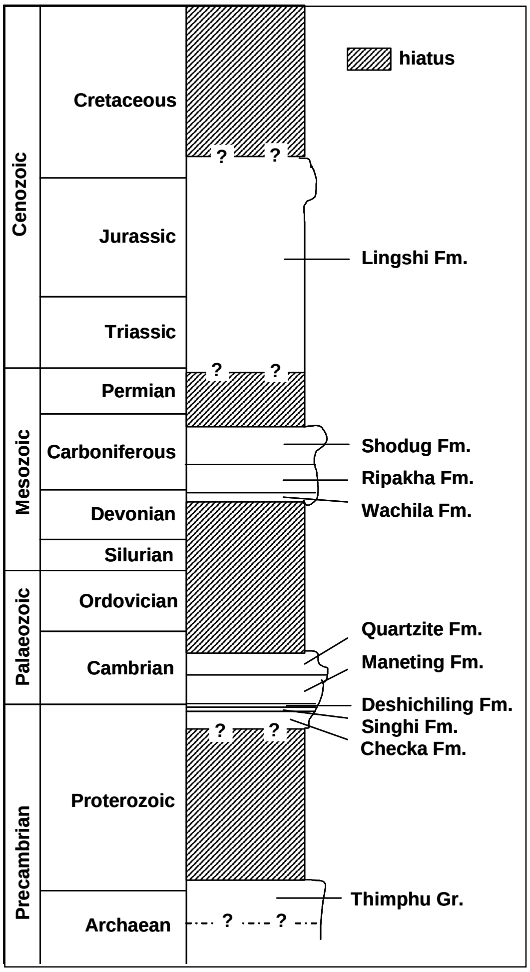

Fig. 13: Lithocolumn of the Tethyan Sequence in Bhutan after Bhargava (1995).

corrected to an Early Cambrian age (Mamgain & Roy 1989, Tangri et al. 2003). One of the intermediate horizons (PK 139/4) is rich in mica, which suggests a polygenetic regolith. Polygenesis is further supported by the step-wise coarsening of the grain size as detected in the field, and the frequent occurrence of fossil A horizons in the area. The properties of the uppermost, aeolian-influenced stratigraphic layer (horizons PK 139/1-3) are decisive in classifying this soil as a Dystri-Vetic Andosol.

PK 156 (Appendix 3, page 156) is developed on a small leucogranite intrusion near Rukubji Village, Central Bhutan. The granite consists of quartz (30-34%), plagioclase (32-37%), orthoclase (23-30%), muscovite (3-7%) and biotite (1-3%) (Gansser 1983). Similar compositional data are given by Guillot & Le Fort (1995) for the Manaslu leucogranite in Central Nepal. Ilmenite, apatite, tourmaline and garnet are common accessory minerals (Dietrich & Gansser 1981). Guillot & Le Fort (1995) mention aluminous schists and gneisses as the likely sources for peraluminous leucogranitic magmas. The upper part of the soil profile may have received aeolian additions, although the field indications are not wholly clear. The profile is determined as Dystric Andosol.

PK 158 (Appendix 3, page 156) is an example for soils developed in the diffuse migmatitic zone south of Chasilakha in South Bhutan. Volcanic melts intercalated between the phyllitic, late Precambrian sediments of the Shumar Formation in the south, and the large crystalline thrustmass in the north. The soil parent material at this site is most probably derived from intrusive migmatitic bodies, metamorphosed to amphibolite. XRD results reveal that it is strikingly different from PK 138 and PK 139 (*Fig. 11*). The dark-coloured matrix is constituted of mainly (meta-) amphiboles, chlorite and plagioclase feldspars. Quartz contents are negligible and illite/mica has not been detected. This is in accordance with the findings of Dasgupta (1995) for basic rocks of the Shumar Formation. The associated pedon is strongly leached and classified as Veti-Humic Ferralsol (Alumic, Hyperdystric, Xanthic).

4.2 Major elements

The results of the major element geochemistry are summarised in *Table 5*.

The gneiss of PT 053 is the most felsic among the examined lithologies, with SiO_2 values of more than 70% throughout the profile and 80% in the A horizon. The contents of Al_2O_3 and Fe_2O_3 are correspondingly the lowest, at about 17 and 5 weight-%, respectively. Podzolisation is reflected by a profile maximum of 5.9% Fe_2O_3 in the Bhs horizon. K_2O steadily increases with depth, from 2.5% in the topsoil to 4.4% in the saprolite, and proves the illitic rather than smectitic character of the profile. MgO, with contents increasing from 0.1 to 1.2% mass, follows the same pattern, whereas CaO and Na_2O are constant with about 1% mass throughout. MnO, TiO_2 and P_2O_5 are below 1% mass each. Major element data of this profile match well with those given by Sarkar & Dasgupta (1995) for a biotite granitic gneiss from the Takhtsang area.

PT 056 on the metamorphosed Naspe Formation (Paro Metasediments) has slightly lower SiO_2, and higher Al_2O_3 and Fe_2O_3 average contents compared to PT 053. This may be due to higher contents of kyanite and staurolite (Golani 1995), or result from higher contents of biotite included in the two-mica schists, as mentioned by Gansser (1983) for the Bumthang-Djüle La facies of this lithological unit.

PK 138 belongs to the still less metamorphosed Deshichiling formation within the Tethyan Pele La Group. Its phyllitic character is reflected by high K_2O values of up to

4.3% mass. Compared to the other metamorphic profiles, it has lower average contents of SiO_2 (65.5%), and higher ones for Al_2O_3 (21.6%) and Fe_2O_3 (7.6%). MgO, CaO and Na_2O values are low throughout. One possible explanation is the more basic regolith of PK 138, in comparison to PT 053 and PT 056, suggesting that quartz increases and Al_2O_3 and Fe_2O_3 decrease with intensifying metamorphism.

Table 5: Total contents of major element concentrations of the selected soil samples. Concentrations for Upper Continental Crust (UCC) are from Taylor & McLennan (1985).

Sample/ horizon		depth [cm]	SiO_2	Al_2O_3	Fe_2O_3	MnO	MgO	CaO	Na_2O	K_2O	TiO_2	P_2O_5
			weight-%									
PT 053												
/1	A	-15	79.64	12.99	1.48	0.02	0.09	1.12	1.36	2.54	0.65	0.11
/2	Bhs	-27	73.51	14.85	5.87	0.06	0.37	0.95	1.16	2.57	0.54	0.11
/3	Bs	-49	70.91	17.29	5.14	0.11	0.71	1.17	1.10	3.10	0.39	0.08
/4	CB	-70	70.57	17.67	4.67	0.13	1.00	1.16	1.08	3.22	0.47	0.03
/5	C1	-120	71.04	17.06	4.58	0.14	1.03	0.72	0.90	4.06	0.46	0.00
/6	C2	ca. 400	70.53	16.43	4.50	0.13	1.20	0.98	1.43	4.39	0.40	0.01
PT 056												
/1	A	-17	72.43	15.57	7.65	0.06	0.30	0.55	0.65	1.62	1.04	0.13
/2	AB	-24	74.39	14.86	6.73	0.03	0.32	0.34	0.53	1.51	1.21	0.09
/3	B1	-49	67.46	19.50	8.53	0.04	0.40	0.23	0.67	1.98	1.09	0.09
/4	B2	-101	67.42	20.20	7.48	0.06	0.43	0.33	0.77	2.34	0.86	0.10
/5	B3	-148	68.69	19.26	6.89	0.07	0.48	0.32	0.66	2.64	0.89	0.11
/6	CB	-200	71.52	19.08	4.66	0.06	0.55	0.05	0.37	2.92	0.70	0.08
PK 158												
/1	A1	-47	54.72	18.90	16.83	0.31	2.51	1.94	1.57	0.69	2.27	0.25
/2	B1	-78	52.87	20.13	16.81	0.30	3.48	1.96	1.58	0.48	2.12	0.27
/3	2B2	-135	48.94	21.70	18.40	0.33	3.90	2.24	1.65	0.29	2.31	0.25
/4	2B3	-210	46.97	21.99	20.78	0.31	3.73	2.07	1.62	0.26	2.07	0.21
/5	2C	-250	48.01	20.86	19.78	0.30	5.07	1.43	2.19	0.29	1.92	0.15
PK 138												
/1	Ah	-5	64.07	17.81	12.55	0.20	0.83	0.06	0.13	3.31	0.93	0.11
/2	B1	-32	64.14	22.38	9.11	0.08	0.40	0.17	0.31	2.42	0.86	0.13
/3	B2	-63	65.15	22.83	7.02	0.11	0.48	0.23	0.40	2.75	0.87	0.15
/4	2A	-70	65.72	23.17	5.95	0.11	0.33	0.04	0.24	3.51	0.79	0.15
/5	2B	-115	67.50	21.63	4.85	0.10	0.37	0.05	0.17	4.34	0.87	0.12
/6	2C	-160+	66.62	21.68	6.06	0.24	0.38	0.06	0.14	4.22	0.48	0.12
PK 139												
/1	A	-14	72.26	15.72	8.06	0.10	0.41	0.20	0.41	1.81	0.90	0.14
/2	B1	-33	66.35	20.42	8.65	0.09	0.54	0.12	0.48	2.26	0.95	0.14
/3	B2	-54	69.35	18.69	6.99	0.09	0.73	0.27	0.53	2.49	0.75	0.11
/4	2B3	-84	77.22	13.93	4.96	0.14	0.45	0.05	0.15	2.48	0.56	0.06
/5	2CB	-115	81.87	11.32	4.75	0.46	0.21	0.08	0.06	0.87	0.30	0.07
/6	3C	-150+	86.53	2.60	6.20	1.19	0.22	0.57	0.03	1.57	0.97	0.12
PK 156												
/1	A1	-16	74.69	14.69	6.03	0.03	0.20	0.23	0.69	2.53	0.76	0.16
/2	2B1	-40	66.07	20.63	9.25	0.03	0.25	0.23	0.60	2.00	0.83	0.11
/3	2B2	-79	65.60	22.24	7.84	0.04	0.28	0.17	0.61	2.43	0.68	0.11
/4	2BC	-104	73.92	18.63	2.02	0.05	0.11	0.06	0.59	4.46	0.13	0.03
/5	2C	-140	74.64	18.12	1.00	0.08	0.05	0.13	0.68	5.20	0.08	0.02
UCC			66.00	15.2	5.0	0.07	2.20	4.2	3.9	3.4	0.5	-

Another possibility is admixture of the metamorphosed Late Precambrian Singhi Volcanic rocks, which underlie the Deshichiling Formation. These have not been described in the sampled area. However, with average 57.2% SiO_2, 16.7% Al_2O_3, 6.8% Fe_2O_3 and 3.2% K_2O (Tangri & Pande 1995), they accord with the geochemical features of PK 138/6 (*Table 5*). Parallel increases in Ba and Th corroborate the admixture hypothesis (*Table 6*).

Major element data for PK 139 indicate that the soil profile is polygenetic. The first stratum including PK 139/1-3 is characterised by high Al_2O_3 (18.3%), Fe_2O_3 (7.9%) and TiO_2 (0.9%). PK 139/4-5 have SiO_2 values of around 80% but clearly lower Al_2O_3 (12.6%), Fe_2O_3 (4.9%) and TiO_2 (0.4%). PK 139/6 is strikingly different. Its major element profile reveals the highest SiO_2 (86.5%) and MnO (1.2%), as well as the lowest Al_2O_3 (2.6%) and Na_2O (0.03%) of all horizons studied. Besides the manganese nodules found at the site, the very high concentration of quartz in this horizon is an indication of the marine provenance of the source bedrock. This may also explain the exceptionally high As and Co concentrations, which we have found nowhere else in Bhutan (*Table 6*).

The leucogranitic saprolite (PK 156/4-5) is potassium- and aluminium-rich, with 4.5-5.2% K_2O and 18.1-18.6% Al_2O_3. At the same time, values for TiO_2, MgO and Fe_2O_3 are remarkably low, and increase manifold towards the surface. Guillot & Le Fort (1995) mention aluminous schists and gneisses as likely sources for peraluminous leucogranitic magmas, which could explain this macro-element behaviour. According to these authors, biotite fractionation can be deduced from the decrease of TiO_2 content, whereas K-feldspar generally is a late phase to crystallize, particularly in the presence of tourmaline (Benard et al. 1985), resulting in the observed high K_2O values. Our saprolite data are comparable to leucogranite rock analyses by Sarkar & Dasgupta (1995). The only differences are higher Al_2O_3 and lower CaO and Na_2O at our site, which is thought to result from saprolite weathering. Rb values and K/Rb ratios are also within the range given by Sarkar & Dasgupta (1995).

PK 158 on migmatitic materials in southern Bhutan is geochemically quite distinct from the other sites. With SiO_2 values below 55% and Fe_2O_3 around 20%, it is the most mafic one in comparison. The substantial contributions from hornblende are reflected by CaO and MgO concentrations about 10-fold higher than those in the other profiles (*Table 5*).

Table 6: Total trace element concentrations of selected soil samples

Sample/ horizon		Rb	Cs	Ba	Sc	V	Co	As	Th
		mg kg^{-1}							
PT 053									
/1	A	64.0	2.8	452.1	6.2	62.6	1.5	3.8	23.4
/2	Bhs	95.0	6.2	542.9	8.3	104.2	4.6	4.9	23.3
/3	Bs	132.9	7.9	511.1	10.9	82.7	9.4	2.1	28.6
/4	CB	165.8	7.7	505.8	11.0	60.1	11.6	< 1.7	25.9
/5	C1	197.7	7.3	596.3	11.5	58.5	10.9	< 1.7	24.6
/6	C2	195.1	7.1	506.8	11.9	66.9	10.6	< 1.7	25.7
PT 056									
/1	A	89.5	11.1	363.2	11.6	144.3	5.0	17.6	23.9
/2	AB	65.1	8.7	221.5	11.4	163.4	3.8	17.6	22.3
/3	B1	97.2	16.1	326.9	15.2	155.1	13.6	22.4	22.9
/4	B2	114.9	19.4	347.2	15.5	135.5	21.0	26.8	23.0
/5	B3	119.6	20.3	378.7	16.5	137.2	14.3	22.3	24.3
/6	CB	131.6	13.0	558.6	13.9	93.6	13.4	6.5	22.6
PK 158									
/1	A1	23.0	2.0	< 89.9	45.7	330.9	52.6	< 3.1	8.2
/2	B1	30.0	1.8	< 90.4	49.5	368.4	50.5	< 3.2	7.1
/3	2B2	< 7.6	0.8	< 93.8	51.8	377.0	58.0	< 3.3	6.1
/4	2B3	< 7.9	0.5	< 97.7	53.6	426.0	59.3	6.7	6.9
/5	2C	< 8.2	<0.3	< 99.7	55.8	407.7	72.8	< 3.6	4.2
PK 138									
/1	Ah	214.4	27.7	542.1	18.8	138.9	30.2	31.2	28.5
/2	B1	119.5	15.5	379.4	15.8	118.6	8.2	42.1	25.6
/3	B2	150.6	18.2	509.3	16.5	111.4	13.6	43.3	25.1
/4	2A	166.4	16.6	543.6	17.0	93.0	9.1	45.5	23.2
/5	2B	203.0	15.4	730.7	16.4	104.1	9.5	35.9	21.2
/6	2C	194.0	12.4	1021.6	17.6	74.7	28.5	59.8	29.3
PK 139									
/1	A	106.5	25.9	374.7	12.3	122.5	9.4	36.0	22.8
/2	B1	121.8	30.9	411.3	15.3	127.8	15.6	33.9	24.1
/3	B2	144.9	35.4	434.8	15.5	111.3	19.3	25.4	22.1
/4	2B3	126.6	35.6	418.8	11.2	73.1	21.2	31.9	15.5
/5	2CB	86.6	36.5	292.8	11.3	47.9	51.2	44.6	21.9
/6	3C	70.3	29.4	363.5	60.1	< 65.9	191.2	99.3	28.8
PK 156									
/1	A1	184.0	31.1	289.1	8.2	102.0	3.1	15.0	18.7
/2	2B1	146.2	25.5	231.8	12.4	141.9	4.2	21.9	24.6
/3	2B2	197.5	35.2	219.2	14.9	110.4	7.5	24.6	23.1
/4	2BC	385.6	58.9	184.2	4.9	21.7	4.7	4.3	10.3
/5	2C	419.8	61.4	153.3	3.1	< 6.1	5.2	< 1.0	6.6

4.3 Indications for the state of weathering

The grain size distribution can be taken as a proxy for the intensity of soil development (Torrent & Nettleton 1979, Bäumler 2001a). In the course of weathering, the size distribution of minerals is shifted towards smaller size ranges, whereas for authigenic soil minerals the opposite trend is observed. As shown in *Table 7*, the gneissic profile (PT 053) is the coarsest with over 60% sand throughout the profile below the organic topsoil. The other profiles on metamorphic lithologies (PT 056, PK 138, and PK 139) are dominated by the silt and clay fractions, and high values for the > 63 µm fraction only occur in the saprolites, e.g. horizons PT 056/6 (59.3%), PK 139/5-6 (53.7% and 55.6%) and PK 156/4-5 (60.7% and 75.8%). The highest clay contents occur in the topsoils of PT 056 and PK 156, and approach 50 weight-%. Both profiles are situated at approximately 3,000 m a.s.l., where frequent freeze-thaw cycles strongly contribute to the overall weathering intensity. PK 138 and 139 are at similar elevation, but the continuing local redistribution of regolith materials seems to diffuse the effects of weathering (see Section 5.1). In all soils from metamorphic parent materials, the most frequent grain sizes are in the fine silt fraction, with peaks at about 5 µm and 10 µm (see *Fig. 21* on page 65). For PT 053, PT 056 and PK 156, a clear coarsening of the matrix with depth is visible. The same trend is apparent in PK 139, but to a lesser degree, because the silt contents of the subsoil (PK 139/5-6) decrease, whereas clay contents remain high. This again indicates some stratification of the solum. PK 139/6 clearly reflects the arenaceous nature of some beds in the Maneting Formation. PK 138 shows no major variations in grain size throughout the profile. This may indicate homogenisation by slope processes, or that we had not yet reached the saprolite. No clear trend has also been found for the migmatitic profile in South Bhutan (PK 158). High clay and silt contents were detected in all horizons, and a significant shift from clay- to silt-sized particles occurs only in the lowest horizon.

Using the major element data, the chemical indices of alteration (CIA = $Al_2O_3/(Al_2O_3+CaO+Na_2O+K_2O) \cdot 100$) have been calculated. The findings are summarised in *Table 7* and graphically illustrated in an A-CN-K (Al_2O_3 - $CaO+Na_2O$ - K_2O) plot (*Fig. 14*). It shows that all profiles are at an advanced stage of weathering, with high proportions of clay minerals relative to feldspars. Compared to the UCC, a high proportion of the Ca and Na has been leached from these materials, i.e. most plagioclase destroyed. Due to the heavier monsoon, the Bhutanese soils are generally more weathered compared to Nepalese profiles from similar lithologies and at similar altitudes (e.g. Bäumler 2001a).

Table 7: Particle size and weathering indices of the selected profiles.

Sample/ horizon		cS	mS	fS	cSi	mSi	fSi	C	CIA	Fe_d	Fe_o	Fe_t	Fe_{d-o} / Fe_t	pH_{KCl}
		weight-%							[-]	mg g^{-1}			[-]	[-]
PT 053														
/1	A	7.2	22.8	11.6	10.2	12.4	11.8	23.9	72	2.7	2.7	10.3	0.00	3.1
/2	Bhs	16.4	35.2	9.3	3.8	5.8	6.3	23.3	76	12.7	19.6	41.1	-0.17	3.6
/3	Bs	27.2	30.6	11.6	4.1	5.4	6.3	14.8	76	8.8	7.7	36.0	0.03	4.3
/4	CB	24.2	32.9	14.6	3.8	6.3	6.8	11.4	76	2.1	1.7	32.7	0.01	4.3
/5	C1	18.4	47.3	16.5	4.3	4.9	3.5	5.2	75	1.2	0.8	32.0	0.01	4.4
/6	C2	36.1	31.4	18.6	3.6	3.1	2.5	4.8	71	0.8	0.1	31.4	0.02	4.6
PT 056														
/1	A	3.4	7.0	8.3	8.9	12.0	13.1	47.2	85	28.6	12.0	53.5	0.31	4.0
/2	AB	0.3	1.1	7.6	7.6	16.5	17.4	49.6	86	31.8	11.8	47.1	0.43	4.0
/3	B1	0.4	8.2	11.4	7.2	13.5	21.6	37.7	87	41.3	9.6	59.7	0.53	4.6
/4	B2	1.9	15.8	13.3	7.7	13.7	19.7	27.9	85	36.8	7.1	52.3	0.57	4.9
/5	B3	1.3	4.8	14.0	8.5	14.7	19.5	37.2	84	32.3	13.7	48.2	0.39	4.9
/6	CB	21.9	21.4	16.0	4.2	6.8	7.7	22.1	85	15.5	6.6	32.6	0.27	4.6
PK 158														
/1	A1	4.2	13.3	6.7	4.4	17.5	20.1	33.9	82	43.2	13.6	117.7	0.25	4.1
/2	B1	3.5	9.6	11.9	5.6	16.9	22.0	30.3	83	44.4	15.8	117.5	0.24	4.3
/3	2B2	3.8	7.1	9.0	6.4	18.0	20.5	35.3	84	51.3	15.5	128.7	0.28	4.5
/4	2B3	2.6	4.4	11.1	10.1	18.0	17.4	36.5	85	60.7	15.6	145.4	0.31	4.6
/5	2C	2.3	5.8	18.1	16.0	24.7	14.6	18.7	84	39.4	3.4	138.4	0.26	4.2
PK 138														
/1	Ah	4.7	4.4	15.0	11.4	21.6	19.7	23.2	84	21.2	7.3	87.8	0.16	4.0
/2	B1	0.9	4.2	10.2	9.3	23.8	25.0	26.5	89	30.0	13.9	63.7	0.25	4.3
/3	B2	1.5	2.7	12.9	9.2	23.9	25.6	24.2	87	22.1	7.6	49.1	0.30	4.5
/4	2A	2.6	4.1	10.3	10.6	26.0	23.7	22.8	86	17.1	6.7	41.6	0.25	4.5
/5	2B	6.9	4.6	11.9	9.8	23.3	16.9	26.6	83	17.0	2.1	33.9	0.44	4.6
/6	2C	5.5	4.0	5.4	13.1	30.0	18.6	23.2	83	23.1	2.2	42.4	0.49	4.6
PK 139														
/1	A	0.7	6.2	12.4	10.0	15.8	18.8	36.2	87	28.3	10.8	56.4	0.31	4.6
/2	B1	0.4	7.1	15.7	9.0	19.4	23.5	25.0	88	26.0	12.0	60.5	0.23	4.6
/3	B2	0.6	4.6	15.6	8.3	17.4	20.5	33.0	85	24.5	11.0	48.9	0.27	4.6
/4	2B3	3.3	12.3	23.5	14.3	17.9	10.6	18.2	84	12.5	3.7	34.7	0.25	4.3
/5	2CB	2.5	30.3	20.9	7.6	9.3	6.7	22.8	92	15.4	2.8	33.2	0.38	4.3
/6	3C	18.7	21.1	15.8	4.3	5.9	5.7	28.6	55	26.7	4.0	43.4	0.52	4.4
PK 156														
/1	A1	3.0	9.5	6.0	3.5	12.2	17.2	48.6	81	22.5	15.7	42.2	0.16	3.8
/2	2B1	4.1	20.9	21.1	6.5	15.9	15.3	16.2	88	34.4	13.4	64.7	0.33	4.5
/3	2B2	4.1	21.8	17.6	5.7	16.5	17.5	16.9	87	29.5	9.4	54.9	0.37	4.7
/4	2BC	12.8	25.9	22.0	3.6	8.5	9.1	18.0	78	6.3	3.3	14.1	0.21	4.4
/5	2C	22.3	36.8	16.7	4.6	7.4	5.9	6.4	75	0.9	0.3	7.0	0.08	4.5

The samples do not plot along an "ideal" alteration trend, as indicated by the arrows in *Fig. 14*. This is not surprising, as we do not have any data from the unweathered parent materials, and all examined saprolites (C horizons) are strongly weathered. Analogous to the findings from weathering as reflected by particle size, the profile on gneiss (PT 053) is the least weathered within the examined set. It has an average CIA of 75, whereas those in the other metamorphic profiles (PT 056, PK 138, and PK 139) are in the range of 81 to 88. The lowest and highest CIA values occur in adjacent subsoil horizons in profile PK 139: 55 in PK 139/6 (3C), and 92 in PK 139/5 (2CB).

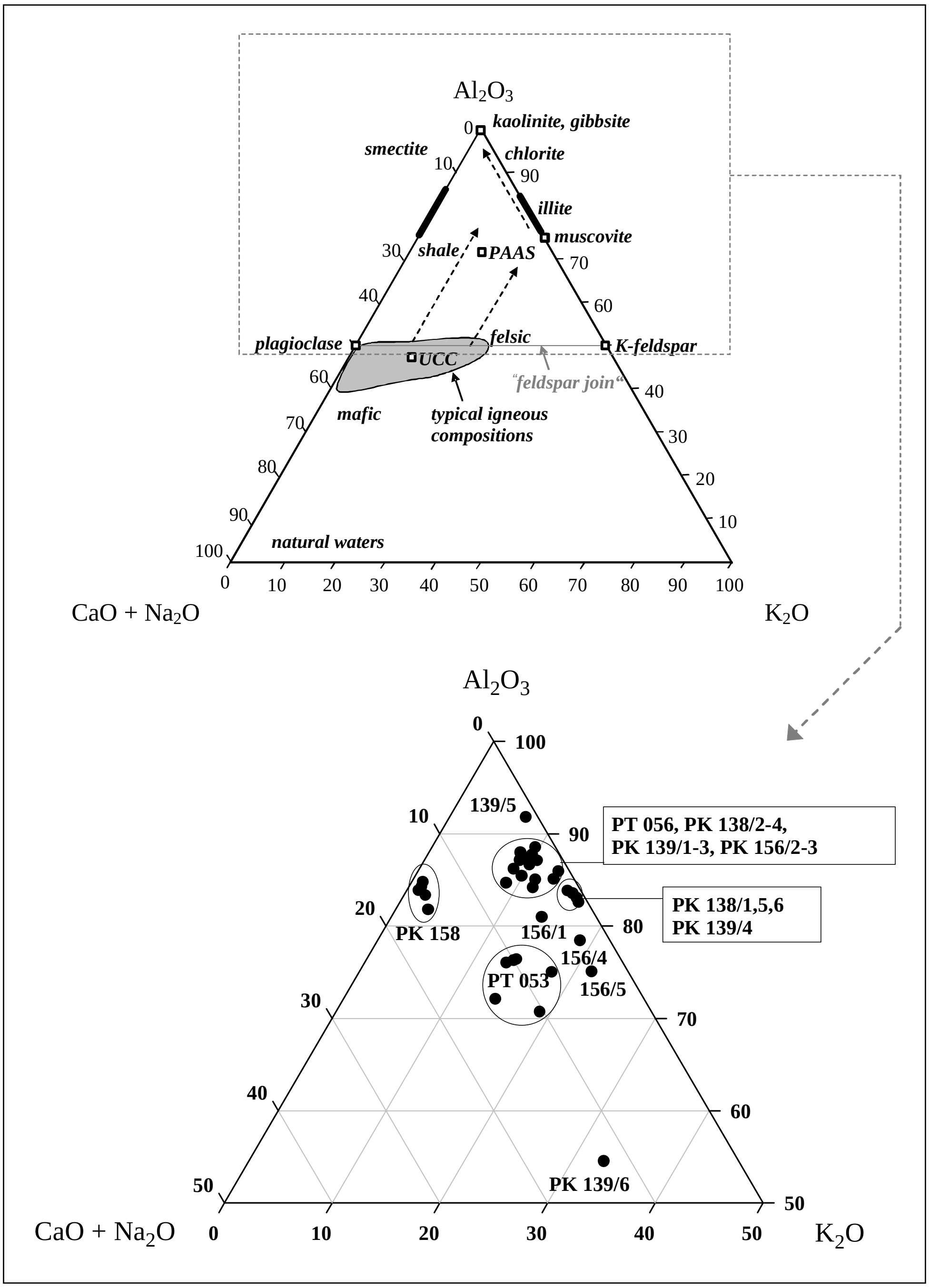

Fig. 14: A-CN-K ternary plot of selected Bhutanese soil and saprolite samples (below); the location of common minerals and possible weathering trends are indicated in the upper plot; UCC = Upper Continental Crust; PAAS = Post-Archaean Australian Shale (both after Taylor & McLennan 1985); dotted lines indicate alteration trends; diagram after Nesbitt & Young (1984).

This highlights the heterogeneity in and polygenetic structure of PK 139. The characteristics of this profile are best examined in terms of its physiographic setting. It is located on a small E-W ridge in the central Bhutanese Phobjikha Valley, close to the head of one of the side valleys, and has not been subject to intense pedoturbation during Pleistocene (*Fig. 15*). As a consequence, palaeosol material (PK 139/5) as well as parts of the unmetamorphosed Tethyan sediments (PK 139/6) are preserved. The low CIA of 55 of the latter sample is due to the extraordinarily high SiO_2 content (86.5%) and isolates this horizon from all others in the A-CN-K diagram (*Fig. 14*).

Fig. 15: Location of profile PK 139 within the landscape of Phobjikha Valley.

Both of the magmatic materials range similarly high in the CIA index. The saprolite of the granitic profile PK 156 is exceptional in so far that it contains less aluminous clay minerals and therefore plots lower in the A-CN-K diagram. The upper horizons, especially 2B1 and 2B2, show a huge increase in CIA, associated with a sudden change to finer particle sizes. This may be due to marked differences in in-situ weathering, or to an addition of pre-weathered, silt-sized materials. The uppermost horizon, PK 156/1, is incongruent with the rest of the profile, as it has three times as much clay, suggesting increased weathering, but this is contradict by the drop in CIA from 88 to 81. This profile is obviously covered by a more felsic, less weathered stratum. PK 158 from migmatitic materials in South Bhutan forms a separate cluster in *Fig. 14*, due to its substantially different geochemistry. In terms of chemical weathering, however, it shows a similarly advanced degree with a profile weighted average of 84 CIA units.

The degree of weathering is also reflected by the Fe_{d-o}/Fe_t index, which ranges from 0.00 to 0.57, i.e. 57% of well-crystallised iron oxides in relation to total iron contents (*Table 7*). A negative value of -0.17 is encountered in the PT 053/2 horizon, reflecting the accumulation of poorly crystallised Fe oxides during the podzolisation process. The weighted profile averages decrease in the order PT 056 (0.42) > PK 138 (0.38) > PK 139 (0.35) > PK 158 (0.28) > PK 156 (0.24) > PT 053 (0.01), which indicates that there is no direct correlation between weathering intensity and elevation a.s.l.. However, soil formation on the steep subtropical Bhutanese foothills (PK 158) is subject to monsoon- and earthquake-induced landslides, which decrease the periods for in-situ soil formation. Furthermore, the low Fe_{d-o}/Fe_t values for PK 158 may also be explained by high contents of silicate-bound Fe_t in the amphibolites (*Table 7*). A positive correlation between the Fe and CIA indeces has been found ($r^2 = 0.58^{***}$, n = 33, excluding the marine sediment of PK 139/6). And this despite the Fe_o dynamics in the podzolised horizon (PT 053/2), and the immobilisation of well-crystallised Fe_d within aggregates during the formation of non-volcanic Andosols like PT 056 (Bäumler et al. 2005).

A general pattern for all profiles is that the maxima of physical weathering (as reflected by the particle size distribution) are located towards the top of the profiles, whereas those for chemical weathering (as reflected by CIA and the Fe index) are located in subsoil horizons (*Table 7*). This reflects the dominace of acid organic leachates and freeze-thaw processes – major factors in physical weathering – in near-surface horizons, whereas clay minerals and well-crystallised Fe compounds, which are used in the chemical weathering indices, accumulate in lower horizons by pedogenic illuviation.

4.4 Rare earth elements

The range of REE contents in the soil and regolith samples is listed in *Table 8*. There are few other data from the southern slopes of the Eastern Himalayas for comparison. Gansser (1983) provides measurements for leucogranites sampled in different parts of Bhutan, all of which compare well with the patterns from PK 156 (*Table 9*). *Table 9* also shows that our findings for PK 138 (Deshichiling Formation) fit well into the range of the underlying Late Precambrian, metamorphosed volcanic rocks of the Singhi area, western Central Bhutan, as given by Tangri & Pande (1995). Bergamaschi et al. (2002)

measured La, Ce and Sm data in soils of different altitudes (1,350-5,200 m) in Nepal in order to determine their enrichment in lichens. They found ranges of 12.5-25.1 mg kg^{-1}, 24.7-78.9 mg kg^{-1} and 2.8-4.5 mg kg^{-1}, respectively (M. Gallorini, private communication). In Bhutan we have detected such low values only in the granitic saprolite of PK 156.

Table 8: Total rare earth element contents of selected soil samples; [a] Anders & Grevesse (1989); [b] Taylor & McLennan (1985); n.d.: Tb peaks could not be fitted because of interference with Sc; La_N/Yb_N ratios (column 12) have been calculated from chondrite-normalised values (subscript "N" denotes normalised).

Sample/ horizon		La	Ce	Nd	Sm	Eu	Tb	Dy	Yb	Lu	La_N/Yb_N	Σ LREE	Σ HREE	Σ REE
		mg kg^{-1}												
PT 053														
/1	A	47.1	92.2	41.1	7.09	0.88	0.93	4.43	2.97	0.48	10.7	187.5	9.7	197.2
/2	Bhs	41.0	78.4	26.9	6.56	0.97	0.93	4.79	3.22	0.50	8.6	152.8	10.4	163.2
/3	Bs	48.0	90.9	30.9	8.08	1.16	1.07	5.67	3.35	0.53	9.7	178.0	11.8	189.8
/4	CB	46.1	84.3	30.6	7.39	1.04	0.98	4.86	3.43	0.53	9.1	168.4	10.8	179.2
/5	C1	39.9	74.6	29.3	6.93	0.95	0.98	5.04	3.33	0.51	8.1	150.7	10.8	161.5
/6	C2	42.5	79.3	25.3	5.90	0.92	0.91	4.54	3.32	0.45	8.6	153.1	10.1	163.2
PT 056														
/1	A	56.6	113.4	43.7	9.22	1.26	1.20	6.23	4.41	0.60	8.7	223.0	13.7	236.7
/2	AB	60.0	110.2	40.1	9.49	1.19	1.08	6.74	4.10	0.59	9.9	219.8	13.7	233.5
/3	B1	55.1	113.3	40.7	9.57	1.50	1.09	6.15	3.78	0.55	9.8	218.6	13.1	231.7
/4	B2	53.7	111.1	37.0	10.11	1.63	1.12	7.51	4.58	0.58	7.9	211.9	15.4	227.3
/5	B3	59.4	111.8	42.1	10.40	1.60	1.21	8.27	4.48	0.55	8.9	223.6	16.1	239.7
/6	CB	50.0	101.6	40.3	8.88	1.30	1.53	5.29	3.35	0.47	10.1	200.8	11.9	212.8
PK 158														
/1	A1	56.0	106.8	30.6	12.29	3.20	n.d.	7.81	4.42	0.55	8.6	205.8	16.0	225.0
/2	B1	48.6	99.8	36.5	11.45	2.96	n.d.	8.20	3.98	0.65	8.2	196.4	15.8	215.6
/3	2B2	40.8	85.7	41.2	10.59	2.56	n.d.	6.43	3.84	0.50	7.2	178.3	13.3	191.9
/4	2B3	47.2	97.4	30.1	11.18	2.87	n.d.	7.71	4.87	0.61	6.5	185.9	16.1	202.2
/5	2C	43.6	53.7	19.7	10.08	2.69	n.d.	9.14	4.89	0.57	6.0	127.1	17.3	144.7
PK 138														
/1	Ah	59.7	133.3	32.1	7.63	1.21	1.13	4.15	2.93	0.43	13.7	232.7	9.9	242.6
/2	B1	41.6	87.8	30.8	6.21	1.07	0.88	5.13	3.30	0.50	8.5	166.4	10.9	177.3
/3	B2	45.1	100.2	31.8	7.22	1.22	0.88	5.48	3.35	0.51	9.1	184.4	11.4	195.8
/4	2A	49.6	111.3	36.4	7.60	1.36	1.11	6.50	3.66	0.54	9.1	204.9	13.2	218.1
/5	2B	58.5	117.0	45.1	8.15	1.38	1.31	7.41	3.92	0.57	10.1	228.7	14.6	243.3
/6	2C	65.5	132.2	35.0	7.38	1.25	0.94	4.62	4.24	0.61	10.4	240.1	11.7	251.8
PK 139														
/1	A	47.9	106.1	36.5	7.66	1.23	1.11	5.58	3.17	0.53	10.2	198.2	11.6	209.8
/2	B1	47.1	108.0	39.8	8.90	1.53	1.33	6.74	3.49	0.52	9.1	203.7	13.6	217.3
/3	B2	48.4	116.7	47.8	9.29	1.57	1.61	6.21	3.82	0.57	8.5	222.2	13.8	236.0
/4	2B3	30.5	83.4	25.8	5.79	1.02	0.91	3.91	2.79	0.44	7.4	145.5	9.1	154.6
/5	2CB	33.6	122.1	21.5	5.15	0.90	0.69	1.95	1.84	0.27	12.3	182.3	5.7	187.9
/6	3C	45.7	736.5	21.0	7.08	1.20	n.d.	3.36	1.74	0.39	17.7	810.2	7.0	817.2
PK 156														
/1	A1	41.0	82.1	40.4	6.37	0.88	0.81	4.21	3.35	0.54	8.2	169.7	9.8	179.5
/2	2B1	44.0	89.6	40.7	7.67	1.31	0.97	5.73	3.25	0.49	9.1	182.0	11.7	193.8
/3	2B2	40.7	92.1	40.7	8.45	1.51	1.13	6.02	2.67	0.46	10.3	181.9	11.8	193.7
/4	2BC	14.2	36.7	12.6	3.47	0.40	0.50	2.61	1.16	0.21	8.3	67.0	4.9	71.8
/5	2C	9.1	22.8	9.3	2.62	0.27	0.39	1.77	0.78	0.10	7.8	43.8	3.3	47.2
Chondrite[a]		0.24	0.60	0.45	0.15	0.06	0.04	0.24	0.16	0.02	-			
UCC[b]		30.0	60.0	27.0	5.30	1.30	0.65	3.80	2.00	0.35	10.1			

In order to facilitate the comparison of the REE data sets, the absolute rare earth contents have been normalised relative to the chondritic abundances of Anders & Grevesse (1989). The normalised patterns were then plotted on a logarithmic scale versus a linear scale of atomic number (*Fig. 16a-f*). Absolute abundances range from an average 190-fold chondritic for La, 180 for Ce, 70 for Nd, 52 for Sm, 24 for Eu, 29 for Tb, 22 for Dy, 21 for Yb and 20 for Lu. The resulting patterns have features typical for sedimentary post-Archaean materials, such as: (i) steep LREE (La-Sm) distributions, which are generally attributed to a partial melting of mantle or crustal rocks leading to an overall enrichment of large ion lithophile (LIL) elements compared to the fundamental mantle sources (McLennan 1989), (ii) mostly flat HREE (Eu-Lu) distributions, suggesting that there has been no dominant control on crustal compositions from a HREE-fractionating phase like garnet, and (iii) a distinct negative Eu anomaly, which is caused by the substitution of Ca^{2+} by Eu^{2+} in plagioclase feldspars (McLennan 1989).

Table 9: Comparison of the REE data with those of other studies; leucogranite data include rock samples from Gansser (1983) (GH 197, GH 471), and our leucogranitic saprolite (PK 156/4-5); metamorphic data are of the metamorphosed Singhi Volcanic rocks (Tangri & Pande 1995) (V2, V12, V24) and our saprolites from Phobjikha Valley, Central Bhutan (PK 138, PK 139); n.d. *= not determined.*

sample	La	Ce	Nd	Sm	Eu	Tb	Dy	Yb	Lu
	mg kg^{-1}								
Leucogranitic materials									
GH 197	10.4	22.3	10.3	2.83	0.34	0.53	n.d.	0.68	0.09
GH 471	16.9	35.0	16.6	3.91	0.41	0.59	n.d.	1.59	0.24
PK 156/4 (2BC)	14.2	36.7	12.6	3.47	0.40	0.50	2.61	1.16	0.21
PK 156/5 (2C)	9.1	22.8	9.3	2.62	0.27	0.39	1.77	0.78	0.10
Metamorphic materials									
V2	97.0	186.0	79.0	16.00	2.70	1.50	n.d.	5.20	0.77
V12	44.0	98.0	49.0	6.50	1.10	0.55	n.d.	1.50	0.18
V24	59.0	118.0	57.0	8.80	1.40	0.49	n.d.	1.40	0.17
PK 138/6 (2C)	65.5	132.2	35.0	7.38	1.25	0.94	4.62	4.24	0.61
PK 139/6 (3C)	45.7	736.5	21.0	7.08	1.20	n.d.	3.36	1.74	0.39

The C horizons show some deviations from this general pattern (*Fig. 17b*). This behaviour has been explained by the occurrence of less weathered heavy mineral suites in the sand fraction, which display particular REE patterns such as HREE enrichment (McLennan 1989). The influence of the various controls on the observed REE patterns are discussed in the following sections.

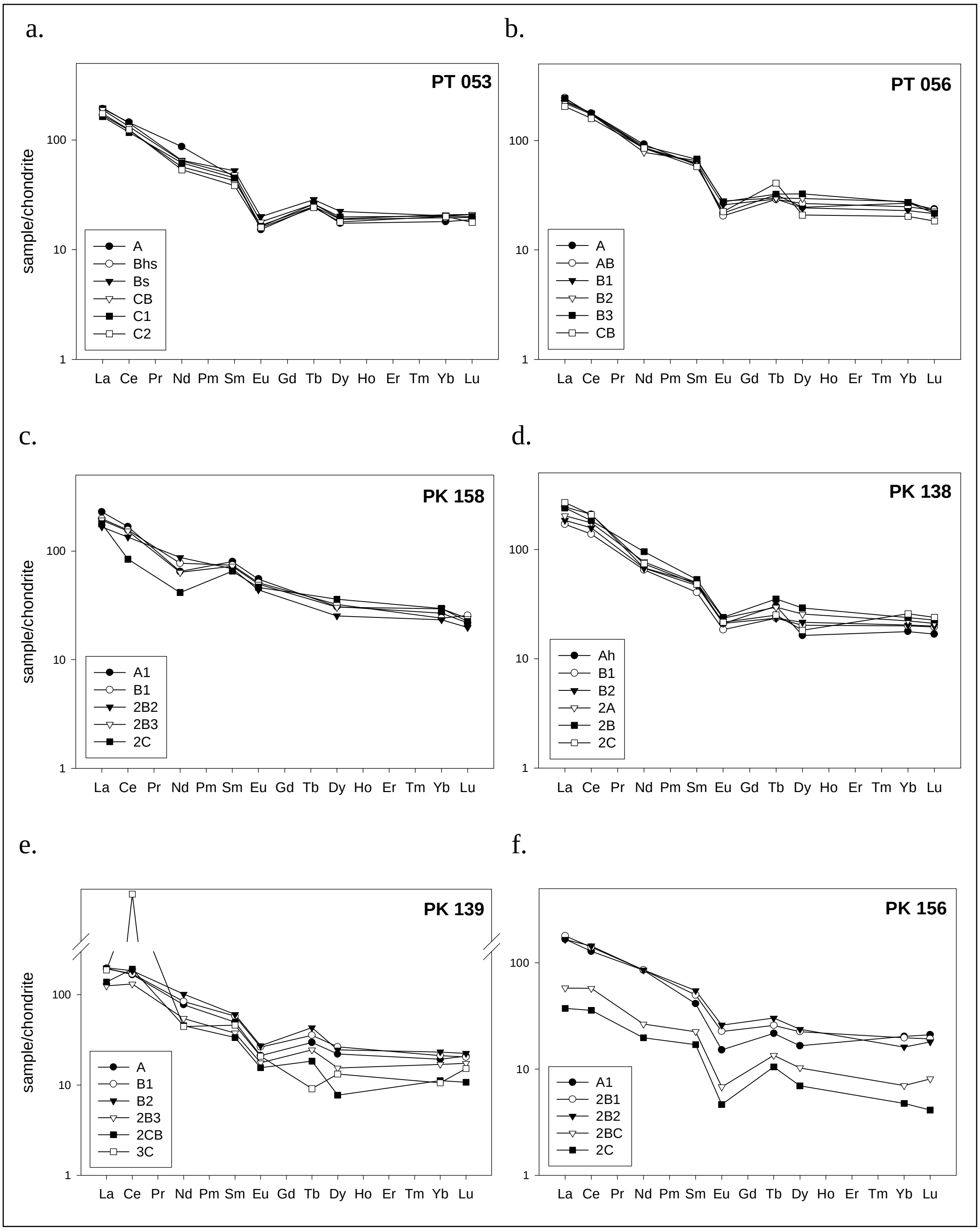

Fig. 16: Chondrite-normalised REE patterns for bulk soil of the examined horizons: a. Granitic gneiss, Takhtsang Formation, Thimphu Group; b. Mica schists, Naspe Formation (Paro Metasediments), Thimphu Group; c. Migmatitic intrusives, Shumar Formation; d. Quartzitic phyllites, Deshichiling Formation, Pele La Group; e. Fossil-bearing Maneting Formation (3C); f. Intrusive leucogranites. The undetected elements are shown as linear interpolations in the relative abundance curves.

4.5 Passive enrichment of REE during weathering

In the course of weathering, a shift to smaller particle sizes results in the passive enrichment of the lanthanides as refractory elements. Apart from the low concentrations of the leucogranitic saprolite (PK 156/4-5), the lanthanide concentrations are mostly higher when compared to UCC, in subsoils as well as in topsoils (*Fig. 17*, *Fig. 18*). It is interesting to note that among the rare earths, europium (Eu) shows the least enrichment and is even slightly negative for PT 053, PK 138 and PK 139 (*Fig. 18*).

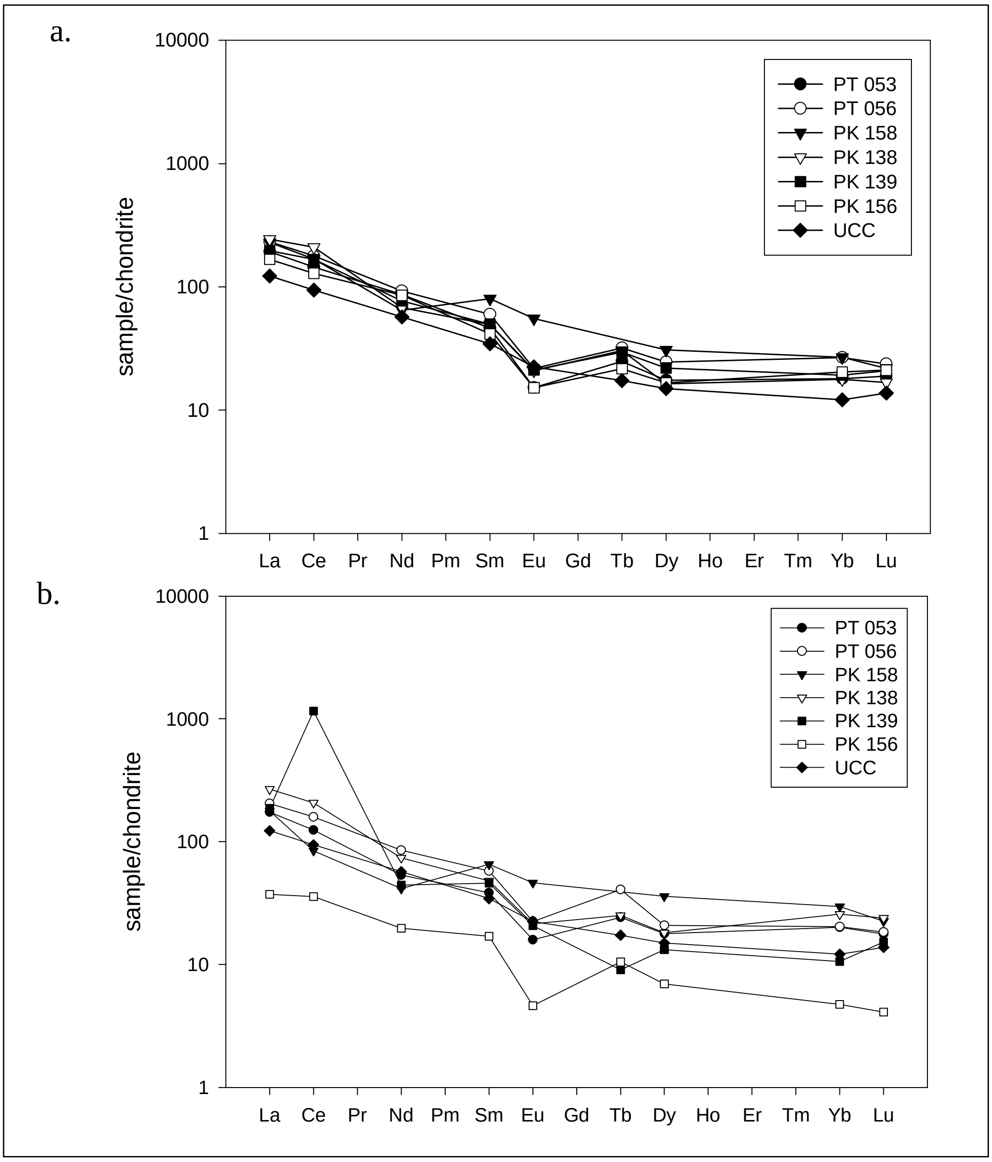

Fig. 17: Comparison of the chondrite-normalised REE patterns of (a) the uppermost, and (b) the lowest soil horizons of the examined profiles in comparison to Upper Continental Crust (UCC). See caption of Fig. 16 for short profile explanations.

Table 10 shows significant correlations between grain size fractions and REE contents: Positive correlations between clay content and REE are all significant at the $p = 0.05$ level except for Eu and Tb. The silt fraction shows significantly positive correlations with all lanthanides except Tb. The correlation between ∑REE and the cumulative grain size fraction < 63 µm (C+Si) has been found to be the most significant with $r = 0.62$***. Even though r^2 values do not exceed 0.40, the data show the substantial influence which the grain size exerts on REE abundances, in spite of the considerable differences in mineralogy, pedogenic processes, climatic conditions and possible anthropogenic influence. This confirms the results of many authors who found that REE reside in the silt and clay fraction (e.g. Cullers et al. 1979).

If we assume that weathering has gone on longer at the top of a soil profile, we would expect particle size – as a proxy for physical weathering – to *in*crease and REE concentrations to *de*crease with depth. The resulting chondrite-normalised REE patterns would show sub-parallel curves with the A horizons on top, and the C horizon at the bottom of the graph. In PT 053, PT 056 and PK 156, which are all thought to have formed in-situ, the grain size clearly decreases with depth (*Table 7*). The REE behaviour, however, does not match the expectations: Whereas we indeed find systematic depth sub-parallel REE patterns in case of the leucogranitic profile (PK 156, *Fig. 16f*), the profile in the metamorphosed Naspe Formation (PT 056, *Fig. 16b*) shows sub-parallel patterns only for the HREE from Eu to Lu. And the intensively weathered, podzolised gneiss profile of PT 053 shows no significant variation in the rare earths throughout the profile (*Fig. 16a*). Does this indicate that weathering is not the dominant control behind the observed REE distribution patterns?

The picture becomes clearer when we look at the results for chemical weathering processes as assessed by the Chemical Index of Alteration (CIA) and the Fe index. Here, the granitic profile is the least weathered, with profile-weighted values of 72.1 and 0.01 respectively; PK 156 has 82.0 and 0.24, and those of PT 056 amount to 85.2 and 0.42. Tectonic, geological and climatic controls may be responsible for these differences between the profiles, apart from different time spans for soil formation. There is evidence that tectonic uplifts in the region have not been substantial during the Quaternary (Fort 1996). Geological controls are discussed in the following section. It is the difference in elevation a.s.l. of these three profiles which observes a closer look.

Table 10: Correlation matrix for major and rare earth elements, particle size classes, C_{org} and Fe fractions. n = 33 (marine sediments of PK 139/6 excluded).

*Pairwise missing data selection (Tb values of PK 158). Correlations significant at the p = 0.05 level are displayed in **bold**. Significant values of r are 0.35 (p = 0.05) and 0.55 (p = 0.001).*

	La	Ce	Nd	Sm	Eu	Tb	Dy	Yb	Lu	Al	Fe	Ca	K	Na	sand	silt	clay	C_{org}	Fe_d	Fe_o
La	1.00																			
Ce	**0.84**	1.00																		
Nd	**0.72**	**0.69**	1.00																	
Sm	**0.70**	**0.50**	**0.59**	1.00																
Eu	**0.40**	0.24	0.25	**0.87**	1.00															
Tb	**0.70**	**0.66**	**0.82**	**0.84**	**0.84**	1.00														
Dy	**0.62**	0.32	**0.51**	**0.90**	**0.80**	**0.75**	1.00													
Yb	**0.79**	**0.50**	**0.56**	**0.85**	**0.70**	**0.69**	**0.87**	1.00												
Lu	**0.82**	**0.58**	**0.69**	**0.79**	**0.59**	**0.70**	**0.80**	**0.92**	1.00											
Al	0.19	0.06	0.17	**0.35**	**0.43**	0.25	**0.50**	0.33	0.27	1.00										
Fe	0.28	0.14	0.10	**0.73**	**0.91**	**0.46**	**0.65**	**0.59**	**0.47**	**0.42**	1.00									
Ca	0.07	-0.16	-0.06	**0.54**	**0.72**	-0.05	**0.44**	**0.42**	0.34	0.08	**0.68**	1.00								
K	-0.25	-0.24	-0.24	**-0.68**	**-0.75**	-0.29	**-0.53**	**-0.50**	**-0.44**	0.01	**-0.77**	**-0.56**	1.00							
Na	-0.05	**-0.39**	-0.16	**0.44**	**0.60**	-0.13	**0.44**	**0.37**	0.25	0.06	**0.57**	**0.90**	**-0.46**	1.00						
sand	**-0.55**	**-0.56**	**-0.54**	**-0.54**	**-0.46**	**-0.37**	**-0.53**	**-0.56**	**-0.55**	-0.34	**-0.48**	0.03	**0.49**	0.15	1.00					
silt	**0.45**	**0.48**	**0.37**	**0.40**	**0.43**	0.31	**0.48**	**0.45**	**0.45**	**0.56**	**0.46**	-0.11	-0.31	-0.20	**-0.89**	1.00				
clay	**0.48**	**0.47**	**0.57**	**0.52**	0.34	0.34	**0.40**	**0.49**	**0.49**	-0.07	0.33	0.07	**-0.55**	-0.04	**-0.79**	**0.42**	1.00			
C_{org}	0.21	0.18	**0.43**	0.04	-0.10	0.05	0.04	0.10	0.25	-0.18	-0.06	-0.08	-0.18	-0.08	**-0.38**	0.20	**0.48**	1.00		
Fe_d	**0.40**	0.33	**0.36**	**0.78**	**0.82**	**0.41**	**0.69**	**0.63**	**0.53**	**0.46**	**0.85**	**0.42**	**-0.79**	0.31	**-0.71**	**0.58**	**0.63**	0.08	1.00	
Fe_o	0.26	0.22	**0.43**	**0.52**	**0.46**	0.30	**0.43**	**0.39**	**0.43**	0.14	**0.51**	0.30	**-0.60**	0.19	**-0.51**	0.26	**0.66**	**0.48**	**0.67**	1.00

The elevation is linked to the different climatic site conditions: PT 053 lies at 3,768 m a.s.l. and therefore substantially higher than PT 056 (3,025 m) and PK 156 (2,866 m). Increasing elevation in Bhutan is equivalent to a decrease in precipitation as well as in temperature, resulting in a lesser degree of chemical weathering. Precipitation is likely to be crucial in this context, because leaching is the driving force for translocation of released REEs within the soil profile. Both, increased temperature and moisture increase the activity of microbes which contribute to the release of lanthanides via destruction of REE phosphates (Taunton et al. 2000). Pandey & Palni (1998) found that microbial populations in Himalayan soils decreased with increasing altitude, among them strains with phosphate solubilising properties.

Looking at the conditions *within* profiles, the maxima of chemical weathering do not lie in the top or bottom horizons, but towards the middle of the profiles (*Table 7*). At the same time, these intermediate horizons plot as the upper ones in the chondrite-normalised REE patterns (*Fig. 16a-f*). This trend is observed for PT 053 (/2 = Bs), PT 056 (/5 = B3), PK 138 (/5 = 2B), PK 139 (/3 = B2) and PK 156 (/3 = 2B2). The only exception is PK 158, where all horizons show high chondrite-normalised values, especially the MREE and HREE. The highest measured Sm, Eu, Dy, Yb and Lu values for all examined horizons are all located within this profile (*Table 8*). Nevertheless, correlations between total REE contents and the degree of chemical weathering (CIA, Fe index) are not significant, as was expected at least for the intra-profile comparisons of in-situ soils. The only profile to show a significantly positive correlation between ∑REE and CIA, is the leucogranitic PK 156 (r^2 = 0.82). Besides physical and chemical weathering, there are other major controls for rare earth behaviour in Bhutan.

4.6 Active enrichment of REE by pedogenic processes

Besides passive enrichment, the active accumulation of elements may also occur during podzolisation and lessivation, especially during summer monsoonal rains. In case of PT 053, these processes are weak: Not even the slight podzolisation process, which is typical for Bhutanese soils at 3,500 - 4,000 m a.s.l. (Baillie et al. 2004), and associated low pH values (*Table 7*) are expressed in the chondrite-normalised REE pattern (*Fig. 16a*).

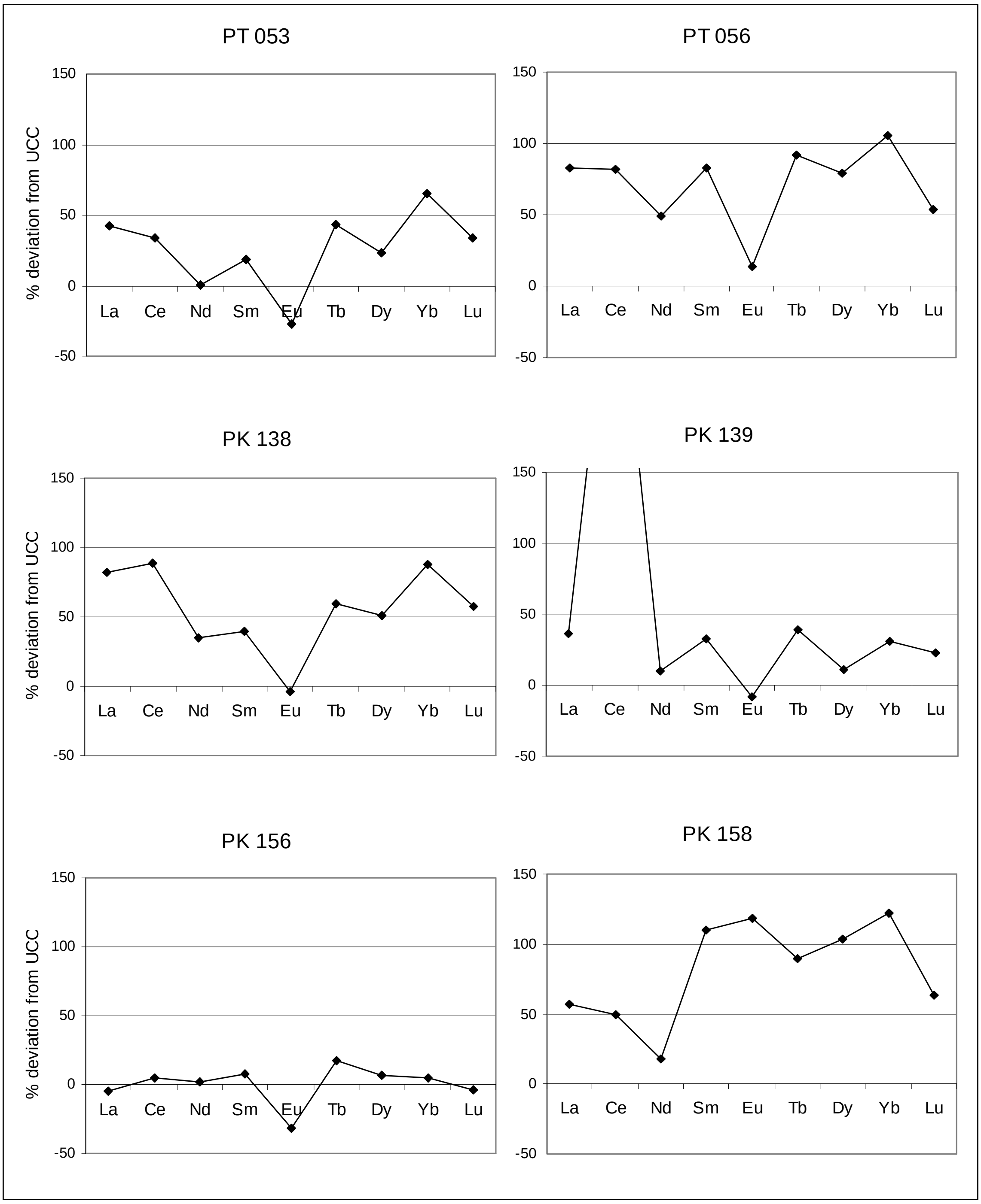

Fig. 18: Deviation of REE contents from upper continental crust (UCC, Taylor & McLennan 1985)

It is notable, however, that La, Sm, Eu, Tb, Dy and Lu have their maxima in the Bs horizon (*Table 8*), suggesting that they have probably been leached from the more acid horizons (especially Ah) above, and accumulated in the Bs horizon, which is 1.2 pH units less acid. Both, REE and Fe are regarded as refractory during weathering, which is supported by the significant positive correlation of DCB-extractable iron oxides (Fe_d) with all rare earths except Ce, and of labile iron compounds (Fe_o) with all REE except La, Ce and Tb (*Table 10*).

In contrast to podzolisation, clay illuviation occurs in Bhutan only to a minor degree (Baillie et al. 2004). In the present synopsis, the only horizons to show initial lessivation in the form of weakly pronounced clay cutans, are PK 139/2-3 and PK 158/4. In PK 139, those horizons plot highest in the respective REE diagram (*Fig. 16e*). However this is not necessarily due to the influence of clay-attached REE. The translocation of REE^{3+} in carbonate complexes or attached to Fe compounds (as indicated in case of the weak podzolisation in PT 053) are generally possible, but do not appear to be significant influences on the observed patterns.

It has been concluded by several authors that the REE become fractionated during weathering, i.e. some of them are preferentially translocated (e.g. the HREE) and some rather enriched (e.g. Ce) within the soil profile (Ronov et al. 1967, Cantrell & Byrne 1987, McLennan 1989). There are indications that this is also the case in the Bhutanese context. To quantify the degree of HREE/LREE fractionation, normalised La/Yb ratios (La_N/Yb_N) have been calculated. They range from 6.0 to 17.7, and vary substantially within the single profiles (*Table 8*, page 47). In case of preferential HREE depletion, La_N/Yb_N values would *in*crease with *in*creasing weathering for “leached” horizons, and *de*crease in lower horizons where HREE may accumulate. No significant correlations were found between La_N/Yb_N ratios and the degree of chemical (CIA, Fe index) or physical weathering (particle size fractions), either within single profiles or for the whole data set (n = 34). However, there is a general trend that geologically young materials like the magmatic saprolites of PK 156 and PK 158 indeed have very low ratios (< 8), and older materials like the Tethyan sediments (PK 139/5-6) rather high ratios (> 12). From *Table 8* it is also evident that the intra-profile maxima of HREE are located beneath those of LREE (PT 053, PK 158, PK 138, PK 156) or are at least in the same horizon (PT 056, PK 139).

The significant correlations among the rare earths themselves (*Table 10*) are another argument that they are geochemically similar in these soils, and that their fractionation is *not* advanced. In the REE correlation matrix, Ce shows the weakest correlations with the rest. *Table 8* shows that in 4 out of 6 profiles, it has the highest absolute inner-profile concentrations in the A horizon. No other rare earth shows this behaviour, indicating that Ce is more recalcitrant than the other REEs. Other authors have explained the same finding with the fact that – as tetravalent cation in CeO_2 – Ce is less soluble than the other REEs (Mongelli 1993).

4.7 Control of parent material

The potentially fundamental difference between REE patterns of metamorphic and magmatic materials lies in their genesis. Most of the metamorphic materials in Bhutan are thought to have evolved from sediments, which probably represented a mixture of components from different provenances, and which were also pre-weathered to a certain degree. In this process, lithological and chemical diversities have been smoothed out, such that the resulting material does not allow insights into single provenance components any more (McLennan 1989). Whereas temperature and pressure conditions during metamorphosis are not sufficient to modify REE patterns, this does occur during diagenesis, in which the REE are fractionated by incorporation into heavy minerals. When comparing the different parent materials for soil formation in this study, we should also be aware that the leucogranites (PK 156) are the only post-collisional lithology. All other materials are originally at least 500 Ma old. In theory, lithogenic differences in REE will be most apparent in the lowest horizons of a soil profile. This is because they represent those materials which are the least mixed and weathered, and also because most heavy mineral suites reside in the sand fraction, causing preferentially HREE-enriched patterns. *Fig. 17* has already shown that the REE patterns of the Bhutanese soils tend to a more varied, “edgy” appearance in the subsoils.

More detailed examination of the rare earth concentrations and patterns of the regoliths shows that the quartzitic phyllite of PK 138, the mica schist of PT 056 and the gneiss of PT 053 are very similar (*Fig. 18*). Compared to the UCC, they are slightly enriched for all rare earths except Eu, indicating stronger than average negative Eu anomalies for the Bhutanese metamorphic lithologies. In contrast to the other parent materials, they show a slight but continuous increase in HREE. The polygenesis of PK 139 – apparent in its contents and distribution of *major* elements – is also reflected in its inconsistent REE patterns. Whereas the loessic substrates of the uppermost layer (PK 139/1-3) appear largely homogeneous, the lower layer (PK 139/4-5) is heavily REE-depleted, most probably as a consequence of high SiO_2 values (*Table 8, Fig. 16*). PK 139/6 is different from all other examined horizons because of its striking positive Ce anomaly with a normalised concentration above 1000 units. Rankin & Childs (1987) reported similar patterns from yellow-grey earth soils with Fe-Mn concretions in New Zealand. The Ce accumulation is further evidence for the marine provenance of this sample and confirms its affiliation with the Tethyan Palaeozoic Sequence. Under the palaeoredox conditions of a marine environment, the then tetravalent Ce ions precipitate together with Mn and other elements of the Fe group. Thus, it is preferentially removed from the sea water and fractionated from the other, trivalent rare earth elements. As a consequence, sea water shows negative Ce anomalies, whereas marine sediments are characterised by positive values (Piper 1974, Takahashi et al. 2000). Temporary anaerobic conditions cannot be considered as cause for the observed REE pattern, as the growth rate of ferromanganese nodules is in the order of a few millimetres per million years (Dubinin & Sval'nov 2003). Zircon also features positive Ce anomalies, however its presence would be visible by clear HREE enrichment (Ayres & Harris 1997).

Both of the magmatic saprolites (PK 156, PK 158) are markedly different from the UCC pattern. The migmatitic material of PK 158/4-5 lacks a distinct Eu anomaly and shows the strongest relative LREE depletion (*Fig. 16c*). Both phenomena can be attributed to the influence of hornblende. This mineral is characterised by more or less flat chondrite-normalised REE patterns without Eu anomaly and enrichments as low as 20-fold (El-Sayed 2003) or even 10-fold (Kato et al. 1996). Sharma & Rajamani (2000) found that REE patterns in a weathering profile of komatiitic amphibolite in South India were sub-parallel, with the chondrite-normalised concentrations increasing with the degree of weathering.

The granitic saprolite of PK 156 displays a REE pattern sub-parallel to the metamorphic materials, but with clearly lower chondrite-normalised concentrations. A distinct Eu anomaly (PK 156/4-5) has been described by Guillot & Le Fort (1995) and Ayres & Harris (1997) to be characteristic for tourmaline leucogranites. The REE depletion may be partly related to grain size, however this cannot explain the lower than UCC concentrations. Several authors working on leucogranites have illustrated that rare earths are drastically fractionated in the presence of monazite, which contains REE as essential structural components (ESC) (Gromet & Silver 1983, Bea et al. 1994, Ayres & Harris 1997). From a mineralogical point of view, the presence of monazite is not unlikely, as it is frequently hosted in biotite (Vidal et al. 1982, Cuney et al. 1984), and biotite fractionation has been indicated from the major element geochemistry of this saprolite. The hypothesis that the leucogranite of PK 156 stems from a silicic, monazite-bearing, REE-undersaturated melt is further indicated by (i.) a strong decrease of Th within the profile (*Table 6*, page 41) as mentioned by Ayres & Harris (1997), and (ii.) a simultaneous lack of transition minerals (Sc, V, Ti, Cr, Fe) and surplus of incompatible elements (Rb, Cs, K) (*Table 6*). The values for PK 156/5 fit into the range of chondrite-normalised REE patterns for tourmaline leucogranites as modelled by Ayres & Harris (1997). The values also match those compiled by Gansser (1983) for the leucogranites of the close-by Pele La pass.

5 In-depth view of particular soil forming processes

Besides the geochemical study of soil profiles and their connexion with landscape and geology, a further task has been to examine the soil forming processes which currently transform these materials.

Section 5.1 will shed light on the pedogenesis in a central Bhutanese valley system, where the redistribution of silty sediments is a major control on soil properties. The frequent occurrence of Andosols within the non-volcanic Bhutanese environment will be elucidated and discussed in Section 5.2.

5.1 Redistribution of local sediments and its influence on soil formation in Phobjikha Valley, Central Bhutan

5.1.1 Natural setting of the study area

Phobjikha Valley is part of the Bhutanese N-S valleys and ranges (*Table 1*, page 3). It is located between 27°23’-27°30’ N and 90°10’-90°14’ E within Wangdue-Phodrang District, to the west of the Black Mountain Range which separates West from Central Bhutan (*Fig. 8*). Altitudes range from 2,800 m a.s.l. at the riverbed of the Nake Chhu river, to 4,000 m a.s.l. on the surrounding mountain tops (*Fig. 10*, page 25).

The climate can be described as cool temperate, having moderately warm summers and frosty winters. It is strongly influenced by the southwest Indian monsoon, with 75% of rainfall occurring between May and September (Baillie & Norbu 2004). Dorji (1995) gives 650-850 mm for annual precipitation and 13°C as mean annual temperature. Direct measurements from Phobjikha Valley over an unknown period of time suggest more humid and cooler conditions (1,516 mm; 10.3°C). Absolute minimum temperatures in the valley are around -12°C, and the area receives substantial snowfall in winter (RSPN 2003).

Fig. 19: View into Phobjikha Valley from NNW to SSE; the picture was taken from the area above profile PK 151 (see Fig. 10, page 25).

Fig. 20: Arrows indicate examples for the mass movement sediments in the main valley; their dissection by periglacial processes and fluvial erosion is visible; view from profile PK 150 to NNW.

Phobjikha Valley is subjected to strong along-valley winds in upward direction (S-N), which act as driving force for the entrainment and transport of aeolian material. Whiteman (2000) shows their role in the overall mountain wind system and elucidates how strong diurnal wind systems develop in dry, high elevation climates. The local morphology provides the ideal setting: Wide and deep valley structures enable a great volume of air, which can flow virtually undisturbed with no major terrain constrictions or even segmentations of the valley to the south of Gangtey Goempa (*Fig. 10*, *Fig. 19*). The wind system shows seasonal variations and is most intense during dry periods in spring and autumn. Clouds and rain during summer monsoon as well as snow cover in winter time modify the surface energy budget such that the diurnal winds are weakened or absent. Whiteman (2000) points out that if larger scale wind systems (like monsoonal winds) interfere with or overpower the along-valley wind system, turbulent conditions with sudden increases in wind speed at the ground may result. This effect is more intense, if the axis of the valley lies in the same direction of the larger scale winds aloft, which is the case in our study area. For the Himalayas, diurnal mountain-valley wind systems are described by Ohata et al. (1981), Egger et al. (2000) and Hindman & Upadhyay (2002).

The bedrock underlying Phobjikha Valley consists of phyllite, phyllitic quartzite, white quartzite, limonitic grey quartzite, sub-greywacke, and intrusive granite. A recent study by the Geological Survey of Bhutan (GSB) has assigned the area to the Gangphey formation (named after a local village), newly defined as part of the low grade metasediments of the Chekha Group within the Tethyan Sequence (RGoB 2001a). During their extensive mapping in the Black Mountain Range, Chaturvedi et al. (1983) proposed a more complex lithostratigraphy, and gave a detailed listing of fossils which indicate a Cambrian to Late Ordovician age of the metasediments. After lingulellid (Brachiopod) fossil finds, these ages have been corrected to Early Cambrian (Mamgain & Roy 1989, Tangri et al. 2003). The valley bottom is largely covered by dwarf bamboo (*Yushania microphylla*) wetland and the foothills and hill slopes are mostly covered by grazed grasslands. Arable agriculture with potato, wheat, millet and buckwheat as the main crops dominates the northern part of the main valley and the floors of the side valleys. Coniferous forests on the higher and steeper slopes mainly consist of blue pine (*Pinus wallichiana*) with hardwoods, such as birch (*Betula utilis*) and several species of rhododendron, wild rose and maple in the midstorey, and fern and herbaceous species such as *Primula sp.*, *Rubus sp.* and *Fragaria sp.* in the understorey.

5.1.2 Valley morphology and description of selected profiles

Six out of 21 profiles have been selected for a more detailed analysis: PK 135, PK 138, PK 143, PK 150, PK 151 and PK 155. They are thought to reflect the whole range of soil types within the study area. Appendix 3 (page 156ff.) contains colour photographs of the profiles.

Phobjikha is characterised by a wide and flat valley bottom, and the bed of the Nake Chhu river is gently graded (*Fig. 19*). This provides favourable conditions for the preservation of local sediments. There are a number of well defined rounded hillocks on the margins of the valley floor and gently graded lower slopes. Whereas the main valley is symmetrically basin-like, the lateral valleys display a clear asymmetry with higher gradients and often shallower pedons on their southern slopes. The strongly weathered and leached soil of profile PK 138 is an example for the soils developed on the N-facing slopes (*Table 11*). Slope movements are indicated by a distorted, “patchy” 2A horizon, above which the topsoil displays bright orange colours.

Table 11: Profile description for PK 138.

PK 138	**South of Pelam (lower side valley); 27°25’N, 90°14’E; 3,185 m; situated on a shoulder of a slightly terraced 19° lower slope; pasture; grassland; Dystric Andosol**	
0-5 cm	**A1**	**10YR 3/3 (dark brown); moderately moist; silt loam; subangular blocky, breaking to crumb; granite stones < 5%; common fine and medium pores; abundant medium and fine roots; clear, wavy boundary to:**
5-32 cm	**B1**	**7.5YR 6/8 (reddish yellow); moderately moist; silt loam; subangular blocky, breaking to crumb; weakly thixotropic; granite stones < 10%; common fine and medium pores; common medium and fine roots; clear, pocket-like boundary to:**
32-63 cm	**B2**	**10YR 5/4 (yellowish brown); moist; silt loam; subangular blocky; thixotropic; stones < 10%; many fine and medium pores; common fine roots; clear, wavy boundary to:**
63-70 cm	**2A2**	**discontinuous horizon; 10YR 3/3 (dark brown); moist; silt loam; subangular blocky, breaking to crumb; thixotropic; many stones < 5 cm; many fine and medium pores; moderate fine roots; diffuse boundary to:**
70-115 cm	**2B3**	**10YR 6/6 (brownish yellow); moist; sandy loam; subangular blocky; abundant stones < 5 cm; common fine pores; very few fine roots; clear, wavy boundary to:**
115-160+ cm	**2C**	**5Y 6/2 (light olive grey) with mottles of 5YR 5/6 (yellowish red); moist; clay loam; coherent; weathered parent material (phyllitic quartzite)**

Mass movement sediments are abundant within the study area (*Fig. 20*). They are most pronounced along the eastern slope of the main valley north of Gangyu, along the western slope below Takche Goempa and on the lower reaches of the S-facing slopes in the lateral valleys (*Fig. 10*, page 25). In a confluence area below Gangtey Goempa they are manifest as massive, well-rounded terrace structures. All of these materials appear to be of fluvial origin, and consist of well-rounded and sorted gravels of different sizes. These terraces have been eroded and dissected – probably most heavily under periglacial conditions – and are covered by up to 4 metres of silty loess-like material. Profile PK 135 is a typical example of these regoliths, which are characterised by a homogeneous, fine-grained matrix. Their recent A horizons are only weakly developed and shallow, and sometimes hardly distinguishable. Buried topsoils generally appear in the upper 1-2 m depth and are more pronounced and darker than the recent topsoils. The “fossil” topsoils and the adjacent stratigraphic layers are often characterised by thixotropy and the occurrence of charcoal. Below, we encounter massive, yellowish-brown subsoil horizons with < 5% skeletal material. These are denser than the topsoils and some have clay skins and dark organic coatings along cracks and root channels. Below this, a clear boundary occurs, and well stratified, grey fine sandy to gravelly materials extend to the base of profiles, as shown in PK 143 (*Table 12*).

Table 12: Profile description for PK 143.

PK 143		**600 m south of Gangtey Goempa; 27°28’N, 90°10’E; 2,885 m; situated towards the western edge of a flat 20 m terrace; pasture, grassland; Andic Ferralsol**
0-20 cm	**A1**	**7.5YR 4/6 (strong brown); dry; silt loam; crumb; no stones; many fine and medium pores; common medium and fine roots; diffuse boundary to:**
20-50 cm	**AB1**	**7.5YR 4/4 (brown); nearly dry; silt loam; subangular blocky, breaking to crumb; no stones; many fine and medium pores; common medium and fine roots; diffuse boundary to:**
50-100 cm	**AB2**	**7.5YR 4/3 (brown); nearly dry; silt loam; subangular blocky; weakly thixotropic; no stones; few fine black iron concretions; many fine and medium pores; few fine roots; charcoal; diffuse boundary to:**
100-123 cm	**2A2**	**7.5YR 3/3 (dark brown); slightly moist; silt loam; subangular to angular blocky; no stones; few fine black iron concretions; many fine and medium pores; few fine roots; charcoal; clear, regular boundary to:**
123-184 cm	**2B1**	**10YR 5/6 (yellowish brown); moderately moist; silty clay loam; subangular to angular blocky; weak clay skins; no stones; few fine black and dark red iron concretions; many fine and medium pores; very few fine roots; diffuse boundary to:**
184-214+ cm	**2B2**	**10YR 4/6 (dark yellowish brown); moist; silty clay loam; subangular blocky; weak clay skins; no stones; few fine black and dark red iron concretions; many fine and medium pores; no roots**
		no changes found in augering to 375 cm; “connecting” profile established approx. 2 m below at the outer edge of the terrace:
375-384 cm	**3BC**	**10YR 6/2 (light brownish grey); moist; loamy sand; subangular blocky to massive; few stones; few fine dark red iron concretions; many fine pores; no roots; clear, regular boundary to:**
384-430 cm	**3CB**	**10YR 5/6 (yellowish brown); moist; loamy sand; single grain, abundant rounded gravels up to 5 cm diameter; many macro-pores; no roots; clear, slightly wavy boundary to:**
430-465+ cm	**4C**	**5Y 5/2 (olive grey); moist; sand; coherent; no stones; common macro-pores; no roots**

The clearly defined 3CB horizon with its well-rounded gravels indicates fluvial deposition. The same origin is assumed for the fine sandy sediments of the 3BC horizon in this profile. Profile PK 150, approximately 5 km down-valley, to the north of Gangyu (*Fig. 10*), shows a comparable stratification and depth sequence. The 2A buried topsoil has been eroded, but is visible in a nearby roadcut. The absence of A or E horizons due to erosion prior to anew burial by loess, is a common feature in palaeosols (Bronger et al. 1998).

Deep silty sediments also mantle the southern slope of a SW-NE oriented ridge, starting NE of Gangtey Goempa. On this slope, profile PK 151 is located at the corner of a fresh landslide. It is in patchy coniferous forest used for grazing and the collection of pine needles. More than 4 metres of aeolian materials have accumulated in spite of a slope gradient of 18°. Below the upper third of the solum, clay translocation is evidenced by clay coatings on the outer ped surfaces. In a few sites within the Phobjikha main valley, slope debris lies on top of the loess. Besides recent rockfall, it may have been transported by periglacial slope processes or flash floods. In Tabeding Village (*Fig. 10*) we discovered conglomerates in the form of well-rounded pebbles, cemented in a finer-grained silicic matrix. A similar conglomerate constitutes the 2BC horizon of profile PK 155 (*Table 13*). This profile is located across the valley from Tabedin and in contrast to the other profiles, it is in a site with little human influence. Due to the steep terrain, this area appears never to have been deforested, and is today covered by dense blue pine (*Pinus wallichiana*) forest with thick undergrowth. The current topsoil accounts for more than 20% of the solum depth, and there is no buried fossil topsoil.

Table 13: Profile description for PK 155.

PK 155	**750 m south of Gophu; 27°27'N, 90°11'E; 3,010 m; culmination site on 38° NW-facing slope; *Pinus wallichiana*, *Juniperus sp.*, *Rhododendron sp.*, *Yushania sp.*; Humic Umbrisol**	
0-35 cm	**A**	**10YR 3/2 (very dark greyish brown); slightly moist; silt loam; crumb; no stones; abundant fine pores; abundant medium and fine roots; clear, slightly wavy boundary to:**
35-73 cm	**B1**	**10YR 6/6 (brownish yellow); moist; silt loam; crumb; thixotropic; no stones; abundant fine pores; many medium and fine roots; diffuse boundary to:**
73-103 cm	**B2**	**10YR 6/6 (brownish yellow); moist; silt loam; subangular to angular blocky; thixotropic; few fine black iron concretions; no stones; many fine and few medium pores; few fine roots; diffuse boundary to:**
103-125 cm	**2B3**	**10YR 6/8 (brownish yellow); moist; silt loam; subangular blocky; slightly thixotropic; few small stones; few fine black iron concretions; abundant medium and fine pores; few fine roots; clear, slightly wavy boundary to:**
125-160+ cm	**2BC**	**10YR 7/4 (very pale brown); moist; sandy loam; angular blocky to platy; weak clay skins; abundant fine black and dark red iron concretions; conglomerates with sandstone, quartz and granite as clasts; abundant medium and fine pores; few fine roots**

5.1.3 Analytical results

All analytical results for this section are listed in *Table 14* and *Table 15*.

5.1.3.1 Soil physical characteristics

Bulk density

In all topsoils, fine earth bulk densities are below 0.8 g cm^{-3}. Under old growth forest (PK 155), values are low throughout the profile, but they increase below the buried A horizons at all other sites. Maximum values are 1.3-1.4 g cm^{-3} in the matrices of the gravelly subsoils.

Surface area (BET)

Values of the < 2 mm fraction range from 7 to 53 m^2 g^{-1}. Typical topsoil values are around 30 m^2 g^{-1}, and increase with soil depth, especially where clay translocation has been observed. In the C horizons, however, BET readings do not exceed 25 m^2 g^{-1}.

Particle size distribution (PSD)

Except for profile PK 138, coarse material > 2 mm accounts for less than 5% in all profiles. Silt and clay dominate the < 2 mm fraction, and the sand fraction rarely exceeds 15 weight-% in the solum. In case of PK 138, silt is dominant with about 60 weight-% throughout the profile. Most frequent particle sizes are in the range of 2-20 µm (*Fig. 21*), which is lower compared to the 10-50 µm usually observed in aeolian environments (Livingstone & Warren 1996).

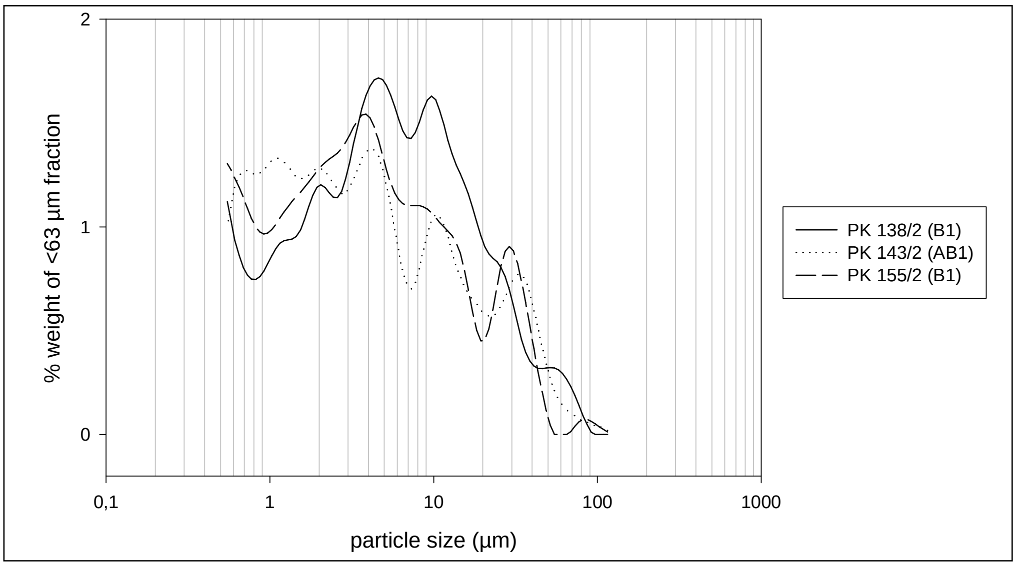

Fig. 21: Grain size distribution of selected B horizons (< 63 µm fraction).

Fig. 22 shows the cumulative mass curves for all horizons in profile PK 143. The differences between the strata are significant: The base of the profile (3BC, 3CB, 4C) is the coarsest, the palaeosol (2A2, 2B1, 2B2) is characterised by the highest quantities of fine clay, and the current soil (A1, AB1, AB2) is similar to the palaeosol except for lower amounts of fine silt and clay. This textural pattern is found throughout the study area.

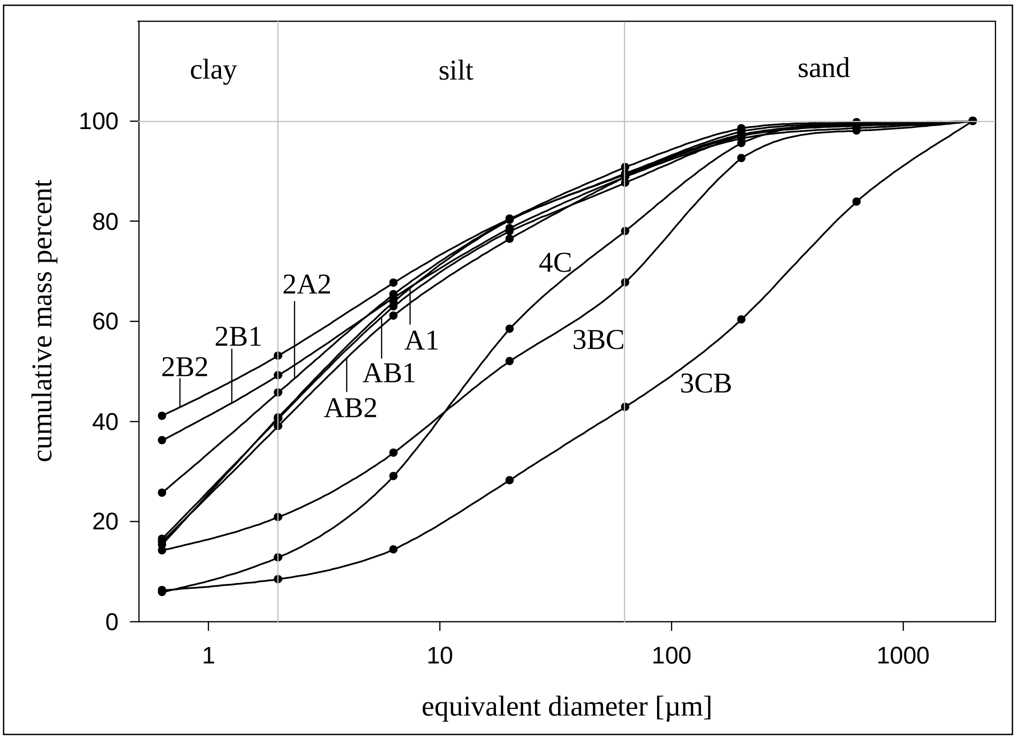

Fig. 22: Grain size distribution of horizons in profile PK 143 (< 2 mm fraction).

<u>*Clay mineral analyses (XRD)*</u>

Kaolinite (°2θ = 14.4), illite (10.2-10.3), mixed-layer minerals and chlorite (7.2-7.3) represent the main phyllosilicates within the study area (*Fig. 23a-c*). Most of the chlorite is assumed to be pedogenic, i.e. in the form of Al-hydroxy interlayered minerals, because primary chlorites are considered unstable under acidic weathering conditions (Barnhisel & Bertsch 1989). Indeed, most of the pedogenic chlorite collapsed to 10Å after heating to 300°C for 1 hour. Plateau-like structures in the region of °2θ = 7-10 are interpreted as diffraction signals from illite-vermiculite and chlorite-vermiculite mixed-layer minerals. Among the non-clay minerals, α-quartz (high) has the most intense line at °2θ = 30.5 and dominates all horizons tested.

Table 14: Analytical results of the soil profiles selected for the study of Phobjikha Valley.

sample ID	horizon	depth (cm)	colour (moist)	pH KCl	pH H_2O	C_{org} ($g\ kg^{-1}$)	N_{tot} ($g\ kg^{-1}$)	C/N ratio	effective cation exchange capacity ($cmol_c\ kg^{-1}$) Na^+	K^+	Ca^{2+}	Mg^{2+}	Mn^{2+}	Al^{3+}	Σ	base saturation (%)	skeleton > 2mm (%)	particle size fraction < 2 mm (w.-%) sand	silt	clay	surface area ($m^2\ g^{-1}$)
PK 135: 2,880 m; southeast of Dechen Goempa; pasture, grassland; Humic Acrisol																					
/1	A1	0-25	7.5YR 4/4	4.5	5.1	42.5	3.5	12.1	0.1	0.3	0.2	0.1	0.0	1.6	2.4	30	< 5	11	48	41	22
/2	B1	25-63	10YR 4/4	4.3	5.4	13.9	1.4	9.9	0.1	0.2	0.2	0.1	0.0	2.5	3.1	20	< 5	8	46	46	25
/3	B2	63-92	10YR 4/6	4.4	5.4	10.9	1.2	9.1	0.1	0.3	0.2	0.1	0.0	1.6	2.3	27	< 5	8	44	48	32
/4	B3	92-142	10YR 4/6	4.3	5.4	10.6	1.2	8.8	0.1	0.3	0.4	0.5	0.0	1.8	3.1	40	< 5	9	35	56	46
/5	B4	142-183	10YR 5/6	4.2	5.6	8.6	1.1	7.8	0.1	0.3	0.7	0.7	0.0	2.0	3.9	47	< 5	8	36	56	52
/6	2A2	183-205+	10YR 4/4	4.0	5.5	20.6	1.6	12.9	0.0	0.3	0.7	0.8	0.0	1.9	3.7	50	< 5	9	48	43	37
PK 138: 3,185 m; south of Pelam; pasture, grassland; Dystric Andosol																					
/1	A1	0-5	10YR 3/3	4.0	5.1	42.0	2.9	14.5	0.1	0.6	1.5	0.4	0.0	3.0	5.7	46	< 5	24	53	23	17
/2	B1	5-32	7.5YR 5/6	4.3	5.0	63.8	2.4	26.6	0.1	0.2	0.4	0.1	0.0	4.9	5.8	14	5-10	15	58	27	32
/3	B2	32-63	10YR 5/4	4.5	5.3	50.7	2.3	22.0	0.1	0.2	0.3	0.1	0.0	3.2	3.9	17	5-10	17	59	24	19
/4	2A2	63-70	10YR 3/3	4.5	5.0	72.4	2.9	25.0	0.1	0.1	0.8	0.1	0.0	2.6	3.7	30	10-30	17	60	23	11
/5	2B3	70-115	10YR 6/6	4.6	5.4	14.8	0.9	16.4	0.0	0.1	0.3	0.1	0.0	1.3	1.8	28	50-70	23	50	27	12
/6	2C	115-160+	5Y 6/2, 5YR 5/6	4.6	5.4	6.6	0.8	8.3	0.0	0.1	0.2	0.0	0.0	0.7	1.1	33	70-90	15	62	23	25
PK 143: 2,885 m; south of Gangtey Goempa; pasture, grassland; Andic Ferralsol																					
/1	A1	0-20	7.5YR 4/6	4.5	5.4	39.2	4.0	9.8	0.1	0.4	1.3	0.7	0.1	0.9	3.5	72	-	10	49	41	26
/2	AB1	20-50	7.5YR 4/4	4.6	5.5	24.6	3.1	7.9	0.1	0.5	0.3	0.3	0.0	0.8	2.0	60	-	12	47	41	30
/3	AB2	50-100	7.5YR 4/3	4.5	5.6	23.5	2.9	8.1	0.1	0.6	0.3	0.4	0.0	0.9	2.3	61	-	11	50	39	31
/4	2A2	100-123	7.5YR 3/3	4.3	5.6	28.8	3.0	9.6	0.1	0.3	0.4	0.9	0.0	1.9	3.6	47	-	9	45	46	29
/5	2B1	123-184	10YR 5/6	4.2	5.6	9.1	1.3	7.0	0.1	0.2	0.5	1.4	0.0	1.7	4.0	57	< 1	11	40	49	40
/6	2B2	184-214	10YR 4/6	4.1	5.4	5.6	1.1	5.1	0.1	0.2	0.8	1.5	0.0	1.9	4.6	57	< 1	11	36	53	46
/7	3BC	375-384	10YR 6/2	4.2	5.3	5.4	0.8	6.8	0.1	0.1	0.5	0.3	0.0	1.5	2.6	41	< 1	32	47	21	16
/8	3CB	384-430	10YR 5/6	4.3	5.6	2.5	0.5	5.0	0.1	0.1	0.3	0.2	0.0	0.9	1.5	42		57	34	9	10
/9	4C	430-465	5Y 5/2	4.3	5.7	0.6	0.7	0.9	0.1	0.1	0.4	0.3	0.0	1.0	2.0	49	-	22	65	13	13

Table 14 (continued): Analytical results of the soil profiles selected for the study of Phobjikha Valley.

sample ID	horizon	depth (cm)	colour (moist)	pH KCl	pH H_2O	C_{org} ($g\ kg^{-1}$)	N_{tot} ($g\ kg^{-1}$)	C/N ratio	effective cation exchange capacity ($cmol_c\ kg^{-1}$) Na^+	K^+	Ca^{2+}	Mg^{2+}	Mn^{2+}	Al^{3+}	Σ	base saturation (%)	skeleton > 2mm (%)	particle size fraction < 2 mm (w.-%) sand	silt	clay	surface area ($m^2\ g^{-1}$)
PK 150: 2,923 m; southeast of Kinkhorthang; pasture, bamboo (*Yushania sp.*); Vetic Andosol																					
/1	A	0-35	10YR 4/3	4.6	5.8	35.2	3.4	10.4	0.1	0.3	1.6	0.4	0.0	1.5	3.9	62	-	13	46	41	31
/2	B1	35-75	10YR 5/6	4.6	5.7	14.0	1.8	7.8	0.1	0.2	0.8	0.2	0.0	1.1	2.4	55	-	8	45	47	36
/3	B2	75-130	10YR 5/6	4.5	5.8	11.3	1.5	7.5	0.1	0.2	0.5	0.6	0.0	1.4	2.8	49	< 1	8	38	54	47
/4	B3	130-210	10YR 5/6	4.3	5.8	5.3	1.2	4.4	0.1	0.5	0.7	0.9	0.0	1.5	3.7	58	< 1	7	40	53	44
/5	2B4	210-290	10YR 4/6	4.0	5.3	3.7	1.1	3.4	0.1	0.2	0.5	0.2	0.0	3.1	4.1	23	-	6	46	48	41
/6	2B5	290-310	10YR 5/8	4.1	5.5	5.8	1.1	5.3	0.1	0.2	0.3	0.2	0.0	2.9	3.7	21	-	9	42	49	41
/7	3CB	310-322	2.5Y 6/3	4.0	5.2	3.2	0.9	3.6	0.1	0.1	0.2	0.1	0.0	2.4	2.9	19	-	14	55	31	23
/8	3C	322-385+	2.5Y 5/1	4.2	5.4	1.2	0.7	1.7	0.1	0.1	0.2	0.1	0.0	0.7	1.1	37	-	16	74	10	7
PK 151: 3,049 m; northeast of Gangtey Goempa; *Pinus wallichiana*., *Cotoneaster sp.*, grass; Vetic Ferralsol																					
/1	A1	0-30	7.5YR 4/6	4.7	5.6	24.2	2.7	9.0	0.1	0.7	0.4	0.2	0.1	0.5	1.9	68	-	12	46	42	33
/2	2A2	30-45	10YR 3/2	4.2	5.5	39.4	3.1	12.7	0.1	0.3	1.6	1.3	0.1	2.5	5.9	56	-	6	37	57	29
/3	2B1	45-58	10YR 5/4	4.5	5.6	18.8	2.0	9.4	0.0	0.3	0.4	0.3	0.0	1.0	2.1	50	-	10	39	51	35
/4	2B2	58-76	10YR 5/4	4.6	5.6	12.6	1.6	7.9	0.1	0.3	0.3	0.3	0.0	0.9	1.9	50	-	11	46	43	35
/5	2Bt1	76-141	10YR 4/6	4.6	5.8	10.0	1.4	7.1	0.1	0.4	0.6	0.8	0.0	0.6	2.4	76	-	11	43	46	38
/6	2Bt2	141-186	10YR 5/4	4.5	5.8	8.8	1.3	6.8	0.1	0.4	0.9	1.6	0.0	0.6	3.5	82	-	13	37	50	41
/7	2Bt3	186-224	10YR 5/4	4.3	5.7	8.4	1.2	7.0	0.0	0.4	0.8	1.5	0.0	1.2	4.0	69	< 1	8	33	59	51
/8	3A3	224-250	10YR 5/4	4.1	5.7	6.2	1.1	5.6	0.1	0.5	0.8	1.4	0.0	2.0	4.7	58	-	8	34	58	53
/9	3B3	250-285	10YR 5/4	4.0	4.9	5.0	1.0	5.0	0.1	0.5	0.9	1.1	0.0	2.5	5.0	50	-	8	36	56	49
/10	3CB	285-361	10YR 5/4	3.9	5.4	3.6	1.0	3.6	0.1	0.4	0.8	0.8	0.0	2.9	5.1	42	-	8	42	50	44
/11	3C1	361-396	10YR 5/4	3.9	5.3	3.1	0.8	3.9	0.1	0.3	0.5	0.5	0.0	2.4	3.8	37	1-2	16	45	39	25
/12	4C2	396-416+	10YR 4/4	4.0	5.5	2.0	0.6	3.3	0.1	0.2	0.4	0.3	0.0	1.2	2.2	44	> 50	42	32	26	20
PK 155: 3,010 m; south of Gophu; *Pinus wallichiana*, dense understorey with *Juniperus sp.*, *Rhododendron sp.*, *Yushania sp.*; Humic Umbrisol																					
/1	A	0-35	10YR 3/2	4.1	5.2	86.3	5.6	15.4	0.1	0.4	1.7	0.9	0.2	4.9	8.1	38	-	10	39	51	21
/2	B1	35-73	10YR 6/6	4.8	5.4	21.2	1.9	11.2	0.2	0.3	0.3	0.1	0.0	1.3	2.2	39	-	14	50	36	44
/3	B2	73-103	10YR 6/6	4.9	5.6	16.0	1.6	10.0	0.2	0.2	0.2	0.1	0.0	0.6	1.4	53	-	13	48	39	43
/4	2B3	103-125	10YR 6/8	4.8	6.1	9.4	1.2	7.8	0.1	0.1	0.3	0.1	0.0	0.5	1.1	53	1-2	14	46	40	39
/5	2BC	125-160+	10YR 7/4	4.2	5.5	3.1	0.7	4.4	0.1	0.1	0.4	0.3	0.0	1.1	2.0	42	10-30	22	47	31	25

The range of °2θ = 20-25 contains feldspars, e.g. K-feldspars at °2θ = 24.5. Sharp signals at °2θ = 21.3 and 23.6 (23.9) in subsoils are attributed to gibbsite. Among the examined profiles, the scans of PK 138 and PK 155 have a similar pattern. The only clear difference is for gibbsite, which is present in PK 155 only in traces, whereas it dominates the feldspar range in all subsoil horizons of PK 138. Profile PK 143 shows significant deviations from this pattern (*Fig. 23c*): Pedogenic chlorite has high relative abundance only in the buried soil (2A2, 2B3), with lower amounts of kaolinite and illite. Towards the top of this profile, Al-interlayering is reduced and amounts of interstratified illite type minerals increase. There are sharp gibbsite signals in the 3CB horizon, and – to a lower extent – in the overlying 3BC horizon. In general, transitions between the horizons are rather smooth and the XRD results do not indicate any sharp stratifications.

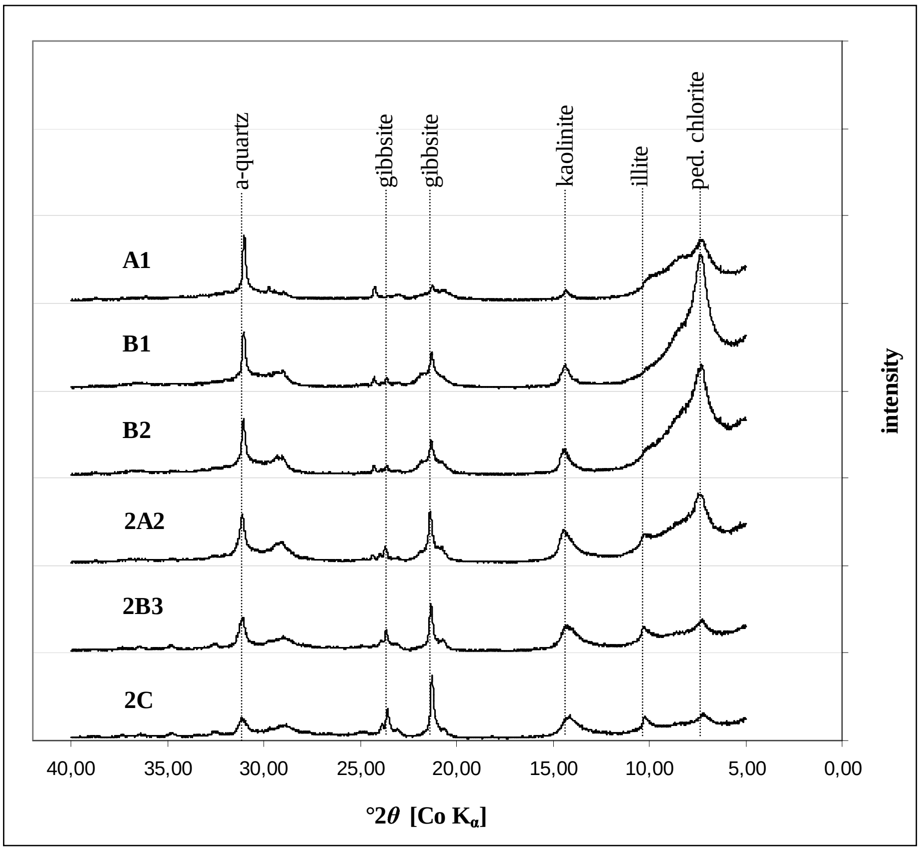

Fig. 23a: XRD graph of Mg^{2+}-saturated clay mineral preparations of profile PK 138.

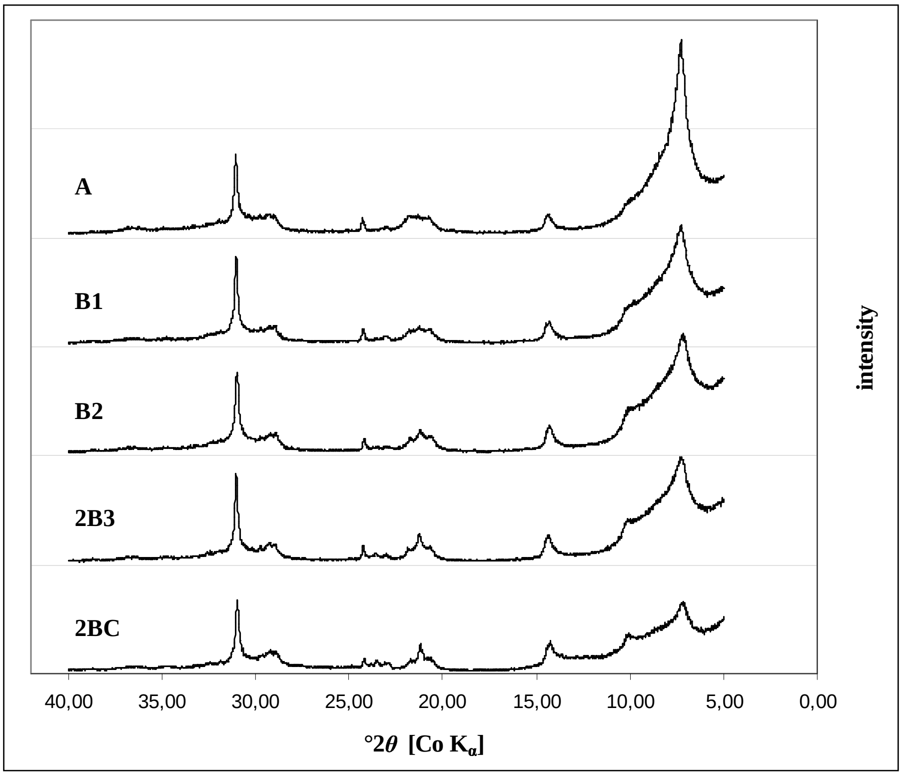

Fig. 23b: XRD graph of Mg^{2+}-saturated clay mineral preparations of profile PK 155.

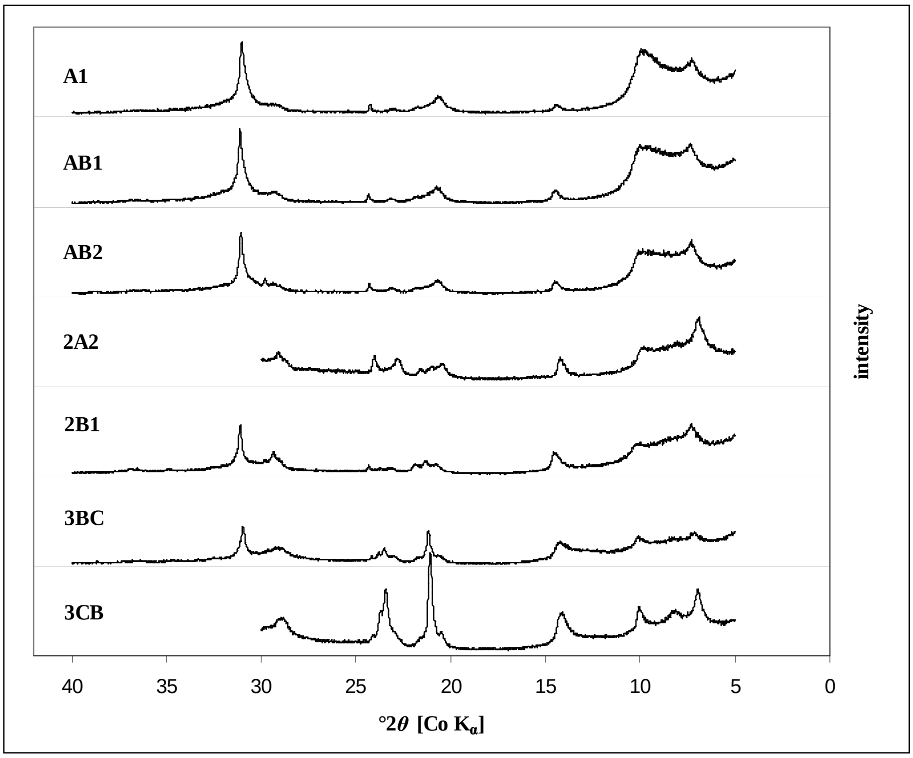

Fig. 23c: XRD graph of Mg2+-saturated clay mineral preparations of profile PK 143.

5.1.3.2 Soil chemical characteristics

pH

As a result of the felsic, carbonate-free substratum and the strong leaching conditions during summer monsoon, all horizons are acid with pH_{KCl} values ranging from 3.9 to 4.9 and pH_{H2O} from 4.9 to 6.1.

Cation exchange capacity

CEC_{eff} values are very low and do not exceed 10 $cmol_c$ kg^{-1} in the fine earth fraction, pointing to a dominance of low-activity clays or highly protonated variable/positive charge conditions. Al^{3+} is the dominant cation at the exchange sites of most horizons. Where clay contents are high, however, exchangeable Mg^{2+} and Ca^{2+} increase the base saturation to 50% and above, in spite of low pH values.

Carbon and nitrogen

Organic carbon (OC) contents are around 40 g kg^{-1} in the topsoils of grazed areas and can reach more than double of that under forest (profile PK 155). OC does not usually fall below 10 g kg^{-1} *above* the buried topsoils, and in PK 135 it is still as high as 20 g kg^{-1} at 2 m depth. In the lower subsoils, values mostly range from 5 to 10 g kg^{-1} and are as low as 0.6 g kg^{-1} in the gravelly substrata at the base of the profiles. Generally, buried topsoils can be identified by second maxima of C_{org} within the solum. C/N ratios are around 10-15 in topsoils, and decrease to 5-10 in most buried soils. Higher values of > 20 are only found in PK 138/2-4.

The two buried topsoils selected for radiocarbon analysis, PK 143/4 (2A2, KIA19867) and PK 144/4 (2A2, KIA19868), gave ages of 1,667 ± 19 and 2,024 ± 20 conventional ^{14}C years before present, respectively.

5.1.3.3 Statistics

Taking the laboratory data as the variables, cluster analysis of the soil horizons as cases identifies three main clusters, containing 21 (I), 11 (II) and 14 (III) soil horizons (= cases) respectively (*Fig. 24*). Cluster I mainly consists of topsoils, including buried ones. Cluster II represents intermediate horizons, and Cluster III the base of the profiles. PK 138 does not follow the general pattern and all of its horizons qualify for Cluster III. Whereas the Euclidean distance between Clusters I and II is about 130, Cluster III is significantly different, at a distance of 355 from the other two clusters.

Table 15: Analytical results related to andic features; n.d. = not determined.

Profile ID	*Horizon*	*Depth (cm)*	*Bulk Density ($g\ cm^{-3}$)*	*Pedogenic oxides ($g\ kg^{-1}$)* Fe_{tot} ($g\ kg^{-1}$)	Al_{tot} ($g\ kg^{-1}$)	Fe_d ($g\ kg^{-1}$)	Fe_o ($g\ kg^{-1}$)	Al_d ($g\ kg^{-1}$)	Al_o ($g\ kg^{-1}$)	Al_o+½Fe_o (%)	*thixotropic*	*P retention (%)*
PK 135	A1	0-25	0.7	48.3	95.5	22.0	8.4	13.5	13.5	1.8		88
	B1	25-63	1.0	47.1	98.3	17.5	7.9	8.0	8.5	1.2		81
	B2	63-92	1.0	49.1	95.9	14.2	9.5	7.2	10.2	1.5		84
	B3	92-142	1.0	55.4	104.7	21.5	13.2	9.1	9.1	1.6		86
	B4	142-183	1.0	60.8	107.6	25.1	15.2	8.0	5.6	1.3		79
	2A2	183-205+	1.3	49.9	101.4	21.3	8.0	5.1	3.9	0.8		59
PK 138	A1	0-5	0.8	87.8	94.3	21.3	7.3	6.8	5.6	1.0		61
	B1	5-32	0.5	63.7	118.5	30.0	13.9	24.1	20.9	2.8	ü	99
	B2	32-63	0.7	49.1	120.8	22.1	7.6	22.4	22.1	2.6	ü	98
	2A2	63-70	0.7	41.6	122.6	17.1	6.7	22.3	19.7	2.3	ü	97
	2B3	70-115	1.2	33.9	114.5	17.0	2.1	7.9	6.2	0.7		65
	2C	115-160+	-	42.4	114.7	23.1	2.2	5.6	3.3	0.4		50
PK 143	A1	0-20	0.7	51.2	82.8	19.8	4.5	9.0	15.7	1.8		90
	AB1	20-50	0.8	53.3	83.7	26.2	5.1	9.2	14.4	1.7		89
	AB2	50-100	0.7	52.3	84.9	26.1	6.2	9.4	37.6	4.1	ü	89
	2A2	100-123	0.7	52.1	85.6	25.4	7.6	10.0	n.d.	n.d.		85
	2B1	123-184	1.0	54.2	87.6	13.1	9.2	5.8	19.3	2.4		77
	2B2	184-214	1.0	55.1	87.3	24.5	8.5	3.9	12.1	1.6		67
	3BC	375-384	1.2	32.0	93.9	5.2	1.6	2.0	2.7	0.4		39
	3CB	384-430	-	30.3	77.1	3.9	1.1	1.6	5.3	0.6		28
	4C	430-465	1.3	29.8	111.9	1.8	0.6	1.5	7.0	0.7		35
PK 150	A	0-35	0.7	55.1	86.4	21.3	10.1	13.9	15.4	2.0		n.d.
	B1	35-75	0.8	53.9	85.5	19.9	11.8	10.2	13.8	2.0		n.d.
	B2	75-130	1.0	56.4	97.5	20.1	13.4	10.9	8.9	1.6		n.d.
	B3	130-210	1.0	52.3	93.1	21.9	9.8	7.8	7.8	1.3		n.d.
	B4	210-290	1.1	48.3	90.6	19.2	7.6	6.0	5.6	1.0		n.d.
	B5	290-310	1.0	46.2	96.2	24.3	10.3	8.2	7.0	1.2	ü	n.d.
	2CB	310-322	1.3	26.1	102.9	7.2	3.2	2.8	3.4	0.5		n.d.
	2C	322-385+	1.3	27.4	85.9	1.2	0.2	0.9	1.5	0.2		n.d.
PK 151	A1	0-30	0.7	55.3	82.1	35.1	6.9	16.3	15.1	1.9		n.d.
	2A2	30-45	0.7	53.8	74.3	29.1	10.8	14.1	9.3	1.5		n.d.
	2B1	45-58	0.7	54.6	81.2	22.7	13.6	12.6	14.5	2.1	ü	n.d.
	2B2	58-76	0.9	53.9	84.8	20.9	9.2	10.4	10.8	1.5		n.d.
	2Bt1	76-141	1.0	55.2	84.5	25.4	11.6	9.8	8.5	1.4	ü	n.d.
	2Bt2	141-186	1.0	56.9	93.7	27.1	10.8	11.1	7.9	1.3	ü	n.d.
	2Bt3	186-224	0.9	59.8	112.2	22.8	15.4	9.5	7.8	1.6	ü	n.d.
	3A3	224-250	1.1	58.9	98.1	29.7	11.3	9.1	4.2	1.0	ü	n.d.
	3B3	250-285	1.1	59.3	86.9	30.0	11.3	8.0	4.1	1.0	ü	n.d.
	3CB	285-361	1.2	57.6	94.5	24.8	8.2	6.3	3.2	0.7	ü	n.d.
	3C1	361-396	1.4	48.2	91.5	23.0	5.8	5.2	2.7	0.6		n.d.
	4C2	396-416+	-	47.7	99.3	20.8	4.3	4.9	2.1	0.4		n.d.
PK 155	A	0-35	0.5	83.1	141.8	22.5	10.8	13.2	12.9	1.8		94
	B1	35-73	0.6	51.3	108.9	32.7	15.0	11.3	12.2	2.0	ü	97
	B2	73-103	0.6	46.7	95.4	32.9	12.1	12.4	15.4	2.1	ü	97
	2B3	103-125	0.8	35.5	99.4	30.3	11.1	9.0	8.9	1.4	ü	91
	2BC	125-160+	-	15.3	85.7	25.3	4.5	3.9	2.4	0.5		44

In the factor analysis, the first four Varimax axes explain more than 70% of the total variation (*Table 16*). Their eigenvalues range from 7.8 (axis 1) to 2.1 (axis 4). No single factor explains more than a quarter of the total variation, meaning that – instead of one dominant factor – there are several subdominant factors. *Table 17* shows the factor loadings for each of the variables. The first factor explains 24% of the total variation and is strongly positively correlated with clay content and surface area. Another positive correlation is observed for pedogenic iron oxides. There are negative loadings for coarse silt, fine sand and medium sand. Factor 2 is responsible for 25% of the variance and is positively related with carbon and nitrogen contents, loss on ignition, extractable aluminium and the fine silt fraction. Axis 3 eliminates further 11% of the total variation. It is negatively related to amounts of exchangeable Al^{3+}, and positively with pH. Axis 4 accounts for another 13% of the variance and has positive loadings for all exchangeable cations, except Al^{3+}, and negative loadings for fine and medium-sized silt.

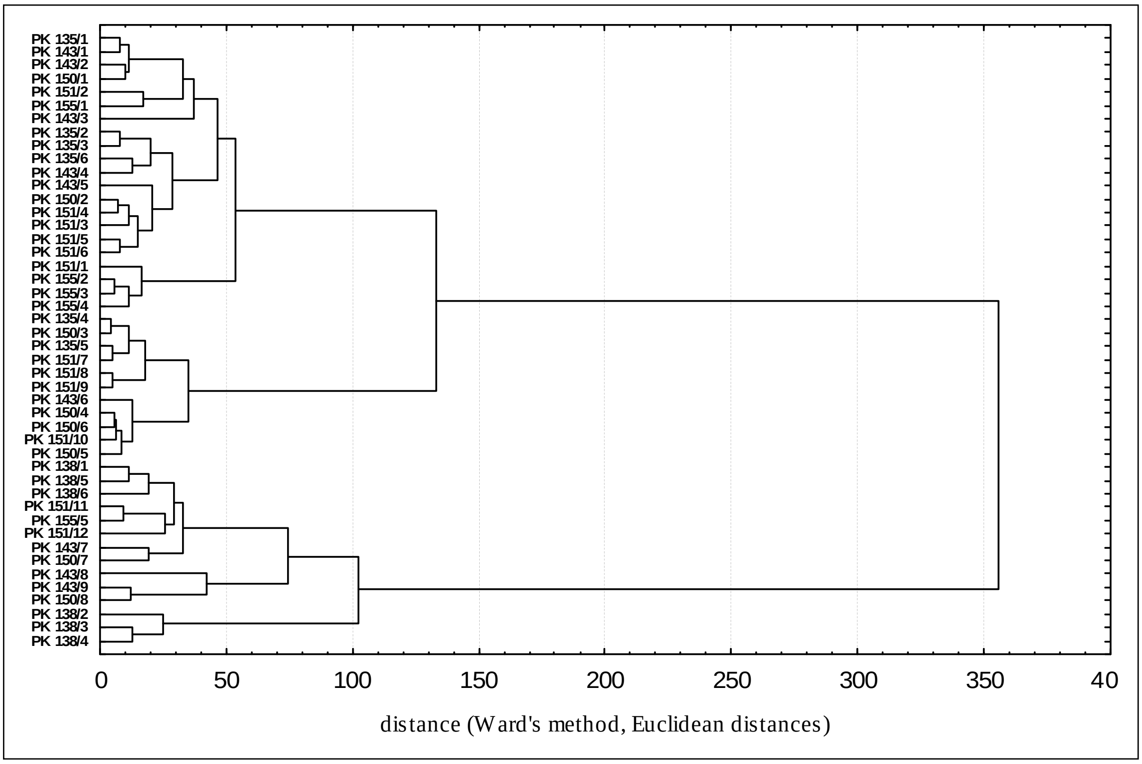

Fig. 24: Dendrogram of cluster analysis (n = 46 horizons). It was performed on 24 variables: Bulk density, pH_{KCl}, pH_{H2O}, C, N, loss on ignition, Fe_d, Fe_o, Al_d, Al_o, CEC data (Na^+, K^+, Ca^{2+}, Mg^{2+}, Mn^{2+}, Al^{3+}), surface area and particle size distribution (cS, mS, fS, cSi, mSi, fSi, C).

Table 16: Eigenvalues, explained variance and cumulative percent of variance for the first four factors of the factor analysis.

axis	eigenvalue	variance explained (%)	cumulative variance (%)
1	7,78	32,40	32,40
2	4,67	19,44	51,85
3	2,80	11,66	63,51
4	2,06	8,59	72,09

*Table 17: Factor loadings as resulting from factor analysis (n = 46 horizons); factor loadings > 0.7 are shown in **bold** figures.*

variable	factor 1	factor 2	factor 3	factor 4
bulk density	-0.27	**-0.88**	-0.17	-0.17
pH_{KCl}	0.04	0.49	**0.74**	-0.34
pH_{H2O}	0.22	-0.23	**0.75**	0.03
N_{tot}	0.02	**0.84**	-0.11	0.36
C_{tot}	-0.11	**0.90**	-0.32	0.21
loss on ignition	0.14	**0.86**	-0.26	0.14
Fe_d	0.62	0.38	0.21	0.23
Al_d	0.26	**0.84**	-0.05	-0.05
Fe_o	**0.78**	0.26	0.13	0.23
Al_o	0.08	**0.72**	0.26	-0.07
exchangeable Na^+	-0.14	0.15	0.42	0.26
exchangeable K^+	0.39	0.24	0.03	0.48
exchangeable Ca^{2+}	0.08	0.23	-0.29	**0.71**
exchangeable Mg^{2+}	0.44	-0.25	-0.06	0.64
exchangeable Mn^{2+}	-0.02	0.48	-0.09	0.59
exchangeable Al^{3+}	0.08	0.30	**-0.80**	0.23
surface area	**0.86**	-0.18	0.22	0.22
coarse sand (cS)	**-0.71**	-0.18	0.15	0.18
medium sand (mS)	**-0.75**	-0.09	0.28	0.13
fine sand (fS)	**-0.80**	-0.17	0.03	-0.00
coarse silt (cSi)	**-0.72**	-0.20	-0.07	-0.31
medium silt (mSi)	-0.45	0.09	-0.35	-0.69
fine silt (fSi)	0.35	**0.73**	-0.05	-0.42
clay (C)	**0.89**	-0.05	0.04	0.39
proportion of total variance	**0.24**	**0.25**	**0.11**	**0.13**

5.1.4 Soil classification

During fieldwork, the very low bulk densities and the regular occurrence of thixotropic features suggested assignment of the soils to the WRB Andosols reference group. According to ISSS (1998), andic horizons often display “smeary consistence” and “may exhibit thixotropy” (p. 21). The high fine silt and clay contents and the low bulk densities are likely to result in high water holding capacities, which – in combination with the orientation of soil particles by frequent freeze-thaw cycles – may be an explanation for the thixotropic properties.

PK 138 is classified as Dystric Andosol and PK 150 as Vetic Andosol. The Vetic qualifier applies because of a CEC_{eff} value below 6 $cmol_c$ kg^{-1} clay. In addition to these two profiles, three individual horizons in other profiles are also andic (PK 143/3 and PK 155/2-3). However, they do not qualify the whole profiles as Andosols because they start at more than 25 cm below the soil surface. PK 151/3 also shows andic features, but is less than 30 cm thick. The silty horizons in many subsoils miss the andic requirements, especially the (Al_o + ½Fe_o) > 2% criterion, because the poorly crystallised oxidic iron compounds (Fe_o) are already aged to well-crystallised iron oxides (Fe_d). These horizons can be distinguished from the horizons above the buried A horizons by their higher clay contents and surface areas (> 40 m^2 g^{-1}) as well as bulk densities > 1 g cm^{-3}. Following the WRB system, the AB1 horizon of profile PK 143 (PK 143/2) with its lack of andic characteristics, its fine-grained texture, and its low CEC_{eff} per kg clay qualifies as ferralic. The AB2 horizon (PK 143/3) is andic, and the profile therefore classified as Andic Ferralsol. Similar ferralic properties are found in profile PK 151. The 2B2 and 2Bt1 (PK 151/4-5) are ferralic horizons, and the extremely low CEC_{eff} values throughout identify this profile as a Vetic Ferralsol. All of the horizons of PK 135 have comparatively high bulk densities and low (Al_o + ½Fe_o) values and therefore miss the andic criteria. PK 135/4 (B3) fulfils the requirements of an argic horizon, and – in combination with its low CEC_{eff} and base saturation – the profile is classified as Humic Acrisol. The pedon under natural forest (PK 155), though having an andic horizon at 35-103 cm from the soil surface, finally keys out as Umbrisol. The high C_{org} contents which are present throughout the profile make it a Humic Umbrisol.

5.1.5 Environmental framework for sediment redistribution

During fieldwork, we observed currently active aeolian transport and deposition, mainly during early afternoon in the area between Gangyu and Gangtey Goempa (*Fig. 10*, *Fig. 25*). How does the environmental setting of Phobjikha Valley encourage the redistribution of silt-sized sediments? Firstly, large amounts of silt are generated during weathering of the low-grade metasediments of the local Gangphey Formation. This can best be seen in PK 138, the profile with only few aeolian additions, where the silt fraction constitutes 60% w/w of the fine earth. Values of 40-50% w/w are common at the other sites. Secondly, surface-near material is subjected to frequent freeze-thaw cycles, which can occur daily during spring and autumn. Frost has long been recognised as an important mechanical agent in pedogenesis (Van Vliet-Lanoë 1998). According to McGowan (1997), frost shattering makes the surfaces highly susceptible to deflation following a thaw. Granular disintegration as an early stage of weathering was also noted by Gardner (1994) in the Middle Hills of Nepal. The strong along-valley winds are the third decisive factor. They not only represent the driving force behind sediment redistribution, but also suppress cloud cover and rainfall, thus causing a general dryness especially at the valley floors (Baillie et al. 2004). Low surface moisture of the valley bottom promotes deflation and is most pronounced during the dry season from October to March. Semi-open conditions in the form of short, grazed grassland vegetation and arable land cover facilitate entrainment and transport of silt-sized particles. Other possible local origins include farm roads, riverbanks and landslides developed during the monsoon.

Fig. 25: Accumulation of silt-sized particles behind a temporary windbreak, set up during the Black Necked Crane Festival on 11 November 2001.

Within this explanatory framework, it is not necessary to invoke aeolian additions by long-distance transport. The grain size curves in *Fig. 21* (page 65) show that the < 63 µm fractions are comprised of multiple end members. Pye (1987) noted that long-distance aeolian sediments often display a bi-modal (or poly-modal) grain size distribution. Consequently, long distance transport does not appear to be likely in case of the Phobjikha soils. This is supported by Bäumler (2001a) from eastern Nepal, where invariant Ti/Zr ratios were interpreted as reflecting a single and local source or local redistribution of fine-grained sediments. Wake & Mayewski (1994) showed that the High Himalayas act as an effective barrier and hinder dust movement from arid and semiarid regions of High Asia to the north (e.g. the Chinese loess plateau) from reaching the southern slopes of the Eastern Himalayas. They also cite Middleton (1989) who found it unlikely that dust from SW Asia is transported far enough eastward to affect the study area.

5.1.6 Macro-morphological indications for sediment redistribution

Signs of deflation are generally rare in Phobjikha, except for some areas on the lower E-facing slopes of the main valley, markedly between Gangphey and Dechhen Goempa (*Fig. 10*, page 25), where there are numerous small (< 20 cm diameter) blocks spread in a fairly regular pattern, forming a "stone pavement" (*Fig. 26*). They may represent rockslide material transported from the comparatively steep slopes above during periglacial conditions, and subsequently stripped of fine material by deflation.

Fig. 26: Blocky materials between Gangphey and Dechhen Goempa.

When loess-like aeolian sediments are transported through Phobjikha Valley, deposition seems to preferentially occur at the windward side of hills, which is in accordance with the findings from Goossens & Offer (1990). Locations under natural forest (profile PK 155) and on leeward northern slopes, like profile PK 138, receive less aeolian material and are therefore characterised by more stable surfaces and more apparent in-situ weathering. This is evidenced by shallower depths of soil development (mostly less than 2 m) and an almost linear decrease in Fe_{tot} with depth (*Table 15*). Considering the geomorphology of Phobjikha Valley, the SW-NE oriented ridge starting from Gangtey Goempa represents the first main barrier for NNW-directed sediment transport. This – apart from additions by slope erosion – may explain the 4 metres of stone-free soil despite a gradient of 18° as recorded in PK 151. Other areas of preferred sedimentation are on the lower valley slopes (e.g. PK 135, PK 150), the hillocks below Gangtey Goempa (PK 143) and the upper part of Taphu side valley (*Fig. 10*).

During the wet season from May to September, monsoonal rains collect and transport erodible material in the opposite direction, leaving it on slopes and river banks, deposited in marshy areas, or transported outside the valley. The vigorous plant growth may be more effective in trapping mobile sediments during this period of the year. However, we made no observations during monsoonal conditions. Although our macroscopic observations corroborate the redistribution of silt-sized sediments, it remains unclear at present to what extent these materials are involved in geologically quick cyclic processes as suggested by Gardner & Rendell (1994).

5.1.7 Analytical and statistical indications

If local redistribution is a slow, hidden process, in which pre-weathered silty materials are continuously included in soil formation at a new location where in-situ weathering continues without a major climatic discontinuity, it is doubtful if differences in the particle size distributions would be visible. *Table 14* (page 67f.), however, shows that one of the non-aeolian profiles, PK 138, has a generally coarser texture than all other profiles, displaying higher percentages of skeletal material (> 2 mm) and sand (2-0.063 mm). Within the < 63 µm fraction, the silt/clay ratio is higher than at any other site. XRD results show that profiles regarded as non-aeolian (PK 138, PK 155) have relatively higher amounts of pedogenic chlorite. It is in these sites that andic features are most pronounced. Delvaux et al. (2004) examined an Andosol-Cambisol toposequence derived from granite in North Austria, and postulated that in non-allophanic Andosols, weathering of primary minerals overshadows the neo-formation of crystalline minerals, resulting in net Si leaching and Al release. As a consequence, stable Al-humus complexes in association with poorly crystalline secondary minerals are formed, which may then facilitate organic matter longevity and accumulation. The same authors describe studies in which comparatively high C/N ratios, similar to those in our in-situ profile PK 138 (*Table 11*), can be interpreted as resulting from very stable organic material, low biological activity or the decay of plant roots. They further explain high clay contents in their soils by a possible contribution of large amounts of organo-mineral complexes. We appear to have similar soil forming processes in the Phobjikha Valley, with the development of andic features in non-volcanic parent materials and a strong weathering environment accompanied by dominance of pedogenic chlorite (Al-hydroxo interlayered vermiculite) minerals and C accumulation. The factor analysis corroborates this hypothesis: Factor 2 has a high fine silt loading of + 0.73, whereas the other particle size fractions are significantly loaded on other factors (*Table 16*). In addition to fine silt, Factor 2 has high positive loadings for organic matter and extractable Al (Al-humus complexes), and negative loadings for bulk density. This factor is therefore specified as the *andic factor*.

At depositional sites like PK 143, interstratified illite type minerals dominate over pedogenic chlorite. This could indicate that the episodically active land surface causes weathering to proceed on continually rejuvenated materials, thus attenuating the effect of weathering in space and time. Johnson et al. (1990) point out that additions of aeolian dust may generally have regressive effects on soil formation. This is especially so if part of the loess incorporated into new topsoils is comprised of less weathered (subsoil) material. In most cases, however, the wind-blown materials are the product of pre-depositional (Bäumler 2001a), syn- or post-depositional (Kemp 2001) weathering.

The continuous input of inorganic material, which is trapped by and partly covers the vegetation during the dry season, impairs the undisturbed development of a C-rich topsoil. This explains the markedly shallow and sometimes virtually non-existent recent A horizons within the study area. Instead, the mixture and imbrication of organic and inorganic materials leads to the development of deep AB horizons, as can be seen e.g. in profile PK 143 (*Table 12*, page 63). The topsoil C_{org} contents of depositional sites are only half those in protected sites, such as 86 g kg^{-1} in PK 155/1 or 72 g kg^{-1} in PK 138/4. Where pedons are comparatively stable after deposition (PK 143, PK 150, PK 151), fine silt is weathered to clay-sized particles which are then translocated into deeper horizons. The weathering and textural fining allows ferralic features to develop in former andic horizons: In profile PK 151, andic features in the 2B1 horizon are directly followed by ferralic properties in the underlying, older 2B2 and 2Bt1 horizons (*Table 15*). This process is reflected by Factor 1 of the factor analysis, the loadings of which show the connection between high surface area and clay contents developed from silt and sand fractions (*Table 17*). Whereas the andic factor is associated with Al compounds, Factor 1 is characterised by a positive relation with Fe_o and Fe_d, and is therefore designated as the *ferralic factor*. This distinction is important, as Fe and Al are usually assumed to behave similarly conservative during weathering. In the Himalayan context, development of ferralic features has also been noted by Bäumler et al. (1991).

A precise quantification of the local sediment redistribution is not feasible. The only indication is provided by the ^{14}C measurements. If we assume the ^{14}C ages of the buried topsoils (1,667 ± 19 conventional ^{14}C years BP in PK 143/4 and 2,024 ± 20 years in PK 144/4) to be approximately correct, about one metre of aeolian material has been deposited in these locations over the last 1.5-2 millennia, corresponding to a deposition rate of about 0.5-0.6 mm a^{-1}. These radiocarbon ages are most probably underestimates, because younger C-containing material from the overlying A horizon(s) can infiltrate and contaminate the sampled horizons. Translocation of organic material has been described as an important process in the soils of this altitudinal zone of Bhutan (Baillie et al. 2004). Weathering indices and comparable approaches to relative dating have not been applied, because they generally assume Al and often also Fe to be immobile within the solum. The high Al_o values and Al_o/Al_d ratios indicate that Al is mobile in the soils of the study area. Both, Al and Fe translocation have been shown to occur during column experiments on similar soils from Central Bhutan (see Chapter 5.2.6). Clay contents are often positively correlated with amounts of exchangeable K^+, Ca^{2+}, Mg^{2+} and Mn^{2+}, which further blurs the pedogenetic clarity of weathering indices.

The cluster analysis (*Fig. 24*, page 73) shows that horizons of most of the profiles are split between the three identified clusters, which suggests that the soils result from a common suite of pedogenic processes. In contrast, PK 138 with all of its horizons assigned to Cluster III, suggests that this profile is the result of in-situ soil formation from autochthonous material. The clustering thus supports the hypothesis that northward directed aeolian processes contribute to soil formation in most sites of the study area. Profile PK 155, covered by natural forest – at least since favourable conditions for tree growth were attained during the Holocene – is expected to display a similar pattern. However, only its lowest horizon, formed in Tertiary conglomerates, is within Cluster III, whereas horizons PK 155/2-4 constitute a distinct subcluster within the lower end of Cluster I. The topsoil horizon (PK 155/1) with a C_{org} content of 86 g kg^{-1}, a fine earth CEC_{eff} of 8 $cmol_c$ kg^{-1} and a clear dominance of pedogenic chlorite in the clay fraction indicates strong weathering and seems to demonstrate the potential of undisturbed in-situ soil formation under forest within the study area.

5.2 Andic features in non-volcanic soils in Bhutan

5.2.1 Non-volcanic Andosol samples

Soils in temperate Bhutan within the altitude range of 2,500 and about 3,300 m a.s.l. are often well-developed in terms of depth as well as crumb structure, and display bright reddish-yellow colours. This phenomenon is most pronounced in unshaded areas at approximately 3,000 m a.s.l. (Baillie et al. 2004).

For a closer examination, a profile (PT 056) has been established in the Lame Goempa Research Forest, Bumthang District, eastern Central Bhutan, at 3,025 m a.s.l. (90°43.98' E and 27°32.19' N) (*Fig. 8*, page 23). A detailed profile description is given in *Table 18*. The site is covered by dense mixed conifer and silver fir forest up to the tree line on the ridges at about 4,000 m a.s.l. (RGoB 2000b). The dominant tree species is *Pinus wallichiana* on lower slopes and in pioneer stands on midslopes, and *Abies densa, Tsuga dumosa, Picea spinulosa* and various *Rhododendron* species higher up. The climate is monsoonal, with mean annual temperatures of about 8°C. The mean annual precipitation amounts to 1,100 mm (1994-1997) at this altitude, with the maximum during summer. Parent materials consist of mica schist of the Thimphu Gneiss Group with quartzite beds and quartz veins, and the landscape is partly covered by (probably autochthonous) aeolian deposits (RGoB 2000b, Caspari et al. 2002, Baillie et al. 2004).

Table 18: Profile description for PT 056.

PT 056	**Lame Goenpa Research Forest; road cutting near Jakar, Bumthang District; 27°32.19' N, 90°43.98' E; 3,025 m; 12° NE-facing slope; *Pinus wallichiana*, *Rosa sp.*, *Berberis sp.*, *Yushania sp.*; non-volcanic Andosol; indigenous classification: Yellow Hill Soil**	
2.5-0 cm	**O**	**Partially fragmented and decomposed litter. The structure and origin of most of the litter is still visible, non-sticky and non-plastic.**
0-17 cm	**A**	**Very dark greyish brown (2.5Y 3/2) clay, fine and medium granular to subangular blocky structure, friable to very friable, no mottles, no concretions, common fine roots, no stones, clear regular boundary.**
17-24 cm	**AB**	**Olive brown (2.5Y 4/4) silty clay, medium granular to subangular blocky structure, friable, no mottles, no concretions, very few fine roots, no stones, clear wavy boundary.**
24-49 cm	**B1**	**Brownish yellow (10YR 6/8) silty clay loam, coarse subangular blocky to angular blocky structure, friable to slightly firm, weak discontinuous clay skins, no mottles, no concretions, very few fine roots, no stones, diffuse wavy boundary.**
49-101 cm	**B2**	**Yellowish brown (10YR 5/8) clay loam, coarse angular blocky structure, firm, weak discontinuous clay skins, no mottles, no concretions, no roots, no stones, diffuse regular boundary.**
101-148 cm	**B3**	**Yellowish brown (10YR 5/8) silty clay loam, coarse subangular blocky structure, firm, no mottles, no concretions, no roots, no stones, clear wavy boundary.**
148-200 cm	**CB**	**Brownish yellow (10YR 6/8) sandy clay loam, massive to granular structure, friable, no mottles, no concretions, no roots, abundant subangular and angular stones, weathered mica schist, clear regular boundary.**
200+ cm	**C**	**Mica schist, slightly weathered, massive.**

5.2.2 Basic soil chemical and physical properties

All analytical results are given in *Table 19*. pH_{KCl} values vary between 4.0 and 4.9. They increase with depth and are 0.5-0.9 units lower than pH_{H2O}. The pH_{H2O} values are > 4.9 in all but the two upper horizons, which is generally considered the lower limit for the formation of short range order minerals of the allophane and imogolite types (Shoji & Fujiwara 1984). The soils have extremely low bulk densities of 0.5-0.8 g cm^{-3} down to 1.5 m depth, which is typical for soils having andic properties.

Cation exchange capacity at field pH varies between 0.5 and 14 $cmol_c$ kg^{-1}, and decreases sharply below the AB horizon. Even in the top horizons, the values are low, considering the high contents of organic carbon and clay. This points either to a predominance of low-activity clays, or to high variable and/or positive charge, as shown by Gustafsson et al. (1995) for imogolite-type minerals in Podzol B horizons. There is a dominance of Ca^{2+} and Al^{3+} on the exchange sites of all horizons. The distinct maxima of Ca^{2+} and Al^{3+} in the A and AB horizon are caused by biogenic cycling (Ca^{2+}) and the low pH values (Al^{3+}). In the AB horizon, the Al saturation amounts to 79%, but drops to 25% with increasing depth.

Organic carbon values are high throughout the solum and continuously decrease with depth. But even in the B3 horizon the values are > 1%, which is a typical feature of andic and “cryptopodzolic” properties (Blaser et al. 1997). No second maximum indicating illuvial processes could be observed. There is a strong correlation with total nitrogen, and C/N-ratios vary between 22 and 11.

Except for the lowest horizon, P retention is > 85%. ODOE values are > 0.25 throughout the profile due to the high amount of organic carbon. pH_{NaF}, which is not used as a classification criterion for Andosols anymore, is > 10.5 in all horizons, slightly increasing with soil depth. All three properties are in accordance with andic and podzolic features, and indicate a predominance of amorphous and organic compounds.

Surface area of the < 2 mm fraction is high. The highest values of about 50 $m^2\ g^{-1}$ soil material were found in the subsoil B horizons, despite the fact that the highest clay contents and the lowest bulk densities are in the upper horizons. In combination with other physicochemical parameters, this may point to a stratification by different parent materials within the solum. However, it may also be caused by the high amount of organic matter in the top horizons which decreases the surface area values.

5.2.3 Pedogenic oxides and mineralogy

The data for the Fe, Al and Si fractions are also given in *Table 19*. Except for Si_o, all values are comparatively high, similar to intensively weathered soils of interglacial origin at the southern slopes of the Himalayas, and to Andosols developed in volcanic materials (Bäumler 2001b, Kleber et al. 2004). There are two maxima: One in the A horizon, as is typical for recent weathering processes or young soils, and the second one in the subsoil B horizons, but varying between B1 and B3 depending on the fraction.

There is no clear indication of depletion typical of eluviation and podzolisation. The absolute values again point to a lithological discontinuity between the second and the third horizon. This is further indicated by the pyrophosphate soluble Fe and Al exceeding the oxalate soluble fractions, and even the amounts of Fe_d in the A and AB horizons. This has been found by Bäumler & Zech (1994a) in soils with similar features in East Nepal. The amount of oxalate soluble Si, however, is low (<< 0.6%). It shows a clear maximum in the B1 horizon pointing to in-situ weathering and mineral trans- or neoformation. Again this is in accordance with the soils from East Nepal, and with (alu-)andic properties in general.

Table 19: Analytical data of the soil from the Lame Goempa Forest area, Central Bhutan (PT 056).

Horizon	Depth [cm]	Colour (moist)	Colour (dry)	pH_{KCl}	pH_{H2O}	Bulk density [g cm^{-3}]	CEC [cmol kg^{-1}]	C_{org} [g kg^{-1}]	N_{tot} [g kg^{-1}]	C/N ratio	P-Ret. [%]	ODOE	pH_{NaF}	Surface area [m^2 g^{-1}]
A	0-17	2,5Y3/2	10YR3/3	4.0	4.8	0.49	13.96	116.9	6.2	18.9	91	>4.0	10.5	17.9
AB	17-24	2,5Y4/4	10YR4/4	4.0	4.8	0.59	9.19	57.7	2.6	22.2	88	2.93	10.9	32.7
B1	24-49	10YR6/8	10YR6/4	4.6	5.1	0.46	1.46	22.7	1.5	15.1	99	2.83	11.3	51.1
B2	49-101	10YR5/8	10YR6/6	4.9	5.4	0.69	0.49	21.8	1.4	15.6	99	>4.0	11.7	47.9
B3	101-148	10YR5/8	10YR6/8	4.9	5.7	0.84	0.59	12.0	1.0	12.0	94	1.80	11.5	50.7
CB	148-200+	10YR6/8	2,5Y6/4	4.6	5.5	1.24	1.01	4.5	0.4	11.3	46	0.33	11.0	20.6

Horizon	Depth	Fe_d	Al_d	Fe_o	Al_o	Si_o	Fe_p	Al_p	Na^+	K^+	Ca^{2+}	Mg^{2+}	Mn^{2+}	Al^{3+}
	[cm]	[g kg^{-1}]							[cmol kg^{-1}]					
A	0-17	28.57	10.95	11.95	8.46	0.45	31.17	9.31	0.03	0.33	6.21	1.0	0.12	5.87
AB	17-24	31.83	8.88	11.80	7.46	0.33	35.15	9.54	0.01	0.10	1.51	0.28	0.03	7.26
B1	24-49	41.27	12.35	9.63	15.54	3.71	14.69	7.22	0.02	0.04	0.34	0.12	0.01	0.93
B2	49-101	36.75	13.15	7.07	17.95	1.25	10.93	6.30	0.02	0.06	0.21	0.02	0.01	0.17
B3	101-148	32.31	8.28	13.66	11.46	0.83	20.88	5.83	0.01	0.04	0.24	0.05	0.01	0.15
CB	148-200+	15.51	3.30	6.57	2.37	0.30	9.27	1.95	0.02	0.05	0.29	0.17	0.02	0.46

Horizon	Al_o+½ Fe_o [%]	Fe_o/Fe_d	Fe_p/Fe_d	Al_p/Al_d	Al_o/Si_o	Al_p/Al_o	Fe_p/Fe_o	Al_o-Al_p /Si_o	cS [%]	mS [%]	fS [%]	cSi [%]	mSi [%]	fSi [%]	C [%]
A	1.44	0.42	1.09	0.85	18.8	1.10	2.61	-1.89	1	2	8	10	13	14	52
AB	1.34	0.37	1.10	1.07	22.6	1.28	2.98	-6.30	<1	1	8	8	16	17	50
B1	2.04	0.23	0.36	0.58	4.2	0.46	1.52	2.24	<1	8	11	7	14	22	38
B2	2.15	0.19	0.30	0.48	14.4	0.35	1.55	9.32	2	16	13	8	13	20	28
B3	1.83	0.42	0.64	0.70	13.8	0.51	1.53	6.78	1	5	14	8	15	20	37
CB	0.57	0.42	0.60	0.59	7.9	0.82	1.41	1.4	22	21	16	4	7	8	22

Ratios of Fe_p/Fe_d and Al_p/Al_d are close to unity in the top layer (*Table 19*), indicating that nearly all of the released Fe and Al are in close combination with organic compounds, although this conclusion is somewhat tenuous because of the known defects of the pyrophosphate extraction method (Bäumler & Zech 1994a, Kaiser & Zech 1996). In the subsoil B horizons, however, Al_p/Al_o values of < 0.9 indicate favourable conditions for short range order minerals of the allophane and imogolite type. Those minerals are absent in the upper layer because of negative values of $(Al_o\text{-}Al_p)/Si_o$, and as corroborated by the XRD and SEM data. However, despite the beneficially low pyrophosphate ratios, the low pH and Si_o values, the XRD results, and $Fe_d:Fe_o > 2$ do not favour or indicate the formation of short range order minerals in the subsoil horizons.

Mixed-layer minerals, Al-hydroxy interlayered vermiculite, minerals of the mica group, and kaolinite are the dominant aluminosilicates in the clay fraction (*Fig. 27*, page 86). There are strong differences in the clay mineral composition between the upper layer (A and AB horizon), and the subsoil B horizons. The lower horizons are characterised by a clear dominance of micaceous minerals, which are inherited from the mica schist parent material. The upper horizons, however, show a predominance of poorly ordered mixed-layer minerals. Allophane and imogolite could not be identified by XRD and SEM in any horizon. Given their short range, non-planar and weak crystallinities, this does not absolutely exclude the presence of these minerals. However, their absence is further corroborated by the extractable Al and Si fractions (Wada 1989, Kleber et al. 2004).

5.2.4 Particle size distribution and the formation of pseudosand

Particle size fractions also appear to indicate a regolithic discontinuity between the AB and B1 horizons, with a dominance of clay of about 50%, and lower fine silt and fine sand fractions in the two uppermost horizons. In the subsoil B horizons, silt predominates with about 40%, which is typical for mica schist weathering. Besides the possibility of pre-weathered aeolian additions, there is another hypothesis to explain the observed discontinuity: The SEM data revealed that almost all particles within the sand fractions are pseudosand-like microaggregates (*Fig. 28*), which proved to be highly resistant against dispersion by sodium pyrophosphate and ultrasonic treatment.

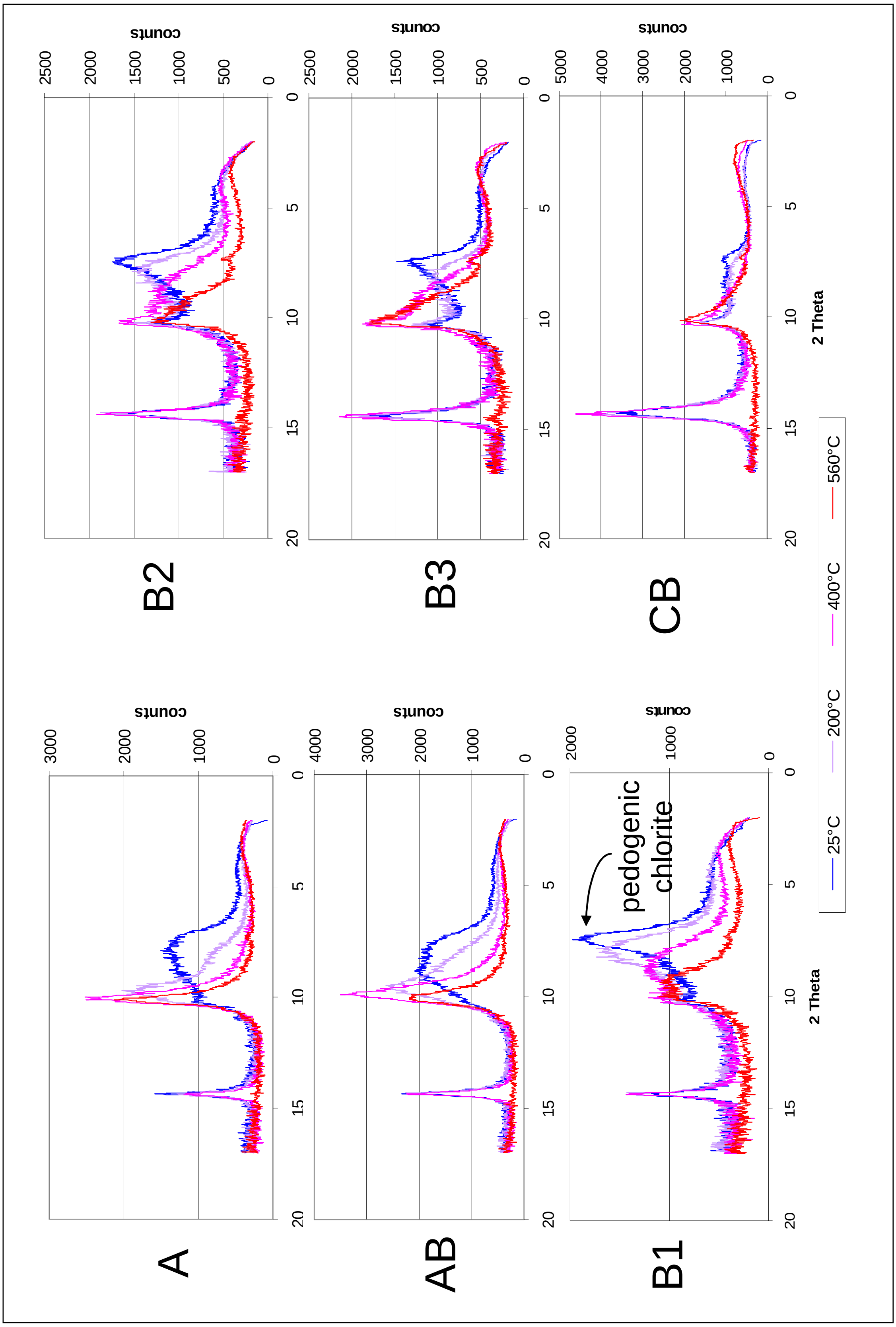

Fig. 27: XRD patterns of the K^+-saturated clay fractions of all PT 056 horizons at different temperatures.

Obviously, the conditions for the formation of stable aggregates are more favourable in the B horizons, leading to their slower destruction during particle size analysis when compared to the topsoil samples. We consequently have to interpret the significantly higher clay contents in the upper horizons as an analytical artefact. This would also explain why the field indications on clay migration – some weak and discontinuous clay skins in the B1 and B2 horizons – have not been more pronounced.

Energy-dispersive X-ray element mapping (SEM-EDX) of the microaggregates showed only small contents of C, but high contents of evenly distributed Fe and Al on the surfaces (*Fig. 29*). This particularly emphasises a stronger influence of Fe compounds with regard to the specific properties than previously thought, and indicates a ferro-(alu-) andic suite of properties.

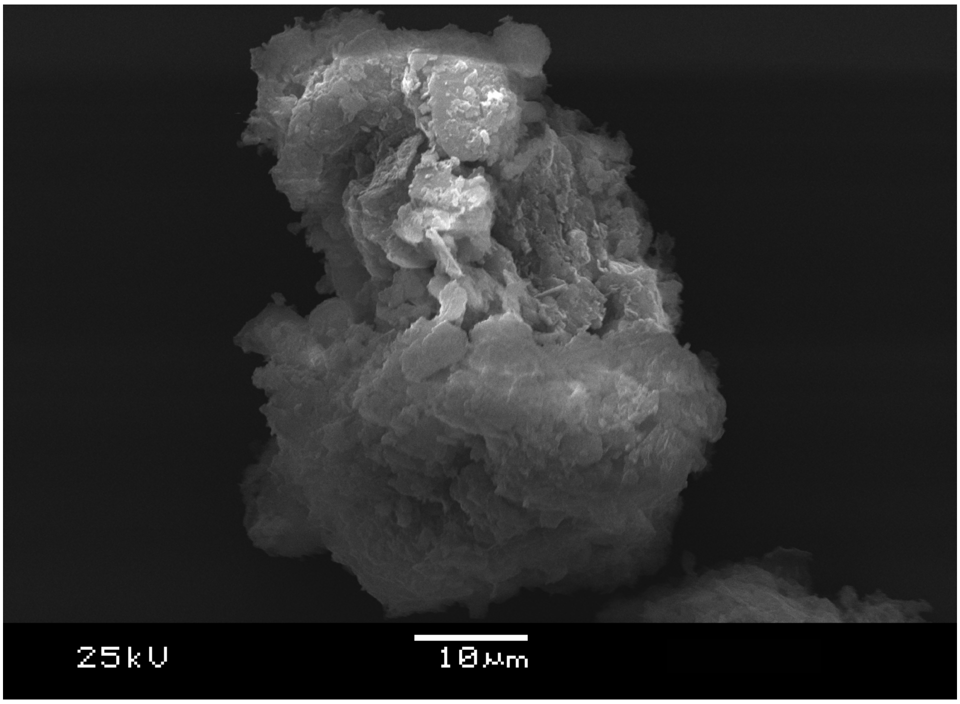

Fig. 28: SEM of one of the pseudosand-like microaggregates of the B1 horizon.

5.2.5 Longevity of the organic matter

Calibrated radiocarbon ages of the organic compounds in the B horizons are expected to be relatively old, compared to subsoils, which have not been buried or with fossil A horizons recently subjected to biogenic processes. The soil organic matter (SOM) of the CB horizon was dated at 15,790 ± 250 yr BP (KI-4987). This indicates stabilisation against biodecay despite recent rooting of the forest vegetation. SOM radiocarbon ages do not exceed 4-6 kyr in in-situ weathered well drained soils at non-contaminated sites, because of more or less continuous biodegradation and rejuvenation/translocation processes, especially with regard to podzolisation.

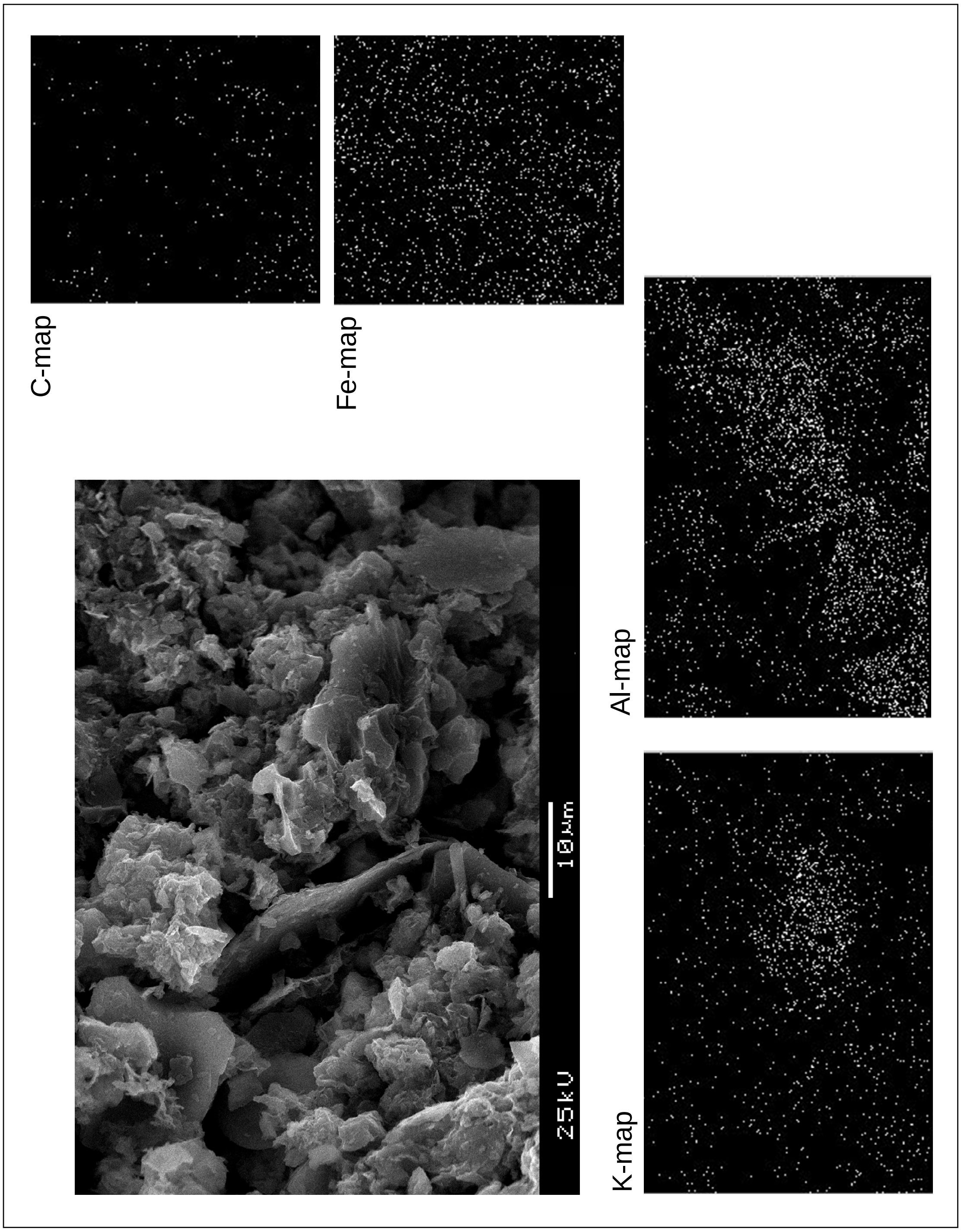

Fig. 29: SEM-EDX element mapping of a pseudosand-like microaggregate from the B1 horizon.

^{13}C solid state NMR spectroscopy may help to understand the unexpected longevity of the SOM in this subsoil. The NMR results of the soil organic matter indicate a comparatively high dominance of aryl- and carbonyl-carbon compounds (*Fig. 30*, left). This accords with the high radiocarbon age, as such organic groups are known to be at least partly resistant to biodegradation. The results are clearly different from illuvial B horizons of a Podzol located 400 m upslope of the examined site (*Fig. 30*, right; RGoB 2000b). Podzols are generally known to have strong signals of O-alkyl and alkyl carbon (Wilcken et al. 1997). However, it is not yet clear how these findings relate to the specific soil properties.

High radiocarbon ages of soil organic matter might also be the result of contamination with inactive organic particles like coal or graphite. However, the SEM analysis of the samples does not identify elemental carbon as an important element (*Fig. 29*).

5.2.6 Column experiments

The column experiments show the release of both organic and mineral solutes and colloids from topsoil (AB) and subsoil (B2) horizons (*Fig. 31*). The analysis of the conservative tracer (chloride) reveals a moderate advection-dominated flow regime with a sigmoidally shaped breakthrough curve. A pulse of three pore volumes of chloride was completely eluted from the columns after seven pore volumes in the AB material and after ten pore volumes in the B2 material. Column dispersivities were high – 8 mm for the AB and 9 mm for the B2 material – reflecting the impact of the strong aggregation on the transport regime. The retardation factor was approximately one ($R = 0.94$) for the AB material, indicating almost ideal conservative transport conditions. In the B2 horizon, however, a significant chloride retardation is observed ($R = 1.4$). This might be due to anion-exchange caused by predominantly positively charged surfaces of the B2 material under these leaching conditions, which is likely in face of the low CEC values (*Table 19*). Release of DOM and Al was higher for the AB than for the B2 horizon. Significant iron release was only observed in case of the AB material. This indicates that, under the given flow conditions, iron mobilisation is restricted to the AB horizon. Aluminium, in contrast, is mobilised both in the AB and the B2 horizon and a distinct first flush behaviour can be observed. Aluminium appears to be present in mobile and readily available forms.

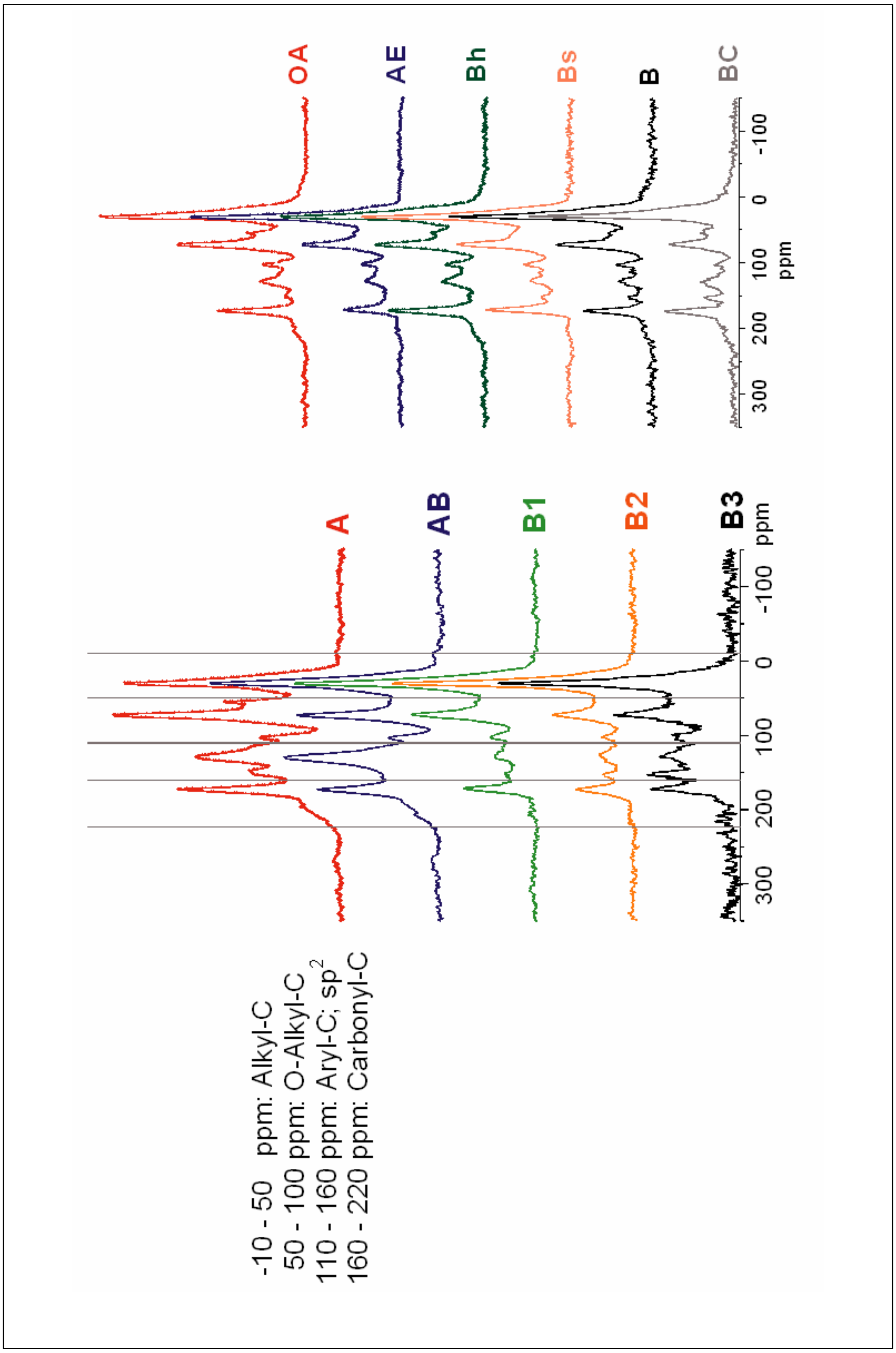

Fig. 30: Results of the ^{13}C CPMAS NMR spectroscopy of the soil organic matter in the non-volcanic Andosol (PT 056, left) and a Haplic Podzol (PT 055, right) situated 400 m upslope.

No significant response to flow interruptions could be observed indicating equilibrium release processes for both mineral and organic phases. In contrast, strong mobilisation effects were caused by the pulse of deionised water. The decline of the ionic strength, thought to be from 120 µS mm^{-1} to values below 10 µS mm^{-1}, resulted in large increases of DOM, Al and Fe outputs from the AB horizon and of DOM and Al from the B2 (*Fig.* 31). The reduction of the ionic strength causes an expansion of the diffuse double layer, which leads to an increase of repulsive forces (Münch et al. 2002). Under such conditions, colloidal materials are readily re-dispersed for translocation in the forms of oxidic Fe compounds and DOM. The simultaneous increase of DOM together with Fe and Al in the AB horizon may have also been caused by the release of colloidal phase organic Al and Fe complexes. As the ionic strength increases, the DOM, Fe and Al outputs quickly decrease to the pre-pulse levels within one exchanged pore volume of the background solution after the deionised water input. This again stresses the presence of colloidal materials and their importance in the translocation of iron and aluminium.

In the B2 horizon, the situation is different. There is no release of iron, and the mobilisation of DOM and aluminium is disconnected. DOM reacts instantly to the change in the ionic strength. The pool of mobilisable DOM, however, seems to be small compared to that in the AB horizon, as the minor *in*crease *de*creases rapidly within one pore volume. The response of aluminium is delayed and is not concurrent with the export of DOM. This points to the possibility that aluminium is present in non-organically bound, potentially colloidal forms.

In general, the results of the column experiments support dynamics of the podzolic type, with re-stabilisation of translocated (metal-)organic phase complexes, which cause the high soil organic matter contents in the subsoil B horizons. Translocation processes, however, are generally thought to be of minor importance or even excluded from Andosols/Andisols.

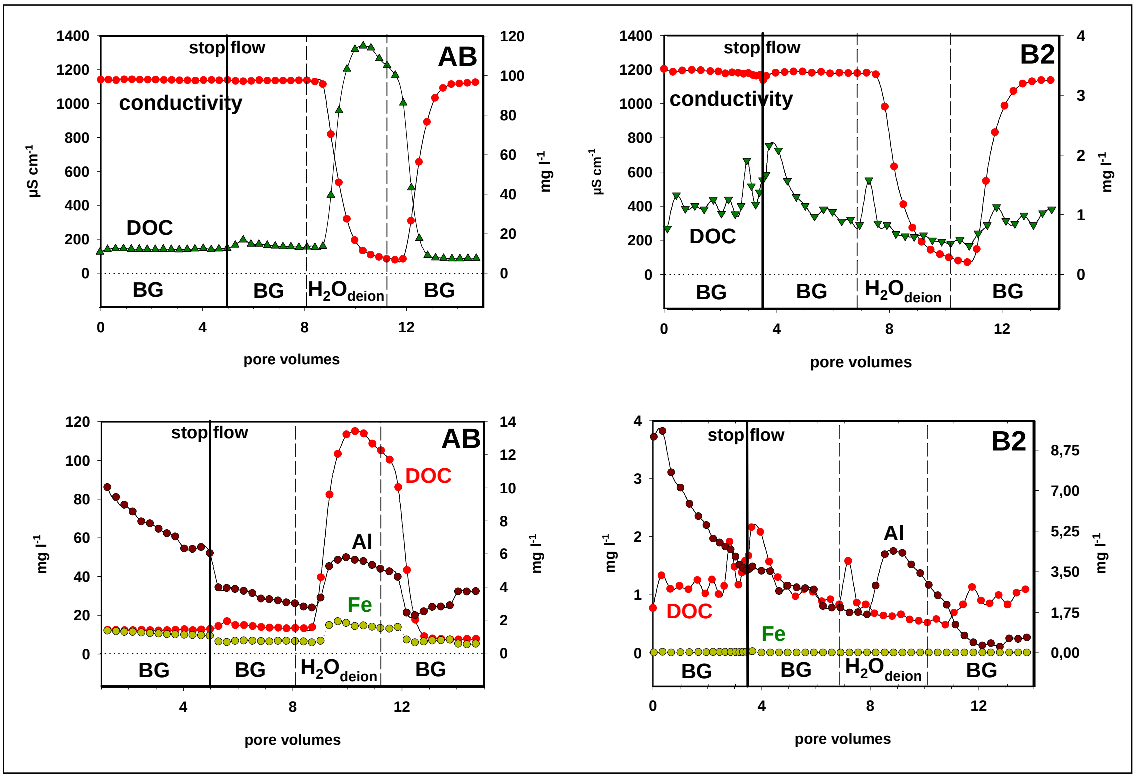

Fig. 31: Results of the column experiments (BG = background solution).

5.2.7 Implications for soil classification

Except for the CB, all horizons in the Lame Goempa soil meet most of the requirements for spodic and andic features in Soil Taxonomy (Soil Survey Staff 1999) and WRB (ISSS 1998) including horizon thickness, $Al_o + ½Fe_o > 0.5$ or $> 2\%$, $pH_{H2O} < 5.9$, $C_{org} \geq 0.6$ and $\leq 25\%$, ODOE > 0.25, bulk density ≤ 0.90 g cm^{-3}, and P retention > 70 or 85%. However, these soils have unusual features with regard to both podzolisation and andosolisation. In both cases the colour requirements are not fulfilled. Visible eluvial and illuvial horizons could be identified neither in the field by colour and structure, nor by chemical analyses. There is no albic horizon, and no second maximum of organic carbon commonly used to separate Andosols from Podzols in contentious cases. Sand grains without humus or sesquioxide coatings, or cracked coatings on sand grains could not be identified.

Translocation of Al and DOM, however, is indicated by the column experiments. This is typical for podzolisation, and defined critical levels for precipitation of translocated Fe- and Al-humus complexes appear to be exceeded in the subsoil horizons. Minor translocation may also occur during andosolisation, and its occurrence is not yet a criterion for exclusion from the Andosols/Andisols. Clay migration and clay coatings, which were found in the B horizons, are also not usually thought to occur in Andosols and Podzols *sensu stricto*, and clay contents of between 40-50% – even if partially an artefact as dicussed above – might be too high to hold favourable conditions for podzolisation. However, Podzols with textures finer than normal have been noted under montane forest, e.g. in the Bavarian Alps (Bäumler 1995) and in Taiwan (Li et al. 1998).

Surface area measurements provide little further information. Both, Podzols and Andosols generally have maxima in their B horizons caused either by illuviation or by in-situ weathering with the formation of short range order or amorphous materials, especially oxidic iron compounds. The obviously high degree of weathering, which has similarly been detected in non-volcanic Andosols of East Nepal, is not in line with the general concepts of the formation of Andisols/Andosols and Podzols/Spodosols.

The Lame Goempa and similar soils most probably tend to have alu-andic properties characterised by a dominance of Al-humus complexes, as neither short range order minerals nor volcanic glass have been identified up to now. However, the results indicate that the role of Fe might have been underestimated so far. For non-volcanic and most probably non-allophanic andic features I concur with Adjadeh & Inoue (1999), that the (Al_o + ½Fe_o) requirement should be omitted, although the implications of this still have to be studied in detail. Any references on Al_p should also be dropped, because of the defects of the pyrophosphate extraction method (Bäumler & Zech 1994a; Kaiser & Zech 1996; Poulenard & Herbillon 2000).

Another point of discussion are the different climatic conditions at the sites where non-volcanic andic soils have been described, including the southern slopes of the Himalayas (*Table 2*, page 17). Most are characterized by humid conditions to some extent. A dry season, however, e.g. monsoon climate, might cause ageing of amorphous materials, and is thus not favourable for the preservation of andic features (Duchaufour 1982). But this has to be seen in connection with inhibition of ageing or crystallisation of iron oxides as well as allophane and imogolite type alumino-silicates by soil organic matter (Schwertmann 1966, Shoji & Ono 1978, Huang 1991), and/or by the formation of metal-organic complexes. These complexes also stabilise the organic matter against biodecay and further translocation (Blaser & Klemmedson 1987, Aran et al. 1998).

Besides present climatic conditions – and this connects to the following chapter – it can be discussed in how far palaeoclimatic aspects might have been necessarily involved in the formation of non-volcanic Andosols. The present occurrence of this soil type within Bhutan is restricted to altitudes of between 2,200 and 3,500 m a.s.l., and therein to areas which have neither been directly influenced by glaciation (see Section 2.3) nor by fluvial sedimentation. We may therefore interpret the geographical extension of these soils as indication that glaciers at the southern slopes of the Eastern Himalayas did not exceed below 3,500 m a.s.l. during the local Last Glacial Maximum (LGM). At that time, the periglacial environment may have contributed to the formation of these soils, but the extent and the possible mechanisms have to remain largely unclear at present.

6 Indicative value of Bhutanese soils for landscape history and palaeoclimate

Among the many natural archives from which palaeoclimatic records may be extracted, soils have the advantage of being small-scale local indicators. This however requires that soil materials of a certain age are present – which is not self-evident within a dynamic landscape such as Bhutan's – and that the available information can be read and interpreted.

This section describes two different approaches from Central Bhutan. Firstly, the morphological findings and profile stratifications in Phobjikha Valley (see Section 5.1) are used to build a tentative local Quaternary chronology. The second study introduces a chronosequence of 28 river terraces along the Chamkhar Chhu river. As a means of relative dating, weathering indices have been calculated on the basis of detailed pedochemical analyses. Radiocarbon dates from selected buried topsoils of both study areas provide valuable additional information.

6.1 Indications from Phobjikha Valley, western Central Bhutan

The major pedogenic, geomorphic and sedimentary processes of this study area have been highlighted in Section 5.1. Now it shall be discussed in how far indications of large-scale climatic changes can be distilled from the available data. The basic idea behind this task is that – in the redistribution of local, silt-sized sediments – climatic changes will directly affect the balance between rates of silt accumulation and chemical weathering. The stratification of Phobjikha's soils may therefore provide pointers to palaeoclimatic changes on the southern slopes of the Eastern Himalayas. Within the framework of this study, extensive dating of organic and inorganic soil materials has not been possible. The chronology suggested in this section must therefore remain preliminary and speculative.

In connection with the building of a regional Quaternary chronology, the possibility of glaciation during Late Pleistocene is an essential consideration. The smooth, gentlysloped landforms and the abundance of sediments within the study area have encouraged previous assumptions of glacial origin. Basin-like structures of several hundred metres diameter in the upper part of Thang/Hal side valley and to the north of Kumbu Goempa, may indeed be glacial cirques (*Fig. 10*, page 25). At the base of the profiles PK 143 and PK 150, grey-coloured, sandy-gravelly horizons represent fluvial sediments lying on top of the weathered parent material. This suggests accumulation during phases of intensive precipitation and massive fluvial sediment transport, but the time of their formation remains unclear. The subsoils of PK 143, PK 150 and PK 151, together with other horizons of predominantly fluvial origin, form a clearly separated common group in the cluster analysis (*Fig. 24*, page 73). Their clay fractions contain gibbsite, which usually indicates strong and prolonged leaching conditions. The presence of gibbsite-bearing Pleistocene fluvial sediments suggests the absence of glaciers during the Last Glacial Maximum (LGM), because they would have eroded these materials. This hypothesis is weakened by the fact that – in case of Andosols – gibbsite formation may happen within a few hundred to a few thousand years by transformation of short-range order minerals or precipitation from soil solution in deeper parts of the profile (Huang et al. 2002). The findings therefore cannot completely discount cirque glaciation with small tongues advancing into the valley system. However, our insights from Central Bhutan (Caspari et al. 2004b) and observations by other authors working in Bhutan corroborate the idea that the glaciation during the LGM did not extend below 3,500 m a.s.l., and that the morphology of Phobjikha Valley was consequently shaped by weathering and aeolian processes rather than glacial abrasion. For the NW Himalayas, Holmes & Street-Perrott (1989) concluded that glacial advances in Kashmir were less extensive than previously assumed and that local sediments resulting from mass movements – similar to those in Phobjikha Valley – had been misinterpreted as moraines and glacial outwash.

If not influenced by glacial activities directly, Phobjikha Valley was certainly part of a *peri*glacial environment. Indications are present in the form of debris slopes on ridge lines above 3,500 m a.s.l. and the asymmetric shapes of the lateral valleys. Clearest evidence, however, are the massive loess-like sediments themselves. As explained above, I assume that they formed during Pleistocene and Holocene as a result of wind-driven redistribution of local silty sediments. During and in the aftermath of the LGM, decreased precipitation and a lack of vegetation would have provided ideal conditions for this process. Evidence from Greenland ice cores shows that the atmosphere around 18,000 years BP was forty times dustier than today (Taylor et al. 1993). Within the uppermost parts of these massive aeolian sediments, we find the buried topsoils, indicating a period of advanced soil development under wetter and warmer climate than today. Judging from the sharpness of the horizon boundaries, this change must have been abrupt, rather than gradual. The two ^{14}C ages of 1,667 ± 19 and 2,024 ± 20 years BP allocate the decline of the associated vegetation, i.e. the end of this soil forming period to be around 2,000 years ago, suggesting a formation of the buried topsoils during the Middle Holocene climate optimum. These radiocarbon data represent minimum ages, but correspond well with buried topsoil ages from the 85 m alluvial terrace in the Bumthang Valley, Central Bhutan (2B horizon: 1,715 years BP, Caspari et al. 2004b), glacial sediments in NW Bhutan (top and bottom of 2A horizon: 1,690 and 2,080 years BP, Iwata et al. 2002b) and a buried peat layer sampled in Lake Kyopreng, Modi Khola Valley, Central Nepal and dated to 1,938 ± 132 years BP (Zech et al. 2001).

Following the Middle Holocene climate optimum, conditions for plant growth became less favourable. From deposits overlying palaeosols in the Thakkhola Basin, Central Nepal, Saijo & Tanaka (2002) concluded stronger summer monsoon and increased rainfall during 6,200 and 4,500 ^{14}C yr BP, followed by drier climate, decreased vegetation cover and accelerated transportation of surface material. Lehmkuhl et al. (2000) inferred cooler conditions from 3,000 years BP from glacier advances in South Tibet. Caine et al. (1982) and Yasuda & Tabata (1988) describe similar conditions for adjacent regions.

Gardner & Rendell (1994) list human activity among the variables within their loess cycle concept. And Lehmkuhl et al. (2000) point out that it is sometimes impossible to distinguish between anthropogenic and climatic influences on the palaeoecological environment during the Late Holocene. The occurrence of charcoal in the stratigraphic surrounding of the buried topsoils in Phobjikha suggests larger-scale anthropogenic deforestation in combination with slash-and-burn agriculture, starting from at least 2,000 years BP. Charcoal-bearing buried soil horizons are also common in Central and East Nepal, and in South-East Tibet (Saijo & Tanaka 2002).

The drier climate in combination with increasing human activities would have hampered humus accumulation and strengthened aeolian processes, resulting in a gradual re-establishment of wind-induced local sediment transport, which is still active today. In protected sites, the topsoils are not buried. Profile PK 155 e.g., situated under natural forest, has no fossil A horizon and its current topsoil has the highest C_{org} content within the data set. This might represent what would have been an extensive soil type within the study area in the absence of human disturbance.

6.2 Indications from Bumthang Valley, eastern Central Bhutan

6.2.1 Site description

The study area is located at 27°37’N and 90°42’E, along the Chamkhar Chhu river between the villages Thangbi and Go’ling in Bumthang District, eastern Central Bhutan (*Fig. 8*, page 23; *Fig. 9*). The site is approximately 10 km north of the river terraces examined by Gurung (2001). The Bumthang area is part of the Bhutanese Inner Valleys (Norbu et al. 2003a) and is characterised by comparatively flat, basin-like sections with straight or concave lower slopes. Like in other intramontane basins, the speed of the river is reduced and large volumes of sediments have been deposited over long time periods.

Within the field area, the present river is at 2,655 m a.s.l., and a German-Bhutanese expedition in 2000 found associated fluvial and fluvioglacial terraces rising to at least 266 meters above this level. Additional terraces were identified in 2002 within the same valley near the Kiki La pass about 20 km south of the study area, which are 280 m, 305 m, 318 m, 330 m, 345 m and 364 m above the recent river level. However they are not included in the present study.

Land use ranges from arable (lower terraces) through pasture (middle terraces) to natural blue pine forest (*Pinus wallichiana*), which is used for firewood and timber. Barley, wheat and buckwheat are the staple crops in the cool temperate climate with mean temperatures of 4.0°C in December/January and 17.5°C from June-August. The mean annual rainfall is about 800 mm, of which 75% precipitate during the monsoon, i.e. June-September, mostly as falls of low or moderate intensity (RGoB 1998, 2003).

According to the most recent geological summary based on field data of the Geological Surveys of India and Bhutan (Bhargava 1995), the site is underlain by rocks of the Thimphu Group. This group consists of highly metamorphosed rocks, mainly gneiss, some of which is granitic, with mixed muscovite and biotite micas, plagioclase feldspars and quartz as the main minerals (see Section 1.1.4). The deposits of the studied terrace system consist of well-rounded leucogranite boulders and granitic gneiss having been deposited after longer-distance transport. Gurung (2001) identified gneiss, granite and granitic gneiss as the main country rocks in his field area.

6.2.2 Field observations and selected profiles

The field studies in 2000 and 2002 showed that the Thangbi terrace system consists of at least 28 associated river terraces (*Fig. 9*, page 24). In terms of terrace morphology, it clearly falls into two main sections: The first comprises terrace 1 up to terrace 7 (T1-T7), and consists of horizontal terraces with clear edges and sharp steps. Little weathered material, including huge blocks stemming from catastrophic floods, can be observed frequently. Relative terrace heights at the study site are at 4 m, 9 m, 17 m, 27 m, 30 m, 34 m, and 41 m, and the land is mainly used for arable farming.

The second part of the system consists of terrace 8 and all terraces upslope (T8-T28). Here, we find inclined terraces with unclear steps and rounded edges. The parent material consists of intensively weathered but highly rounded and clearly alluvial gravels. Pasture and forest are the main land use forms. Relative terrace heights are at 57 m, 74 m, 86 m, 94 m, 104 m, 113 m, 118 m, 126 m, 130 m, 136 m, 144 m, 153 m, 160 m, 167 m, 176 m, 191 m, 202 m, 211 m, 222 m, 230 m, and 266 m, including additional intermediate sublevels.

This division initially suggests that the sediments forming the lower terraces (T1-T7) were deposited at the end of and after the last main glacial period in this area, and have not since been significantly disrupted by periglacial processes. The highest of these younger terraces, T7, is more than 500 m wide and is suggested to represent the sediments accumulated during the last main melting period of glaciers in northern Bumthang (*Fig. 32*, *Fig. 33*). On the basis of embedded driftwood, the terrace has been dated to 27,340 ± 180 years BP by Gurung (2001).

Fig. 32: The Thangbi river terrace system; view from the T10 terrace onto the main terrace (T7). The Chamkhar Chhu river is located near the lower edge of the forest. View is upstream (from S to N).

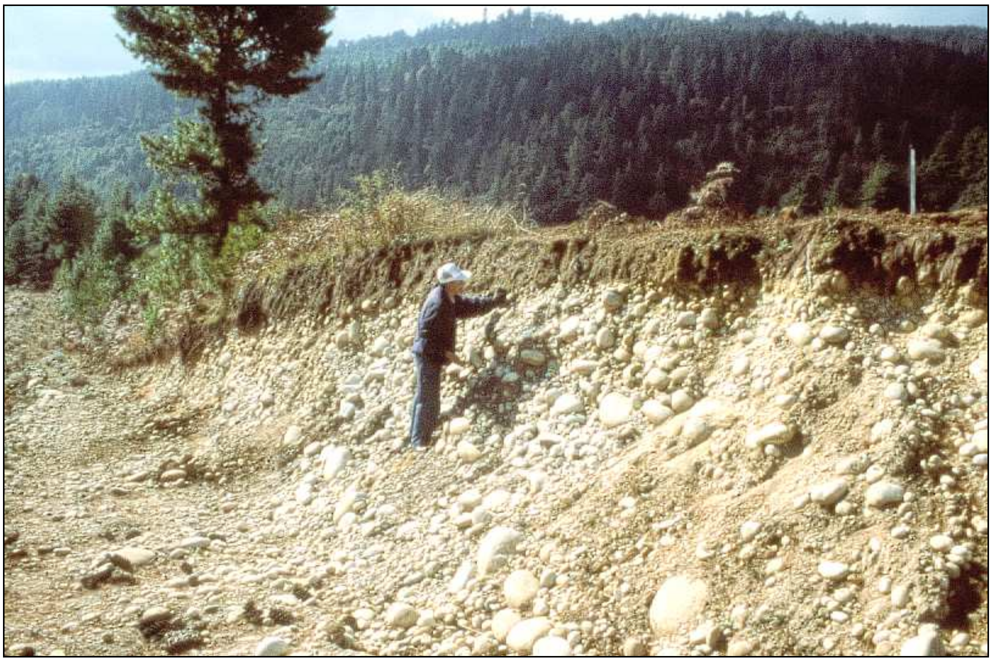

Fig. 33: Leucogranite boulders forming the sediments of the main terrace (T7) at 40 m relative height above the current riverbed.

All terraces above T7 are older and show clear signs of periglacial processes such as solifluction and several generations of re-worked loess covers. Fossil ice wedges were observed at the roadcuts around Kiki La pass. This indicates that these terraces were deposited before and overlaid during the last main glacial period in this area. Gurung (2001) has dated carboniferous debris on top of Terrace V (at approx. 2,640 m a.s.l. and 10 km south of our study area) at 65-70 m above the current riverbed, which corresponds to our T8 or T9 level. He found 29,940 ± 180 years BP, which evidences increasing age of the terrace materials with increasing elevation above the riverbed. It is interesting to note that this site forms the lower end of a slope with massive debris flow deposits, on whose upper reaches the Lame Goempa site (3,025 m a.s.l.) is located, where the non-volcanic Andosol samples discussed in Section 5.2 stem from. This again highlights the extraordinarily high age of the materials involved and the periglacial influence during the formation of these soils.

Aeolian sediments are missing on all terraces below T7. This suggests that last major loess deposits within the study area occurred during Late Pleistocene or Early Holocene, and that most of the polygenesis observed results from re-working of local materials (solifluction) during colder Holocene periods. *Table 20* summarises the field descriptions of the profiles T4 and T19 as examples of the soils on the young and the old terraces, respectively. Silt and clay contents generally *in*crease with *in*creasing height of the terrace above the current river level. This is accompanied by more strongly developed pedal structures in the upper part of the system.

In autumn 2000, 18 profile pits were sited so as to cover the whole range of the terrace system (*Fig. 9*, page 24). Six typical profiles have been selected for discussion, including PT 036 (T4), PT 039 (T7), PT 049 (T10), PT 043 (T17), PT 042 (T19) and PT 041 (T28). *Fig. 34* depicts the location and main morphological features of the six profiles. In general, the older terraces show much deeper B horizons. The soils on the upper terraces also have one or more buried topsoils, manifest as darker colours and lower bulk densities. Among the whole set of 18 profiles, the only ones to show the characteristics of a Bt horizon, were located on the terraces T19 (153 m, PT 042) and T20 (160 m, PT 040). In both cases, the Bt occurs beneath a buried A horizon, which indicates a period of pedogenic stability and a long interruption in sedimentation.

Increases in clay content with depth appear to be mainly due to in-situ weathering and the complex histories of alluvial, aeolian and periglacial deposition, rather than argilluviation. However, some clay translocation has been noted in similar Bhutanese soils (Baillie et al. 2004).

Table 20: Profile descriptions of the soils on terraces T4 (PT 036) and T19 (PT 042).

T4, lower terrace soil (27 m terrace) 27°37’N, 90°42’E; 2,682 m a.s.l.; arable (wheat) Endoskeleti-eutric Cambisol		T19, upper terrace soil (153 m terrace) 27°36’N, 90°42’E; 2,808 m a.s.l.; pasture (cattle) Hapli-eutric Cambisol	
0-16 cm (A)	10YR 3/3; sandy loam; subangular to platy; slightly moist; few fine pores; common fine roots; granite gravels, many well-rounded, partly weathered boulders throughout the whole profile; diffuse boundary	0-20 cm (A)	10YR 3/4; clay loam, probably aeolian sediment; friable consistence; almost dry; common fine pores; common medium and fine roots; no stones; diffuse boundary
16-28 (B1)	10YR 4/3; sandy loam; subangular; almost dry; few fine pores; few fine roots; frequent quartz stones; diffuse boundary	20-47 (B1)	10YR 4/4; sandy loam, probably aeolian sediment; subangular blocky; almost dry; common fine pores; few medium and fine roots; no stones; diffuse boundary
28-39 (B2)	10YR 3/4; sandy loam; subangular; almost dry; few fine pores; very few fine roots; few quartzitic gravels; clear wavy boundary	47-118 (2B2)	2.5Y 5/4; sandy loam, probably solifluction layer; subangular to platy; almost dry; few fine pores; very few fine and medium roots; few stones from granite, gneiss, quartzite and amphibolite; diffuse boundary
39-64 (CB)	2.5Y 6/3; sand; single grain structure; almost dry; few fine pores; very few fine roots; granitic gneiss; clear wavy boundary	118-190 (2B3)	10YR 5/4; sandy clay loam; subangular to platy; almost dry; few fine pores; very few fine roots; very few stones; diffuse boundary
64-90+ (C)	2.5Y 7/4; sand; granitic parent material weathered to single grain structure; almost dry; very few fine pores; no roots	190-230 (2B4)	10YR 4/4; silty loam; subangular to polyhedral; almost dry; common fine pores; no roots; very few stones; diffuse boundary
		230-295 (2B5)	10YR 4/4; sandy clay loam; subangular blocky; almost dry; common fine pores; no roots; very few stones; clear horizontal boundary
		295-305 (3A)	10YR 3/3; silty loam; subangular blocky; clay skins; almost dry; common fine pores; no roots; very few stones; clear horizontal boundary
		305-380 (3Bt)	10YR 5/8; clay loam; subangular to polyhedral; clay skins; almost dry; common fine pores; no roots; very few stones; diffuse boundary
		380+ (3C)	weathered parent material; not sampled

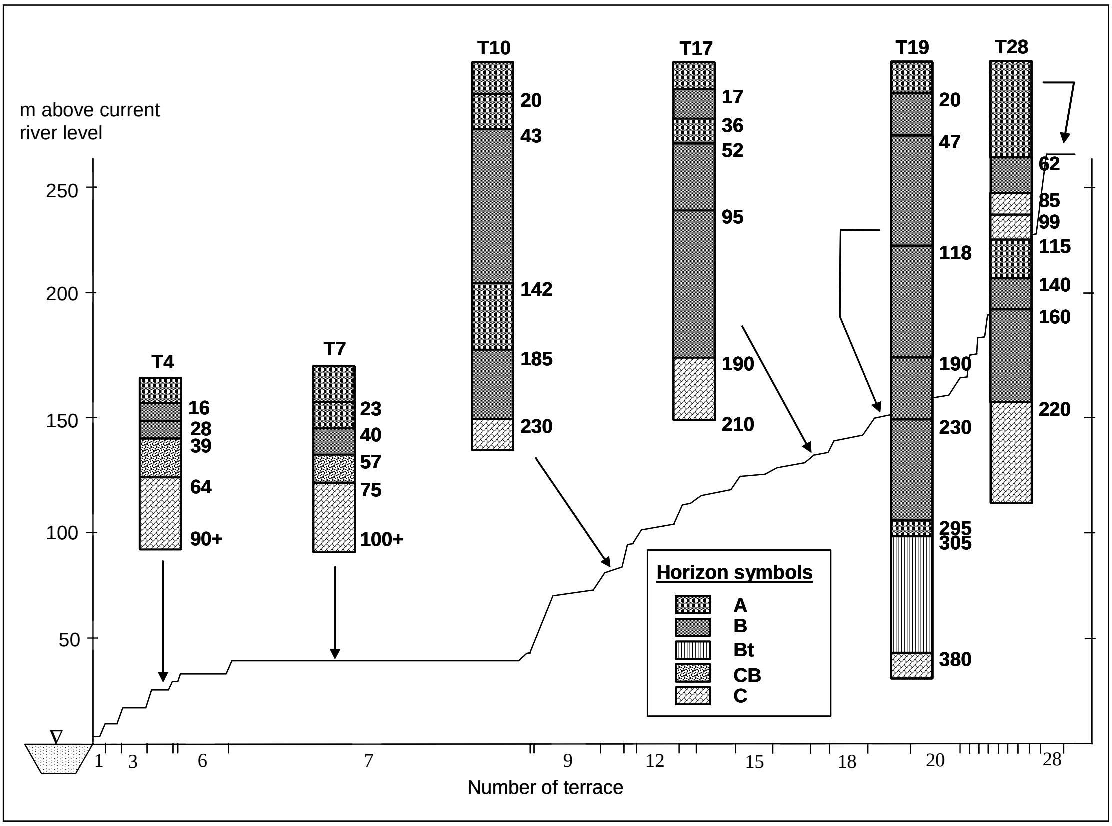

Fig. 34: Selected standard profiles and their horizon designations after ISSS (1998); arrows show the location of the sampling sites within the terrace system; numbers indicate horizon boundaries in cm below the surface.

6.2.3 Basic laboratory analyses

Analytical data for the selected profiles are summarised in *Table 21*. The depth functions of base status indicators and organic carbon content (C_{org}) for an exemplary profile (T19, PT 042) are shown in *Fig. 35*. pH values are low throughout, reflecting the felsic origins of the granitic alluvial and gneissic periglacial deposits. All samples are carbonate-free. The organic C profile shows a significant increase at about 3 m, which confirms the field indications of a deeply buried fossil topsoil. At the same depth, the N_{tot} profile only shows a minor bulge, possibly because of N losses since burial or because of the nature of the original litter. Within the terrace system, there is no significant increase of C or N values with increasing height above the current river level. The CEC values are low throughout, mostly below 6 $cmol_c$ kg^{-1}. This reflects the soil's coarse texture but the values are still low for soils with presumed illitic and micaceous clays. This points to a dominance of low activity clays. In *Fig. 35*, the maxima of the CEC profile correspond with those for organic C and confirm the existence of a buried palaeosol. The intermediate maximum at approximately 2 m corresponds to increasing clay contents. Bulk densities are generally low and range from 0.8-1.5 g cm^{-3}. These low values may reflect the aeolian origin of some of the sediments.

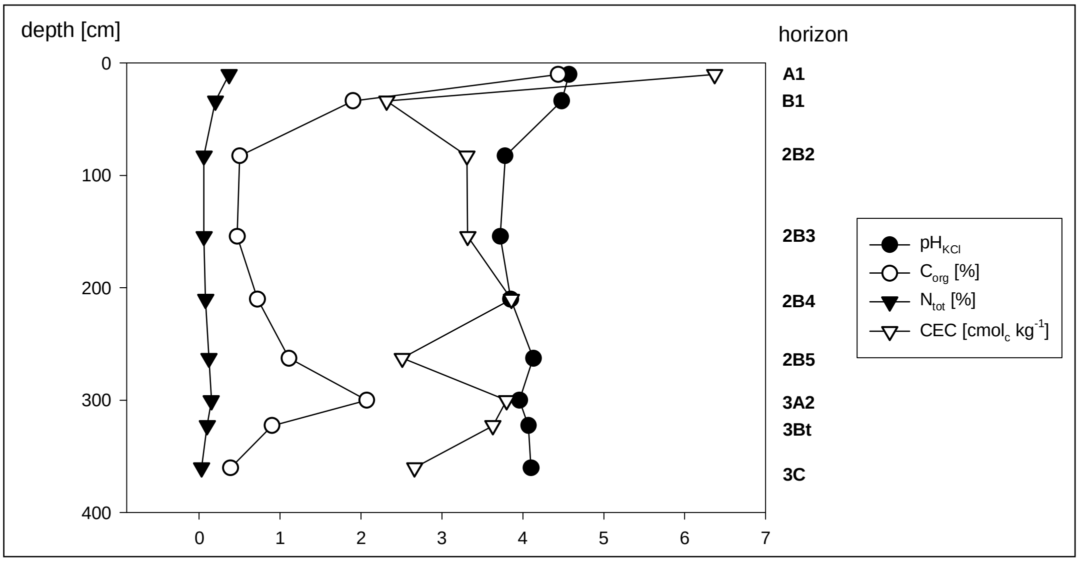

Fig. 35: Depth functions of pH_{KCl}, C_{org}, N_{tot} and CEC for profile PT 042 (T19).

Following the WRB classification, most soils are identified as Cambisols. Whereas some of the lower terraces showed partly skeletic properties, the soils in the upper parts of the terrace system appear to be more intensively weathered. However, the WRB classification – like many profile-based systems – takes insufficient account of the polygenetic structure of the solum. Polygenesis has been detected on the main terrace, T7, and for all terraces upslope. This shows that during the formation of the terrace system, soil development was interrupted several times. Besides the continuous and low intensity slope processes, sediments might have been deposited during or immediately after high intensity events such as earthquakes or glacial lake outbursts. Periglacial processes during colder periods resulted in solifluction layers and the deposition of aeolian material.

Table 21: Selected analytical data of six typical profiles.

profile/ horizon	depth [cm]	bulk density [$g\ cm^{-3}$]	pH_{H2O}	C_{org} [%]	CEC [$cmol_c\ kg^{-1}$]	Fe_d	Fe_o	Al_d	Al_o	sand, silt, clay [%]	surface area [$m^2\ g^{-1}$]
						[$g\ kg^{-1}$]					
T4, PT 036, 27 m above the current river level											
A	0-16	1.3	5.4	1.8	4.8	5.8	3.4	1.1	1.8	54, 22, 24	6.0
B1	16-28	1.2	5.6	1.1	4.5	4.7	3.2	1.2	2.0	53, 24, 23	7.9
B2	28-39	1.2	5.8	0.7	3.3	3.2	2.2	1.0	1.5	67, 19, 14	6.1
BC	39-64	1.3	6.1	0.1	1.1	0.7	0.6	0.3	0.5	88, 6, 6	1.9
C	64-90+	1.3	6.2	0.1	0.5	0.4	0.4	0.2	0.4	90, 4, 6	1.2
T7, PT 039, 40 m above the current river level											
A	0-23	-	5.2	2.9	2.9	5.5	3.3	5.0	9.5	46, 35, 19	7.5
2A	23-40	-	5.8	1.7	3.1	3.3	1.5	4.0	7.8	49, 34, 17	8.2
2B	40-57	-	5.8	0.9	1.2	2.3	1.1	2.1	10.2	80, 14, 6	1.8
2CB	57-75	-	5.9	0.5	0.7	1.8	0.6	1.3	9.0	85, 8, 7	1.2
2C	75-100+	-	5.9	0.1	0.4	1.3	0.2	0.6	2.5	89, 5, 6	1.2
T10, PT 049, 85 m above the current river level											
A	0-20	1.0	5.4	3.3	4.1	5.4	4.0	4.5	6.9	49, 35, 16	9.3
2A2	20-43	1.0	5.5	2.3	3.4	5.8	4.1	4.0	5.6	49, 30, 21	10.3
2B	43-142	1.3	5.6	0.4	3.0	7.3	4.1	2.2	2.7	48, 30, 22	18.6
3A3	142-185	1.1	5.6	0.9	1.6	8.5	4.7	3.7	5.8	49, 30, 21	18.1
3B	185-230	1.2	6.1	0.2	4.2	7.2	1.9	2.1	1.1	62, 28, 10	16.3
3C	230+	-	6.2	0.1	6.3	8.5	1.9	1.5	1.3	69, 24, 7	15.2
T17, PT 043, 136 m above the current river level											
A	0-17	0.8	5.4	3.1	2.5	9.7	4.2	3.8	7.6	50, 30, 20	11.0
B1	17-36	0.9	5.5	2.0	2.5	9.1	4.2	3.5	5.4	49, 32, 19	12.6
2A	36-52	1.1	5.5	1.1	3.3	10.1	4.2	2.5	2.5	50, 29, 21	14.0
2B2	52-95	1.3	5.4	0.6	3.5	9.4	3.9	2.1	1.8	51, 29, 20	13.4
2B3	95-190	1.3	5.5	0.5	3.7	9.6	3.8	2.2	1.7	51, 29, 20	13.9
2C	190-210	-	5.9	0.1	3.9	4.5	0.9	0.9	1.5	81, 12, 7	3.5
T19, PT 042, 153 m above the current river level											
A	0-20	0.9	5.5	4.4	6.4	7.3	3.7	4.4	7.6	51, 26, 23	8.4
B1	20-47	1.0	5.7	1.9	2.3	9.5	3.7	3.0	6.1	55, 2, 18	10.7
2B2	47-118	1.3	5.8	0.5	3.3	8.8	4.0	1.4	1.1	53, 26, 21	11.2
2B3	118-190	1.4	5.7	0.5	3.3	13.0	3.7	2.3	1.4	52, 26, 22	16.0
2B4	190-230	1.3	5.3	0.7	3.9	15.5	4.6	3.1	2.5	46, 29, 25	18.7
2B5	230-295	1.1	5.3	1.1	2.5	12.9	5.4	4.7	6.0	42, 32, 26	20.9
3A	295-305	0.9	5.4	2.1	3.8	17.7	9.2	5.2	5.5	27, 35, 38	23.4
3Bt	305-380	1.0	5.4	0.9	3.6	22.5	8.9	4.8	4.6	22, 36, 42	33.6
3C	380+	-	5.4	0.4	2.7	12.9	4.1	2.4	2.0	47, 30, 23	17.8
T28, PT 041, 266 m above the current river level											
A	0-62	0.8	5.7	2.3	1.2	18.8	4.5	4.5	11.7	25, 40, 35	35.0
B	62-85	1.0	5.6	1.4	2.7	15.3	5.8	3.5	4.6	28, 42, 30	29.6
C	85-99	1.0	5.8	0.7	1.9	7.7	3.0	1.8	2.3	52, 29, 19	18.7
2C	99-115	1.3	5.9	0.3	1.2	8.1	1.8	1.3	1.3	69, 20, 11	11.0
3A	115-140	0.9	5.8	1.6	2.7	29.6	10.7	6.4	6.3	14, 42, 44	43.9
3B2	140-160	1.0	5.9	0.4	2.9	25.9	3.5	5.7	2.6	19, 38, 43	43.0
3B3	160-220	1.2	6.0	0.3	2.4	14.7	2.5	3.0	1.8	30, 37, 33	33.0
3C	220-265+	1.4	6.1	0.1	1.6	7.0	1.5	2.4	1.2	60, 24, 16	15.8

6.2.4 Radiocarbon dating

Table 22 summarises the AMS ^{14}C dating results and their interpretation. Translocation of organic material is a common process in the soils of this part of Bhutan (Baillie et al. 2004), so that younger C-containing material can infiltrate the sampled horizons from the overlying A horizon(s). The ages therefore represent the minima for the main phases of pedogenesis and are most probably underestimates for the ages of the parent materials.

Table 22: Results and interpretation of AMS ^{14}C dating of selected horizons; conventional age according to Stuiver & Polach (1977).

Terrace	Sample	Horizon	Conventional radiocarbon age	Interpretation
T19	PT 042/8 KIA14502	3Bt	10,175 ± 60 BP	Soil formed during temperature fluctuations in the Younger Dryas (Zhisheng et al. 1993, Zhou et al. 1996)
T28	PT 041/6 KIA14503	3B2	8,710 ± 55 BP	Fairly warm and moist conditions during Early Holocene, but still before the climate optimum (Winkler & Wang 1993)
T9	PT 050/X KIA14500	2B	4,055 ± 30 BP	Mid to Late Holocene cooling period (4,000-3,000 BP); solifluction and distinct redistribution of aeolian sediments all over Central and High Asia (Bäumler 2001a)
T10	PT 049/4 KIA14501	3A3	1,715 ± 25 BP	Probably marking another period of temperature fluctuations accompanied by enhanced solifluction during the Subatlantic period (Late Holocene)

Lehmkuhl & Haselein (2000) mention three major intervals of Holocene soil formation from the neighbouring Tibetan Loess Plateau (4,000-4,500 m a.s.l.): 9,900-8,000 years BP, 7,400-4,600 years BP and 3,400-2,000 years BP. This suggests that – compared to the study area – pedogenesis on the Tibetan Plateau was interrupted several hundred years earlier each time, which can be explained by the higher elevation of Tibet and the regional variations in monsoonal climate. Saijo & Tanaka (2002) also mention mid-Holocene (6,200-4,500 years BP) palaeosol formation from the Nepalese Thakkhola Basin at elevations of 2,770-3,860 m a.s.l.. The youngest conventional ^{14}C age for the soil on T10 (1,715 ± 25 BP) is in accordance with the findings of Iwata et al. (2002b) close to Raphsthreng, North Bhutan at approximately 4,400 m a.s.l.. They dated humic soil materials covered by 0.4 m of moraine material to 1,690 ± 40 and 2,080 ± 40 ^{14}C years BP.

The ^{14}C datings of Gurung (2001) mentioned above are clearly higher, however not in contrast to ours. Whereas his findings refer to woody debris as part of the alluvial sedimentation, our dating is based on the C_{org} accumulated during post-alluvial pedogenesis. Gurung's data suggest that the retreat or melting of the source glaciers in our study area began earlier than the conventional global LGM (18-25 ka). The almost ideally rounded granite boulders which constitute the terrace deposits must result from longer-distance transport and therefore indicate that at this time, the maximum extent of the glaciers was still several decakilometres upstream of the study area. According to geological mapping (Gansser 1983, RGoB 2001b), the leucogranites outcrop 50 km north of our study area at approximately 4,500 m a.s.l..

6.2.5 Pedogenic indicators of relative dating

Fig. 36 depicts the whole-profile weighted mean particle size distribution for all analysed profiles. As indicated by the grey arrow, a trend from more sandy soils close to the river to more silty/clayey soils on higher terraces is evidenced. There is a significant positive correlation between relative height above the river versus clay+silt ($r^2 = 0.50^{**}$).

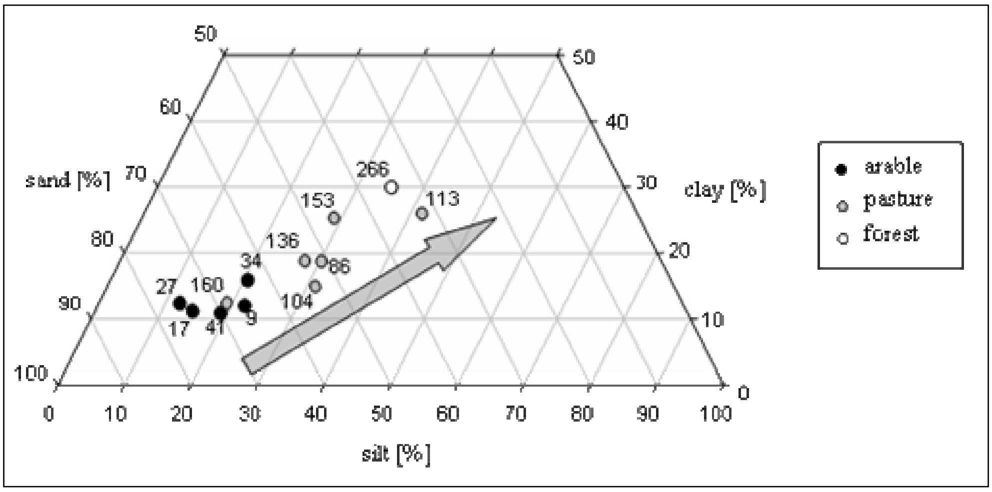

Fig. 36: Ternary plot showing whole-profile weighted means of particle size distributions; numbers indicate altitude of the terraces in m above the current river level.

Terrace T20, which is at 160 m above the current river level does not fit into the general pattern. It is located at the foot of the steepest part of the terrace system (*Fig. 34*, page

103), and has probably received coarser textured and less weathered material from upslope, or it is simply more eroded in comparison to the other terraces.

The observed correlation is not necessarily evidence for increasing weathering intensity with increasing relative height above the current river level. Older sediments might have already been finer or "pre-weathered" at the time of their deposition (Bäumler 2001b), and can therefore significantly influence the results for the profile-weighted means which do not take account of individual horizons or genetic units.

The results for the whole-profile weighted means of specific surface area (*Fig. 37*) of the < 2 mm fraction show a similar pattern. Increasing surface area with increasing terrace level can be taken as another proof for more pronounced weathering upslope. The correlation of the weighted mean clay contents against the surface area measurements produces a highly significant correlation ($r^2 = 0.96^{***}$).

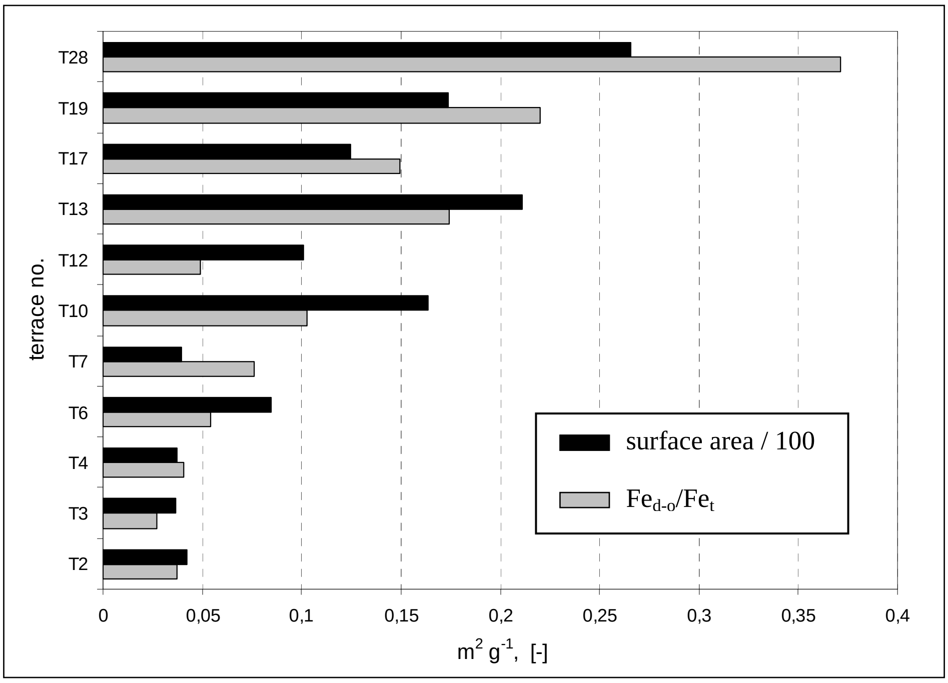

Fig. 37: Whole-profile weighted means of surface area and Fe index for selected profiles; Fe index = ratio of well-crystallised iron oxides (Fe_{d-o}) to total iron content (Fe_t).

Besides the neo- and transformation of silicate minerals, the transformation of iron components represents a reliable indicator for the state of pedogenesis. During weathering, iron is released, oxidised and – after some time as poorly crystallised oxidic compounds – finally transformed into well-crystallised Fe compounds. Within the study area, the percentage of silicate-bound iron steadily *de*creases with *in*creasing elevation above the river, whereas well-crystallised iron oxides (Fe_{d-o}) *in*crease (*Table 21, Fig. 38*). There are almost constant Fe_o values over time, which indicates that we observe a state of equilibrium between the rate of Fe release from silicate weathering, the formation of Fe_o and the subsequent crystallisation to Fe_{d-o}. The iron oxide-based weathering index, Fe_{d-o}/Fe_t, is also plotted in *Fig. 37*. It shows a continuous increase from less weathered sites in the lower part of the terrace system to more strongly weathered terraces upslope. Terraces T12 and T20 do not follow the general trend, which is also observed in case of the particle size distribution (*Fig. 36*).

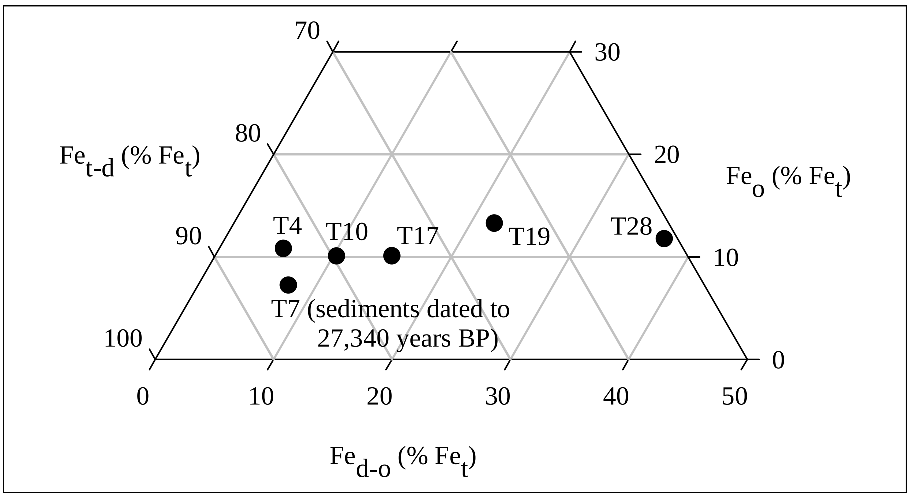

Fig. 38: Whole-profile weighted means of silicate-bond iron (Fe_{t-d}), well-crystallised Fe oxides (Fe_{d-o}) and poorly crystallised oxidic Fe compounds (Fe_o), plotted as percentage of total iron (Fe_t).

Other elements can also be used to trace the course of weathering. Parker's (1970) weathering index uses the unequal release and leaching of sodium, potassium, calcium and magnesium during weathering. *Fig. 39* shows that the lower terraces have the highest values (= least weathering), but the increase with height is irregular.

XRD analyses of the clay fractions also indicate the intensity of soil development and its trend within the terrace system (*Fig. 40*). The dominant phyllosilicate is kaolinite, which is sharply peaked in all samples, including the lowest terraces. Besides in-situ weathering, some of the kaolinite is presumably inherited from the alluvium, at least at the lower sites. The synoptic illustration elucidates the alteration of illite to interstratified minerals and to hydroxy-Al interlayered minerals and pedogenic chlorite with increasing height above the current riverbed. This supports the findings of Bäumler et al. (1997), who observed similar mineralogical changes in a soil chronosequence in moraine deposits of Central Nepal. The ordinate values of the XRD plots can also be taken as a measure for the degree of crystallisation and therefore relative age.

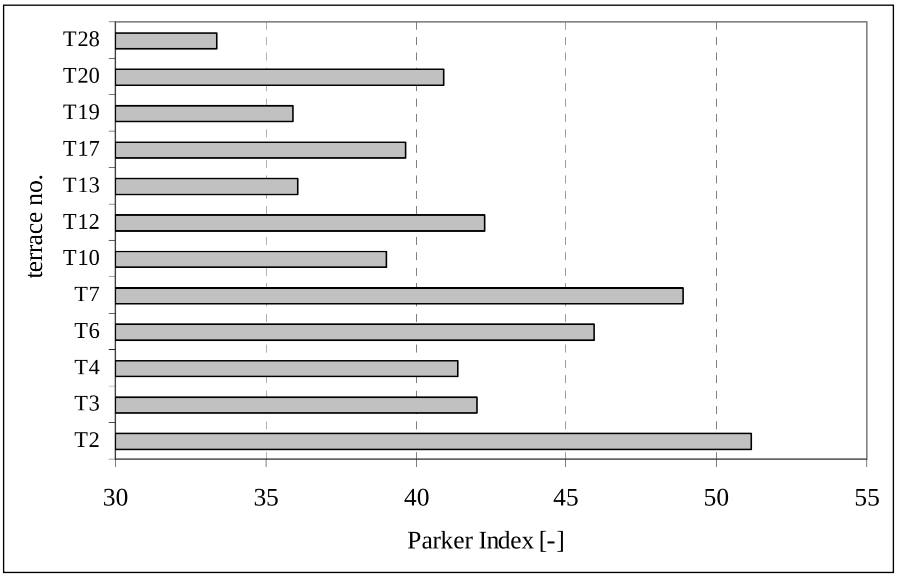

Fig. 39: Whole-profile weighted means of Parker Index values.

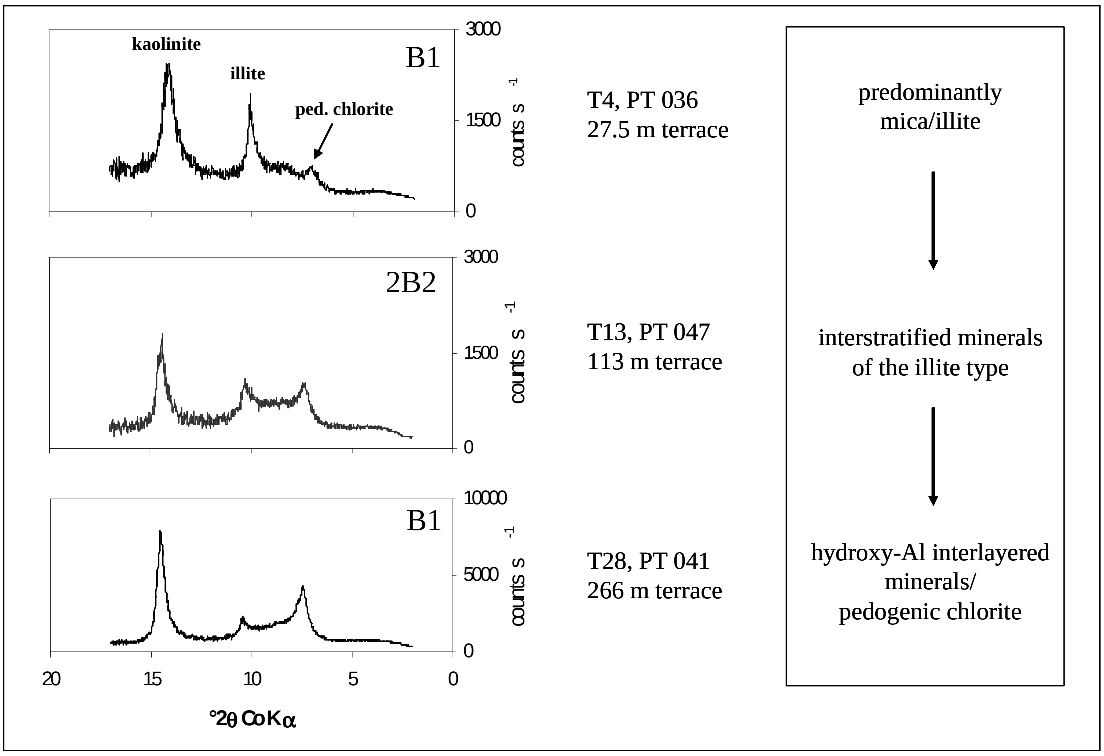

Fig. 40: Comparison of XRD scans of the Mg^{2+}-saturated clay fractions; B horizons from terraces T4, T13 and T28.

All of the profile-weighted parameters show distinctive, more or less “smooth” trends when plotted against increasing relative height above the current river level. This outcome was not necessarily expected, especially when we take into account the different genesis of the two main sections of the Thangbi river terrace system: The sediments of the lower terraces (T1-T6) are younger than 27,340 years BP; and no palaeosols were detected, indicating that the soils have developed without any major interruptions until present. In contrast, the valley structures of terraces T8 and above existed before Late Pleistocene or at least the global LGM, and were repeatedly disturbed by periglacial processes.

The clarity of the trends also suggests that tectonic movements within the valley structure, which could have lead to “offsets” or even reversals, seem unlikely to have occurred since Late Pleistocene. However, this does not exclude the moderate regional uplift as mentioned by Baillie & Norbu (2004).

7 Conclusions

7.1 Comparative geochemical investigation of Bhutanese soils

This work compiles the first systematic data on major and trace elemental compositions as well as REE abundances for saprolites and their associated soils on the southern slopes of the Eastern Himalayas. The close geochemical relationship between the metamorphic materials of Central Bhutan is reflected in similar REE abundances and patterns of the gneissic, metasedimentary and phyllitic lithologies. Magmatic materials show greater heterogeneity because their REE patterns have not been smoothed out during weathering, transport and sedimentation. The existence of marine Tethyan sediments in the central Bhutanese Phobjikha valley is confirmed by a large positive Ce anomaly.

Major element data indicate an advanced state of weathering for all examined materials. The synopsis of the profiles shows that physical weathering which dominates at higher elevations has been effective in the passive enrichment of lithophile elements. In this process, the rare earths become residually associated with the clay and silt sized fraction, however transport and fractionation appear negligible.

Only below altitudes between 3,200 and 3,700 m a.s.l. increasing temperature and rainfall intensify chemical weathering, resulting in the release *and* transport of REE. Especially the HREE seem to be preferentially translocated within the soil profiles, whereas Ce is more refractory than other lanthanides. Both initial mineralogy and climate are identified as major controls on REE patterns. The influence of the former becomes increasingly visible with increasing depth of the soil profile, where the coarser fractions reveal the less altered chemical fingerprint of the parent materials.

In the Bhutanese landscape, residual soils are not widespread. Vertical pedogenetic processes like podzolisation or lessivation combine with horizontal processes in the form of aeolian and fluvial additions or slope processes and landslides. The geochemical variations within the examined profiles, however, are generally less clear than morphologic features as indicators of polygenetic discontinuities within sola.

7.2 Soil forming processes

7.2.1 Redistribution of local sediments and its influence on soil formation

The smooth morphology of the Central Bhutanese Phobjikha Valley, as well as the particular geological and climatic setting of this study area promote the production and redistribution of silty sediments. Deflation, entrainment, transport, deposition and erosion probably represent a local cycling of silt-sized materials. The extent, to which the studied profiles are affected by aeolian additions, influences their properties. Whereas andic properties dominate in leeward, protected sites, a tendency to ferralic and argic features is observed for soils developed from pre-weathered, entrained, transported and deposited fine-silty materials. The redistribution of loess-like sediments therefore represents an essential process within the local ecosystem without which soil formation in the study area cannot be understood. This allows us to postulate that the age of the soil material reflected by its state of weathering is not identical with the age of the pedon in situ. The study also shows that horizons can certainly develop ferralic features in a high mountain environment.

7.2.2 Andic features in non-volcanic Andosols

Collation of our results with published data (*Table 2*, page 17) indicates that the development of non-volcanic and non-allophanic Andosols/Andisols most probably requires:

- Humid conditions for several consecutive months, with or without dry season,
- adequate drainage to maintain leaching environments (Delvaux et al. 2004),
- a relatively large amount of organic matter by input or accumulation, and
- an intensive weathering environment.

Intensive weathering may result from significant contents of readily weatherable minerals (Delvaux et al. 2004), and also because the sites were never glaciated, but were under the influence of frequent freeze-thaw cycles during the Quaternary. This holds especially for the southern slopes of the Himalayas even at higher elevations (Section 5.1.5, Bäumler 2004, Baillie et al. 2004).

The distinct soil forming conditions and features of these soils need to be recognised within in the existing soil classification systems. This means either that the criteria for the Andosols and Podzols need to be relaxed to allow the inclusion of these soils, or that provision needs to be made for a separate taxon of non-allophanic soils with andic features that have developed in non-volcanic materials.

7.3 Soils as indicators for landscape history and palaeoclimate

7.3.1 Indications from Phobjikha-Valley, Wangdue-Phodrang

Buried topsoils within Phobjikha Valley suggest that the redistribution of local sediments weakened or stopped during the Late Holocene climatic optimum, when warmer and wetter climate shifted the balance towards in-situ soil formation. Before then, geology and climate were the decisive controls, but the arrival of humans helped to re-establish the sediment redistribution by deforestation, grazing and arable agriculture since at least 2,000 years.

7.3.2 Indications from the Chamkhar Chhu Valley near Jakar, Bumthang

The study provides insight into basic properties of soils regarded as typical for the inner valleys of Central Bhutan. Field observations and geomorphological analyses helped to build a preliminary chronology of events. Wood remnants in the sediments of the main terrace, T7 at 41 m above the current river level, were dated to 27,340 ± 180 years BP by Gurung (2001). If we assume that this massive sediment load represents the materials accumulated towards the end of the last glaciation, it suggests that the last local maximum glaciation may have predated the global LGM, which confirms recent findings from East Nepal and from the southern Kamchatka Peninsula (Bäumler 2004, Bäumler & Zech 2000).

The same assumption makes all of the terraces above T7 of at least early Late Pleistocene age or older. They can be clearly distinguished from the members of the lower part by their deeper profiles and higher contents of silt and clay indicating that they are more strongly weathered. Furthermore, they show polygenetic structures, which means that soil development was interrupted several times by periglacial phenomena under cold and dry conditions. As no aeolian materials were detected below

T7 (= 27,340 years BP), the interruptions identified at 10,175, 8,710, 4,055 and 1,715 years BP represent solifluction events, rather than depositions of fresh loess.

The terraces below T7 are of Late Pleistocene and Holocene age. No polygenetic features can be found which indicates that “catastrophic floods” did not occur during this period, and that the Chamkhar Chhu cut into the valley fill by continuous depth erosion.

The identified trends in the determination of relative ages by particle size distribution, surface area, clay mineral development and weathering indices, do not show a distinctive “gap” between the two parts of the terrace system. Even *within* the upper part, relative ages *in*crease with *in*creasing level of the terraces. This might be evidence that during the formation of the soils we observe today, in-situ weathering played an important role, reinforcing the possible pre-weathering of aeolian sediments.

The Thangbi terrace system can therefore be regarded as a chronosequence of fluvial sediments and their associated pedal structures. Its vertical amplitude of nearly 300 m makes it comparable with others in the Himalayas, which include many of the biggest river terrace systems in the world.

8 References*

Adjadeh T.A. & Inoue K. (1999): Andisols of the Kitakami mountain range, northeastern Japan: their characterization and classification. *Soil Science and Plant Nutrition* **45**: 115-130.

Ageta Y., Iwata S., Yabuki H., Naito N., Sakai A., Narama C. and Karma (2000): Expansion of glacier lakes in recent decades in the Bhutan Himalayas. *In*: Debris-Covered Glaciers (M. Nakawo, C.F. Raymond and A. Fountain eds.), *IAHS Publication No.* **264**, IAHS Press, Wallingford, England, UK; pp. 165-175.

Agrawal D.P., Dodia R., Kotlia B.S., Razdan H. and Sahni A. (1989): The Plio-Pleistocene geologic and climatic record of the Kashmir Valley, India: A review and new data. *Palaeogeography, Palaeoclimatology, Palaeoecology* **73**: 267-286.

Aleksandrova L.N. (1960): The use of sodium pyrophosphate for isolating humic substances and their organic-mineral compounds from soil. *Soviet Soil Science* **2**: 190-197.

Alexander E.B., Shoji S. and West R. (1993): Andic soil properties of Spodosols in nonvolcanic materials of southeast Alaska. *Soil Science Society of America Journal* **57**: 472-475.

Anders E. & Grevesse N. (1989): Abundances of the elements: meteoritic and solar. *Geochimica et Cosmochimica Acta* **53 (1)**: 197-214.

Aran D., Gury M., Zida M., Jeanroy E. and Herbillon A.J. (1998): Influence de la roche-mère et du climat sur les propriétés andiques des sols en région montagnarde tempérée (Vosges, France). *European Journal of Soil Science* **49**: 269-281.

Arduino E., Barberis E., Carraro F. and Former M.G. (1984): Estimating relative ages from iron-oxide/total-iron ratios of soils in the western Po Valley, Italy. *Geoderma* **33**: 39-52.

* all online resources were available at the date of submission

Arduino E., Barberis E., Ajmone Marsan F., Zanini E. and Franchini M. (1986): Iron oxides and clay minerals within profiles as indicators of soil age in Northern Italy. *Geoderma* **37**: 45-55.

Ayres M. & Harris N. (1997): REE fractionation and Nd-isotope disequilibrium during crustal anatexis: constraints from Himalayan leucogranites. *Chemical Geology* **139 (1-4)**: 249-269.

Bäumler R. (1995): Dynamik gelöster Stoffe in verschiedenen Kompartimenten kleiner Wassereinzugsgebiete in der Flyschzone der Bayerischen Alpen - Auswirkungen eines geregelten forstlichen Eingriffs. *Bayreuther Bodenkundliche Berichte* **40**.

Bäumler R. (2001a): Pedogenic studies in aeolian deposits in the high mountain area of eastern Nepal. *Quaternary International* **76/77**: 93-102.

Bäumler R. (2001b): Vergleichende bodenkundliche Untersuchungen in Hochasien und Kamtschatka - Böden als Zeugen der quartären Landschafts- und Klimageschichte. *Relief, Boden, Paläoklima* **16**, Bornträger, Berlin & Stuttgart, Germany.

Bäumler R. (2004): Pedogenic studies in eastern Nepal – new aspects about the last glaciation. *Quaternary Science Reviews* **23**: 1777-1783.

Bäumler R. & Zech W. (1994a): Characterization of Andisols developed from nonvolcanic material in eastern Nepal. *Soil Science* **158**: 211-217.

Bäumler R. & Zech W. (1994b): Soils of the high mountain region of eastern Nepal: classification, distribution and soil forming processes. *Catena* **22**: 85-103.

Bäumler R. & Zech W. (2000): Quaternary paleosols, tephra deposits and landscape history in South Kamchatka, Russia. *Catena* **41 (1-3)**: 199-215.

Bäumler R., Zech W., Heuberger H. & Weberdiefenbach K. (1991): Investigations on the intensity of weathering of soils developed from glacial and fluvioglacial deposits and their relationship with the history of the landscape in the Mt. Everest region. *Geoderma* **48**: 223-243.

Bäumler R., Madhikermi D.P. & Zech W. (1997): Fine silt and clay mineralogical changes of a soil chronosequence in the Langtang Valley (Central Nepal). *Zeitschrift für Pflanzenernährung und Bodenkunde* **160**: 413-421.

Bäumler R., Caspari T., Totsche K.U., Dorji T., Norbu C. and Baillie I.C. (2005): Andic features in non-volcanic soils in Bhutan. *European Journal of Soil Science* (submitted).

Baillie I. & Norbu C. (2004): Climate and other factors in the development of river and interfluve profiles in Bhutan. *Journal of Asian Earth Sciences* **22**: 539-553.

Baillie I.C., Tshering K., Dorji T., Tamang H.B., Dorji T., Norbu C., Hutcheon A.A. and Bäumler R. (2004): Regolith and soils in Bhutan, Eastern Himalayas. *European Journal of Soil Science* **55** (1): 9-27.

Balashov Y.A., Ronov A.B., Migdisov A.A. and Turanskaya N.V. (1964): The effect of climate and facies environment on the fractionation of the rare earths during sedimentation. *Geochemistry International* **5**: 951-969.

Barnhisel R.I. & Bertsch P.M. (1989): Chlorites and hydroxy-interlayered vermiculite and smectite. *In*: Minerals in soil environments (J.B. Dixon & S.B. Weed eds.), *Soil Science Society of America Book Series No.* **1**, Madison, WI, USA; pp. 729-788.

Bea F., Pereira M.D. and Stroh A. (1994): Mineral/leucosome trace-element partitioning in a peraluminous migmatite (a laser ablation-ICP-MS study). *Chemical Geology* **117 (1-4)**: 291-312.

Benard F., Moutou B. and Pichavant M. (1985): Phase-relations of tourmaline leucogranites and the significance of tourmaline in silicic magmas. Journal of Geology **93 (3)**: 271-291.

Benn D. & Owen L.A. (1998): The role of the Indian Summer Monsoon on Himalayan glaciation. *Journal of the Geological Society* **155**: 353-364.

Bergamaschi L., Rizzio E., Valcuvia M.G., Verza G., Profumo A. and Gallorini M. (2002): Determination of trace elements and evaluations of their enrichment factors in Himalayan lichens. *Environmental Pollution* **120 (1)**: 137-144.

Bhargava O.N. (1995): Stratigraphy. *In*: The Bhutan Himalaya: A geological account (O.N. Bhargava ed.), *Geological Survey of India Special Publication* **39**, Calcutta, India; pp. 173-181.

Blakemore L.C., Searle P.L. and Daly B.K. (1987): Methods for chemical analysis of soils. *New Zealand Soil Bureau Scientific Report* **80**, DSIR, Lower Hutt, New Zealand.

Blaser P. & Klemmedson J.O. (1987): Die Bedeutung von hohen Aluminiumgehalten für die Humusanreicherung in sauren Waldböden. *Zeitschrift für Pflanzenernährung und Bodenkunde* **150**: 334-341.

Blaser P., Kernebeek P., Tabbens L., van Breemen N. and Luster J. (1997): Cryptopodzolic soils in Switzerland. *European Journal of Soil Science* **48**: 411-423.

Bronger A. & Heinkele T. (1989): Micromorphology and genesis of palaeosols in the Luochuan loess section, China: pedostratigraphic and environmental implications. *Geoderma* **45**: 123-144.

Bronger A., Winter R. and Heinkele T. (1998): Pleistocene climatic history of East and Central Asia based on paleopedological indicators in loess-palaeosol sequences. *Catena* **34**: 1-17.

Brunauer S., Emmett P. and Teller E. (1938): Adsorption of gases in multimolecular layers. *Journal of the American Chemical Society* **60**: 309-319.

Caine N., Ives J.D., Kienholz H. and Messerli B. (1982): A buried Podzol near Namche Bazar, Solu-Khumbu, Nepal. *Mountain Research and Development* **2**: 405-406.

Caner L., Bourgeon G., Toutain F. and Herbillon A.J. (2000): Characteristics of non-allophanic Andisols derived from low-activity clay regoliths in the Nilgiri hills (Southern India). *European Journal of Soil Science* **51**: 553-563.

Cantrell K.J. & Byrne R.H. (1987): Rare earth element complexation by carbonate and oxalate ions. *Geochimica et Cosmochimica Acta* **51 (3)**: 597-606.

Caspari T. (2003): Origin and properties of the soils of Phobji-Gangtey Valley. *Bhutan Soil Survey Project (BSSP) Technical Report*, Ministry of Agriculture, Royal Government of Bhutan, Thimphu, Bhutan.

Caspari T., Dorji T. and Bäumler R. (2002): Böden als Indikatoren der Landschafts- und Klimageschichte Zentralbhutans. *In*: Planet Erde: Vergangenheit, Entwicklung, Zukunft (B. Niebuhr ed.), *Schriftenreihe der Deutschen Geologischen Gesellschaft* **21**; p. 91.

Caspari T., Norbu C. and Bäumler R. (2004a): Relevance of soils for Gross National Happiness. *Proceedings of the International Seminar on "Operationalising the Concept of Gross National Happiness"*, 18-20 February 2004, The Centre for Bhutan Studies, Thimphu, Bhutan.

Caspari T., Bäumler R., Dorji T., Norbu C., Tshering K. and Baillie I.C. (2004b): Pedochemical characterisation and landscape history of the Thangbi river terrace system, Central Bhutan. *Zeitschrift für Geomorphologie N.F.* **48(2)**: 145-165.

Caspari T., Bäumler R., Norbu C., Tshering K. and Baillie I. (2005): Redistribution of local sediments and its influence on soil formation in Phobjikha Valley, Bhutan. *Catena* (submitted).

Castelli D. & Lombardo B. (1988): The Gophu La and western Lunana granites: Miocene muscovite leucogranites of the Bhutan Himalaya. *Lithos* **21 (3)**: 211-225.

Catt J.A. (1991): Soils as indicators of Quaternary climatic change in mid-latitude regions. *Geoderma* **51**: 167-187.

Chang Q., Mishima T., Yabuki S., Takahashi Y. and Shimizu H. (2000): Sr and Nd isotope ratios and REE abundances or moraines in the mountain areas surrounding the Taklimakan Desert, NW China. *Geochemical Journal* **34 (6)**: 407-427.

Chaturvedi R.K., Mishra S.N. and Mulay V.V. (1983): On the Tethyan palaeozoic sequence of Black Mountain region, Central Bhutan. *Himalayan Geology* **10**: 224-249.

Chhetri I.K. & Gurung C.R. (2001): Report on the litho-structural mapping of Wangduephodrang and Punakha dzongkhag. Geological Survey of Bhutan, Department of Geology and Mines, Royal Government of Bhutan, Thimphu, Bhutan.

Copeland P., Harrison T.M. and Le Fort P. (1990): Age and cooling history of the Manaslu granite: implications for Himalayan tectonics. *Journal of Volcanology and Geothermal Research* **44**: 33-50.

Cullers R.L., Chaudhuri S., Arnold B., Lee M. and Wolf C.W. (1975): Rare earth distributions in clay minerals and in the clay-sized fraction of lower Permian Havensville and Eskridge shales of Kansas and Oklahoma. *Geochimica et Cosmochimica Acta* **39 (12)**: 1691-1703.

Cullers R.L., Chaudhuri S., Kilbane N. and Koch R. (1979): Rare earths in size fractions and sedimentary rocks of Pennsylvanian-Permian age from the mid-continent of the U.S.A. *Geochimica et Cosmochimica Acta* **43 (8)**: 1285-1301.

Cuney M., Le Fort P. and Wang Z.X. (1984): Uranium and thorium geochemistry and mineralogy in the Manaslu leucogranite (Nepal, Himalaya). *In*: Geology of Granites and their Metallogenetic Relations (Xu Keqin & Tu Guangchi eds.), Proceedings of the International Symposium, University Sciences Editions, Nanjing, China; pp. 853-873.

Das B.K. & Haake B.-G. (2003): Geochemistry of Rewalsar Lake sediment, Lesser Himalaya, India: implications for source-area weathering, provenance and tectonic setting. *Geosciences Journal* **7 (4)**: 299-312.

Dasgupta S. (1995): Quaternary sediments. *In*: The Bhutan Himalaya: A geological account (O.N. Bhargava ed.), *Geological Survey of India Special Publication* **39**, Calcutta, India; pp. 19-22.

Delvaux B., Strebl F., Maes E., Herbillon A.J., Brahy V. and Gerzabek M. (2004): An Andosol-Cambisol toposequence on granite in the Austrian Bohemian Massif. *Catena* **56**: 31-43.

Dietrich V. & Gansser A. (1981): The leucogranites of the Bhutan Himalaya. Crustal anatexis versus mantle breeding. *Schweizerische Mineralogische und Petrographische Mitteilungen* **61**: 177-202.

Dorji K. (1995): An Analysis of Comparative Advantages in Bhutanese Agriculture. PhD Thesis, ETH Zurich, Switzerland.

Dubinin A.V. & Sval’nov V.N. (2003): Geochemistry of the manganese ore process in the ocean: evidence from rare earth elements. *Lithology and Mineral Resources* **38 (2)**: 91-100.

Duchaufour P. (1982): Pedology: Pedogenesis and classification. George Allen & Unwin, Boston, MA, USA.

Duddy I.R. (1980): Redistribution and fractionation of rare-earth and other elements in a weathering profile. *Chemical Geology* **30 (4)**: 363-381.

Egashira K., Aramaki K., Yoshimasa M., Takeda A. and Yamasaki S. (2004): Rare earth elements and clay minerals of soils of the floodplains of three major rivers in Bangladesh. *Geoderma* **120 (1-2)**: 7-15.

Egger J., Bajrachaya S., Egger U., Heinrich R., Reuder J., Shayka P., Wendt H. and Wirth V. (2000): Diurnal winds in the Himalayan Kali Gandaki Valley. Part I: observations. *Monthly Weather Review* **128**: 1106-1122.

Eguchi T. (1987): Topographic features in the central part of the Bhutan Himalayas. *In*: Life Zone Ecology of the Bhutan Himalaya (M. Ohsawa ed.), Laboratory of Ecology, Chiba University, Japan; pp. 185-208.

Eguchi T. (1991): Regional and seasonal change in precipitation in Bhutan – analysis of daily precipitation in 1988. *In*: Life Zone Ecology of the Bhutan Himalaya II (M. Ohsawa ed.), Laboratory of Ecology, Chiba University, Japan; pp. 1-20.

El-Sayed M.M. (2003): Neoproterozoic magmatism in NW Sinai, Egypt: magma source and evolution of collision-related intracrustal anatectic leucogranite. *International Journal of Earth Sciences* **92 (2)**: 145-164.

FAO-ISRIC (1990): Guidelines for soil description. 3rd Edition (revised), Soil Resources, Management and Conservation Service, Land and Water Development Division, Food and Agriculture Organization of the United Nations, Rome, Italy.

FAO (1991): Master Plan for Forestry Development in Bhutan - Wood Energy Sectoral Analysis. *Regional Wood Energy Development Programme in Asia Field Document No.* **32** (GCP/RAS/154/NET), Food and Agriculture Organization of the United Nations (FAO) Regional Office for Asia and the Pacific, Bangkok, Thailand [Online at http://www.rwedp.org/acrobat/fd32.pdf].

FAO (1995): Shifting Cultivation in Bhutan: A Gradual Approach to Modifying Land Use Patterns. A case study from Pema Gatshel District, Bhutan. *Community Forestry Case Study Series* **11**, Food and Agriculture Organisation of the United

Nations, Rome, Italy [Online at http://www.fao.org/documents/show_cdr.asp?url_file=/DOCREP/006/V8380E/V8380E00.htm].

Fort M. (1996): Late Cenozoic environmental changes and uplift of the northern side of the central Himalaya: a reappraisal from field data. *Palaeogeography, Palaeoclimatology, Palaeoecology* **120 (1-2)**: 123-145.

Gallet S., Jahn B., Van Vliet Lanoe B., Dia A. and Rossello E. (1998): Loess geochemistry and its implications for particle origin and composition of the upper continental crust. *Earth and Planetary Science Letters* **156 (3-4)**: 157-172.

Gansser A. (1983): Geology of the Bhutan Himalaya. *Denkschriften der Schweizer. Naturforschenden Gesellschaft* **96**, Birkhaeuser, Basel, Switzerland.

Garcia-Rodeja E., Silva B.M. and Macias F. (1987): Andisols developed from non-volcanic materials in Galicia. *Journal of Soil Science* **38**: 573-591.

Gardner R.A.M. (1994): Silt production from weathering of metamorphic rocks in the Southern Himalaya. *In*: Rocks, rock weathering and landform evolution (D.A. Robinson & R.B.G. Williams eds.), Wiley, London, UK; pp. 387-503.

Gardner R.A.M. & Rendell H.M. (1994): Loess, climate and orogenesis: implications of South Asian loesses. *Zeitschrift für Geomorphologie N.F.* **38 (2)**: 169-184.

Gehrels G.E., DeCelles P.G., Ojha T.P., Pinhassi G. and Upreti B.N. (2003): Initiation of the Himalayan orogen as an early Paleozoic thin-skinned thrust belt. *GSA Today* **13 (9)**: 4-9.

Gerasimov I.P. (1973): Chernozems, buried soils and loesses of the Russian Plain: their age and genesis. *Soil Science* **116**: 202-210.

Gillespie A. & Molnar P. (1995): Asynchronous maximum advances of mountain and continental glaciers. *Reviews of Geophysics* **33**: 311-364.

Golani P.R. (1995): Thimphu Group. *In*: The Bhutan Himalaya: A geological account (O.N. Bhargava ed.), *Geological Survey of India Special Publication* **39**, Calcutta, India; pp. 89-108.

Goossens D. & Offer Z.I. (1990): A wind-tunnel simulation and field verification of desert dust deposition. *Sedimentology* **37**: 7-22.

Grierson A.J.C. & Long D.J. (1983): Flora of Bhutan. Vol. 1 Part 1. Royal Botanic Garden, Edinburgh, Scotland. [homepage at http://www.rbge.org.uk/rbge/web/science/research/biodiversity/flbhut.jsp]

Gromet L.P. & Silver L.T. (1983): Rare earth element distributions among minerals in a granodiorite and their petrogenetic implications. *Geochimica et Cosmochimica Acta* **47 (5)**: 925-939.

Grujic D., Hollister L.S. and Parrish R.R. (2002): Himalayan metamorphic sequence as an orogenic channel: insight from Bhutan. *Earth and Planetary Science Letters* **198 (1-2)**: 177-191.

Guggenberger G., Bäumler R. and Zech W. (1998): Weathering of soils developed in eolian material overlying glacial deposits in eastern Nepal. *Soil Science* **163 (4)**: 325-337.

Guillot S. & Le Fort P. (1995): Geochemical constraints on the bimodal origin of High Himalayan leucogranites. *Lithos* **35 (3-4)**: 221-234.

Gupta A.K. & Ura K. (1992): Indigenous Farming Technologies and Environment: Experiences in Bhutan. *In*: Sustainable Mountain Agriculture (N.S. Jodha, M. Banskota and T. Partap eds.), Vol. 2, Oxford & IBH Publishing Co Pvt. Ltd., New Delhi, India; pp. 540-568.

Gurung D.R. (2001): Quaternary system in the Chamkhar and Tang Valley floor, Bumthang. *Bhutan Geology Newsletter* **4**: 1-6.

Gustafsson J.P., Bhattacharya P., Bain D.C., Fraser A.R. and McHardy W.J. (1995): Podzolisation mechanisms and the synthesis of imogolite in Northern Scandinavia. *Geoderma* **66**: 167-184.

Harris (2000): Grassland resource assessment for pastoral systems. *FAO Plant Production and Protection Papers* **162**, Food and Agriculture Organization of the United Nations, Rome, Italy.

Hindman E.E. & Upadhyay B.P. (2002): Air pollution transport in the Himalayas of Nepal and Tibet during the 1995–1996 dry season. *Atmospheric Environment* **36**: 727-739.

Hodges K.V. (2000): Tectonics of the Himalaya and southern Tibet from two perspectives. *Geological Society of America Bulletin* **112 (3)**: 324-350.

Holmes J.A. & Street-Perrott F.A. (1989): The Quaternary Glacial History of Kashmir, North-West Himalaya: A Revision of de Terra and Paterson's Sequence. *Zeitschrift für Geomorphologie N.F. Suppl.* **76**: 195-212.

Honda M., Yabuki S. and Shimizu H. (2004): Geochemical and isotopic studies of aeolian sediments in China. *Sedimentology* **51 (2)**: 211-230.

Huang P.M. (1991): Ionic factors affecting the formation of short-range ordered aluminosilicates. *Soil Science Society of America Journal* **55**: 1172-1180.

Huang P.M., Wang M.K., Kämpf N. and Schulze D.G. (2002): Aluminum Hydroxides. *In*: Soil Mineralogy with Environmental Applications (J.B. Dixon & D.G. Schulze eds.), *SSSA Book Series* **No. 7**, Madison, WI, USA; pp. 261-289.

Hunter C.R., Frazier B.E. and Busacca A.J. (1987): Lytell series: a nonvolcanic Andosol. *Soil Science Society of America Journal* **51**: 376-383.

ICIMOD, UNEP RRC.AP and RGoB (2002): Inventory of glaciers, glacier lakes, glacier lake outburst floods monitoring & early warning systems in the Hindu Kush-Himalayan Region Bhutan [Online at http://www.rrcap.unep.org/glofbhutan/guide/movie.html].

ISSS Working Group Reference Base (1998): World Reference Base for Soil Resources. *FAO World Soil Resources Reports* **84**, Rome, Italy.

Iwata S. (1987): Mode and rate of uplift of the central Nepal Himalaya. *Zeitschrift für Geomorphologie N.F. Suppl.* **63**: 37-49.

Iwata S., Ageta Y., Naito N., Sakai A., Narama C. and Karma (2002a): Glacial lakes and their outburst flood assessment in the Bhutan Himalaya. *Global Environmental Research* **6 (1)**: 3-17.

Iwata S., Narama C. and Karma (2002b): Three Holocene and Late Pleistocene glacial stages inferred from moraines in the Lingshi and Thanza Village areas, Bhutan. *Quaternary International* **97/98**: 69-78.

Iwata S., Naito N., Narama C. and Karma (2003): Rock glaciers and the lower limit of mountain permafrost in the Bhutan Himalayas. *Zeitschrift für Geomorphologie N.F. Suppl.* **130**: 129-143.

Jangpangi B.S. (1978): Stratigraphy and structure of Bhutan Himalaya. *In*: Tectonic Geology of the Himalaya (P.S. Saklani ed.), Today and Tomorrow's Printers and Publishers, New Delhi, India; pp. 221-242.

Johnson D.L., Keller E.A. and Rockwell T.K. (1990): Dynamic pedogenesis: new views on some key soil concepts, and a model for interpreting Quaternary soils. *Quaternary Research* **33**: 306-319.

Kaiser K. & Zech W. (1996): Defects in estimation of aluminum in humus complexes of podzolic soils by pyrophosphate extraction. *Soil Science* **161**: 452-458.

Karan P.P. (1967): Bhutan – A Physical and Cultural Geography. University of Kentucky Press, Lexington, KY, USA.

Karma, Ageta Y., Naito N., Iwata S. and Yabuki H. (2003): Glacier distribution in the Himalayas and glacier shrinkage from 1963 to 1993 in the Bhutan Himalayas. *Bulletin of Glaciological Research* **20**: 29-40.

Kato Y., Kawakami T., Kano T., Kunugiza K. and Swamy N.S. (1996): Rare-earth element geochemistry of banded iron formations and associated amphibolite from the Sargur belts, south India. *Journal of Southeast Asian Earth Sciences* **14 (3-4)**: 161-164.

Kemp R.A. (1999): Micromorphology of loess-palaeosol sequences: a record of paleoenvironmental change. *Catena* **35**: 181-198.

Kemp R.A. (2001): Pedogenic modification of loess: significance for palaeoclimatic reconstructions. *Earth-Science Reviews* **54**: 145-156.

Kemp R.A. & Derbyshire E. (1998): The loess soils of China as records of climatic change. *European Journal of Soil Science* **49**: 525-539.

Kleber M., Mikutta C. and Jahn R. (2004): Andosols in Germany – pedogenesis and properties. *Catena* **56**: 67-83.

Koike T. (2001): New finding of Trilobite from the Dang Chhu formation, along Pe Chhu, Wangdue-Phodrang. *Bhutan Geology Newsletter* **4**: 9-11.

Koike T., Chettri I.K., Tapa T.P. and Ghaley K.S. (2002): Stratigraphy and correlation of the Tethyan sediments in Bhutan. *Bhutan Geology Newsletter* **6**: 26-36.

Kukla G. (1987): Loess stratigraphy in Central China. *Quaternary Science Reviews* **6**: 191-219.

Laskar T. (1995): Quaternary sediments. *In*: The Bhutan Himalaya: A geological account (O.N. Bhargava ed.), *Geological Survey of India Special Publication* **39**, Calcutta, India; pp. 19-22.

Le Fort P. (1981): Manaslu leucogranite: a collision signature of the Himalaya, a model for its genesis and emplacement. *Journal of Geophysical Research* **86 (NB11)**: 10545-10568.

Lehmkuhl F. & Haselein F. (2000): Quaternary paleoenvironmental change on the Tibetan Plateau and adjacent areas (western China and western Mongolia). *Quaternary International* **65/66**: 121-145.

Lehmkuhl F., Klinge M., Rees-Jones J. and Rhodes E.J. (2000): Late Quaternary aeolian sedimentation in central and south-eastern Tibet. *Quaternary International* **68/71**: 117-132.

Li S.-Y., Chen Z.-S. and Liu J.-C. (1998): Subalpine loamy Podzols in Taiwan: characteristics, micromorphology and genesis. *Soil Science Society of America Journal* **62**: 710-716.

Livingstone I. & Warren A. (1996): Aeolian geomorphology. An introduction. Addison Wesley Longman Lmt., Singapore.

Mamgain V.D. & Roy P.K. (1989): Delineating extension of Tang Chu Formation and establishing its bio and lithostratigraphy. *In*: Extended abstracts of progress reports; field season 1987-88 (D.P. Dhoundial ed.), *Records of the Geological Survey of India* **122**, Calcutta, India; pp. 210-213.

McGowan H.A. (1997): Meteorological controls on wind erosion during foehn wind events in the eastern Southern Alps, New Zealand. *Canadian Journal of Earth Sciences* **34 (11)**: 1477-1485.

McLennan M.C. (1989): Rare earth elements in sedimentary rocks: influence of provenance and sedimentary processes. *In*: Geochemistry and Mineralogy of Rare Earth Elements (B.R. Lipin & G.A. McKay eds.), *MSA Reviews in Mineralogy* **21**: 169-200.

Mehra O.P. & Jackson M.L. (1960): Iron oxide removal from soils and clays by dithionite-citrate systems buffered with sodium bicarbonate. *Clays and Clay Minerals* **7**: 317-327.

Meyer M., Häusler H., Leber D. and Wangda D. (2003): The glacial chronology of eastern Lunana (NW-Bhutan - Himalaya). Poster presented on 28 July 2003 at the INQUA congress in Reno, NV, USA.

Middleton N.J. (1989): Climatic controls on the frequency, magnitude and distribution of dust storms: examples from India/Pakistan, Mauritania and Mongolia. *In*: Paleoclimatology and paleometeorology: modern and past patterns of global atmospheric transport (M. Leinen & N. Sarnthein eds.), Kluwer Academic Publishers, Boston, MA, USA; pp. 97-132.

Mongelli G. (1993): REE and other trace elements in a granitic weathering profile from “Serre”, southern Italy. *Chemical Geology* **103**: 17-25.

Moore D.M. & Reynolds R.C. (1989): X-ray diffraction and the identification and analysis of clay minerals. Oxford University Press, London, England, UK.

Motegi M. (2002): Geology and Neighbouring Areas – generalization and geostructural problems. *Bhutan Geology Newsletter* **6**: 1-9.

Münch J.-M., Totsche K.U. and Kaiser K. (2002): Physicochemical factors controlling the release of dissolved organic carbon from columns of forest subsoils. *European Journal of Soil Science* **53 (2)**: 311-320.

Munsell A.H. (1994): Munsell Soil Color Charts. Revised Edition, MacBeth Division of Kollmorgen Instruments Corp., New Windsor, NY, USA.

Nath B.N., Kunzendorf H., Plüger W.L. (2000): Influence of provenance, weathering, and sedimentary processes on the elemental ratios of the fine-grained fraction of the bedload sediments from the Vembanad Lake and the adjoining continental shelf, southwest coast of India. *Journal of Sedimentary Research* **70 (5)**: 1081-1094.

Navara G. (1997): The lay of the land. *In*: Bhutan: Mountain Fortress of the Gods (C. Schicklgruber & F. Pommaret eds.), Bookwise, Delhi, India; pp. 31-42.

Nesbitt H.W. (1979): Mobility and fractionation of rare earth elements during weathering of a granodiorite. *Nature* **279 (5710)**: 206-210.

Nesbitt H.W. & Young G.M. (1982): Early Proterozoic climates and plate motions inferred from major element chemistry of lutites. *Nature* **299 (5885)**: 715-717.

Nesbitt H.W. & Young G.M. (1984): Predictions of some weathering trends of plutonic and volcanic rocks based upon thermodynamic and kinetic considerations. *Geochimica et Cosmochimica Acta* **48 (7)**: 1523-1534.

Nesbitt H.W. & Markovics G. (1997): Weathering of granodioritic crust, long-term storage of elements in weathering profiles, and petrogenesis siliciclastic sediments. *Geochimica et Cosmochimica Acta* **61 (8)**: 1653-1670.

Norbu C., Baillie I.C., Dorji Tshering, Dorji Tsheten, Tamang H.B., Tshering K. and Hutcheon A.A. (2003a): A provisional physiographic zonation of Bhutan. *Journal of Bhutan Studies* **8**: 54-87.

Norbu C., Baillie I.C., Dema K., Jamyang, Dema Y., Tamang H.B., Tshering K., Turkelboom F. and Norbu S. (2003b): Types of land degradation in Bhutan. *Journal of Bhutan Studies* **8**: 88-114.

Ohata K., Higuchi K. and Ikegami K. (1981): Mountain-valley windsystem in the Khumbu Himal, east Nepal. *Journal of the Meteorological Society of Japan* **59**: 753-762.

Ohsawa M. (1987): Vegetation zones in the Bhutan Himalaya. *In*: Life Zone Ecology of the Bhutan Himalaya (M. Ohsawa ed.), Laboratory of Ecology, Chiba University, Japan; pp. 1-72.

Okazaki M. (1987): Soils of the Bhutan Himalaya. *In*: Life Zone Ecology of the Bhutan Himalaya (M. Ohsawa ed.), Laboratory of Ecology, Chiba University, Tokyo, Japan; pp. 145-184.

Pal D. & Srivastava R.A.K. (1982): Landform configuration of the Karewa floor and its implications on the Quaternary sedimentation – Kashmir Valley. *In*: Himalaya – landforms and processes (V.K. Verma & P.S. Saklani eds.), Today & Tomorrow Publications, New Delhi, India.

Pandey A. & Palni L.M.S. (1998): Microbes in Himalayan soils: biodiversity and potential applications. *Journal of Scientific & Industrial Research* (India) **57 (10-11)**: 668-673.

Parfitt R.L. & Clayden B. (1991): Andisols – The development of a new order in Soil Survey Staff. *Geoderma* **49**: 181-198.

Parker, A. (1970): An index of weathering for silicate rocks. *Geological Magazine* **107**: 501-504.

Parker J.C. & van Genuchten M.Th. (1984): Determining transport parameters from laboratory and field tracer experiments. *Virginia Agricultural Experiment Station Bulletin* **84 (3)**, Blacksburg, VA, USA.

Patriat P. & Achache J. (1984): India-Eurasia collision chronology has implications for crustal shortening and driving mechanisms of plates. *Nature* **311 (5987)**: 615-621.

Piper D.Z. (1974): Rare earth elements in the sedimentary cycle: A summary. *Chemical Geology* **14**: 285-304.

Poulenard J. & Herbillon A.J. (2000): Identification of three categories of andic horizons in Andosols. *Comptes Rendus de l'Academie des Sciences Series IIA Earth and Planetary Science* **331 (10)**: 651-657.

Prasad C. & Verma V.K. (1974): A study of Quaternary sediments around Asan Valley, Dehradun. *Himalayan Geology* **4**: 361-370.

Pye K. (1987): Aeolian Dust and Dust Deposits. Academic Press, London, England, UK.

Ramesh S. & Ramasamy S. (1997): Rare earth element geochemistry of a sediment core from the Lower Bengal Fan. *Journal of the Geological Society of India* **50 (4)**: 399-406.

Rankin P.C. & Childs C.W. (1987): Rare earths and other trace elements in iron-manganese concretions from a catenary sequence of yellow-grey earth soils. *New Zealand Journal of Geology and Geophysics* **30**: 199-202.

RGoB (1997): 8th Five Year Plan, Main Document. Department of Planning, Ministry of Finance, Royal Government of Bhutan, Post Box 127, Thimphu, Bhutan.

RGoB (1998): Technical Report on the detailed soil survey of Jakhar RNR Research Centre site, Bathpalathang farm. Report No. 2(a), Bhutan Soil Survey Project, Ministry of Agriculture, Royal Government of Bhutan, Thimphu, Bhutan.

RGoB (2000a): The weather in Bumthang 1999. Report from the Forestry Sector, RNR-RC Jakar, Ministry of Agriculture, Royal Government of Bhutan, Thimphu, Bhutan.

RGoB (2000b): Technical Report on semi-detailed soil survey of Lame Gompa Research Forest, Jakar. Report No. 7, Bhutan Soil Survey Project, Ministry of Agriculture, Royal Government of Bhutan, Thimphu, Bhutan.

RGoB (2001a): Report on the litho-structural mapping of Wangduephodrang and Punakha Dzongkhag. Geological Survey of Bhutan, Department of Geology and Mines, Royal Government of Bhutan, Thimphu, Bhutan.

RGoB (2001b): Geological map of Bhutan and neighbouring area (1:1000 000). Department of Geology and Mines, Ministry of Trade and Industry, Royal Government of Bhutan, Thimphu, Bhutan.

RGoB (2003): National Statistical Bureau, Royal Government of Bhutan [Online at http://www.bhutan.gov.bt/govataglance.php].

RGoB (2004): Selected RNR Statistics 2003. Ministry of Agriculture, Royal Government of Bhutan, Post Box 252, Thimphu, Bhutan.

Roaldset E. (1973): Rare earth elements in Quaternary clays of the Numedal area, southern Norway. *Lithos* **6**: 349-372.

Roder W., Calvert O. and Dorji T. (1993): Effect of burning on selected soil parameters in a grass fallow shifting cultivation system in Bhutan. *Plant and Soil* **149**: 51-58.

Ronov A.B., Balashov Y.A. and Migdisov A.A. (1967): Geochemistry of the rare earths in the sedimentary cycle. *Geochemistry International* **4 (1)**: 1-17.

Rowley D.B. (1996): Age of initiation of collision between India and Asia: A review of stratigraphic data. *Earth and Planetary Science Letters* **145**: 1-13.

RSPN (2003): Integrated Conservation and Development Program (ICDP). Royal Society for Protection of Nature, Post Box 325, Thimphu, Bhutan [Online at http://www.rspn-bhutan.org/pics/icdp/icdp-document.pdf].

Saijo K. & Tanaka S. (2002): Palaeosols of Middle Holocene age in the Thakkhola Basin, Central Nepal, and their paleoclimatic significance. *Journal of Asian Earth Sciences* **21**: 323-329.

Sarkar A. & Dasgupta S. (1995): The granitic rocks. *In*: The Bhutan Himalaya: A geological account (O.N. Bhargava ed.), *Geological Survey of India Special Publication* **39**, Calcutta, India; pp. 143-171.

Schicklgruber C. & Pommaret F. (1997): Bhutan – Festung der Götter. Verlag Paul Haupt, Bern, Switzerland.

Schwertmann U. (1966): Inhibitory effect of soil organic matter on the crystallization of amorphous ferric hydroxide. *Nature* **212**: 645-646.

Sharma A. & Rajamani V. (2000): Major element, REE, and other trace element behavior in amphibolite weathering under semiarid conditions in southern India. *Journal of Geology* **108**: 487-496.

Shiraiwa T. & Watanabe T. (1991): Late Quaternary glacial fluctuations in the Langtang Valley, Nepal Himalaya, reconstructed by relative dating methods. *Arctic and Alpine Research* **23 (4)**: 404-416.

Shoji S. & Ono T. (1978): Physical and chemical properties and clay mineralogy of Andisols from Kitikami, Japan. *Soil Science* **126**: 297-312.

Shoji S. & Fujiwara Y. (1984): Active aluminium and iron in the humus horizons of Andosols from northeastern Japan: their forms, properties and significance in clay weathering. *Soil Science* **137**: 216-226.

Singh P. (1973): A note on the fossiliferous formations in Lesser Himalaya of Nepal and Bhutan. *Himalayan Geology* **3**: 372-380.

Soil Survey Staff (1999): Soil Taxonomy. A basic system of soil classification for making and interpreting soil surveys. Handbook 210, USDA Natural Resources Conservation Service, Washington,

Stuiver M. & Polach H.A. (1977): Reporting of 14C data – discussion. *Radiocarbon* **19(3)**: 355-363.

Survey of Bhutan (1999): Topographic map of Trongsa/Bumthang, 1:50000. Survey of Bhutan, Thimphu, Bhutan.

Takada M. (1991): Landform and Quaternary geohistory of the Bhutan Himalaya. *In*: Life Zone Ecology of the Bhutan Himalaya (M. Ohsawa ed.), Laboratory of Ecology, Chiba University, Japan; pp. 41-88.

Takahashi Y., Shimizu H., Kagi H., Yoshida H., Usui A. and Nomura M. (2000): A new method for the determination of CeIII/CeIV ratios in geological materials; application for weathering, sedimentary and diagenetic processes. *Earth and Planetary Science Letters* **182 (3-4)**: 201-207.

Tangri S.K. & Pande A.C. (1995): Tethyan sequence. *In*: The Bhutan Himalaya: A geological account (O.N. Bhargava ed.), *Geological Survey of India Special Publication* **39**, Calcutta, India; pp. 109-141.

Tangri S.K., Bhargava O.N. and Pande A.C. (2003): Late Precambrian – Early Cambrian trace fossils from Tethyan Himalaya, Bhutan and their bearing on the Precambrian-Cambrian boundary. *Journal of the Geological Society of India* **62 (6)**: 708-716.

Taunton A.E., Welch S.A. and Banfield J.F. (2000): Microbial controls on phosphate and lanthanide distributions during granite weathering and soil formation. *Chemical Geology* **169 (3-4)**: 371-382.

Taylor S.R. & McLennan S.M. (1985): The continental crust: Its composition and evolution. Blackwell, Oxford, England, UK.

Taylor K.C., Lamorey G.W., Doyle G.A., Alley R.B., Grootes P.M., Mayewski P.A., White J.W.C. and Barlow L.K. (1993): The 'flickering switch' of late Pleistocene climate change. *Nature* **361 (6411)**: 432-436.

Torrent J. & Nettleton W.D. (1979): A simple textural index for assessing chemical weathering in soils. *Soil Science Society of America Journal* **43**: 373-377.

Trüby P. & Aldinger E. (1989): Eine Methode zur Bestimmung austauschbarer Kationen in Waldböden. *Zeitschrift für Pflanzenernährung und Bodenkunde* **152**: 301-306.

Ura K. (2001): Deities and Environment. A four-part series appearing in the national newspaper *Kuensel* between 17 November and 8 December, Thimphu, Bhutan.

Van Reeuwijk L.P. (ed.) (2002): Procedures for Soil Analysis. 6th Edition, *ISRIC Technical Paper* **9**, Wageningen, The Netherlands.

Van Vliet-Lanoë B. (1998): Frost and soils: implications for palaeosols, paleoclimates and stratigraphy. *Catena* **34**: 157-183.

Vidal P., Cocherie A. and Le Fort P. (1982): Geochemical investigations of the origin of the Manaslu leucogranite (Himalaya, Nepal). *Geochimica et Cosmochimica Acta* **46**: 2279-2292.

Wada K. (1989): Allophane and Imogolite. *In*: Minerals in soil environments (J.B. Dixon & S.B. Weed eds.), *Soil Science Society of America Book Series No.* **1**, Madison, WI, USA; pp. 1051-1087.

Wake C.P. & Mayewski P.A. (1994): Modern eolian dust deposition in Central Asia. *Tellus* **46B**: 220-233.

Wake C.P. & Mayewski P.A. (eds.) (1995): Report from the International Himalayan/ Tibetan Plateau Palaeoclimate Workshop in Kathmandu 2-7 April 1995. Himalayan Interdisciplinary Paleoclimate Project – Science and Implementation Plan [Online at http://www. ccrc.sr.unh.edu/hipp/KduWkshp_contents/KduWkshp_rep.html].

Wangchuck T., Bäumler R., Caspari T. and Tshering K. (2003): The landslides and depressions of TshoGoempa (Lumang geog) – causes and recommendations. *RNR-RC East Technical Document No.* **28**, Khangma, Bhutan.

Weigand H. & Totsche K.U. (1998): Flow and reactivity effects on dissolved organic matter transport in soil columns. *Soil Science Society of America Journal* **62**: 1268-1274.

Whiteman C.D. (2000): Mountain Meteorology - Fundamentals and Applications. Oxford University Press, Oxford, England, UK.

Wilcken H., Sorge C. and Schulten H.-R. (1997): Molecular composition and chemometric differentiation and classification of soil organic matter in Podzol B-horizons. *Geoderma* **76**: 193-219.

Winkler M.G. & Wang P.H. (1993): Late-Quaternary vegetation and climate of China. *In*: Global Climates Since the Last Glacial Maximum (H.E. Wright, J.E. Kutzbach, T. Webb III, W.F. Ruddiman, F.A. Street-Perrott and P.J. Bartlein eds.), University of Minnesota Press, Minneapolis, MN, USA; pp. 221-264.

Xing B. & Dudas M.J. (1993): Trace and rare earth element content of white clay soils of the three river plain, Heilongjiang Province, P.R. China. *Geoderma* **58 (3-4)**: 181-199.

Xiong S., Sun D. and Ding Z. (2002): Aeolian origin of the red earth in southeast China. *Journal of Quaternary Science* **17 (2)**: 181-191.

Yamanaka H., Yoshida M. and Arrita K. (1982): Terrace landforms and Quaternary deposits around Pokhara Valley, Central Nepal. *Journal of Nepal Geological Society* **2**: 113-142.

Yasuda Y. & Tabata H. (1988): Vegetation and climatic changes in Nepal Himalayas II. A preliminary study of the Holocene vegetational history in the Lake Rara National Park area, West Nepal. *Proceedings of the Indian National Science Academy* **54A (4)**: 538-549.

Yoshida M. & Igarashi Y. (1984): Neogene to Quaternary lacustrine sediments in the Kathmandu Valley, Nepal. *Journal of Nepal Geological Society* **4**: 73-100.

Young A. (1994): Land degradation in South Asia: its severity, causes, and effects upon the people. *World Soil Resources Report* **78**, UNDP/UNEP/FAO, Rome, Italy [Online at http://www.fao.org/documents/show_cdr.asp?url_file=/docrep/V4360E/V4360E00.htm].

Zech W., Bäumler R., Sovoskul O. and Sauer G. (1996): Zur Problematik der pleistozänen und holozänen Vergletscherung Süd-Kamtschatkas – erste Ergebnisse bodengeographischer Untersuchungen. *Eiszeitalter und Gegenwart* **46**: 132-143.

Zech W., Glaser B., Ni A.A., Petrov M. and Lemzin I. (2000): Soils as indicators of the Pleistocene and Holocene landscape evolution in the Alay Range (Kyrgystan). *Quaternary International* **65/66**: 161-169.

Zech W., Bäumler R., Madhikarmi D., Gerl T. and Beck E. (2001): Zur pleistozänen Landschaftsgeschichte des Modhi Khola-Tals (Annapurna, Nepal). *Zeitschrift für Gletscherkunde und Glazialgeologie* **37 (2)**: 159-190.

Zhisheng A., Porter S.C., Zhou W., Yanchou L., Donahue D.J., Head M.J., Xihuo W., Jianzhang R. and Hongbo Z. (1993): Episode of Strengthened Summer Monsoon Climate of Younger Dryas age on the Loess Plateau of Central China. *Quaternary Research* **39**: 45-54.

Zhou W., Donahue D.J., Porter S.C., Jull T.A., Xiaoqiang L., Stuiver M., Zhisheng A., Matsumoto E. and Guangrong D. (1996): Variability of Monsoon Climate in East Asia at the End of the Last Glaciation. *Quaternary Research* **46**: 219-229.

Zöller L. (2000): Chronology of upper Pleistocene ‘red silts’ in the Siwalik system and constraints for the timing of the upper Palaeolithic in Nepal. *Catena* **41**: 229-235.

9 Appendices

This last part compiles all analytical data from the geochemical measurements conducted in the TUM laboratories (Appendix 1), as well as total element contents determined by INAA (University of Missouri Research Reactor MURR, Columbia, MO, USA) (Appendix 2). Appendix 3 contains colour photographs of the profiles discussed in Chapters 4-6.

The data are sorted according to chronological order of the fieldwork:

<u>2000 Expedition</u>

- PT 034-PT 052: River terrace system along the Chamkhar Chhu, near Thangbi, Bumthang District, eastern Central Bhutan,
- PT 053: Thrumsing La-pass, eastern Central Bhutan,
- PT 054-PT 056: Lame Goempa Research Forest, near Jakar, Bumthang District, eastern Central Bhutan, and
- PT 057-PT 062: River terrace system along the Puna Tsang Chhu, near Bajo RNR-RC, Wangdue-Phodrang District, western Central Bhutan.

<u>2001 Expedition</u>

- PK 135-PK 152, PK 154-PK 155: Phobjikha Valley, Wangdue-Phodrang District, western Central Bhutan,
- PK 153, PK 156: Near Rukubji, Wangdue-Phodrang District, western Central Bhutan, and
- PK 157-PK 159: North of Phuentsholing, south-western Bhutan.

For location of the profiles within Bhutan, see *Fig. 8* on page 23.

Appendix 1: Soil analytical data

Sample	Hori-zon	Bulk density	Colour field	Colour dry	pH KCl	pH H_2O	C	N	C/N	LOI	Cation Exchange Capacity Na^+	K^+	Ca^{2+}	Mg^{2+}	Mn^{2+}	Al^{3+}	total	Pedogenic Oxides Fe_d	Al_d	Fe_o	Al_o	Particle Size Distribution cS	mS	fS	cSi	mSi	fSi	C	Surface area
		[g cm^{-3}]			[-]	[-]	[g kg^{-1}]		[-]	[%]	[cmol$_c$ kg^{-1}]							[g kg^{-1}]				[%]							[m^2 g^{-1}]
PT034/1	A	1.06	10YR3/3	2.5Y4/2	4.4	5.3	26.0	2.6	10.1	7.6	0.1	0.3	1.5	0.2	0.0	2.6	4.7	2.9	2.3	2.0	3.1	21.1	20.5	18.0	8.8	8.7	9.2	13.9	3.9
PT034/2	B1	1.08	10YR3/3	2.5Y5/2	4.4	5.7	11.3	0.9	12.5	3.2	0.0	0.2	1.3	0.2	0.0	1.5	3.2	3.5	1.5	2.6	2.0	22.9	25.2	19.4	7.1	7.4	5.8	12.2	5.3
PT034/3	B2	1.24	10YR3/2	10YR4/1	4.3	5.8	7.3	0.5	15.6	2.4	0.1	0.1	1.3	0.2	0.0	0.8	2.5	2.3	1.2	1.7	1.3	16.0	29.4	25.0	7.2	7.2	5.6	9.5	4.2
PT034/4	CB	1.24	10YR3/2	2.5Y5/1	4.3	5.8	7.7	0.5	17.1	3.7	0.1	0.1	1.7	0.2	0.0	0.9	3.0	1.6	0.8	1.2	1.3	21.2	29.3	22.9	4.3	7.8	5.6	9.0	4.4
PT034/5	C1	1.26	2.5Y4/2	2.5Y5/1	4.5	5.9	5.3	0.3	17.5	3.1	0.1	0.1	1.9	0.3	0.0	0.2	2.7	1.1	0.5	0.6	0.8	13.9	41.9	18.8	3.9	9.2	4.9	7.5	2.6
PT034/6	C2	0.86	2.5Y2.5/1	5Y3/1	4.6	5.8	33.7	1.5	22.0	9.3	0.1	0.3	8.6	1.3	0.0	0.2	10.6	2.3	2.1	1.7	2.7	9.2	18.2	21.6	7.3	11.2	12.5	20.1	4.8
PT035/1	A	n.d.	10YR4/4	10YR4/3	4.4	5.4	32.4	2.7	11.9	7.6	0.1	0.4	0.7	0.2	0.1	1.6	3.1	4.9	4.0	4.0	6.2	14.6	20.8	18.8	6.1	8.8	11.5	19.4	5.5
PT035/2	B	n.d.	10YR3/3	10YR4/2	4.5	5.4	19.3	1.2	15.8	3.7	0.0	0.1	0.3	0.0	0.0	1.1	1.5	5.3	3.1	4.0	6.6	36.7	19.8	11.7	4.4	6.9	7.0	13.5	3.8
PT035/3	C	n.d.	2.5Y6/4	2.5Y6/3	4.8	5.8	3.2	0.2	16.1	0.8	0.0	0.0	0.2	0.1	0.0	0.3	0.6	1.7	0.7	1.2	2.4	63.9	20.0	5.3	2.0	2.0	1.6	5.2	2.7
PT036/1	A	1.28	10YR3/3	2.5Y5/3	4.5	5.4	18.1	1.8	9.9	5.4	0.0	0.2	3.8	0.4	0.2	0.2	4.8	5.8	1.1	3.4	1.8	10.7	21.7	21.5	3.6	7.5	11.2	23.9	6.0
PT036/2	B1	1.24	10YR4/3	10YR5/3	4.5	5.6	11.1	1.1	10.0	4.5	0.0	0.2	3.6	0.5	0.0	0.2	4.5	4.7	1.2	3.2	2.0	9.2	24.0	19.3	4.5	8.1	11.2	23.5	7.9
PT036/3	B2	1.23	10YR3/4	2.5Y5/2	4.5	5.8	7.1	0.6	12.0	2.2	0.0	0.1	2.7	0.3	0.0	0.1	3.3	3.2	1.0	2.2	1.5	18.1	31.0	17.9	4.1	7.3	7.6	13.8	6.1
PT036/4	BC	1.33	2.5Y6/3	2.5Y5/2	4.7	6.1	1.2	0.1	12.1	1.5	0.0	0.1	0.8	0.2	0.0	0.1	1.1	0.7	0.3	0.6	0.5	44.0	35.0	9.5	1.4	2.2	2.2	5.7	1.9
PT036/5	C	1.28	2.5Y7/4	2.5Y6/2	4.8	6.2	0.6	0.0	15.3	1.4	0.0	0.0	0.3	0.1	0.0	0.1	0.5	0.4	0.2	0.4	0.4	42.8	36.8	10.3	1.5	1.1	1.5	5.9	1.2
PT037/1	A	1.14	10YR3/4	2.5Y4/3	4.4	5.1	25.6	2.5	10.1	n.d.	0.0	0.2	0.5	0.1	0.1	1.3	2.2	0.6	2.2	3.9	4.8	11.6	25.5	21.7	5.2	8.7	10.9	16.4	8.0
PT037/2	C1	1.14	2.5Y7/4	2.5Y7/3	4.6	5.9	2.6	0.3	7.4	n.d.	0.0	0.1	0.3	0.0	0.0	0.4	0.9	3.6	1.2	0.6	2.4	6.7	42.6	26.1	3.1	5.5	5.0	11.0	5.9
PT038/1	A	1.34	10YR3/4	2.5Y5/3	4.7	5.5	12.0	1.1	10.9	5.6	0.0	1.2	3.9	0.9	0.1	0.0	6.1	9.1	2.1	4.4	1.8	11.1	23.5	23.3	7.0	7.7	8.1	19.3	9.8
PT038/2	B	1.30	10YR5/8	2.5Y6/4	4.8	5.7	4.7	0.5	9.6	4.8	0.0	0.8	2.1	0.6	0.0	0.0	3.5	11.9	2.0	4.0	1.3	13.6	21.2	28.3	6.2	6.4	6.2	18.1	12.2
PT038/3	C1	1.16	2.5Y6/4	5Y7/3	4.9	5.8	2.3	0.3	7.6	4.9	0.0	0.5	0.9	0.2	0.0	0.1	1.7	2.9	0.9	1.0	2.2	11.0	30.7	33.5	6.6	6.6	4.0	7.6	3.5
PT039/1	A	n.d.	10YR5/6	10YR5/3	4.5	5.2	28.7	3.0	9.7	10.8	0.0	0.5	1.2	0.1	0.0	1.1	2.9	5.5	5.0	3.3	9.5	4.0	14.2	27.5	9.9	12.2	13.1	19.1	7.5
PT039/2	2A2	n.d.	2.5Y4/2	10YR5/3	4.5	5.8	17.4	1.7	10.5	8.4	0.0	0.6	1.8	0.1	0.0	0.6	3.1	3.3	4.0	1.5	7.8	5.0	18.5	25.5	11.5	11.7	11.1	16.7	8.2
PT039/3	2B	n.d.	10YR4/4	2.5Y5/4	4.9	5.8	8.6	0.7	12.6	5.3	0.0	0.2	0.8	0.0	0.0	0.1	1.2	2.3	2.1	1.1	10.2	23.3	42.3	14.7	4.9	4.8	4.0	6.0	1.8
PT039/4	2CB	n.d.	2.5Y6/8	10YR6/6	5.0	5.9	4.8	0.3	14.3	3.9	0.0	0.0	0.4	0.0	0.0	0.2	0.7	1.8	1.3	0.6	9.0	53.0	21.5	10.8	1.9	2.8	3.5	6.5	1.2
PT039/5	2C	n.d.	2.5Y6/3	5Y7/3	5.1	5.9	1.5	0.1	16.4	2.7	0.0	0.0	0.1	0.0	0.0	0.2	0.4	1.3	0.6	0.2	2.5	52.0	28.7	8.3	1.7	1.9	1.8	5.7	1.2
PT040/1	A	1.19	10YR4/3	10YR5/3	4.5	5.4	16.0	1.6	10.3	8.6	0.0	0.2	0.4	0.0	0.1	1.0	1.7	4.3	2.7	2.5	3.3	17.5	26.3	22.0	4.4	10.4	8.8	10.5	6.4
PT040/2	B	1.25	10YR4/4	10YR5/4	4.5	5.8	6.0	0.7	9.0	7.2	0.1	0.2	0.8	0.2	0.1	0.9	2.2	7.2	1.9	2.5	2.4	11.5	25.5	22.7	6.7	10.4	8.0	15.2	12.2
PT040/3	2AB	1.31	10YR3/3	2.5Y4/2	4.1	6.0	8.6	0.6	14.1	7.6	0.1	0.1	1.3	0.3	0.0	1.6	3.5	7.6	1.8	3.8	1.9	16.7	22.7	16.6	3.5	8.6	10.5	21.4	12.3
PT040/4	2Bt	1.16	10YR5/6	2.5Y5/4	4.1	5.9	4.6	0.5	10.0	8.6	0.1	0.2	1.9	0.4	0.0	1.3	3.9	7.2	1.8	3.1	1.7	8.0	30.2	21.9	2.0	7.6	8.6	21.6	15.7
PT040/5	2BC	1.20	2.5Y5/6	2.5Y6/4	4.3	6.1	1.4	0.1	9.3	5.0	0.1	0.1	1.8	0.6	0.0	0.4	3.1	4.5	1.0	1.3	1.0	7.7	46.6	23.1	2.5	5.6	5.7	8.7	8.6
PT040/6	2C	1.28	2.5Y5/4	2.5Y6/4	4.4	6.0	0.7	0.1	10.4	0.0	0.1	0.2	2.7	0.8	0.0	0.3	4.1	3.8	0.6	1.0	0.5	9.5	50.1	18.1	2.5	7.4	5.2	7.3	6.4
PT041/1	A	0.78	7.5YR4/6	10YR5/4	4.6	5.7	23.1	2.2	10.7	10.7	0.1	0.2	0.3	0.1	0.0	0.5	1.2	18.8	4.5	4.5	11.7	3.3	7.4	13.9	4.5	14.9	21.1	35.0	34.9
PT041/2	B	0.95	10YR5/6	10YR5/4	4.4	5.6	13.7	1.1	12.5	8.7	0.0	0.2	0.1	0.5	0.0	1.9	2.7	15.3	3.5	5.8	4.6	3.4	7.9	17.0	12.9	16.1	13.0	29.6	25.6
PT041/3	C	0.98	10YR6/6	10YR6/4	4.3	5.8	6.5	0.6	10.7	5.8	0.0	0.1	0.1	0.2	0.0	1.4	1.9	7.7	1.8	3.0	2.3	4.6	14.2	33.4	9.2	10.7	9.2	18.7	17.5
PT041/4	2C2	1.26	2.5Y6/6	2.5Y6/4	4.4	5.9	2.5	0.3	9.1	4.8	0.0	0.1	0.1	0.2	0.0	0.7	1.2	8.1	1.3	1.8	1.3	20.5	25.5	23.0	6.6	7.9	5.6	11.0	9.9
PT041/5	3A2	0.88	10YR4/4	10YR5/4	4.4	5.8	16.2	1.1	14.6	10.8	0.1	0.2	0.0	0.3	0.0	2.2	2.7	29.6	6.4	10.7	6.3	1.3	3.6	9.4	11.9	13.5	16.5	43.9	40.0
PT041/6	3B2	0.97	10YR5/8	10YR6/6	4.2	5.9	4.3	0.6	7.8	8.3	0.1	0.1	0.1	0.3	0.0	2.3	2.9	25.9	5.7	3.5	2.6	2.3	5.1	12.0	8.6	13.5	15.6	43.0	35.8
PT041/7	3B3	1.20	10YR6/8	10YR6/4	4.3	6.0	2.5	0.4	6.1	6.7	0.1	0.1	0.8	0.3	0.0	1.2	2.4	14.7	3.0	2.5	1.8	3.9	12.9	13.1	8.8	12.7	15.7	33.0	25.1
PT041/8	3C3	1.35	2.5Y7/6	2.5Y7/4	4.3	6.1	1.2	0.2	6.6	4.4	0.1	0.1	0.7	0.2	0.0	0.5	1.6	7.0	2.4	1.5	1.2	23.4	20.7	15.7	5.8	9.2	9.5	15.8	14.8
PT041/X	-	n.d.	n.d.	10YR6/6	4.3	6.2	0.9	0.1	8.1	5.5	0.1	0.1	0.5	0.4	0.0	0.4	1.5	8.6	1.9	0.6	1.0	18.4	29.7	15.8	8.3	5.9	4.1	17.8	16.4

Appendix 1 (continued)

Sample	Hori-zon	Bulk density	Colour field	Colour dry	pH KCl	pH H_2O	C	N	C/N	LOI	CEC Na^+	CEC K^+	CEC Ca^{2+}	CEC Mg^{2+}	CEC Mn^{2+}	CEC Al^{3+}	CEC total	Fe_d	Al_d	Fe_o	Al_o	cS	mS	fS	cSi	mSi	fSi	C	Surface area
		[g cm^{-3}]			[-]	[-]	[g kg^{-1}]	[g kg^{-1}]	[-]	[%]	[$cmol_c$ kg^{-1}]							[g kg^{-1}]				[%]							[m^2 g^{-1}]
PT042/1	A1	0.89	10YR3/4	10YR4/3	4.6	5.5	44.4	3.7	11.8	13.6	0.0	0.6	4.4	1.0	0.1	0.3	6.4	7.3	4.4	3.7	7.6	9.6	20.6	20.6	4.5	8.8	12.8	23.1	8.4
PT042/2	B1	0.99	10YR4/4	10YR5/4	4.5	5.7	19.0	2.0	9.6	7.8	0.0	0.4	0.9	0.4	0.0	0.6	2.3	9.5	3.0	3.7	6.1	9.2	24.4	20.7	6.0	10.3	11.1	18.3	10.7
PT042/3	2B2	1.34	2.5Y5/4	2.5Y5/3	3.8	5.8	5.0	0.6	7.8	4.7	0.0	0.2	1.4	0.7	0.0	0.9	3.3	8.8	1.4	4.0	1.1	8.7	23.3	20.6	5.4	9.2	11.5	21.4	11.2
PT042/4	2B3	1.38	10YR5/4	2.5Y6/4	3.7	5.7	4.7	0.6	8.0	4.6	0.1	0.1	1.5	0.6	0.0	1.0	3.3	13.0	2.3	3.7	1.4	7.4	23.6	21.4	5.7	9.5	10.8	21.7	16.0
PT042/5	2B4	1.25	10YR4/4	10YR5/4	3.9	5.3	7.2	0.8	8.9	6.4	0.1	0.2	1.2	0.5	0.0	1.9	3.9	15.5	3.1	4.6	2.5	7.3	19.3	19.7	6.7	10.5	11.4	25.2	18.7
PT042/6	2B5	1.07	10YR4/4	10YR5/4	4.1	5.3	11.1	1.2	9.3	7.5	0.0	0.6	0.4	0.1	0.0	1.4	2.5	12.9	4.7	5.4	6.0	5.8	17.1	18.9	6.8	12.0	12.8	26.5	20.9
PT042/7	3A2	0.94	10YR3/3	10YR4/3	4.0	5.4	20.7	1.5	13.6	9.8	0.0	0.3	0.8	0.3	0.0	2.3	3.8	17.7	5.2	9.2	5.5	3.6	9.3	14.3	11.1	11.8	12.5	37.4	23.4
PT042/8	3Bt	0.99	10YR5/8	10YR5/6	4.1	5.4	9.0	1.0	9.4	8.2	0.0	0.3	0.9	0.5	0.0	1.8	3.6	22.5	4.8	8.9	4.6	2.4	6.0	13.3	10.4	13.5	12.7	41.7	33.6
PT042/X	3C	n.d.	n.d.	10YR6/6	4.1	5.4	3.9	0.3	12.1	5.4	0.0	0.4	1.0	0.5	0.0	0.8	2.7	12.9	2.4	4.1	2.0	5.5	18.6	22.6	6.5	10.8	12.7	23.3	17.8
PT043/1	A1	0.83	10YR4/4	2.5Y4/3	4.5	5.4	31.0	2.8	11.0	10.7	0.0	0.2	1.0	0.4	0.0	0.9	2.5	9.7	3.8	4.2	7.6	9.9	21.8	17.8	5.6	11.2	13.6	20.1	11.0
PT043/2	B1	0.92	10YR4/4	2.5Y5/4	4.5	5.5	19.8	2.0	9.9	8.2	0.0	0.1	1.0	0.5	0.0	0.8	2.5	9.1	3.5	4.2	5.4	10.7	18.9	19.6	6.4	13.0	12.5	18.9	12.6
PT043/3	2A2	1.06	10YR5/4	2.5Y5/3	4.3	5.5	11.2	1.2	9.0	6.6	0.0	0.1	1.3	0.9	0.0	1.0	3.3	10.1	2.5	4.2	2.5	7.6	26.2	16.8	5.9	10.7	12.1	20.8	14.0
PT043/4	2B2	1.30	10YR5/4	2.5Y5/4	4.1	5.4	6.0	0.7	8.3	5.2	0.0	0.1	1.5	0.8	0.0	0.9	3.5	9.4	2.1	3.9	1.8	9.6	20.9	20.9	7.7	10.2	10.9	19.8	13.4
PT043/5	2B3	1.32	10YR5/4	2.5Y5/3	4.0	5.5	5.3	0.7	8.2	5.1	0.1	0.1	1.8	0.8	0.0	0.8	3.7	9.6	2.2	3.8	1.7	7.5	23.2	20.0	6.5	10.4	12.3	20.2	13.9
PT043/6	2C	n.d.	n.d.	2.5Y6/3	4.1	5.9	1.3	0.1	9.9	3.5	0.1	0.1	2.0	0.6	0.0	1.1	3.9	4.5	0.9	0.9	1.5	36.0	31.0	14.4	3.6	4.6	3.4	7.0	3.5
PT044/1	A	n.d.	2.5Y5/3	2.5Y5/4	4.4	5.4	27.8	2.4	11.7	9.5	0.0	0.4	2.9	0.6	0.1	0.4	4.3	9.1	3.4	4.9	4.5	11.7	19.0	17.2	7.6	10.6	11.4	22.5	8.5
PT044/2	2B	n.d.	2.5Y6/4	2.5Y6/4	4.2	5.7	2.6	0.3	9.6	4.7	0.0	0.3	1.5	0.6	0.0	0.3	2.7	7.7	0.8	1.3	1.1	20.9	30.7	25.9	5.5	6.4	3.8	6.7	7.3
PT044/3	2C	n.d.	2.5Y8/1	2.5Y7/3	4.2	6.1	0.5	0.1	6.1	3.9	0.0	0.1	1.5	0.7	0.0	0.1	2.4	5.1	0.4	1.2	0.4	25.6	37.1	16.5	6.4	5.2	2.9	6.2	6.3
PT045/1	A	1.07	10YR3/3	10YR5/3	3.9	5.3	17.1	1.3	13.3	8.0	0.1	0.1	2.2	0.4	0.1	1.8	4.6	13.7	3.2	6.4	3.2	6.4	14.6	22.2	8.6	12.2	11.7	24.3	16.3
PT045/2	2A2	1.09	10YR4/4	10YR5/3	4.3	5.6	17.2	1.6	11.0	8.7	0.1	0.1	2.9	1.2	0.0	0.8	5.1	12.9	4.1	7.8	6.0	3.4	8.8	12.8	9.3	13.1	18.2	34.4	24.1
PT045/3	2B	0.92	10YR6/8	10YR6/6	4.5	5.6	9.2	0.8	11.1	8.5	0.1	0.1	0.8	0.3	0.0	0.6	1.9	24.4	4.5	9.9	8.1	1.3	4.1	13.7	13.0	13.6	14.8	39.4	35.8
PT045/X	-	n.d.	n.d.	10YR6/6	4.5	5.7	1.8	0.2	7.4	6.7	0.1	0.2	1.8	1.1	0.0	0.3	3.6	14.9	3.0	2.5	1.5	11.3	18.0	16.3	6.6	8.6	10.6	28.6	25.1
PT047/1	A1	1.41	10YR5/4	10YR5/3	4.5	5.5	18.8	1.8	10.6	8.6	0.1	0.7	2.6	0.7	0.1	0.4	4.6	10.8	3.3	4.7	3.1	15.7	12.5	17.2	8.1	11.2	12.7	22.5	12.8
PT047/2	B1	1.39	10YR5/4	10YR6/4	4.6	5.9	7.4	0.9	8.3	6.7	0.1	0.5	3.0	0.9	0.0	0.2	4.7	10.5	3.7	4.9	2.8	9.4	14.4	16.3	9.4	13.9	13.7	22.9	18.8
PT047/3	2B2	0.97	10YR4/4	10YR5/4	4.7	5.9	14.6	1.5	10.0	8.5	0.0	0.5	2.2	0.6	0.0	0.2	3.5	13.0	4.9	6.3	7.6	4.1	10.1	14.5	14.5	16.7	15.9	24.2	23.2
PT047/4	3A2	0.91	10YR3/2	10YR4/2	4.7	6.0	28.2	1.7	16.2	11.9	0.1	0.5	5.1	1.2	0.0	0.1	6.9	12.0	5.4	7.6	6.1	4.2	9.6	12.0	11.8	13.9	17.2	31.2	22.8
PT047/5	3B3	1.33	2.5Y6/4	2.5Y6/4	4.8	6.1	3.5	0.4	9.7	5.5	0.1	0.5	2.2	1.0	0.0	0.0	3.7	10.6	2.8	2.0	1.4	6.4	19.4	21.1	9.8	12.2	11.8	19.2	17.4
PT048/1	A	n.d.	10YR3/4	10YR5/3	4.6	5.6	25.5	2.4	10.6	9.3	0.1	0.3	1.4	0.3	0.1	0.7	2.9	5.1	3.6	4.1	5.5	14.5	16.7	18.4	9.8	11.7	11.5	17.5	10.7
PT048/2	B1	1.20	10YR5/4	2.5Y5/3	4.3	5.4	12.1	1.4	8.8	6.7	0.1	0.1	0.9	0.5	0.0	1.1	2.7	4.3	2.1	4.0	3.3	11.6	19.9	15.6	8.2	12.5	12.7	19.4	11.5
PT048/3	B2	1.15	10YR4/4	10YR6/4	4.3	5.5	8.8	1.1	8.1	5.9	0.1	0.1	1.0	0.2	0.0	0.9	2.4	6.4	1.9	4.3	3.4	10.3	19.3	17.0	7.9	12.1	13.6	19.8	12.8
PT048/4	C	1.56	5Y8/2	2.5Y7/3	4.5	6.0	0.7	0.1	6.7	3.8	0.0	0.1	0.9	0.3	0.0	0.0	1.4	4.2	0.4	0.7	0.5	15.0	27.0	22.7	8.2	12.1	7.3	7.7	7.4
PT049/1	A1	0.99	10YR4/4	10YR5/3	4.4	5.4	33.2	2.9	11.6	10.7	0.1	0.4	2.0	0.5	0.1	1.1	4.1	5.4	4.5	4.0	6.9	12.1	19.5	16.8	11.5	13.4	10.3	16.3	9.3
PT049/2	2A2	0.96	10YR3/3	10YR5/3	4.4	5.5	23.5	2.1	11.0	9.1	0.1	0.2	1.7	0.4	0.1	0.9	3.4	5.8	4.0	4.1	5.6	10.6	19.7	18.6	7.5	10.4	12.6	20.6	10.3
PT049/3	2B	1.26	10YR4/4	2.5Y5/4	4.0	5.6	4.5	0.4	10.1	5.5	0.1	0.0	0.6	0.0	0.1	2.2	3.0	7.3	2.2	4.1	2.7	9.6	20.4	17.7	7.8	11.2	11.3	22.0	18.6
PT049/4	3A3	1.08	10YR3/4	10YR5/3	4.3	5.6	9.1	0.9	10.5	6.2	0.1	0.0	0.3	0.0	0.1	1.1	1.6	8.5	3.7	4.7	5.8	8.8	22.2	18.0	8.4	10.9	11.0	20.7	18.1
PT049/5	3B2	1.15	2.5Y5/6	2.5Y6/4	4.4	6.1	1.8	0.2	10.3	6.8	0.1	0.1	2.9	0.7	0.0	0.3	4.2	7.2	2.1	1.9	1.1	6.0	27.0	29.6	8.0	10.8	9.1	9.6	16.3
PT049/6	3C	n.d.	n.d.	2.5Y6/4	4.6	6.2	1.2	0.1	11.0	6.2	0.2	0.1	3.6	2.4	0.0	0.1	6.3	8.5	1.5	1.9	1.3	11.9	33.3	23.5	8.5	10.2	5.2	7.4	15.2
PT052/2	B1	1.14	10YR4/3	10YR5/4	4.7	5.9	12.9	1.7	7.6	5.9	0.1	0.1	1.5	0.2	0.0	0.1	2.0	10.0	3.4	4.1	1.5	10.8	10.8	13.8	16.7	20.0	11.7	16.3	12.4
PT052/3	B2	1.33	2.5Y8/3	10YR6/4	4.2	5.8	5.0	0.7	6.7	6.0	0.1	0.3	2.8	2.8	0.1	0.2	6.2	16.3	3.8	2.6	1.3	4.4	6.9	11.5	12.0	16.5	16.2	32.5	28.5
PT052/4	B3	1.57	2.5Y8/3	2.5Y6/4	4.6	6.1	3.1	0.5	6.1	4.6	0.1	0.2	2.1	1.3	0.0	0.0	3.7	11.0	2.3	2.7	1.1	4.2	9.6	17.0	14.5	13.9	14.9	25.9	23.3
PT052/5	2B4	1.57	2.5Y6/6	2.5Y6/4	4.8	6.3	1.7	0.3	5.0	3.9	0.1	0.1	2.9	2.4	0.1	0.0	5.5	7.8	1.5	1.4	1.0	12.0	20.2	15.6	8.3	11.1	11.2	21.6	16.6
PT052/6	2C	n.d.	2.5Y5/4	2.5Y6/4	4.7	6.0	3.4	0.6	6.2	4.5	0.1	0.2	3.0	2.6	0.1	0.0	6.0	11.5	1.9	1.9	1.1	11.4	16.4	13.2	9.5	13.5	11.8	24.2	19.5

Appendix 1 (continued)

Sample	Hori-zon	Bulk density	Colour field	Colour dry	pH KCl	pH H_2O	C	N	C/N	LOI	CEC Na^+	K^+	Ca^{2+}	Mg^{2+}	Mn^{2+}	Al^{3+}	total	Pedogenic Oxides Fe_d	Al_d	Fe_o	Al_o	Particle Size Distribution cS	mS	fS	cSi	mSi	fSi	C	Surface area
		[g cm^{-3}]			[-]	[-]	[g kg^{-1}]		[-]	[%]	[cmol$_c$ kg^{-1}]							[g kg^{-1}]				[%]							[m^2 g^{-1}]
PT053/1	A	n.d.	n.d.	10YR3/1	3.1	3.6	110.0	7.5	14.6	24.5	0.1	0.2	0.3	0.3	0.0	3.3	4.1	2.7	1.8	2.7	1.5	7.2	22.8	11.6	10.2	12.4	11.8	23.9	1.4
PT053/2	Bhs	n.d.	10YR3/2	10YR3/3	3.6	3.9	75.5	3.7	20.5	20.6	0.0	0.1	0.4	0.2	0.0	7.7	8.5	12.7	5.6	19.6	5.7	16.4	35.2	9.2	3.8	5.8	6.3	23.3	4.6
PT053/3	Bs	n.d.	7.5YR4/4	2.5Y5/4	4.3	4.7	14.7	0.8	18.5	8.0	0.0	0.0	0.3	0.1	0.0	2.0	2.4	8.8	4.7	7.7	5.0	27.2	30.6	11.6	4.1	5.4	6.3	14.8	17.4
PT053/4	CB	n.d.	2.5YR5/6	2.5Y6/3	4.3	5.1	4.3	0.3	16.2	5.1	0.0	0.1	0.1	0.0	0.0	1.2	1.4	2.1	1.5	1.7	2.2	24.2	32.9	14.6	3.8	6.3	6.8	11.4	9.1
PT053/5	C1	n.d.	5Y6/3	2.5Y7/2	4.4	5.4	2.1	0.1	25.0	4.5	0.0	0.1	0.1	0.0	0.0	0.8	0.9	1.2	0.9	0.8	1.6	18.4	47.3	16.5	4.3	4.9	3.5	5.1	7.3
PT053/6	C2	n.d.	5Y7/2	5Y7/1	4.6	5.6	0.4	0.0	9.1	3.6	0.0	0.0	0.1	0.0	0.0	0.4	0.5	0.8	0.4	0.1	0.7	36.1	31.4	18.6	3.5	3.1	2.5	4.8	3.6
PT054/1	A	0.59	10YR3/2	10YR3/2	3.8	4.2	87.6	5.9	14.9	21.7	0.0	0.3	4.2	1.1	0.2	3.7	9.4	13.0	3.9	12.2	3.3	4.2	14.6	18.5	7.3	10.1	11.1	34.2	4.9
PT054/2	AB	0.59	10YR4/4	10YR4/4	4.1	4.5	52.5	2.7	19.7	16.7	0.0	0.1	1.1	0.2	0.0	4.1	5.6	22.5	7.7	21.9	8.1	4.2	15.8	18.6	6.7	7.7	9.9	37.0	27.1
PT054/3	B1	0.58	10YR5/6	10YR5/4	4.2	4.7	49.9	2.3	21.7	17.0	0.0	0.1	0.7	0.2	0.0	3.1	4.2	21.4	11.4	20.0	10.8	2.7	15.3	21.2	6.7	9.6	11.4	33.1	24.5
PT054/4	B2	0.78	2.5Y5/6	2.5Y6/4	4.5	5.2	27.4	1.5	18.6	10.4	0.0	0.0	0.4	0.1	0.1	1.7	2.3	12.9	9.8	8.4	11.0	4.6	18.9	21.9	6.8	9.7	10.6	27.5	19.5
PT054/5	CB	1.09	2.5Y5/4	2.5Y5/4	4.6	5.3	17.1	1.1	15.4	9.5	0.1	0.0	0.2	0.0	0.0	1.1	1.4	9.8	6.5	5.2	8.5	5.9	23.3	23.5	7.8	9.9	10.3	19.2	17.4
PT054/6	C	1.15	2.5Y6/4	2.5Y7/3	4.6	5.8	1.4	0.1	13.1	5.8	0.0	0.0	0.1	0.0	0.0	0.6	0.8	2.1	1.0	0.6	1.9	21.0	40.4	17.6	4.9	5.1	3.5	7.5	7.4
PT055/1	OA	n.d.	10YR2/2	10YR3/2	2.8	3.6	153.3	8.6	17.8	33.8	0.1	0.3	2.6	0.6	0.0	4.0	7.6	3.9	1.9	3.1	1.6	1.5	7.0	11.7	12.7	15.9	18.9	32.3	2.7
PT055/2	AE	0.80	2.5Y4/1	10YR3/2	2.9	3.7	90.2	4.8	18.7	21.2	0.0	0.2	1.5	0.4	0.0	7.6	9.7	7.5	2.0	8.4	2.5	2.4	10.1	12.2	11.7	13.3	14.0	36.3	3.9
PT055/3	Bh	n.d.	7.5YR4/4	10YR2/2	3.5	4.0	111.8	5.4	20.8	30.2	0.1	0.2	2.4	0.6	0.0	17.5	20.7	75.0	8.3	30.3	8.4	2.5	9.1	9.8	4.6	7.6	10.4	55.9	14.5
PT055/4	Bs	0.39	7.5YR4/6	10YR5/6	3.8	4.4	66.3	2.9	22.9	22.2	0.1	0.1	0.8	0.2	0.0	10.1	11.3	52.5	10.8	43.0	10.9	3.3	9.9	10.0	4.3	8.5	12.0	51.9	41.8
PT055/5	B	0.43	10YR5/8	10YR4/6	4.0	4.6	44.1	2.1	21.1	16.8	0.1	0.1	0.4	0.1	0.0	6.1	6.8	46.0	10.2	25.6	9.3	2.9	13.3	14.7	6.2	10.2	14.3	38.4	38.8
PT055/6	BC	0.91	2.5Y5/6	2.5Y5/4	4.3	4.8	30.0	1.6	18.9	13.9	0.0	0.0	0.2	0.0	0.0	3.2	3.5	20.4	14.3	7.5	13.6	4.4	18.2	13.6	6.6	12.2	14.7	30.3	22.1
PT056/1	A	0.49	2.5Y3/2	10YR3/3	4.0	4.8	116.9	6.2	19.0	29.0	0.0	0.3	6.2	1.4	0.1	5.9	14.0	28.6	11.0	11.9	8.5	3.4	7.0	8.3	8.9	12.0	13.1	47.2	17.9
PT056/2	AB	0.59	2.5Y4/4	10YR4/4	4.0	4.8	57.7	2.6	22.2	17.3	0.0	0.1	1.5	0.3	0.0	7.3	9.2	31.8	8.9	11.8	7.5	0.3	1.1	7.6	7.6	16.5	17.4	49.6	32.7
PT056/3	B1	0.46	10YR6/8		4.6	5.1	22.7	1.5	15.6	13.7	0.0	0.0	0.3	0.1	0.0	0.9	1.5	41.3	12.3	9.6	15.5	0.4	8.2	11.4	7.2	13.5	21.6	37.7	51.1
PT056/4	B2	0.69	10YR5/8	10YR6/6	4.9	5.4	21.8	1.4	15.4	13.8	0.0	0.1	0.2	0.0	0.0	0.2	0.5	36.7	13.2	7.1	17.9	1.9	15.8	13.3	7.7	13.7	19.7	27.9	47.9
PT056/5	B3	0.84	10YR5/8	10YR6/8	4.9	5.7	12.0	1.0	12.1	11.0	0.0	0.0	0.2	0.1	0.0	0.2	0.5	32.3	8.3	13.7	11.5	1.3	4.8	14.0	8.5	14.7	19.5	37.2	50.7
PT056/6	CB	1.24	10YR6/8	2.5Y6/4	4.6	5.5	4.5	0.4	11.8	6.2	0.0	0.0	0.3	0.2	0.0	0.5	1.0	15.5	3.3	6.6	2.4	21.9	21.4	16.0	4.2	6.7	7.7	22.1	20.6

Appendix 1 (continued)

Sample	Hori-zon	Bulk density	Colour field	Colour dry	pH KCl	pH H_2O	C	N	C/N	LOI	Cation Exchange Capacity Na^+	K^+	Ca^{2+}	Mg^{2+}	Mn^{2+}	Al^{3+}	total	Pedogenic Oxides Fe_d	Al_d	Fe_o	Al_o	Particle Size Distribution cS	mS	fS	cSi	mSi	fSi	C	Surface area
		[g cm^{-3}]			[-]	[-]	[g kg^{-1}]		[-]	[%]	[cmol$_c$ kg^{-1}]							[g kg^{-1}]				[%]							[m^2 g^{-1}]
PT057/1	A	1.57	2.5Y6/4	2.5Y5/4	5.5	6.6	8.5	0.9	9.6	5.6	0.0	0.4	5.8	1.3	0.0	0.0	7.6	11.7	0.9	2.2	0.4	8.8	18.8	19.3	6.9	9.8	11.1	25.3	16.4
PT057/2	B1	1.51	2.5Y5/4	2.5Y5/4	5.7	6.6	6.9	0.8	8.6	4.8	0.0	0.2	6.1	1.3	0.0	0.0	7.8	9.5	0.7	2.8	0.2	10.5	19.6	18.5	5.4	10.4	11.2	24.3	15.1
PT057/3	B2	1.27	10YR5/4	2.5Y5/4	5.8	6.6	8.8	1.0	8.8	5.2	0.0	0.3	5.8	1.1	0.0	0.0	7.3	8.5	0.8	2.6	0.2	8.3	20.8	19.0	8.4	11.3	10.5	21.8	14.0
PT057/4	B3	1.41	10YR4/3	2.5Y5/3	5.6	6.7	6.4	0.8	8.6	4.8	0.0	0.3	4.5	1.0	0.0	0.0	5.8	8.9	0.4	2.8	0.2	6.8	16.2	21.0	8.4	10.1	10.5	27.0	14.6
PT057/5	CB1	1.29	10YR6/4	10YR5/4	5.7	6.7	5.6	0.6	9.4	4.0	0.0	0.2	4.3	0.9	0.0	0.0	5.4	8.2	0.4	3.0	0.2	8.0	36.4	20.2	4.7	5.9	6.2	18.6	10.0
PT057/6	CB2	1.58	10YR5/4	2.5Y5/4	5.7	6.7	4.8	0.6	7.7	5.0	0.0	0.3	4.8	1.1	0.0	0.0	6.2	7.9	0.4	2.0	0.2	6.6	23.8	18.8	7.7	7.8	9.9	25.5	17.8
PT057/7	CB3	1.61	10YR5/4	10YR5/3	5.8	6.9	3.5	0.5	7.6	4.7	0.1	0.2	3.9	1.0	0.0	0.0	5.2	11.3	0.9	1.2	0.4	7.2	25.2	21.8	6.0	6.4	7.7	25.7	16.8
PT057/X	-	n.d.	n.d.	5Y8/1	7.8	6.8	3.5	0.1	41.4	1.2	0.0	0.0	10.6	0.1	0.0	0.0	10.8	1.4	0.1	0.4	0.2	0.0	38.2	52.0	4.1	1.3	1.2	3.1	10.1
PT058/1	A	1.29	10YR6/4	2.5Y5/3	5.2	6.1	21.2	1.6	13.3	8.4	0.1	1.4	5.9	1.6	0.1	0.0	9.0	9.2	0.5	4.0	0.5	7.2	16.3	18.5	7.5	10.9	12.5	27.1	13.7
PT058/2	B1	1.62	10YR6/3	2.5Y5/4	6.1	6.4	4.0	0.5	7.7	4.4	0.0	0.2	5.2	1.3	0.0	0.0	6.8	8.6	0.3	2.8	0.5	7.8	22.6	18.8	6.5	9.3	10.2	24.7	16.0
PT058/3	B2	1.51	10YR6/4	2.5Y5/4	6.1	6.5	2.3	0.3	6.6	4.6	0.0	0.3	5.1	1.5	0.0	0.0	6.9	15.3	0.9	2.2	0.6	7.3	22.2	17.4	5.4	9.6	10.3	27.8	20.6
PT058/4	B3	1.58	10YR5/4	2.5Y6/4	6.1	6.2	2.2	0.5	4.8	4.6	0.3	0.3	6.3	1.8	0.0	0.0	8.6	12.9	0.9	2.6	0.5	7.0	21.0	18.9	6.6	8.9	9.7	27.8	18.6
PT058/5	CB	1.46	10YR6/4	2.5Y5/4	6.3	7.0	1.7	0.2	7.7	4.6	0.2	0.1	3.3	0.9	0.0	0.0	4.5	8.1	0.8	1.1	0.3	10.8	34.1	17.8	7.1	7.0	4.9	18.3	12.2
PT058/6	C	1.45	10YR5/4	10YR5/4	6.2	7.3	0.8	0.1	6.5	2.3	0.1	0.1	2.1	0.5	0.0	0.0	2.9	6.1	0.6	0.7	0.2	11.6	39.9	23.1	5.9	4.6	3.7	11.3	8.3
PT059/1	A	1.51	2.5Y6/1	5Y6/3	5.6	6.0	14.0	1.5	9.4	7.5	0.0	0.4	7.0	1.6	0.0	0.0	9.0	5.5	0.3	4.6	0.5	3.7	10.1	15.2	8.2	11.6	14.9	36.2	19.1
PT059/2	B1	1.59	2.5Y6/2	2.5Y5/4	6.6	6.6	4.0	0.5	8.3	4.9	0.1	0.4	7.8	1.9	0.0	0.0	10.3	17.6	0.6	4.3	0.5	7.3	14.7	15.8	5.0	8.7	13.6	34.8	24.4
PT059/3	2B2	1.69	10YR5/4	10YR4/4	6.7	6.8	2.8	0.3	9.3	3.4	0.0	0.3	4.9	1.2	0.0	0.0	6.4	12.6	0.9	2.1	0.5	7.7	21.5	22.4	7.1	7.8	9.3	24.1	15.5
PT059/4	2B3	1.54	7.5YR5/4	10YR4/4	6.6	6.9	1.7	0.3	6.6	4.0	0.0	0.4	5.2	1.4	0.0	0.0	7.0	11.6	1.2	1.3	0.6	2.6	20.6	30.0	6.2	5.6	8.3	26.7	18.9
PT059/5	2B4	1.45	7.5YR5/6	10YR5/6	6.4	7.2	1.1	0.2	6.4	3.7	0.0	0.3	3.7	1.0	0.0	0.0	5.0	9.2	1.1	0.7	0.5	1.3	26.0	34.4	5.7	4.5	6.3	21.8	15.6
PT059/X1	2B5	n.d.	n.d.	7.5YR4/6	6.5	7.1	0.8	0.2	3.8	5.3	0.1	0.8	6.5	2.0	0.0	0.0	9.3	12.8	1.7	0.8	1.1	0.7	14.6	22.6	7.8	7.3	8.8	38.3	33.6
PT059/X2	2B6	n.d.	n.d.	10YR5/6	6.5	7.1	0.7	0.1	4.8	4.1	0.1	0.5	5.4	1.6	0.0	0.0	7.6	10.3	1.3	0.4	0.7	0.6	22.8	29.4	6.9	5.5	6.3	28.4	24.4
PT060/1	A	1.45	2.5Y5/2	2.5Y5/3	5.9	6.9	7.2	0.9	8.1	5.8	0.1	0.3	6.3	1.4	0.0	0.0	8.0	6.6	0.3	4.6	0.5	5.7	11.0	17.5	8.1	12.5	13.0	32.3	18.3
PT060/2	B1	1.44	10YR5/4	2.5Y5/4	6.4	7.0	3.5	0.5	7.5	5.5	0.1	0.3	6.4	1.7	0.0	0.0	8.5	13.5	0.9	3.3	0.9	4.5	11.5	19.1	7.2	9.8	12.1	35.8	25.3
PT060/3	B2	1.50	10YR5/4	2.5Y5/4	6.3	7.0	3.3	0.4	7.6	5.4	0.1	0.3	5.6	1.4	0.0	0.0	7.4	14.4	0.8	3.4	0.8	4.9	11.7	20.2	8.0	10.8	12.3	32.1	24.2
PT060/4	Bt1	1.58	10YR4/4	10YR5/4	6.4	7.0	1.9	0.3	6.2	5.5	0.1	0.4	6.5	1.8	0.0	0.0	8.7	18.9	1.7	1.4	1.0	2.8	8.2	21.2	8.4	9.0	11.3	39.1	29.9
PT060/5	Bt2	1.49	7.5YR4/6	10YR5/6	6.4	7.1	1.8	0.3	5.7	6.1	0.1	0.4	6.0	1.7	0.0	0.0	8.2	22.0	2.0	1.0	1.0	2.9	6.5	18.6	8.3	8.4	11.7	43.6	32.6
PT060/X1	-	n.d.	n.d.	10YR5/4	6.3	7.2	3.5	0.5	7.6	4.9	0.1	0.4	6.6	1.7	0.0	0.0	8.8	14.8	0.7	5.6	0.8	3.5	12.9	20.9	8.8	8.9	11.1	33.9	26.5
PT060/X2	-	n.d.	n.d.	10YR5/4	6.3	7.1	0.9	0.2	4.5	3.7	0.1	0.3	5.4	1.5	0.0	0.0	7.4	10.9	0.9	2.0	0.8	0.3	18.1	33.8	7.0	6.0	6.9	27.9	20.3
PT061/1	A	1.52	10YR6/4	2.5Y5/3	5.0	6.3	11.5	1.1	10.2	6.3	0.0	0.4	4.8	1.3	0.1	0.0	6.6	13.4	0.8	3.5	0.6	5.4	15.1	17.7	7.4	11.7	14.2	28.5	15.5
PT061/2	B1	1.45	10YR5/4	2.5Y5/4	5.8	6.9	5.4	0.6	8.6	5.1	0.1	0.2	5.7	1.4	0.0	0.0	7.5	11.8	0.5	4.1	0.5	5.0	13.4	17.5	7.7	12.2	13.5	30.6	16.1
PT061/3	2B2	1.55	2.5Y5/3	2.5Y5/3	6.2	7.0	2.0	0.5	4.4	5.4	0.1	0.3	5.4	1.3	0.0	0.0	7.2	15.0	1.0	2.0	0.7	6.0	12.4	17.8	7.3	11.3	14.3	31.0	18.6
PT061/4	2B3	1.59	10YR5/6	2.5Y5/3	6.3	7.0	2.9	0.4	8.0	4.4	0.1	0.3	5.5	1.4	0.0	0.0	7.3	14.6	0.9	2.0	0.6	8.0	19.6	20.3	6.7	10.2	10.3	24.9	16.5
PT061/5	2B4	1.55	10YR5/6	10YR5/4	6.4	7.1	2.3	0.3	8.7	3.5	0.0	0.2	4.1	1.1	0.0	0.0	5.4	14.1	1.1	1.8	0.5	12.7	21.3	24.2	6.8	8.7	7.8	18.5	13.8
PT061/X1	-	n.d.	n.d.	10YR4/4	6.4	7.1	1.5	0.2	7.6	3.5	0.0	0.2	3.9	1.1	0.0	0.0	5.2	14.5	0.9	1.3	0.4	22.3	28.4	15.2	2.7	5.3	5.6	20.6	13.5
PT061/X2	-	n.d.	n.d.	7.5YR4/6	6.9	7.1	1.0	0.2	4.1	4.4	0.0	0.3	4.8	1.4	0.0	0.0	6.5	18.0	0.6	0.7	0.4	11.6	19.4	16.8	6.9	9.0	9.2	27.0	22.4
PT062/1	A	1.38	10YR5/4	10YR5/4	6.3	6.8	21.7	1.8	11.7	9.1	0.0	0.4	8.1	1.9	0.0	0.0	10.5	15.2	1.5	1.8	0.9	11.4	14.6	14.7	6.8	8.8	10.1	33.7	17.4
PT062/2	B1	1.47	7.5YR4/6	7.5YR4/6	6.2	7.1	3.1	0.5	6.4	6.1	0.0	0.5	5.9	1.8	0.0	0.0	8.3	18.7	1.9	1.2	1.5	5.0	9.4	10.1	5.6	9.7	10.1	50.0	36.3
PT062/3	B2	1.54	5YR4/6	7.5YR4/6	6.3	7.1	1.4	0.4	3.8	5.6	0.0	0.5	5.7	2.0	0.0	0.0	8.2	17.6	1.5	0.9	1.2	6.3	12.9	11.8	7.3	6.7	8.5	46.4	37.0
PT062/4	B3	1.58	5YR4/6	7.5YR4/6	6.3	7.1	1.2	0.3	4.3	4.8	0.0	0.3	4.4	1.6	0.0	0.0	6.3	19.1	1.8	0.8	0.9	6.7	15.0	13.2	6.9	6.2	8.6	43.5	32.1
PT062/5	CB	1.60	5YR4/4	7.5YR4/6	6.3	7.1	1.0	0.3	4.1	4.4	0.0	0.3	4.6	1.7	0.0	0.0	6.6	20.1	1.6	0.6	0.6	13.4	16.1	14.6	4.4	6.1	8.2	37.3	25.5
PT062/X1	-	n.d.	n.d.	n.d.	6.3	7.1	0.9	0.2	5.4	4.8	0.0	0.2	3.6	1.9	0.0	0.0	5.7	17.8	1.3	0.5	0.4	13.3	20.7	19.9	5.2	8.5	8.1	24.4	19.7

Appendix 1 (continued)

Sample	Hori-zon	Bulk density	Colour field	Colour dry	pH KCl	pH H_2O	C	N	C/N	LOI	Na^+	K^+	Ca^{2+}	Mg^{2+}	Mn^{2+}	Al^{3+}	total	Fe_d	Al_d	Fe_o	Al_o	cS	mS	fS	cSi	mSi	fSi	C	Surface area
		[g cm^{-3}]			[-]	[-]	[g kg^{-1}]		[-]	[%]	[cmol$_c$ kg^{-1}]							[g kg^{-1}]				[%]							[m^2 g^{-1}]
PK 135/1	A1	0.73	7.5YR 4/4	7.5YR 5/6	4.5	5.1	42.5	3.9	12.1	15.2	0.1	0.3	0.2	0.1	0.0	1.6	2.4	22.0	13.5	8.4	13.5	0.8	1.6	8.6	8.9	17.0	22.0	41.0	21.5
PK 135/2	B1	1.04	10YR 4/4	10YR 7/3	4.3	5.4	13.9	1.4	9.7	9.6	0.1	0.2	0.2	0.1	0.0	2.5	3.1	17.5	8.0	7.8	8.5	0.9	1.3	6.1	3.8	17.5	24.2	46.2	25.4
PK 135/3	B2	1.04	10YR 4/6	10YR 7/4	4.4	5.4	10.9	1.2	9.2	9.7	0.1	0.3	0.2	0.1	0.0	1.6	2.3	14.2	7.2	9.5	10.2	0.9	1.4	6.1	3.2	17.6	23.0	47.9	31.5
PK 135/4	B3	1.02	10YR 4/6	10YR 7/4	4.3	5.4	10.6	1.2	9.2	10.8	0.1	0.3	0.4	0.5	0.0	1.8	3.1	21.5	9.1	13.2	9.1	1.2	1.6	6.1	4.4	13.0	18.0	55.7	45.6
PK 135/5	B4	1.01	10YR 5/6	10YR 7/4	4.2	5.6	8.6	1.1	7.9	11.1	0.1	0.3	0.7	0.7	0.0	2.0	3.9	25.1	8.0	15.2	5.6	1.1	1.6	5.4	7.3	12.8	15.6	56.3	52.0
PK 135/6	2A2	1.25	10YR 4/4	10YR 7/4	4.0	5.5	20.6	1.6	13.1	12.1	0.0	0.3	0.7	0.8	0.0	1.9	3.7	21.3	5.1	8.0	3.9	1.0	1.8	6.0	7.0	19.1	21.8	43.3	37.0
PK 136/1	Ap	0.63	10YR 4/3	10YR 6/4	4.2	5.0	72.3	5.1	14.3	21.8	0.1	0.3	0.7	0.3	0.1	3.8	5.2	15.7	15.1	10.0	10.1	0.3	0.9	6.9	7.5	19.3	21.9	43.3	12.9
PK 136/2	E	0.94	10YR 3/6	10YR 7/4	4.5	5.6	19.9	1.5	13.2	8.4	0.1	0.2	0.2	0.1	0.0	1.8	2.4	18.4	11.6	11.6	13.4	0.3	1.1	6.8	9.5	19.5	21.7	41.0	32.1
PK 136/3	Bt1	1.16	10YR 5/4	10YR 7/4	4.4	5.2	12.0	1.2	10.3	10.0	0.1	0.2	0.2	0.1	0.0	1.9	2.5	17.3	8.5	9.5	9.6	0.1	1.0	6.6	8.9	20.8	22.4	40.3	30.9
PK 136/4	2B	1.30	10YR 5/4	10YR 7/4	4.1	5.4	8.1	0.9	8.8	8.3	0.1	0.2	0.2	0.2	0.0	2.4	3.1	18.1	5.8	8.9	5.6	0.3	0.9	6.9	9.9	19.8	21.9	40.5	29.6
PK 136/5	2Bt2	1.34	10YR 5/4	10YR 7/4	4.1	5.4	5.4	0.8	7.1	7.5	0.1	0.2	0.2	0.4	0.0	2.3	3.1	29.8	5.4	10.1	4.0	0.7	1.6	9.5	9.3	18.8	19.1	41.0	30.3
PK 136/6	3BC	1.51	2.5Y 5/3	10YR 6/4	4.0	5.4	3.7	0.6	6.2	6.4	0.1	0.2	0.5	0.4	0.0	1.9	3.1	19.3	5.4	5.3	2.6	1.4	2.4	13.9	13.6	20.5	13.7	34.5	28.3
PK 136/7	3CB	1.37	2.5Y 6/3	10YR 6/6	4.0	5.3	3.7	0.6	5.8	6.7	0.1	0.2	0.3	0.3	0.0	2.2	3.2	16.1	1.4	5.6	3.0	1.8	2.8	15.1	13.0	17.4	13.8	36.1	30.5
PK 136/X	-	n.d.	n.d.	n.d.	4.0	5.5	2.6	0.6	4.7	6.2	0.1	0.2	0.5	0.3	0.0	1.6	2.6	19.4	4.2	5.4	2.1	3.0	3.4	15.8	13.6	18.5	12.9	32.8	28.3
PK 137/1	Ap	n.d.	10YR 4/4	10YR 5/4	4.2	5.1	37.7	3.0	12.5	12.8	0.1	0.3	0.3	0.2	0.0	2.6	3.5	13.0	8.5	8.3	4.8	2.5	3.5	17.6	14.4	18.7	15.0	28.3	13.2
PK 137/2	AE	n.d.	2.5Y 6/3	10YR 7/4	4.2	5.2	4.4	0.6	7.0	6.9	0.0	0.2	0.2	0.1	0.0	2.1	2.5	9.4	4.7	1.6	2.1	1.5	2.5	15.0	13.9	19.5	16.5	31.0	20.9
PK 137/3	2Bsh	n.d.	7.5YR 5/6	10YR 5/3	4.2	5.1	6.1	0.8	7.5	13.1	0.0	0.2	0.1	0.1	0.0	1.4	1.8	53.0	13.8	2.5	3.0	1.0	3.6	19.4	10.4	17.4	10.3	37.9	28.9
PK 137/4	2C	n.d.	10YR 5/4	10YR 7/4	4.0	5.3	1.0	0.4	2.4	4.9	0.0	0.2	0.1	0.2	0.0	1.1	1.6	12.2	0.2	1.5	0.9	3.8	7.4	28.0	19.9	20.8	8.0	12.1	12.2
PK 138/1	A1	0.79	10YR 3/3	10YR 6/8	4.0	5.1	42.0	2.9	14.3	7.1	0.1	0.6	1.5	0.4	0.0	3.0	5.7	21.2	6.8	7.3	5.6	4.7	4.3	15.0	11.4	21.6	19.7	23.2	17.1
PK 138/2	B1	0.54	7.5YR 5/6	10YR 6/4	4.3	5.0	63.8	2.4	26.3	24.1	0.1	0.2	0.4	0.1	0.0	4.9	5.8	30.0	24.1	13.9	20.9	0.9	4.2	10.2	9.3	23.8	25.0	26.5	31.7
PK 138/3	B2	0.66	10YR 5/4	10YR 6/4	4.5	5.3	50.7	2.2	22.4	20.0	0.1	0.2	0.3	0.1	0.0	3.2	3.9	22.1	22.4	7.6	22.1	1.5	2.7	12.9	9.1	23.9	25.6	24.2	18.9
PK 138/4	2A2	0.69	10YR 3/3	10YR 6/4	4.5	5.0	72.4	2.9	24.7	23.6	0.1	0.1	0.8	0.1	0.0	2.6	3.7	17.1	22.3	6.7	19.7	2.6	4.1	10.2	10.6	26.0	23.7	22.8	10.8
PK 138/5	2B3	1.17	10YR 6/6	10YR 7/4	4.6	5.4	14.8	0.9	16.8	9.0	0.0	0.1	0.3	0.1	0.0	1.3	1.8	17.0	7.9	2.1	6.2	6.9	4.6	11.9	9.8	23.2	16.9	26.6	12.4
PK 138/6	2C	n.d.	5Y 6, 5YR 5/6	10YR 7/4	4.6	5.4	6.6	0.9	7.9	7.5	0.0	0.1	0.2	0.0	0.0	0.7	1.1	23.1	5.6	2.2	3.3	5.5	4.0	5.4	13.1	30.0	18.6	23.2	24.5
PK 139/1	A	0.63	10YR 4/6	10YR 5/4	4.6	5.5	53.3	3.6	15.0	17.1	0.0	0.9	1.0	0.2	0.0	1.2	3.4	28.3	12.8	10.8	14.6	0.7	6.2	12.4	10.0	15.8	18.8	36.2	31.5
PK 139/2	B1	0.86	10YR 5/6	10YR 6/4	4.6	5.9	45.9	2.2	21.1	18.9	0.0	0.2	0.3	0.1	0.0	1.7	2.4	26.0	23.4	12.0	20.6	0.4	7.1	15.7	9.0	19.4	23.5	25.0	44.1
PK 139/3	B2	0.78	10YR 4/6	10YR 6/4	4.6	5.4	19.9	1.3	15.2	11.6	0.0	0.2	0.2	0.1	0.0	1.9	2.3	24.5	10.5	11.0	14.8	0.6	4.6	15.6	8.3	17.4	20.5	33.0	32.6
PK 139/4	2B3	1.32	2.5Y 5/4	10YR 7/4	4.3	5.4	3.8	0.5	8.1	5.2	0.0	0.1	0.2	0.1	0.0	1.2	1.6	12.5	8.3	3.7	3.1	3.2	12.3	23.5	14.3	17.9	10.5	18.2	15.2
PK 139/5	2CB	1.55	10YR 4/6	10YR 6/4	4.3	5.4	3.0	0.4	7.0	5.1	0.0	0.1	0.2	0.1	0.1	0.7	1.2	15.4	11.3	2.8	3.2	2.5	30.3	20.9	7.6	9.3	6.6	22.8	20.4
PK 139/6X	3C	-	10YR 2/2	10YR 3/3	4.4	5.2	1.7	0.4	4.1	8.6	0.0	0.1	0.1	0.1	0.1	0.3	0.8	26.7	15.5	4.0	6.3	18.7	21.1	15.8	4.3	5.9	5.7	28.6	60.0
PK 140/1	Ap	0.81	10YR 3/6	10YR 5/4	4.7	5.7	33.6	3.1	10.6	12.8	0.0	0.5	1.6	0.6	0.0	0.5	3.3	24.4	10.4	8.0	13.7	0.5	2.8	9.7	8.3	18.0	23.9	36.7	28.3
PK 140/2	AB	0.58	10YR 4/4	10YR 6/4	4.5	5.3	23.0	1.9	12.0	12.1	0.1	0.3	1.1	0.8	0.0	1.0	3.4	28.7	11.3	15.0	10.6	0.3	2.3	13.2	7.9	15.3	20.9	40.1	44.0
PK 140/3	B1	0.95	10YR 5/4	10YR 6/4	4.6	5.6	13.8	1.4	9.5	10.2	0.0	0.3	0.4	0.2	0.0	0.9	1.8	19.7	8.1	10.4	11.3	0.4	2.2	9.2	6.5	19.3	21.3	41.1	31.9
PK 140/4	B2	1.00	10YR 4/4	10YR 7/4	4.7	5.7	10.8	1.4	7.6	9.3	0.0	0.3	0.4	0.2	0.0	0.8	1.8	21.6	9.4	7.5	11.3	0.5	2.3	7.3	8.4	17.7	21.6	42.1	33.8
PK 140/5	2B3	1.09	10YR 5/8	10YR 7/4	4.4	5.8	7.3	1.2	6.3	8.6	0.0	0.4	1.0	1.0	0.0	0.9	3.3	26.3	7.6	8.5	6.7	0.6	2.3	7.4	8.7	16.3	18.7	46.0	37.8
PK 140/6	2B4	1.25	2.5Y 5/4	2.5Y 7/3	4.2	5.8	6.0	1.1	5.3	9.4	0.0	0.4	1.8	1.2	0.0	1.1	4.7	39.2	6.1	9.1	4.7	0.4	1.9	5.7	7.0	13.6	16.0	55.4	48.8

Appendix 1 (continued)

Sample	Hori-zon	Bulk density	Colour		pH		C	N	C/N	LOI	Cation Exchange Capacity							Pedogenic Oxides				Particle Size Distribution							Surface area
			field	dry	KCl	H_2O					Na^+	K^+	Ca^{2+}	Mg^{2+}	Mn^{2+}	Al^{3+}	total	Fe_d	Al_d	Fe_o	Al_o	cS	mS	fS	cSi	mSi	fSi	C	
		[g cm^{-3}]			[-]	[-]	[g kg^{-1}]		[-]	[%]	[cmol$_c$ kg^{-1}]							[g kg^{-1}]				[%]							[m^2 g^{-1}]
PK 140A/1	Ap	0.73	7.5YR 5/6	10YR 5/4	4.7	5.6	31.1	3.2	9.9	11.9	0.0	0.5	0.9	0.2	0.0	0.5	2.2	27.1	11.8	5.9	13.5	0.6	2.3	10.5	8.9	17.7	23.6	36.4	26.7
PK 140A/2	AB	0.50	10YR 5/8	10YR 5/4	4.5	4.7	24.5	1.9	13.2	13.5	0.0	0.3	1.2	0.8	0.0	1.3	3.6	36.4	12.0	13.7	12.7	0.5	3.6	16.0	5.3	15.7	20.2	38.6	46.5
PK 140A/3	B1	0.65	10YR 4/6	10YR 6/4	4.5	5.7	17.7	1.6	11.1	11.2	0.0	0.2	0.6	0.4	0.0	1.2	2.5	24.3	10.8	9.3	12.7	0.6	2.2	7.1	8.3	17.5	21.9	42.4	33.9
PK 140A/4	2B2	1.05	10YR 6/6	10YR 7/4	4.6	5.7	11.2	1.3	8.7	9.2	0.0	0.2	0.3	0.2	0.0	0.9	1.7	17.0	7.2	6.6	10.5	0.6	2.3	7.8	9.9	20.2	22.6	36.6	27.6
PK 140A/5	3C	1.27	7.5YR 4/4	n.d.	4.1	5.5	5.2	1.0	5.0	9.2	0.0	0.3	1.1	1.8	0.0	0.9	4.3	38.5	7.9	2.4	2.2	0.9	3.6	10.0	6.2	11.0	13.5	54.7	47.1
PK 141/1	Ap	0.81	10YR 5/6	n.d.	4.5	5.5	49.1	4.1	11.9	14.8	0.1	0.5	1.2	0.3	0.0	1.3	3.5	18.2	9.7	5.9	9.6	0.6	4.5	14.7	9.0	16.2	18.3	36.6	16.9
PK 141/2	B1	0.80	7.5YR 4/6	n.d.	4.6	5.6	25.5	1.6	16.3	10.4	0.0	0.3	0.5	0.1	0.0	0.9	1.9	21.6	9.4	6.3	11.0	0.9	6.5	15.1	8.5	16.3	17.5	35.2	23.5
PK 141/3	2A	0.63	10YR 3/6	n.d.	4.3	5.5	24.5	2.2	11.1	11.6	0.0	0.2	0.7	0.3	0.0	2.0	3.3	25.7	8.8	7.3	9.2	0.4	2.5	12.5	7.4	15.0	17.9	44.3	36.4
PK 141/4	2B2	0.64	10YR 5/8	n.d.	4.5	5.5	20.1	1.9	10.7	11.0	0.0	0.2	0.5	0.3	0.0	1.6	2.7	20.2	10.4	12.0	10.2	0.4	2.6	14.2	8.1	15.2	19.9	39.7	36.9
PK 141/5	3A2	1.05	2.5Y 5/4	n.d.	4.5	5.6	9.5	1.3	7.6	7.3	0.0	0.2	0.3	0.1	0.0	1.0	1.7	11.6	5.2	6.1	8.0	0.5	2.2	10.5	8.5	20.3	23.1	34.7	21.8
PK 141/6	3B3	1.07	2.5Y 5/4	n.d.	4.3	5.6	7.9	1.2	6.4	7.9	0.0	0.3	0.6	0.6	0.0	1.2	2.7	19.4	4.9	7.7	7.3	0.6	2.5	9.0	8.8	16.6	19.3	43.3	31.9
PK 142/1	Ah	n.d.	10YR 3/2	n.d.	4.2	5.1	61.5	4.1	14.9	18.1	0.0	0.4	0.7	0.2	0.0	2.9	4.3	18.2	8.1	9.8	10.1	1.0	2.9	19.6	12.9	19.0	15.1	29.5	11.7
PK 142/2	B1	n.d.	10YR 4/3	n.d.	4.4	5.1	37.7	2.6	14.7	14.3	0.0	0.2	0.3	0.0	0.0	2.4	2.9	17.7	10.9	10.4	10.5	1.4	6.8	15.6	14.5	18.6	16.4	26.7	17.0
PK 142/3	2Ah2	n.d.	10YR 3/2	n.d.	4.3	5.0	56.8	4.2	13.7	17.6	0.0	0.2	0.5	0.1	0.0	2.9	3.7	20.4	13.6	10.8	10.7	0.8	2.7	16.2	13.6	17.8	15.0	33.9	18.3
PK 142/4	2B2	n.d.	10YR 5/6	10YR 5/4	4.4	5.3	27.8	1.7	16.0	12.8	0.1	0.1	0.2	0.1	0.0	2.6	3.1	26.1	10.5	14.6	12.0	2.6	3.5	18.2	11.4	20.2	20.0	24.0	35.5
PK 142/5	2BC1	n.d.	2.5Y 5/4	10YR 7/3	4.4	5.5	10.4	1.0	10.9	7.8	0.1	0.1	0.2	0.0	0.0	2.0	2.4	8.2	5.3	3.0	6.7	3.7	7.4	22.9	17.1	20.8	11.7	16.4	13.5
PK 142/6	3CB	n.d.	2.5Y 5/2	10YR 6/2	4.3	5.3	4.3	0.6	7.7	7.1	0.1	0.0	0.2	0.0	0.0	2.1	2.4	6.4	4.3	1.8	12.3	4.9	15.9	25.9	15.4	20.0	6.7	11.3	11.3
PK 142/7	3BC2	n.d.	2.5Y 5/4, 2.5Y 4/1	10YR 7/4	4.0	5.3	1.5	0.3	4.5	7.3	0.1	0.1	0.4	0.1	0.0	2.5	3.1	19.1	7.5	0.8	2.0	2.1	10.0	32.0	13.1	17.3	10.4	15.0	19.3
PK 143/1	A1	0.70	7.5YR 4/6	10YR 5/6	4.5	5.4	39.2	4.0	9.8	14.4	0.1	0.4	1.3	0.7	0.1	0.9	3.5	19.8	9.0	4.5	15.6	0.6	1.5	8.4	9.3	16.4	23.1	40.8	25.6
PK 143/2	AB1	0.77	7.5YR 4/4	10YR 5/6	4.6	5.5	24.6	3.1	7.9	11.4	0.1	0.5	0.3	0.3	0.0	0.8	2.0	26.2	9.2	5.1	14.4	0.7	2.3	9.4	9.7	15.1	22.4	40.5	30.0
PK 143/3	AB2	0.72	7.5YR 4/3	10YR 5/4	4.5	5.6	23.5	2.9	8.1	11.4	0.1	0.6	0.3	0.4	0.0	0.9	2.3	26.1	9.4	6.2	37.6	0.7	2.0	8.5	12.4	15.4	22.1	39.0	31.0
PK 143/4	2A2	0.70	7.5YR 3/3	10YR 5/4	4.3	5.6	28.8	3.0	9.5	13.5	0.1	0.3	0.4	0.9	0.0	1.9	3.6	25.4	10.0	7.6	0.7	0.4	1.0	7.8	10.4	15.0	19.7	45.7	29.1
PK 143/5	2B1	1.04	10YR 5/6	10YR 7/4	4.2	5.6	9.1	1.3	7.1	9.4	0.1	0.2	0.5	1.4	0.0	1.7	4.0	13.1	5.8	9.1	19.3	1.4	2.0	7.7	10.3	13.9	15.5	49.2	40.2
PK 143/6	2B2	1.04	10YR 4/6	10YR 7/4	4.1	5.4	5.6	1.1	5.2	9.0	0.1	0.2	0.8	1.5	0.0	1.9	4.6	24.4	3.9	8.5	12.1	0.9	2.0	7.8	8.8	12.8	14.6	53.1	46.0
PK 143/7	3BC	1.21	10YR 6/2	2.5Y 7/3	4.2	5.3	5.4	0.8	6.7	7.2	0.1	0.1	0.5	0.3	0.0	1.5	2.6	5.2	2.0	1.6	2.7	1.9	5.5	24.8	15.7	18.4	12.8	20.8	15.8
PK 143/8	3CB	n.d.	10YR 5/6	2.5Y 7/3	4.3	5.6	2.5	0.5	5.3	4.9	0.1	0.1	0.3	0.2	0.0	0.9	1.5	3.9	1.6	1.1	5.1	16.1	23.6	17.5	14.6	13.8	5.9	8.4	9.7
PK 143/9	4C	1.33	5Y 5/2	2.5Y 7/2	4.3	5.7	0.6	0.7	0.9	7.0	0.1	0.1	0.4	0.3	0.0	1.0	2.0	1.8	1.5	0.6	7.0	0.3	4.1	17.6	19.6	29.4	16.2	12.8	13.1
PK 144/4	3A	0.70	10YR 2/2	10YR 4/2	4.0	4.9	43.9	3.0	14.8	14.6	0.1	0.1	0.5	0.3	0.0	5.6	6.6	22.6	8.1	12.7	20.5	1.2	3.4	9.9	14.2	15.2	15.1	41.0	21.2
PK 144/5	4B	0.75	10YR 4/4	10YR 6/4	4.3	5.5	13.5	1.3	10.2	9.4	0.1	0.1	0.2	0.1	0.0	2.5	3.0	15.5	7.0	8.2	20.4	2.7	6.2	17.5	9.0	16.7	14.3	33.7	22.2
PK 145/1	Ah	0.79	7.5YR 3/4	10YR 6/4	4.8	5.6	30.1	2.8	10.7	11.3	0.1	0.4	0.9	0.3	0.0	0.5	2.2	14.4	8.0	5.6	11.3	1.2	2.2	15.4	14.8	18.6	18.3	29.5	18.4
PK 145/2	BC	n.d.	2.5Y 6/4	10YR 7/2	4.2	5.5	3.5	0.5	7.4	5.0	0.1	0.2	0.2	0.3	0.0	0.9	1.8	4.2	1.3	2.3	1.9	4.9	16.9	19.9	20.7	18.0	7.8	11.8	10.4
PK 145/3	C	n.d.	2.5Y 6/3	10YR 7/2	4.0	5.5	1.4	0.4	4.0	5.7	0.1	0.2	0.4	0.4	0.0	1.1	2.2	3.5	1.0	1.1	1.3	1.4	6.4	25.0	22.2	22.0	9.2	13.9	13.0
PK 146/1	Ah	0.71	7.5YR 4/4	10YR 5/4	4.8	5.6	53.2	4.2	12.8	17.5	0.1	0.5	0.8	0.2	0.0	0.6	2.2	15.7	10.0	4.1	16.4	0.6	1.1	13.9	20.5	18.6	17.3	27.9	12.7
PK 146/2	B1	0.68	10YR 4/4	10YR 5/4	4.9	5.6	30.0	2.8	10.9	12.6	0.1	0.2	0.2	0.1	0.0	0.4	1.0	17.8	7.8	5.6	13.8	0.4	1.1	15.8	17.9	17.6	16.1	31.2	15.3
PK 146/3	2A	0.92	10YR 3/3	10YR 5/4	4.3	5.6	20.7	1.5	13.5	10.2	0.1	0.3	1.0	0.5	0.0	1.6	3.4	21.4	6.1	7.2	5.2	0.3	0.9	13.3	17.9	16.8	12.9	38.0	21.5
PK 146/4	2B2	1.03	10YR 4/6	10YR 7/4	4.1	5.7	7.7	1.0	7.9	8.0	0.1	0.4	0.8	0.8	0.0	1.5	3.6	21.0	5.1	1.3	1.6	0.5	1.1	9.7	16.2	17.3	15.7	39.6	27.7
PK 146/5	3CB	1.37	7.5YR 4/6	10YR 7/6	4.1	5.7	2.3	0.5	5.2	7.0	0.1	0.2	0.8	0.8	0.0	0.8	2.8	21.0	4.8	6.1	3.2	0.5	1.2	16.8	18.3	20.0	13.0	30.2	24.7
PK 146/6	4C	n.d.	7.5YR 5/6, 2.5Y 5/2	10YR 7/4	4.0	5.6	1.7	0.4	4.2	6.0	0.1	0.3	0.4	0.4	0.0	1.1	2.3	16.0	3.3	1.2	1.1	4.3	11.8	20.6	19.5	17.4	7.0	19.4	18.2

Appendix 1 (continued)

Sample	Hori-zon	Bulk density	Colour field	Colour dry	pH KCl	pH H_2O	C	N	C/N	LOI	Cation Exchange Capacity Na^+	K^+	Ca^{2+}	Mg^{2+}	Mn^{2+}	Al^{3+}	total	Pedogenic Oxides Fe_d	Al_d	Fe_o	Al_o	Particle Size Distribution cS	mS	fS	cSi	mSi	fSi	C	Surface area
		[g cm^{-3}]			[-]	[-]	[g kg^{-1}]		[-]	[%]	[cmol$_c$ kg^{-1}]							[g kg^{-1}]				[%]							[m^2 g^{-1}]
PK 147/1	Ah	1.00	10YR 4/4	10YR 6/4	4.3	5.0	31.1	2.9	10.7	11.9	0.1	0.2	0.3	0.1	0.0	2.3	3.1	11.1	5.1	6.1	5.0	0.7	3.1	21.6	18.0	16.9	13.4	26.4	11.7
PK 147/2	B	1.12	2.5Y 6/4	10YR 7/4	4.1	5.2	6.2	0.9	7.3	6.9	0.1	0.1	0.2	0.1	0.0	2.0	2.4	9.9	3.1	3.6	2.2	0.3	2.0	14.7	23.4	24.2	14.3	21.1	18.8
PK 147/3	2C1	1.26	2.5Y 6/3	10YR 7/2	4.1	5.1	2.3	0.6	4.3	5.9	0.1	0.1	0.1	0.1	0.0	1.9	2.2	4.8	3.3	1.4	1.9	0.0	1.5	32.8	23.3	18.7	8.9	14.7	15.5
PK 147/4	2C2	1.43	2.5Y 6/2	10YR 8/2	4.0	5.5	2.8	0.6	4.6	7.7	0.1	0.1	0.2	0.1	0.0	2.4	2.8	5.4	2.0	1.1	2.0	0.0	0.4	11.8	23.6	30.0	14.4	19.7	21.4
PK 147/5	2C3	1.43	2.5Y 5/2	10YR 7/2	4.2	5.4	1.8	0.5	3.7	4.8	0.1	0.1	0.1	0.0	0.0	1.1	1.4	3.5	1.5	1.0	1.7	1.9	10.8	27.3	26.3	19.5	7.4	6.8	10.1
PK 147/6	2C4	1.45	5Y 6/3	10YR 7/2	3.9	5.4	1.7	0.6	2.8	7.0	0.1	0.1	0.3	0.2	0.0	2.2	2.8	3.4	1.1	0.9	1.6	0.0	0.4	6.5	18.5	37.8	20.4	16.4	19.3
PK 147/7	2C5	1.22	5Y 5/2	2.5Y 7/2	4.5	5.6	1.6	0.5	2.9	4.9	0.1	0.0	0.2	0.0	0.0	0.5	0.8	1.6	2.0	0.9	3.1	0.2	2.0	23.4	33.5	27.8	9.5	3.7	10.6
PK 147/8	2C6	1.30	5Y 5/2	2.5Y 7/3	4.2	5.7	0.8	0.4	2.3	4.1	0.1	0.1	0.3	0.1	0.0	0.6	1.1	1.6	1.1	0.8	1.0	0.4	36.8	32.3	13.0	8.0	4.2	5.3	7.9
PK 148/1	Ah	0.72	10YR 3/3	10YR 5/4	4.4	4.8	50.7	4.6	11.0	16.6	0.1	0.2	0.4	0.1	0.0	2.8	3.6	23.9	14.7	10.4	10.9	0.7	1.2	14.6	8.7	13.4	17.5	43.9	19.9
PK 148/2	B1	0.58	10YR 5/6	10YR 6/4	4.4	5.4	20.4	1.6	13.1	12.3	0.0	0.1	0.3	0.1	0.0	2.7	3.2	27.3	12.1	16.1	12.1	0.7	1.7	18.4	10.0	14.5	17.8	36.9	37.4
PK 148/3	Bt	0.93	10YR 5/4	10YR 7/4	4.4	5.5	9.4	1.0	9.6	8.6	0.0	0.1	0.3	0.0	0.0	1.5	1.9	20.8	7.5	8.2	6.1	1.0	2.3	17.1	8.9	18.9	18.7	32.9	25.6
PK 148/4	2B2	1.29	10YR 5/4	10YR 7/4	4.3	5.4	5.1	0.7	7.1	7.6	0.0	0.1	0.3	0.1	0.0	1.4	1.8	16.6	5.1	6.7	3.4	1.0	2.4	22.0	11.5	15.5	16.2	31.5	25.2
PK 148/5	3C	n.d.	10YR 5/6	10YR 7/6	4.3	5.7	2.0	0.5	4.4	6.5	0.0	0.1	0.3	0.1	0.0	0.7	1.3	17.8	4.0	3.9	1.5	5.5	21.3	34.4	7.2	8.8	6.2	16.6	17.0
PK 149/1	Ah	0.78	10YR 3/4	10YR 5/4	4.4	5.0	50.1	4.3	11.8	16.9	0.0	0.2	0.2	0.1	0.1	2.7	3.3	29.4	14.9	9.7	8.6	1.2	1.2	9.2	10.2	14.6	17.3	46.3	20.2
PK 149/2	B	0.83	10YR 5/4	10YR 7/4	4.6	5.5	12.7	1.5	8.7	9.6	0.0	0.1	0.1	0.0	0.0	1.2	1.5	24.8	10.5	7.9	10.4	1.7	1.9	9.3	12.3	17.2	19.2	38.3	25.9
PK 149/3	2B2	0.99	10YR 5/4	10YR 7/4	4.6	5.6	11.2	1.4	8.0	9.2	0.1	0.1	0.2	0.0	0.0	1.2	1.5	22.0	9.4	7.1	8.5	2.9	2.9	10.0	13.3	17.1	16.6	37.0	26.3
PK 149/4	2Bt	1.50	10YR 4/6	10YR 6/6	4.3	5.9	2.6	0.9	3.1	7.0	0.1	0.1	0.9	0.4	0.0	0.5	2.0	26.1	5.9	5.2	2.3	7.8	7.5	11.4	13.3	14.5	11.4	34.1	30.1
PK 150/1	A	0.71	10YR 4/3	10YR 6/4	4.6	5.8	35.2	3.4	10.3	15.1	0.1	0.3	1.6	0.4	0.0	1.5	3.9	21.3	13.9	10.1	15.4	0.6	3.6	8.3	8.0	16.4	21.7	41.4	30.7
PK 150/2	B1	0.81	10YR 5/6	10YR 7/4	4.6	5.7	14.0	1.8	7.9	10.9	0.1	0.2	0.8	0.2	0.0	1.1	2.4	19.9	10.2	11.8	13.8	0.4	1.9	5.7	8.9	16.5	19.4	47.2	35.7
PK 150/3	B2	0.95	10YR 5/6	10YR 6/6	4.5	5.8	11.3	1.5	7.6	11.4	0.1	0.2	0.5	0.6	0.0	1.4	2.8	20.0	10.9	13.4	8.9	0.5	1.7	6.0	6.9	13.6	16.9	54.4	47.2
PK 150/4	B3	0.99	10YR 5/6	10YR 7/4	4.3	5.8	5.3	1.2	4.5	8.9	0.1	0.5	0.7	0.9	0.0	1.5	3.7	21.9	7.8	9.8	7.8	0.3	1.1	5.4	7.8	15.6	17.1	52.6	44.2
PK 150/5	B4	1.12	10YR 4/6	10YR 7/4	4.0	5.3	3.7	1.1	3.4	7.7	0.1	0.2	0.5	0.2	0.0	3.1	4.1	19.2	6.0	7.6	5.6	0.2	0.8	5.4	10.0	17.3	18.9	47.5	41.0
PK 150/6	B5	1.01	10YR 5/8	10YR 7/4	4.1	5.5	5.8	1.1	5.1	8.9	0.1	0.2	0.3	0.2	0.0	2.9	3.7	24.3	8.2	10.3	7.0	0.4	1.1	7.1	8.2	16.7	17.1	49.4	40.8
PK 150/7	2CB	1.27	2.5Y 6/3	10YR 7/4	4.0	5.2	3.2	0.9	3.7	7.5	0.1	0.1	0.2	0.1	0.0	2.4	2.9	7.2	2.8	3.2	3.4	0.3	0.5	13.7	13.5	22.6	18.5	30.9	23.2
PK 150/8	2C	1.33	2.5Y 5/1	10YR 7/1	4.2	5.4	1.2	0.7	1.8	4.8	0.1	0.1	0.2	0.1	0.0	0.7	1.1	1.2	0.9	0.2	1.5	0.1	2.1	13.5	21.7	35.6	16.7	10.3	6.6
PK 151/1	Ah1	0.66	7.5YR 4/6	10YR 5/6	4.7	5.6	24.2	2.7	9.0	11.5	0.1	0.7	0.4	0.2	0.1	0.5	1.9	35.1	16.3	6.9	15.1	0.9	2.1	9.3	7.8	15.4	22.9	41.5	33.1
PK 151/2	2Ah2	0.73	10YR 3/2	10YR 5/3	4.2	5.5	39.4	3.1	12.6	15.1	0.1	0.3	1.6	1.3	0.1	2.5	5.9	29.1	14.1	10.8	9.3	0.2	0.5	5.3	6.1	14.3	16.9	56.6	29.3
PK 151/3	2B1	0.70	10YR 5/4	10YR 5/6	4.5	5.6	18.8	2.0	9.4	12.3	0.0	0.3	0.4	0.3	0.0	1.0	2.1	22.7	12.6	13.6	14.5	0.3	2.4	7.7	3.4	14.3	21.1	50.7	34.9
PK 151/4	2B2	0.91	10YR 5/4	10YR 6/4	4.6	5.6	12.6	1.6	7.9	10.2	0.1	0.3	0.3	0.3	0.0	0.9	1.9	20.9	10.4	9.2	10.8	0.3	2.7	8.4	9.6	15.6	20.5	42.8	34.7
PK 151/5	2Bt1	0.98	10YR 4/6	10YR 7/4	4.6	5.8	10.0	1.4	7.0	9.8	0.1	0.4	0.6	0.8	0.0	0.6	2.4	25.4	9.8	11.6	8.5	0.4	2.6	8.2	9.2	15.6	18.4	45.5	38.2
PK 151/6	2Bt2	1.00	10YR 5/4	10YR 6/4	4.5	5.8	8.8	1.3	6.8	9.9	0.1	0.4	0.9	1.6	0.0	0.6	3.5	27.1	11.1	10.8	7.9	0.4	1.3	11.1	5.6	13.7	17.8	50.2	41.3
PK 151/7	2Bt3	0.89	10YR 5/4	10YR 6/6	4.3	5.7	8.4	1.2	6.8	11.3	0.0	0.4	0.8	1.5	0.0	1.2	4.0	22.8	9.5	15.4	7.8	0.4	1.1	6.4	5.6	11.8	15.9	58.7	50.8
PK 151/8	3A	1.07	10YR 5/4	10YR 6/6	4.1	5.7	6.2	1.1	5.7	10.4	0.1	0.5	0.8	1.4	0.0	2.0	4.7	29.7	9.1	11.3	4.2	0.3	1.2	6.7	6.3	11.8	16.2	57.5	53.4
PK 151/9	3B3	1.06	10YR 5/4	10YR 6/6	4.0	4.9	5.0	1.0	4.9	10.0	0.1	0.5	0.9	1.1	0.0	2.5	5.0	30.0	8.0	11.3	4.1	0.2	0.9	7.2	6.6	12.7	16.3	56.0	49.3
PK 151/10	3CB	1.20	10YR 5/4	10YR 6/4	3.9	5.4	3.6	1.0	3.6	8.7	0.1	0.4	0.8	0.8	0.0	2.9	5.1	24.8	6.3	8.2	3.2	0.4	1.5	5.7	8.1	16.1	17.9	50.3	44.4
PK 151/11	3C1	1.43	10YR 5/4	10YR 7/4	3.9	5.3	3.1	0.8	4.0	7.1	0.1	0.3	0.5	0.5	0.0	2.4	3.8	22.9	5.2	5.8	2.7	1.7	2.0	12.6	8.9	16.9	19.1	38.8	24.7
PK 151/12	4C2	n.d.	10YR 4/4	10YR 7/4	4.0	5.5	2.0	0.6	3.1	6.7	0.1	0.2	0.4	0.3	0.0	1.2	2.2	20.8	4.9	4.3	2.1	14.1	5.8	22.4	9.7	11.5	10.6	25.9	20.0

Appendix 1 (continued)

Sample	Horizon	Bulk density	Colour field	Colour dry	pH KCl	pH H_2O	C	N	C/N	LOI	Na^+	K^+	Ca^{2+}	Mg^{2+}	Mn^{2+}	Al^{3+}	total	Fe_d	Al_d	Fe_o	Al_o	cS	mS	fS	cSi	mSi	fSi	C	Surface area
		[g cm^{-3}]			[-]	[-]	[g kg^{-1}]		[-]	[%]	[cmol$_c$ kg^{-1}]							[g kg^{-1}]				[%]							[m^2 g^{-1}]
PK 152/1	Ap	0.76	10YR 3/3	10YR 4/4	4.4	5.5	58.5	5.0	11.7	16.6	0.1	0.2	1.3	0.4	0.1	2.1	4.2	20.3	11.6	9.5	10.5	3.8	5.5	18.5	12.1	15.0	14.2	30.9	17.8
PK 152/2	B1	0.72	7.5YR 4/4	10YR 5/6	4.4	5.4	38.0	3.6	10.6	13.5	0.1	0.1	0.3	0.2	0.0	2.0	2.7	25.0	12.3	9.9	11.4	3.4	6.3	17.0	7.2	11.9	15.9	38.3	18.0
PK 152/3	2A	0.85	7.5YR 3/3	10YR 5/4	4.3	5.2	30.8	2.6	11.7	12.1	0.1	0.1	0.2	0.1	0.0	2.8	3.3	21.5	7.3	12.1	6.4	3.1	10.9	14.9	5.6	11.4	14.8	39.3	21.2
PK 152/4	2B2	1.26	10YR 5/6	10YR 6/6	4.2	5.4	6.6	1.1	6.2	7.6	0.1	0.1	0.1	0.1	0.0	2.0	2.5	24.3	6.7	7.8	4.1	2.2	6.8	18.8	6.6	13.0	14.6	38.0	30.2
PK 152/5	3AB	1.23	10YR 6/6	10YR 7/6	4.1	5.3	5.3	1.0	5.4	7.9	0.1	0.1	0.2	0.2	0.0	2.1	2.6	29.1	7.1	6.6	3.5	2.1	6.7	13.9	6.6	14.0	16.2	40.6	33.1
PK 152/6	3B3	1.39	7.5YR 4/6	10YR 6/6	4.0	5.4	3.6	0.8	4.3	7.0	0.1	0.1	0.2	0.2	0.1	1.9	2.6	30.0	4.5	4.2	2.7	1.9	9.8	19.6	6.1	11.9	12.2	38.5	30.7
PK 152/7	4CB	n.d.	10YR 5/6	10YR 6/6	4.2	5.4	2.4	0.6	3.9	6.0	0.1	0.1	0.1	0.1	0.0	1.3	1.7	18.6	3.3	7.0	2.5	6.4	6.8	25.4	13.3	16.8	9.2	22.1	19.0
PK 152/8	4C	n.d.	2.5Y 6/4	10YR 7/4	4.4	5.6	4.5	0.9	5.2	6.4	0.0	0.1	0.1	0.1	0.0	1.2	1.5	12.2	4.3	7.5	5.4	4.3	5.9	28.7	9.5	18.6	12.8	20.3	17.4
PK 154/6	4A3	n.d.	2.5Y 4/2	10YR 4/1	4.3	5.6	18.9	1.0	18.8	7.5	0.3	0.2	0.5	0.1	0.0	1.2	2.3	3.0	2.3	2.2	4.1	0.1	8.2	26.6	15.7	29.6	11.7	8.1	5.7
PK 154/7	4C2	n.d.	5Y 5/2	10YR 7/1	4.6	6.3	2.7	0.6	4.3	3.9	0.1	0.1	0.2	0.0	0.0	0.8	1.2	2.4	1.6	0.4	2.5	0.1	16.2	26.8	13.7	25.2	10.7	7.3	4.7
PK 155/1	A	0.48	10YR 3/2	10YR 4/3	4.1	5.2	86.3	5.6	15.4	24.9	0.1	0.4	1.7	0.9	0.2	4.9	8.1	22.5	13.2	10.8	12.9	0.3	1.4	8.2	5.9	13.6	19.3	51.3	21.4
PK 155/2	B1	0.55	10YR 6/6	10YR 6/4	4.8	5.4	21.2	1.9	11.4	12.5	0.2	0.3	0.3	0.1	0.0	1.3	2.2	32.7	11.3	15.0	12.2	0.4	2.6	10.8	8.4	16.7	24.6	36.5	44.2
PK 155/3	B2	0.64	10YR 6/6	10YR 6/4	4.9	5.6	16.0	1.6	10.0	11.5	0.2	0.2	0.2	0.1	0.0	0.6	1.4	32.9	12.4	12.1	15.4	0.8	3.2	8.9	8.8	16.7	22.6	39.1	43.3
PK 155/4	2B3	0.84	10YR 6/8	10YR 7/4	4.8	6.1	9.4	1.2	7.8	9.8	0.1	0.1	0.3	0.1	0.0	0.5	1.1	30.3	9.0	11.1	8.9	0.9	3.6	9.4	6.9	16.1	22.6	40.5	38.8
PK 155/5	2BC	-	10YR 7/4	10YR 7/4	4.2	5.5	3.1	0.7	4.5	6.1	0.1	0.1	0.4	0.3	0.0	1.1	2.0	25.3	3.9	4.5	2.4	1.0	4.5	16.4	9.5	17.6	19.7	31.4	24.7

Sample	Horizon	Bulk density	Colour field	Colour dry	pH KCl	pH H_2O	C	N	C/N	LOI	Na^+	K^+	Ca^{2+}	Mg^{2+}	Mn^{2+}	Al^{3+}	total	Fe_d	Al_d	Fe_o	Al_o	cS	mS	fS	cSi	mSi	fSi	C	Surface area
		[g cm^{-3}]			[-]	[-]	[g kg^{-1}]		[-]	[%]	[cmol$_c$ kg^{-1}]							[g kg^{-1}]				[%]							[m^2 g^{-1}]
PK 153/1	Ah	0.40	10YR 4/3	10YR 4/2	3.6	4.5	133.3	6.7	20.0	32.2	0.1	0.4	1.1	0.3	0.0	14.2	16.2	29.9	8.1	17.2	8.4	0.6	1.1	5.8	9.3	13.5	17.7	51.9	17.5
PK 153/2	B1	0.41	10YR 5/6	10YR 6/6	4.8	5.2	45.1	2.1	21.1	23.2	0.1	0.1	0.2	0.0	0.0	1.1	1.5	34.0	22.6	8.7	24.3	3.5	17.7	16.8	8.2	16.2	17.3	20.3	56.7
PK 153/3	Bt	0.46	7.5YR 5/6	10YR 6/8	5.0	5.2	47.1	2.0	23.7	26.0	0.1	0.1	0.1	0.0	0.0	0.5	0.9	43.5	24.5	6.8	15.3	4.0	19.0	20.9	8.1	16.5	15.9	15.6	69.4
PK 153/4	2A	0.78	10YR 5/6	10YR 7/6	4.5	5.5	11.9	1.1	11.3	12.5	0.2	0.1	0.1	0.0	0.0	1.6	2.0	27.1	5.7	18.4	6.4	1.4	7.2	9.0	6.4	15.3	19.3	41.5	45.8
PK 153/5	3B2	0.90	10YR 5/6	10YR 7/6	4.4	5.3	6.8	0.8	8.7	8.7	0.1	0.1	0.2	0.0	0.0	1.2	1.6	21.6	5.2	17.1	6.8	8.0	19.3	14.3	5.4	10.4	11.2	31.4	34.5
PK 153/6	3CB	1.09	10YR 6/6	10YR 7/6	4.5	5.4	4.6	0.6	7.9	7.6	0.2	0.2	0.2	0.0	0.0	0.7	1.4	22.0	4.7	12.5	4.8	6.7	23.6	21.7	3.4	7.0	8.4	29.1	25.9
PK 153/7	3C	1.20	2.5Y 6/6	10YR 8/3	4.2	5.4	1.6	0.4	3.9	4.2	0.2	0.1	0.1	0.0	0.0	0.7	1.1	5.1	1.4	2.1	1.6	18.4	37.9	11.3	2.7	5.9	6.7	17.2	11.4
PK 156/1	A1	0.48	10YR 3/3	10YR 4/2	3.8	4.1	107.8	7.3	14.8	27.5	0.2	0.3	0.7	0.3	0.1	8.3	9.8	22.5	10.9	15.7	8.0	3.0	9.5	6.0	3.4	12.2	17.2	48.6	7.9
PK 156/2	2B1	0.36	10YR 4/4	10YR 6/6	4.5	5.1	68.1	3.2	21.4	25.9	0.2	0.1	0.3	0.1	0.0	2.5	3.1	34.4	20.5	13.4	21.9	4.0	20.9	21.1	6.5	15.9	15.3	16.2	33.0
PK 156/3	2B2	0.43	10YR 4/6	10YR 6/6	4.7	5.5	50.9	2.5	20.4	22.9	0.2	0.1	0.2	0.1	0.0	1.2	1.8	29.5	18.9	9.4	19.8	4.1	21.8	17.6	5.7	16.5	17.5	16.9	27.2
PK 156/4	2BC	0.99	10YR 6/6	10YR 8/3	4.4	5.2	5.4	0.5	10.3	6.3	0.2	0.0	0.1	0.1	0.0	1.0	1.4	6.3	2.2	3.3	3.3	12.8	25.9	22.0	3.6	8.5	9.1	18.0	10.9
PK 156/5	2C	1.17	10YR 8/1	10YR 8/1	4.5	5.4	1.2	0.3	4.2	4.2	0.1	0.0	0.1	0.1	0.0	0.4	0.7	0.9	0.4	0.3	0.6	22.2	36.8	16.7	4.6	7.4	5.9	6.4	42.1

Appendix 1 (continued)

Sample	Hori-zon	Bulk density	Colour field	Colour dry	pH KCl	pH H_2O	C	N	C/N	LOI	Cation Exchange Capacity Na^+	K^+	Ca^{2+}	Mg^{2+}	Mn^{2+}	Al^{3+}	total	Pedogenic Oxides Fe_d	Al_d	Fe_o	Al_o	Particle Size Distribution cS	mS	fS	cSi	mSi	fSi	C	Surface area
		[g cm^{-3}]			[-]	[-]	[g kg^{-1}]		[-]	[%]	[cmol$_c$ kg^{-1}]							[g kg^{-1}]				[%]							[m^2 g^{-1}]
PK 157/1	Ah	n.d.	10YR 4/3	10YR 7/2	4.6	5.6	17.4	2.0	8.6	6.6	0.1	0.4	3.4	1.3	0.1	0.1	5.2	10.1	1.7	3.9	1.6	30.3	14.3	9.7	4.6	8.5	12.3	20.4	5.3
PK 157/2	B1	n.d.	10YR 5/4	2.5Y 7/3	4.5	5.7	7.5	1.0	7.5	4.8	0.1	0.3	1.2	0.7	0.0	0.4	2.7	10.8	1.0	3.2	1.6	25.8	17.5	10.3	5.0	9.5	12.3	19.5	7.3
PK 157/3	B2	n.d.	2.5Y 5/4	2.5Y 7/4	4.4	5.5	3.4	0.6	5.9	3.9	0.2	0.2	0.7	0.5	0.0	0.4	2.0	10.0	1.6	2.3	1.0	27.4	15.6	12.3	5.3	9.4	12.7	17.1	7.9
PK 157/4	B3	n.d.	2.5Y 5/4	2.5Y 8/3	4.2	5.6	2.1	0.4	4.9	3.6	0.1	0.2	0.5	0.4	0.0	0.5	1.7	11.4	3.1	1.8	1.0	26.3	17.6	11.2	2.0	8.3	14.1	20.5	9.4
PK 157/5	C	n.d.	2.5Y 5/4	2.5Y 8/3	4.3	6.2	0.5	0.2	2.3	2.6	0.0	0.1	0.4	0.3	0.0	0.2	1.2	5.9	0.7	0.6	0.5	41.5	14.8	11.0	2.7	6.5	11.2	12.2	4.9
PK 158/1	Ah	n.d.	10YR 4/4	10YR 5/4	4.1	4.6	41.4	4.1	10.1	17.4	0.1	0.1	0.3	0.2	0.1	3.7	4.4	43.2	12.5	13.6	6.5	4.2	13.3	6.7	4.4	17.5	20.1	33.9	24.3
PK 158/2	B1	n.d.	10YR 4/4	10YR 5/4	4.3	5.2	30.0	2.8	10.6	15.5	0.1	0.0	0.1	0.1	0.1	2.1	2.5	44.4	12.3	15.8	7.5	3.5	9.6	11.9	5.6	16.9	22.0	30.3	34.9
PK 158/3	2B2	n.d.	10YR 4/6	10YR 6/4	4.5	5.1	17.6	1.8	10.0	13.1	0.1	0.0	0.1	0.1	0.0	0.9	1.3	51.3	9.5	15.5	5.1	3.8	7.1	9.0	6.4	18.0	20.5	35.3	35.1
PK 158/4	2B3	n.d.	10YR 4/6	10YR 5/6	4.6	5.3	12.4	1.2	10.0	12.7	0.1	0.0	0.1	0.1	0.0	0.3	0.6	60.7	12.0	15.6	4.4	2.5	4.4	11.1	10.1	18.0	17.4	36.5	42.2
PK 158/5	2C	n.d.	5Y 4/4	10YR 6/4	4.2	5.5	3.6	0.5	7.4	9.1	0.1	0.0	0.1	0.1	0.0	1.0	1.2	39.4	5.1	3.4	1.7	2.3	5.8	18.1	16.0	24.6	14.6	18.7	16.3
PK 159/1	Ah	n.d.	7.5YR 3/2	10YR 5/3	4.2	4.9	69.8	6.7	10.5	18.6	0.0	0.5	5.7	1.5	0.3	1.1	9.0	18.1	3.2	11.9	2.3	17.6	17.7	11.1	4.4	10.9	10.9	27.5	9.8
PK 159/2	B1	n.d.	7.5YR 4/4	10YR 6/6	4.1	4.9	18.6	2.0	9.4	10.2	0.1	0.1	0.4	0.2	0.0	4.4	5.2	28.0	6.5	14.4	4.6	18.3	10.3	8.1	3.2	9.1	11.9	39.0	33.1
PK 159/3	B2	n.d.	7.5YR 4/6	10YR 6/4	4.1	5.2	8.6	1.3	6.7	10.4	0.1	0.2	0.2	0.1	0.0	4.1	4.7	23.7	6.3	10.7	6.1	4.3	7.3	3.7	1.7	15.6	18.3	49.0	44.4
PK 159/4	B3	n.d.	7.5YR 4/6	10YR 6/6	4.1	5.1	7.4	1.2	5.9	9.3	0.1	0.2	0.1	0.1	0.0	5.1	5.7	26.6	6.1	11.4	5.0	1.4	3.1	2.3	3.9	18.7	20.6	50.0	43.1

Appendix 2: Total element contents (INAA measurements)

sample	Al	As	Ba	Ca	Ce	Co	Cr	Cs	Dy	Eu	Fe	Hf	K	La	Lu	Mn	Na	Nd	Ni	Rb	Sb	Sc	Sm	Sr	Ta	Tb	Th	Ti	U	V	Yb	Zn	Zr
	[ppm]																																
PT034/1	78639	1.4	385	7836	81	4.2	29	14	6.41	1.00	16784	12.2	24488	39	0.68	489	16812	33	< 31	167	0.11	8.5	7.3	73	1.2	1.3	19	1661	7.7	40	4.7	53	307
PT034/2	75707	1.4	352	8256	66	4.6	48	12	7.51	0.89	18418	9.9	23008	32	0.60	520	17730	27	31	161	0.10	8.3	6.1	80	1.4	1.0	16	1560	6.9	47	4.0	49	261
PT034/3	79438	0.8	396	7470	68	5.1	41	12	5.49	0.86	16589	10.5	26493	32	0.48	399	18038	28	< 31	176	0.06	8.6	6.2	87	1.4	1.0	17	1649	6.7	38	3.1	46	263
PT034/4	84929	0.6	423	8581	46	4.9	27	14	3.32	0.82	15593	9.7	26180	22	0.36	330	18952	16	< 31	176	< 0.06	8.6	4.2	99	1.4	0.7	11	1893	5.9	51	2.2	49	251
PT034/5	80023	< 0.9	439	9165	62	4.8	29	14	4.32	0.94	15838	12.1	25983	31	0.44	409	19009	33	< 31	183	< 0.06	8.6	5.7	104	1.3	0.8	14	1799	6.5	38	2.8	54	307
PT034/6	87789	1.8	464	8483	61	5.7	48	23	4.77	1.09	18252	9.2	23092	28	0.62	405	14189	31	< 37	184	0.19	12.0	6.3	73	1.8	0.9	13	2424	16.6	70	3.1	65	301
PT035/1	80734	1.8	422	7912	112	5.8	44	14	6.48	1.18	23399	10.6	22249	55	0.63	1025	12855	52	< 35	173	0.13	9.9	9.7	68	1.5	1.3	26	2033	7.0	63	4.1	67	255
PT035/2	72040	< 1.1	446	10072	115	6.3	48	9	9.07	1.26	30927	9.5	17147	56	0.68	2013	12777	45	< 39	127	< 0.08	12.3	9.2	101	1.2	1.4	26	2644	5.2	41	4.9	65	228
PT035/3	81185	< 1.2	418	10991	101	7.9	58	7	8.98	1.12	42136	18.0	21957	49	1.18	2250	13869	36	< 47	138	< 0.10	17.5	8.2	82	1.4	1.5	23	1815	3.8	53	9.1	98	426
PT036/1	80780	2.8	451	6794	88	6.1	43	15	5.52	1.00	20766	9.9	24728	45	0.54	1020	13242	40	< 33	189	0.14	9.0	7.6	92	1.4	1.1	20	2025	6.9	47	3.5	76	276
PT036/2	84167	3.0	447	7857	81	6.2	44	16	5.22	1.01	21353	11.6	24980	41	0.52	842	13352	36	0	191	0.18	9.5	7.2	102	1.5	1.0	20	2476	7.4	53	3.2	74	287
PT036/3	72609	1.7	353	7414	58	4.4	36	12	4.79	0.76	16027	10.2	25304	29	0.56	631	12998	27	< 34	162	0.09	7.8	5.1	90	1.3	0.9	13	2070	5.9	37	3.7	50	247
PT036/4	58379	< 0.7	283	5552	32	2.3	27	6	2.51	0.49	8649	13.3	23059	16	0.29	467	11633	13	32	129	0.04	4.9	2.7	57	0.8	0.4	8	1133	2.5	23	1.9	31	306
PT036/5	54576	< 0.9	278	6696	93	3.3	23	6	8.42	0.79	15711	15.5	18339	46	0.84	1524	11120	33	< 28	114	< 0.04	6.8	7.3	33	1.3	1.3	21	1668	5.9	22	6.0	46	386
PT038/1	77774	3.5	414	6937	89	6.8	42	14	5.81	0.98	23803	11.7	24641	44	0.51	1180	12190	35	39	189	0.20	9.2	7.1	56	1.4	1.0	21	2082	6.5	56	3.5	69	285
PT038/2	82493	3.5	471	4707	54	5.7	47	17	4.07	0.84	25069	10.2	28352	28	0.34	454	9087	24	< 34	209	0.14	9.6	5.0	< 48	1.7	0.6	14	3043	5.6	62	1.8	50	243
PT038/3	84673	1.4	441	8742	81	6.7	49	16	5.18	0.98	21918	11.0	28455	40	0.46	459	14273	34	< 35	207	0.18	10.3	7.1	103	1.8	1.0	23	2887	7.8	51	2.8	64	268
PT039/1	83771	4.6	443	8441	149	6.6	55	20	8.00	1.40	20961	14.7	24990	73	0.74	913	12503	59	35	201	0.33	10.3	13.6	114	1.5	1.7	36	3100	9.5	66	4.9	83	361
PT039/2	80688	2.9	410	8021	160	5.9	61	20	9.46	1.58	18446	17.2	24973	78	0.79	690	13118	67	< 35	205	0.35	10.5	14.5	67	1.6	1.8	38	3102	9.7	64	5.4	70	406
PT039/3	83728	3.8	410	12359	102	5.7	44	10	6.98	1.21	20245	14.8	23069	49	0.79	1147	17152	37	40	165	0.16	9.6	9.0	100	1.1	1.3	45	1101	7.6	39	5.7	64	361
PT039/4	82957	6.3	383	12126	111	5.2	44	8	8.56	1.09	23262	11.6	22618	55	1.08	1700	16446	49	< 35	150	0.12	10.8	9.3	70	0.9	1.6	25	1136	5.5	47	8.0	68	294
PT039/5	66011	3.4	352	13117	86	4.5	32	10	5.99	0.92	16409	15.5	23822	42	0.60	1172	18458	35	< 30	164	0.09	7.5	7.5	103	1.1	1.1	21	1348	5.1	29	4.5	57	355
PT040/1	84849	1.2	504	6642	87	7.6	24	13	7.07	1.04	23748	12.7	30617	42	0.58	719	9834	37	< 36	230	0.07	10.4	7.9	89	1.7	1.1	24	1855	7.7	47	3.7	53	328
PT040/2	85412	2.2	461	7985	91	11.2	53	14	6.33	1.11	30627	9.6	24985	43	0.50	876	9454	32	< 39	207	0.16	11.9	7.3	68	1.6	1.1	23	2778	7.8	66	3.2	68	246
PT040/3	86825	4.2	451	6646	73	8.8	42	18	4.19	0.94	24511	10.2	27322	36	0.57	852	10055	32	31	248	0.21	9.6	6.8	44	1.7	1.1	19	2433	8.1	50	3.8	63	249
PT040/4	92488	3.2	475	8163	65	15.9	74	13	3.67	0.84	39093	9.8	21112	31	0.45	899	7950	25	45	175	0.32	12.6	5.4	41	1.5	0.7	18	2864	7.0	82	2.8	81	255
PT040/5	89580	< 1.3	565	11223	70	15.5	80	9	3.60	0.87	37710	8.4	21555	34	0.38	733	8651	26	73	161	< 0.08	12.6	5.2	43	1.2	0.6	19	2766	7.3	77	2.3	74	193
PT040/6	87841	0.8	473	11239	73	16.9	85	9	3.52	0.85	37938	8.0	19846	35	0.45	860	8336	29	43	150	< 0.08	12.9	5.4	65	1.2	0.8	19	2443	8.0	70	2.3	78	210
PT041/1	99370	17.5	435	2027	119	12.8	88	19	7.35	1.39	41230	15.3	21134	56	0.62	411	4790	52	79	174	0.81	13.3	9.8	< 59	1.9	1.2	25	4651	8.2	113	4.0	78	379
PT041/2	96622	13.2	403	1652	102	10.6	71	18	6.91	1.26	36517	13.6	23049	49	0.68	304	4744	45	61	192	0.60	12.6	9.0	< 56	2.0	1.3	24	4197	8.5	93	4.5	71	295
PT041/3	103800	6.2	445	2118	82	9.3	51	17	6.99	1.03	28963	11.7	29191	38	0.61	277	5474	35	< 39	231	0.46	11.9	7.6	59	2.1	1.2	22	2995	7.5	69	4.0	59	291
PT041/4	76365	3.3	460	1588	126	6.1	28	12	13.63	1.06	19363	17.8	31724	60	1.11	378	4815	51	< 33	215	0.21	8.7	12.0	57	1.5	2.1	35	2169	9.5	50	8.0	44	357
PT041/5	97962	18.6	418	1798	119	11.8	92	18	6.38	1.40	45751	12.5	19472	56	0.59	504	4521	47	46	159	0.93	13.0	9.7	44	2.0	1.2	25	5141	7.8	114	3.8	80	310
PT041/6	102905	18.5	445	1518	124	15.3	94	21	6.47	1.31	39422	12.0	20646	51	0.58	213	4144	47	68	168	0.87	14.1	9.4	< 60	1.8	1.2	26	5049	7.7	116	4.0	75	322
PT041/7	94815	11.8	447	1718	107	13.5	78	20	7.10	1.33	28588	13.3	24165	52	0.57	219	4133	47	< 41	181	0.73	12.3	9.6	< 56	1.8	1.4	27	3988	7.8	90	3.8	58	329
PT041/8	87460	3.7	402	1885	56	8.4	33	27	3.83	0.64	17904	8.8	35649	25	0.42	365	6523	24	< 32	311	0.30	7.9	4.8	< 46	2.6	0.8	14	1864	7.8	35	2.5	57	208
PT041/X	93960	3.5	417	2157	62	6.4	23	23	4.13	0.76	19781	7.5	30839	29	0.47	598	8598	28	25	343	0.26	7.4	6.3	35	2.1	0.8	17	1469	11.3	35	2.5	67	210

Appendix 2 (continued)

sample	Al	As	Ba	Ca	Ce	Co	Cr	Cs	Dy	Eu	Fe	Hf	K	La	Lu	Mn	Na	Nd	Ni	Rb	Sb	Sc	Sm	Sr	Ta	Tb	Th	Ti	U	V	Yb	Zn	Zr
	[ppm]																																
PT042/1	87983	3.3	530	8741	78	12.9	68	14	4.26	1.04	33366	12.9	23936	38	0.49	960	8870	33	60	201	0.16	12.5	6.8	45	1.5	0.9	20	2398	6.6	69	3.1	93	316
PT042/2	89859	2.1	533	8179	95	13.0	68	14	4.90	1.14	33585	11.9	25103	46	0.54	874	9034	39	< 41	202	0.26	12.9	7.5	58	1.6	1.1	23	2780	7.5	70	3.5	83	287
PT042/3	86127	4.1	532	6571	86	13.9	73	15	4.92	1.06	34186	9.6	25351	42	0.45	826	7620	35	< 41	196	0.23	12.7	7.1	75	1.5	1.0	21	2717	6.9	84	2.8	79	239
PT042/4	93434	4.0	581	5351	90	15.8	81	15	5.30	1.07	37369	11.4	22622	43	0.47	922	6395	35	< 43	195	0.25	13.2	7.3	< 58	1.5	1.0	22	3494	7.6	91	2.9	78	266
PT042/5	92056	8.4	445	4557	89	15.1	87	16	4.84	1.04	38232	10.5	22703	43	0.50	837	5776	40	70	195	0.36	12.9	7.4	28	1.5	1.0	21	3606	7.4	91	3.0	78	250
PT042/6	88284	7.5	489	3833	101	14.7	84	17	5.28	1.18	38642	13.0	21147	48	0.46	903	5645	40	< 42	199	0.42	12.7	8.1	< 58	1.7	1.1	23	3448	7.5	93	2.9	85	296
PT042/7	95125	10.5	389	2993	104	12.5	73	19	6.06	1.13	34680	12.2	22760	52	0.46	1127	5693	45	< 39	186	0.41	10.5	8.6	74	1.6	1.2	23	3528	7.3	90	3.1	79	299
PT042/8	90557	16.6	444	3020	124	14.7	88	22	6.81	1.33	41260	12.9	20313	54	0.55	706	5951	48	51	210	0.67	12.7	10.0	42	1.9	1.3	28	3944	7.5	110	3.6	85	298
PT042/X	85044	7.9	563	3204	120	15.8	69	17	5.89	1.26	31724	15.2	22162	60	0.49	816	4563	57	51	195	0.63	11.6	9.5	65	1.7	1.2	28	3463	8.8	80	3.3	65	403
PT043/1	85976	2.7	528	7511	97	13.8	76	14	4.36	1.08	34874	9.9	22550	50	0.43	833	7383	44	50	187	0.30	12.6	8.2	36	1.5	0.9	24	3130	7.3	84	2.5	82	232
PT043/2	89059	3.3	516	6813	82	14.5	78	15	4.74	1.02	36422	12.5	21739	41	0.44	840	7292	36	40	198	0.23	13.1	6.7	75	1.6	0.9	21	3344	7.2	73	2.7	81	329
PT043/3	89396	4.1	466	7469	91	14.2	77	15	4.31	1.07	35583	9.4	23702	44	0.41	817	7228	41	44	192	0.27	12.8	7.5	< 57	1.5	1.0	23	3172	7.8	77	2.5	76	241
PT043/4	92335	3.1	507	6674	87	14.3	79	15	5.58	1.07	35950	14.4	24099	44	0.46	784	7314	35	162	192	0.24	12.9	7.1	61	1.6	0.9	21	2900	8.1	85	2.7	77	347
PT043/5	91565	4.7	552	6433	84	14.7	80	15	5.04	1.07	36498	11.7	23065	41	0.48	810	7307	31	< 42	187	0.26	13.0	6.6	< 71	1.5	0.9	20	2587	6.0	84	2.7	76	354
PT043/6	84929	< 1.5	387	18757	104	14.7	117	12	4.51	1.10	37780	8.1	17704	52	0.43	738	16361	37	< 47	162	< 0.05	16.2	7.5	144	1.3	0.8	23	3067	5.1	92	2.5	67	194
PT044/3	88876	< 1.2	573	13923	80	11.6	51	8	5.05	1.20	32360	8.7	26247	40	0.49	584	11710	29	< 38	188	< 0.03	10.1	6.7	112	1.1	0.9	22	3053	5.8	64	2.8	64	243
PT047/1	90303	5.7	538	5840	96	13.0	68	19	5.29	1.08	32450	11.4	24260	47	0.55	748	7336	34	< 41	223	0.38	11.6	7.5	< 69	1.7	0.9	24	2609	7.0	85	2.7	78	293
PT047/2	94309	9.0	549	4364	89	12.0	66	22	5.50	1.08	31304	10.8	26178	43	0.50	663	6067	31	49	235	0.47	11.0	7.4	< 67	1.9	0.9	22	2498	7.7	76	2.6	74	298
PT047/3	98121	10.1	479	4529	111	12.3	72	22	5.96	1.23	34067	13.5	23559	54	0.58	793	6637	35	74	219	0.56	11.0	9.2	91	1.8	1.2	26	3797	8.4	92	3.1	79	367
PT047/4	93006	9.1	513	6175	108	10.0	70	20	5.76	1.18	34490	13.7	22662	56	0.51	999	7009	42	< 39	193	0.44	10.3	8.7	51	1.9	1.3	26	3578	6.1	98	2.9	69	362
PT047/5	89276	8.4	544	6709	91	12.3	59	17	6.03	1.01	37058	10.0	25980	45	0.44	390	9840	31	51	206	0.32	10.2	7.3	98	1.6	1.0	23	2966	7.0	83	2.6	74	290
PT048/1	88547	4.6	474	6385	82	10.5	53	20	5.68	1.01	28589	11.6	27606	38	0.42	727	8518	27	< 40	247	0.24	10.6	6.6	45	1.8	1.2	21	2407	7.1	65	2.5	77	313
PT048/2	85995	5.1	450	6793	77	9.7	51	18	4.72	0.94	26543	12.7	26102	38	0.42	777	8149	24	30	233	0.23	9.8	6.4	< 64	1.6	0.8	20	2922	7.3	59	2.4	66	375
PT048/3	86561	5.1	526	6370	78	10.2	53	17	5.11	0.98	27718	12.0	26465	39	0.43	683	8503	27	54	217	0.21	10.2	6.4	93	1.6	0.9	20	2291	6.6	66	2.6	68	323
PT048/4	86462	< 1.1	395	1121	59	3.8	17	30	4.23	0.82	15740	8.0	38114	26	0.42	373	4055	21	< 29	356	0.13	5.6	5.7	< 52	2.1	0.7	15	1032	9.1	29	2.2	60	211
PT049/1	89495	3.8	510	12421	76	14.3	60	17	4.04	0.97	35753	10.6	22254	37	0.39	835	10575	26	< 42	187	0.22	12.3	5.6	113	1.6	0.7	19	2380	6.0	77	2.3	75	247
PT049/2	92268	4.6	411	12680	80	13.8	59	16	4.34	0.97	34551	10.9	20761	40	0.41	882	11078	24	< 41	176	0.25	12.0	6.3	110	1.6	0.8	20	2639	5.4	76	2.5	74	277
PT049/3	98392	3.2	417	11982	80	10.7	47	13	3.93	0.91	27929	7.8	22349	41	0.32	631	11162	28	< 38	148	0.17	10.2	5.5	111	1.3	0.7	20	2367	4.6	63	2.1	62	186
PT049/4	68191	4.5	477	8695	84	14.1	59	19	4.34	1.03	37130	11.8	22072	40	0.40	800	9901	26	< 43	189	0.24	12.2	6.2	78	1.8	0.8	20	2653	6.1	67	2.7	75	313
PT049/5	101459	3.3	255	2990	73	19.6	57	27	4.93	1.08	48614	7.8	15074	36	0.41	795	4648	26	< 48	184	0.19	15.4	6.0	< 80	1.6	1.0	15	3078	6.1	101	2.5	83	188
PT049/6	103612	4.2	314	11940	45	19.8	34	22	3.10	0.87	45608	8.0	14519	22	0.38	808	10883	15	< 47	153	0.11	15.6	4.1	< 79	3.2	0.5	11	2684	6.3	107	1.9	74	253
PT052/1	83242	9.2	706	2908	115	10.2	75	19	5.71	1.25	29721	13.3	27736	58	0.51	514	6318	44	< 40	233	0.44	11.1	9.4	68	1.7	1.2	26	4248	7.0	81	3.0	74	337
PT052/3	97184	16.7	652	3382	89	13.4	97	23	5.07	1.10	45151	10.4	29639	46	0.52	875	6126	36	< 45	262	0.65	13.9	7.5	< 76	1.8	0.9	21	4501	6.0	124	2.9	92	245
PT052/4	86222	15.7	574	3641	112	13.3	78	20	5.72	1.29	41914	11.9	29572	55	0.51	740	8059	40	< 42	241	0.66	11.2	9.3	79	1.8	1.2	25	4011	6.0	96	3.2	75	297
PT052/5	82560	6.1	527	3617	71	7.9	53	23	4.72	0.94	26520	10.6	30280	37	0.43	426	8660	26	< 37	264	0.38	9.4	6.2	43	1.9	0.8	17	2793	6.0	65	2.5	71	286
PT052/6	83994	8.6	592	3442	83	9.7	63	22	5.03	1.04	29869	11.3	26030	42	0.38	540	7695	33	< 39	252	0.43	10.4	7.1	102	1.8	0.9	19	2950	6.0	82	2.5	73	286

Appendix 2 (continued)

sample	Al	As	Ba	Ca	Ce	Co	Cr	Cs	Dy	Eu	Fe	Hf	K	La	Lu	Mn	Na	Nd	Ni	Rb	Sb	Sc	Sm	Sr	Ta	Tb	Th	Ti	U	V	Yb	Zn	Zr
	[ppm]																																
PT 053/1	68759	4	452	8014	92	1	23	3	4.4	0.9	10338	16	21076	47	0.48	138	10125	41	< 27	64	0.5	6	7.1	136	1.5	0.9	23	3884	7.3	63	3.0	17	452
PT 053/2	78618	5	543	6805	78	5	29	6	4.8	1.0	41081	16	21315	41	0.50	377	8623	27	< 37	95	0.3	8	6.6	76	1.8	0.9	23	3211	9.7	104	3.2	41	443
PT 053/3	91502	2	511	8336	91	9	28	8	5.7	1.2	35955	11	25769	48	0.53	647	8159	31	< 41	133	< 0.1	11	8.1	< 70	1.7	1.1	29	2337	10.1	83	3.3	< 3	306
PT 053/4	93538	< 2	506	8259	84	12	25	8	4.9	1.0	32654	11	26731	46	0.53	814	8026	31	< 40	166	< 0.1	11	7.4	73	1.8	1.0	26	2796	9.1	60	3.4	85	292
PT 053/5	90312	< 2	596	5141	75	11	21	7	5.0	0.9	32026	9	33743	40	0.51	829	6677	29	< 41	198	< 0.1	12	6.9	< 71	1.9	1.0	25	2760	9.0	58	3.3	80	259
PT 053/6	86981	< 2	507	6985	79	11	22	7	4.5	0.9	31449	8	36477	42	0.45	763	10643	25	< 41	195	< 0.1	12	5.9	89	1.7	0.9	26	2427	4.6	67	3.3	47	201
PT 054/1	83771	9	453	4550	98	3	55	18	5.7	1.0	32733	13	27569	49	0.52	324	9509	38	< 39	129	0.8	10	8.6	< 70	2.2	1.2	23	4157	7.1	100	3.6	43	307
PT 054/2	93764	8	483	3835	92	4	56	17	5.5	1.0	43654	25	25937	45	0.53	348	9149	35	< 41	127	0.7	10	8.2	130	2.2	1.1	22	4670	7.5	103	4.0	< 3	659
PT 054/3	95589	11	493	3816	86	6	61	19	5.6	1.0	45847	13	25752	43	0.46	430	9563	32	< 42	132	0.7	11	7.8	82	2.2	1.1	21	3712	6.1	96	3.3	47	345
PT 054/4	96978	11	455	3720	87	10	63	23	5.6	1.1	35310	17	27072	45	0.43	556	10241	34	< 42	158	0.8	12	8.4	< 76	2.1	1.1	21	3856	6.3	77	3.0	97	477
PT 054/5	97223	7	420	4919	84	13	61	21	4.4	1.1	33245	11	27738	45	0.41	664	10743	32	< 42	166	0.7	12	8.4	< 75	2.0	1.1	21	3163	6.8	82	2.9	93	290
PT 054/6	91795	< 2	138	7217	94	8	21	20	8.6	1.3	25892	8	15395	46	0.78	625	18831	34	< 42	134	0.6	12	9.8	< 74	2.8	1.8	26	2212	10.8	43	6.0	91	240
PT 055/1	68515	16	413	2369	119	3	68	9	6.4	1.3	16641	22	16904	63	0.53	126	6394	54	< 36	76	1.1	11	10.5	45	1.9	1.2	26	6041	7.0	123	3.7	44	544
PT 055/2	72842	18	382	2121	120	3	75	7	6.3	1.3	24495	26	16974	62	0.53	136	5894	55	< 39	70	1.0	11	9.3	< 69	4.8	1.1	26	6954	9.2	141	3.6	45	702
PT 055/3	85725	33	378	1978	104	4	92	10	5.1	1.1	82439	15	18014	54	0.41	228	5015	31	< 48	78	1.0	12	8.6	< 80	2.1	0.9	23	6918	7.3	177	2.6	< 4	349
PT 055/4	93033	28	438	917	101	7	104	19	5.0	1.2	87371	16	19156	53	0.42	433	5261	31	< 51	106	1.0	13	8.9	< 85	2.0	0.9	24	6644	6.9	158	2.8	< 4	407
PT 055/5	100716	32	467	2095	97	13	117	26	5.0	1.3	73051	13	22889	50	0.37	654	5793	33	< 51	127	0.9	14	8.1	< 88	1.8	0.8	23	5639	6.1	145	2.5	94	367
PT 055/6	112415	34	494	2404	100	20	112	25	5.7	1.4	50669	12	23891	51	0.35	749	7645	35	53	133	0.9	15	8.6	< 88	1.7	1.0	23	4166	6.6	119	2.6	132	324
PT 056/1	82417	18	363	3925	113	5	97	11	6.2	1.3	53477	22	13430	57	0.60	355	4805	44	< 44	89	1.3	12	9.2	< 76	1.9	1.2	24	6256	6.7	144	4.4	64	613
PT 056/2	78643	18	221	2426	110	4	93	9	6.7	1.2	47056	14	12522	60	0.59	173	3948	40	< 43	65	1.3	11	9.5	< 74	2.1	1.1	22	7255	7.5	163	4.1	< 3	337
PT 056/3	103230	22	327	1630	113	14	115	16	6.1	1.5	59689	12	16410	55	0.55	265	4994	41	< 51	97	1.5	15	9.6	< 88	1.8	1.1	23	6551	6.6	155	3.8	93	311
PT 056/4	106919	27	347	2386	111	21	115	19	7.5	1.6	52343	14	19397	54	0.57	390	5731	37	103	115	1.4	16	10.1	< 89	1.6	1.1	23	5158	6.4	135	4.6	120	338
PT 056/5	101938	22	379	2295	112	14	110	20	8.3	1.6	48177	16	21918	59	0.55	399	4883	42	42	120	1.8	17	10.4	< 90	1.7	1.2	24	5311	8.6	137	4.5	97	474
PT 056/6	100964	7	559	385	102	13	78	13	5.3	1.3	32601	16	24258	50	0.47	361	2748	40	36	132	0.7	14	8.9	< 79	1.9	1.5	23	4226	6.7	94	3.3	92	396

Appendix 2 (continued)

sample	Al	As	Ba	Ca	Ce	Co	Cr	Cs	Dy	Eu	Fe	Hf	K	La	Lu	Mn	Na	Nd	Ni	Rb	Sb	Sc	Sm	Sr	Ta	Tb	Th	Ti	U	V	Yb	Zn	Zr
	[ppm]																																
PT 057/1	87953	7	478	5449	69	14	69	14	6.0	1.2	36891	11	29529	35	0.47	647	8477	28	< 44	188	0.7	13	7.2	< 78	1.4	1.0	16	3410	5.1	76	3.1	84	276
PT 057/2	84027	5	521	5419	74	12	65	13	5.1	1.2	31798	12	31247	36	0.42	505	8155	35	< 42	183	0.6	12	7.2	< 74	1.2	0.9	16	3183	4.8	83	3.0	76	270
PT 057/3	77881	4	459	5553	72	11	62	13	4.8	1.2	30754	9	27124	37	0.42	465	8064	35	< 41	180	0.7	12	6.8	124	1.3	1.1	17	3033	5.5	66	3.5	< 3	247
PT 057/4	89987	7	546	6194	75	12	64	14	5.2	1.2	31849	10	31776	39	0.46	478	9371	32	< 43	185	0.7	12	7.0	81	1.4	1.0	17	3358	5.4	88	3.5	< 3	255
PT 057/5	77206	7	564	4636	55	10	55	11	4.8	1.1	27011	10	28950	27	0.39	471	9363	30	28	164	0.6	10	4.9	57	1.0	0.8	12	2639	4.3	67	2.8	59	316
PT 057/6	87385	5	498	6115	70	11	63	14	5.6	1.2	32899	9	29691	36	0.43	466	8677	26	< 43	180	0.7	13	6.6	< 76	1.4	0.9	16	3330	5.3	77	3.3	72	258
PT 057/7	85354	6	465	6001	75	12	61	13	5.1	1.2	34502	9	26815	38	0.47	581	9003	28	39	179	0.8	12	6.9	< 75	1.2	1.0	17	3354	5.2	77	3.2	73	232
PT 057/X	70338	< 2	434	20421	65	7	33	14	4.1	1.0	21096	7	33115	32	0.31	442	17976	33	< 33	185	0.2	8	6.6	174	1.2	0.9	16	2248	5.7	45	2.4	53	179
PT 061/1	95268	6	591	3383	105	16	87	13	7.4	1.6	44270	12	30416	55	0.67	601	5843	36	< 51	205	0.8	17	9.8	< 88	1.5	1.3	23	4845	5.6	103	5.5	< 4	294
PT 061/2	97028	< 3	556	4495	103	15	84	12	8.3	1.6	40567	12	32536	52	0.57	748	5978	33	< 49	193	0.1	16	8.6	< 86	1.4	1.2	22	4794	3.9	104	4.6	93	262
PT 061/3	94209	7	610	3675	119	17	83	14	7.6	1.6	47625	13	29151	60	0.59	548	5403	44	< 32	244	0.5	16	9.6	< 85	1.7	1.4	27	4596	4.8	105	5.0	64	331
PT 061/4	86862	4	675	3314	142	14	80	11	9.0	1.7	41160	14	29908	72	0.59	590	5750	53	< 32	222	0.5	15	11.9	< 81	1.6	1.7	33	4305	5.5	98	5.0	87	405
PT 061/5	78746	3	649	3122	119	14	66	10	6.3	1.6	36180	13	26363	60	0.56	1065	5963	45	< 32	200	0.3	12	9.5	< 75	1.3	1.4	28	3684	3.5	72	4.6	53	323
PT 061/X1	72997	4	621	3034	133	13	58	8	7.3	1.5	32988	12	24675	67	0.59	987	5074	53	< 32	172	0.4	11	10.6	< 70	1.1	1.5	31	2588	5.9	72	4.8	61	372
PT 061/X2	84978	5	597	1982	108	14	77	10	7.1	1.5	43428	14	27888	56	0.59	690	3064	45	< 32	208	0.5	14	8.9	< 80	1.5	1.1	26	4267	5.2	92	4.6	56	370
PT 062/1	89391	8	582	3309	147	15	79	13	9.0	1.7	40676	14	28762	75	0.58	842	3398	55	< 32	207	0.7	14	12.2	< 79	1.7	1.7	35	3546	6.6	92	5.3	55	396
PT 062/2	97046	12	686	3331	135	18	88	16	6.7	1.4	44604	12	28778	63	0.65	975	3056	46	< 32	229	0.8	15	10.3	< 83	1.7	1.2	32	5087	6.2	106	4.8	57	349
PT 062/3	94565	9	608	2186	117	16	77	17	7.1	1.5	42819	12	31632	58	0.63	833	3011	46	< 32	237	0.7	14	9.7	< 81	1.6	1.4	27	3746	4.9	98	5.0	59	279
PT 062/4	95815	9	610	2249	120	16	81	15	6.0	1.5	43612	10	29344	59	0.52	838	2760	45	< 32	226	0.6	14	9.6	< 82	1.6	1.2	28	3984	5.8	100	4.4	83	295
PT 062/5	98415	7	537	1321	109	16	83	12	8.9	1.5	46677	11	27606	60	0.52	835	1939	40	< 32	211	0.5	15	9.5	< 83	1.3	1.2	25	3697	5.7	97	4.3	59	276
PT 062/X1	83044	5	576	1361	89	14	84	8	6.1	1.4	49474	10	23272	51	0.63	913	1336	39	< 32	190	0.4	17	7.6	< 86	1.3	1.0	19	3965	3.4	89	4.0	94	257

Appendix 2 (continued)

sample	Al	As	Ba	Ca	Ce	Co	Cr	Cs	Dy	Eu	Fe	Hf	K	La	Lu	Mn	Na	Nd	Ni	Rb	Sb	Sc	Sm	Sr	Ta	Tb	Th	Ti	U	V	Yb	Zn	Zr
																[ppm]																	
PK 135/1	95519	16	459	1539	117	18	111	19	6.8	1.5	48296	15	19895	54	0.60	741	3959	44	< 32	187	0.9	16	8.9	< 85	2.8	1.2	24	5992	6.5	138	4.6	97	324
PK 135/2	98335	16	499	2648	121	23	118	19	6.9	1.6	47084	13	24218	53	0.59	788	4278	45	< 32	204	1.0	17	9.2	< 87	1.9	1.3	23	5974	5.8	123	3.9	106	353
PK 135/3	95934	16	482	2389	118	22	117	19	7.0	1.6	49090	13	23031	57	0.65	847	3103	47	< 32	194	1.0	17	9.3	< 88	1.8	1.2	26	5373	6.1	137	4.0	110	282
PK 135/4	104690	24	504	1429	124	22	119	21	8.4	1.9	55413	13	21692	54	0.71	827	2285	49	< 32	191	1.2	22	10.8	< 98	1.9	2.0	27	6021	7.2	135	4.7	< 5	293
PK 135/5	107592	25	460	718	125	20	125	22	8.2	1.9	60795	12	19606	53	0.70	791	1803	43	< 32	175	1.6	22	11.1	< 99	2.0	1.9	28	6049	7.4	146	4.9	< 5	227
PK 135/6	101352	19	544	2559	122	22	121	20	6.7	1.6	49940	12	25674	56	0.59	653	3985	47	< 32	197	1.0	17	9.5	< 86	1.7	1.3	25	5809	6.6	137	3.8	78	273
PK 136/1	94323	15	395	2978	116	19	116	20	6.4	1.4	49015	11	23525	53	0.57	575	4303	47	< 32	181	0.8	15	8.9	< 83	1.7	1.2	25	6164	5.7	131	3.6	73	306
PK 136/2	103340	20	595	1198	119	22	112	19	5.9	1.4	52116	11	24080	53	0.56	883	1775	40	< 32	191	1.4	17	8.5	< 90	2.1	1.4	25	5757	7.1	147	3.7	< 4	244
PK 136/3	99114	20	519	2139	116	23	126	19	6.8	1.5	51249	11	27057	53	0.57	863	3030	46	< 32	214	1.2	18	9.0	< 89	1.7	1.1	25	5410	6.8	133	3.8	93	254
PK 136/4	98276	16	643	1946	112	19	117	20	6.6	1.5	50406	11	27265	51	0.63	867	2522	39	< 32	219	1.0	19	9.4	< 92	1.8	1.1	24	5785	7.1	137	3.9	< 4	335
PK 136/5	95053	19	542	1433	105	17	111	22	5.8	1.4	50614	12	25332	46	0.60	842	1879	36	< 32	223	1.0	18	8.5	< 89	1.7	1.0	23	5709	6.7	129	3.8	< 4	276
PK 136/6	86226	13	491	1521	104	13	104	22	5.9	1.3	47467	14	23716	47	0.57	590	1472	39	< 32	192	0.8	16	8.4	< 83	1.8	1.1	24	5554	6.9	121	3.8	84	327
PK 136/7	88509	16	523	1221	106	15	111	24	6.6	1.5	49251	14	25252	51	0.60	544	1364	44	< 32	205	0.7	17	9.0	< 87	1.8	1.2	24	5377	6.3	121	4.2	83	346
PK 136/X	87241	19	572	1352	107	18	110	26	5.3	1.3	49290	13	26373	46	0.55	932	1292	42	< 32	210	0.7	16	7.8	< 84	1.7	1.0	23	5033	6.7	116	3.6	70	304
PK 137/1	86029	14	460	958	91	14	91	22	5.4	1.0	49058	17	24000	42	0.52	850	1925	33	< 32	199	0.6	14	6.7	< 80	1.9	0.9	23	5300	5.7	118	3.3	82	396
PK 137/2	97088	13	528	884	114	21	97	31	4.4	1.0	39985	12	21650	45	0.49	525	1077	30	< 32	214	0.7	15	6.2	< 82	1.8	0.8	30	5031	6.4	110	2.9	92	308
PK 137/3	75191	33	332	880	88	4	66	9	6.0	1.0	40310	20	16400	42	0.68	411	1819	32	< 32	99	0.9	11	6.3	< 68	1.9	1.1	20	6170	6.1	114	4.6	< 2	520
PK 137/4	86274	7	559	448	88	19	86	38	4.9	1.1	53086	11	33874	42	0.48	752	957	32	< 32	254	0.4	17	6.9	< 91	1.7	1.1	28	4244	6.2	111	3.0	< 4	274
PK 138/1	94256	31	542	< 453	133	30	118	28	4.1	1.2	87759	11	27482	60	0.43	1190	949	32	< 32	214	0.9	19	7.6	< 99	1.8	1.1	28	5577	7.5	139	2.9	< 5	249
PK 138/2	118473	42	379	1187	88	8	98	16	5.1	1.1	63698	13	20080	42	0.50	486	2288	31	< 32	120	1.2	16	6.2	< 84	1.6	0.9	26	5174	6.0	119	3.3	< 3	300
PK 138/3	120830	43	509	1634	100	14	95	18	5.5	1.2	49127	12	22805	45	0.51	669	2998	32	< 32	151	1.0	16	7.2	< 85	1.4	0.9	25	5232	5.5	111	3.4	< 3	248
PK 138/4	122629	45	544	280	111	9	86	17	6.5	1.4	41599	18	29161	50	0.54	649	1761	36	< 32	166	1.2	17	7.6	< 84	1.4	1.1	23	4740	5.9	93	3.7	< 3	472
PK 138/5	114457	36	731	< 330	117	9	73	15	7.4	1.4	33913	12	36033	59	0.57	609	1286	45	< 32	203	1.2	16	8.1	< 82	1.4	1.3	21	5245	4.9	104	3.9	< 3	252
PK 138/6	114739	60	1022	< 431	132	29	67	12	4.6	1.2	42390	11	35045	66	0.61	1474	1030	35	< 32	194	1.8	18	7.4	< 87	1.6	0.9	29	2858	5.1	75	4.2	< 4	315
PK 139/1	83183	36	375	1464	106	9	93	26	5.6	1.2	56357	15	15019	48	0.53	592	3016	36	< 32	106	0.8	12	7.7	< 78	1.8	1.1	23	5370	6.3	122	3.2	60	406
PK 139/2	108075	34	411	840	108	16	112	31	6.7	1.5	60521	13	18733	47	0.52	530	3592	40	< 32	122	0.8	15	8.9	< 87	1.7	1.3	24	5676	5.6	128	3.5	95	302
PK 139/3	98932	25	435	1912	117	19	103	35	6.2	1.6	48865	13	20658	48	0.57	553	3956	48	< 32	145	0.8	16	9.3	< 87	1.6	1.6	22	4472	6.4	111	3.8	97	332
PK 139/4	73723	32	419	< 368	83	21	59	36	3.9	1.0	34707	15	20610	31	0.44	860	1122	26	< 32	127	0.5	11	5.8	< 74	1.2	0.9	16	3334	4.9	73	2.8	54	400
PK 139/5	59935	45	293	< 544	122	51	48	36	2.0	0.9	33247	10	7243	34	0.27	2773	454	21	< 32	87	0.9	11	5.2	< 77	0.8	0.7	22	1805	2.9	48	1.8	< 3	336
PK 139/6X	13738	99	364	< 4038	736	191	37	29	< 3.4	1.2	43377	7	< 13025	46	0.39	7199	< 232	21	< 32	70	1.9	60	7.1	< 202	0.7	< 0.3	29	< 5841	7.1	< 66	1.7	< 14	160
PK 140/1	78284	21	429	2766	115	17	112	28	5.3	1.4	54999	14	18141	55	0.54	1067	3502	35	< 32	210	0.9	15	8.6	< 86	1.8	1.3	25	4475	6.8	112	3.5	113	338
PK 140/2	88905	23	438	1752	108	14	117	26	5.3	1.2	60776	12	21327	51	0.54	884	4133	39	< 32	195	0.9	15	8.2	< 84	1.8	1.0	24	5138	6.1	137	3.4	91	312
PK 140/3	98442	20	487	2709	117	24	115	23	6.7	1.4	51152	12	22903	52	0.51	1288	4974	41	< 32	227	1.1	16	8.6	< 87	1.7	1.1	24	5525	7.1	135	3.4	124	317
PK 140/4	99109	20	534	1381	120	24	114	23	6.3	1.6	52078	12	27639	55	0.57	1334	4452	41	< 32	242	1.1	17	9.5	< 89	1.7	1.2	25	3909	5.6	149	3.8	120	322
PK 140/5	95899	22	470	1596	120	22	105	24	5.8	1.4	49247	12	23431	52	0.59	1605	2780	40	< 32	217	1.4	18	9.0	< 91	1.8	1.1	26	5512	6.5	127	4.0	112	252
PK 140/6	108209	25	515	1458	119	19	112	26	6.1	1.3	59272	13	23775	46	0.62	1196	1732	37	< 32	213	1.7	20	8.3	< 99	1.8	0.9	27	5241	7.5	137	3.8	139	289

Appendix 2 (continued)

sample	Al	As	Ba	Ca	Ce	Co	Cr	Cs	Dy	Eu	Fe	Hf	K	La	Lu	Mn	Na	Nd	Ni	Rb	Sb	Sc	Sm	Sr	Ta	Tb	Th	Ti	U	V	Yb	Zn	Zr
	[ppm]																																
PK 140A/1	95441	22	560	1281	108	16	108	25	6.9	1.3	53112	14	18631	55	0.57	1298	4330	36	34	184	0.9	14	8.3	< 79	1.9	1.0	22	6247	6.8	136	4.3	111	363
PK 140A/2	99707	22	337	1190	113	16	115	21	5.6	1.2	61616	11	18131	52	0.56	698	3503	26	< 64	151	1.2	16	8.2	< 81	2.0	0.9	26	6645	7.3	147	3.8	86	246
PK 140A/3	98002	24	435	2907	121	23	116	23	6.6	1.5	52602	12	22220	54	0.54	874	4276	40	< 65	189	1.1	17	9.2	< 84	1.8	1.1	25	5141	7.8	130	4.1	123	317
PK 140A/4	93191	21	510	2093	120	26	111	20	6.2	1.5	44429	14	24244	57	0.56	1078	3927	37	69	200	1.2	15	9.1	< 80	1.7	1.3	25	5224	7.2	127	3.7	< 4	305
PK 140A/5	112979	36	578	652	131	33	123	25	4.9	1.2	60342	12	20326	49	0.59	945	1175	25	81	172	2.5	24	8.0	< 100	2.0	1.2	27	6359	10.0	156	3.9	< 6	270
PK 141/1	80225	18	484	2083	104	10	90	27	5.5	1.2	44124	15	16574	51	0.54	978	3645	44	< 55	162	0.8	12	8.2	< 72	1.7	1.1	21	5176	5.9	125	3.6	91	392
PK 141/2	79630	18	534	2032	100	8	90	27	5.7	1.1	44795	16	18193	51	0.54	955	3418	34	< 55	166	0.8	12	7.8	< 72	1.8	1.0	21	5026	6.2	125	3.7	70	371
PK 141/3	85384	18	416	1466	101	10	100	23	5.6	1.2	50371	12	19256	50	0.48	956	3501	38	< 57	150	0.8	13	8.0	< 76	1.9	1.0	22	6249	6.8	144	3.4	77	350
PK 141/4	89442	18	527	1876	99	12	103	23	6.1	1.2	49330	13	19864	49	0.48	855	4040	37	< 59	152	0.8	13	8.0	< 76	1.8	0.9	21	5666	5.9	140	3.3	94	299
PK 141/5	82529	16	530	2329	108	17	95	22	5.5	1.3	39919	14	25718	53	0.49	1051	5210	31	83	208	0.8	14	8.2	< 76	1.7	0.9	21	4652	6.4	106	3.4	110	361
PK 141/6	80049	24	580	1783	105	17	107	33	5.4	1.3	47398	12	22263	50	0.56	1083	3157	33	70	229	1.0	16	8.5	< 82	1.9	1.1	23	4804	6.5	117	3.5	118	238
PK 142/1	82458	11	582	1952	106	10	85	23	5.1	1.3	45916	14	21959	49	0.56	527	3234	36	47	169	0.5	13	7.6	< 74	1.7	1.1	19	4772	6.0	100	4.0	100	332
PK 142/2	84713	15	553	1761	97	10	82	21	5.0	1.2	45986	13	22800	48	0.55	573	3216	35	< 57	165	0.6	13	8.0	< 74	1.7	1.0	19	4743	5.9	96	3.6	98	324
PK 142/3	79983	14	498	2011	97	8	82	22	5.0	1.2	48958	15	20027	49	0.54	491	3246	37	< 57	163	0.6	13	7.5	< 73	1.8	0.9	20	5286	5.8	99	3.6	< 4	376
PK 142/4	83924	13	525	1738	95	9	86	22	5.5	1.2	51380	21	22516	47	0.57	496	3126	35	< 59	158	0.6	13	7.9	< 75	1.8	1.0	19	5307	5.8	107	4.0	81	487
PK 142/5	81716	7	617	1804	102	12	67	20	6.3	1.5	38325	18	25858	56	0.61	633	2643	44	< 57	175	0.5	13	8.7	< 74	1.6	1.3	18	4038	6.0	79	4.2	107	493
PK 142/6	86003	4	628	1338	108	12	54	16	8.5	1.9	37932	14	25454	67	0.71	712	1271	62	< 57	147	0.2	13	10.8	< 74	1.4	1.7	24	3754	5.4	66	5.4	124	357
PK 142/7	78319	20	515	< 481	305	26	38	43	3.7	1.0	60425	13	18020	34	0.52	1443	363	21	< 69	258	0.9	17	6.1	< 90	1.4	0.7	26	2558	6.2	47	3.6	153	323
PK 143/1	82820	20	569	2315	107	16	103	35	5.2	1.4	51245	15	17674	54	0.54	956	3000	41	< 64	213	0.9	16	9.3	< 84	2.6	1.0	24	4440	7.7	118	3.8	119	388
PK 143/2	83655	18	533	1435	108	15	104	36	5.4	1.4	53281	13	19576	52	0.55	891	2961	31	< 65	219	0.9	16	8.8	< 84	2.2	1.0	24	4627	6.2	115	3.6	110	277
PK 143/3	84916	18	581	1443	105	13	103	36	5.1	1.3	52324	13	18179	51	0.53	865	2921	34	< 63	217	0.8	15	8.6	< 82	2.4	1.0	23	4535	6.9	112	3.7	86	311
PK 143/4	85571	20	545	2095	111	15	106	35	5.5	1.4	52123	13	19492	55	0.53	918	3248	38	84	219	0.9	15	9.0	< 83	2.1	1.1	25	4948	7.2	113	3.6	114	322
PK 143/5	87593	23	598	1369	122	20	110	38	5.7	1.6	54249	12	20268	53	0.61	1047	2286	37	< 71	231	1.3	19	9.6	< 92	2.1	1.1	26	4349	7.2	112	4.3	144	332
PK 143/6	87295	28	579	503	113	18	101	41	5.7	1.5	55104	13	20035	51	0.64	1141	1456	34	< 70	217	1.6	18	9.4	< 92	2.2	1.0	24	4754	7.6	115	3.8	107	261
PK 143/7	93890	10	597	667	120	10	72	57	5.0	1.1	32041	16	25806	41	0.49	377	2732	22	< 62	197	0.6	16	6.6	< 85	3.6	0.9	27	4575	8.7	87	3.2	83	376
PK 143/8	77057	5	601	< 625	87	7	52	57	5.0	1.1	30309	14	24196	36	0.48	493	4563	26	< 56	214	0.2	13	6.3	< 78	4.6	0.8	17	3337	6.9	54	3.2	76	374
PK 143/9	111907	10	699	< 578	119	10	73	75	7.1	2.2	29785	12	30869	68	0.65	452	2596	50	< 63	239	0.3	17	11.9	< 89	3.3	1.2	23	5048	9.2	81	4.0	103	295
PK 144/4	78669	11	571	< 669	89	5	78	38	5.1	1.0	43842	15	20635	47	0.53	330	2964	40	< 55	201	0.5	12	7.2	< 73	2.5	0.9	19	5037	7.8	109	3.5	52	393
PK 144/5	93873	17	564	1444	102	15	94	49	5.7	1.3	44467	16	26843	46	0.54	808	3729	36	< 62	212	0.8	14	8.0	< 83	2.5	1.1	22	4776	7.3	110	3.5	93	437
PK 145/1	96514	11	541	1456	92	15	88	33	5.8	1.2	40366	14	22508	44	0.56	499	2710	36	< 60	178	0.7	15	7.1	< 79	1.7	1.0	20	5113	5.1	114	3.6	66	338
PK 145/2	86031	< 2	583	920	53	11	59	42	3.4	0.7	27646	15	29216	24	0.48	594	1043	20	< 55	202	0.5	13	4.5	< 74	2.1	0.6	14	4517	5.9	86	3.2	44	381
PK 145/3	96174	< 3	669	243	56	13	55	52	3.5	0.8	31561	14	27486	30	0.42	608	851	18	< 61	205	0.5	17	4.2	< 84	1.9	0.6	22	4926	4.4	109	2.9	< 4	327
PK 146/1	94968	7	467	914	107	9	61	61	5.5	1.2	41283	24	19312	31	0.60	543	1422	30	< 59	164	0.3	14	6.7	< 82	2.0	0.9	20	4765	6.2	81	4.4	< 4	608
PK 146/2	94677	8	519	512	105	9	64	64	5.1	1.1	43038	15	20907	33	0.55	587	1325	32	< 59	167	0.3	13	6.5	< 81	2.0	0.9	20	4961	5.1	87	3.9	< 4	348
PK 146/3	96142	9	522	1046	105	8	65	60	4.9	0.9	43714	13	22103	29	0.56	517	1294	20	< 58	164	0.2	13	5.7	< 80	2.0	0.8	20	4874	5.5	88	3.6	< 4	303
PK 146/4	93720	12	539	1155	114	15	90	45	5.8	1.2	45911	18	21848	43	0.57	402	2380	33	< 63	154	0.8	16	7.1	< 84	2.3	0.9	22	5286	6.8	116	3.9	68	435
PK 146/5	100003	13	536	323	84	9	74	67	2.8	0.5	45084	12	23165	17	0.49	435	829	11	< 66	168	0.9	16	2.9	< 89	11.1	0.6	22	4890	11.4	97	2.6	< 4	281
PK 146/6	102047	7	730	397	62	14	65	44	4.5	0.9	39040	11	31061	26	0.55	555	857	15	38	166	0.6	16	4.6	< 84	1.7	0.6	21	4245	5.1	87	3.4	< 4	257

Appendix 2 (continued)

sample	Al	As	Ba	Ca	Ce	Co	Cr	Cs	Dy	Eu	Fe	Hf	K	La	Lu	Mn	Na	Nd	Ni	Rb	Sb	Sc	Sm	Sr	Ta	Tb	Th	Ti	U	V	Yb	Zn	Zr
	[ppm]																																
PK 147/1	85014	9	564	754	83	6	59	41	5.9	1.2	30514	16	22849	42	0.52	425	3111	38	< 54	179	0.5	12	7.3	< 73	2.6	1.0	18	3915	6.2	77	3.5	54	415
PK 147/2	98545	11	609	529	75	6	72	45	5.2	1.0	28629	14	25904	33	0.53	324	2076	22	< 57	179	0.6	14	6.3	< 78	2.4	0.7	20	4502	6.5	90	3.5	< 3	358
PK 147/3	89223	9	509	< 283	68	8	57	43	4.7	0.8	28429	13	22423	32	0.48	403	1439	19	< 55	170	0.4	13	5.1	< 75	2.7	0.7	20	4711	8.0	75	3.3	< 3	290
PK 147/4	122498	20	776	< 298	105	9	69	48	4.5	0.9	26702	11	28557	52	0.50	334	1241	21	< 61	189	0.5	17	5.6	< 84	2.3	0.7	27	4671	7.6	88	3.4	< 4	234
PK 147/5	79233	5	604	708	115	9	47	38	5.5	1.4	25924	12	22445	53	0.47	515	2161	45	< 55	166	0.6	13	8.7	< 75	1.9	1.0	20	3594	6.2	62	3.1	65	290
PK 147/6	122674	11	819	< 237	86	7	72	52	6.0	1.3	23975	11	31813	52	0.59	394	1188	40	< 62	223	0.4	18	7.1	< 86	2.1	1.0	24	5060	6.9	93	3.8	< 4	288
PK 147/7	91495	14	622	1036	90	7	52	55	6.8	1.6	27165	14	30453	44	0.55	453	5238	48	< 55	221	0.4	13	9.2	< 77	3.5	1.2	17	4323	8.2	68	3.9	73	348
PK 147/8	72180	3	475	1017	68	7	33	55	5.2	1.2	26716	13	24768	35	0.46	764	4622	34	< 48	215	0.2	9	6.9	< 69	4.4	0.9	13	3212	8.0	54	2.9	66	317
PK 148/1	92171	15	403	1879	100	9	98	34	4.9	1.1	51384	14	16546	48	0.51	465	3084	36	< 61	153	0.9	14	6.9	< 80	2.2	0.9	22	5352	7.9	125	3.6	64	331
PK 148/2	100837	16	435	1631	96	12	109	31	5.3	1.2	53869	15	19511	44	0.51	374	3281	34	< 63	151	0.9	15	7.5	< 83	2.0	0.8	22	5349	7.4	119	3.5	95	363
PK 148/3	94460	18	421	1690	114	19	104	37	5.6	1.3	41692	14	22033	42	0.55	541	2236	32	100	166	0.9	16	7.7	< 85	2.0	0.9	22	4852	6.5	105	3.7	78	379
PK 148/4	92935	15	535	813	117	19	97	42	4.6	1.0	41484	14	19890	36	0.53	634	1315	21	52	162	1.2	18	6.8	< 89	1.8	0.6	22	4609	6.4	97	3.7	< 4	297
PK 148/5	95396	11	535	544	89	19	69	49	1.7	0.5	38302	13	25474	12	0.39	810	1058	8	< 46	163	0.8	17	2.9	< 94	1.3	0.4	18	4011	5.1	78	2.4	47	295
PK 149/1	80951	21	577	998	106	14	102	30	4.7	1.2	53926	14	21132	49	0.54	910	3282	35	< 44	195	0.9	14	6.9	< 88	1.8	1.1	22	4137	5.0	122	3.9	87	325
PK 149/2	80997	24	507	1726	106	19	107	26	5.2	1.4	51648	12	24363	47	0.59	1013	3334	41	< 47	195	1.1	16	8.1	< 93	1.7	1.2	21	4526	5.8	132	3.8	117	253
PK 149/3	86314	23	572	1573	108	19	102	27	5.7	1.4	50432	13	23853	48	0.61	938	2494	44	< 46	192	1.2	16	7.8	< 92	2.0	1.1	22	4625	6.4	118	4.7	103	277
PK 149/4	85343	26	567	< 547	94	18	79	31	4.9	1.2	50103	12	22085	43	0.56	1277	874	39	< 46	168	1.1	16	6.4	< 92	1.6	1.0	20	3918	5.1	93	3.7	83	273
PK 150/1	86436	20	499	2222	116	19	122	20	5.3	1.5	55119	10	19357	53	0.64	963	3320	37	62	181	0.9	17	8.2	< 94	2.0	1.3	24	4578	6.4	123	3.4	125	308
PK 150/2	85512	22	494	2349	116	21	118	21	6.0	1.6	53898	10	19850	54	0.69	992	2936	43	< 49	189	1.1	18	8.8	< 96	1.7	1.4	24	5047	6.2	118	4.6	130	239
PK 150/3	97529	30	496	1418	115	20	123	22	6.7	1.8	56354	11	19978	51	0.78	897	1456	47	< 54	185	1.4	23	9.5	< 107	1.8	1.4	24	4932	7.6	130	5.5	149	283
PK 150/4	93074	23	550	1546	114	20	107	22	5.3	1.6	52330	11	19543	50	0.68	984	1234	43	< 50	191	1.5	19	8.8	< 99	1.8	1.0	25	5363	7.9	117	4.9	140	260
PK 150/5	90614	16	584	663	114	18	98	22	5.2	1.4	48304	11	19841	56	0.56	908	1118	49	< 47	193	1.2	18	8.3	< 95	1.8	1.2	24	4724	7.7	124	3.9	131	218
PK 150/6	96175	25	600	542	112	12	117	23	7.1	1.9	46237	11	20639	53	0.76	641	1163	47	88	188	1.2	18	10.4	< 94	1.8	1.3	25	5493	6.9	128	5.6	109	281
PK 150/7	102932	15	564	372	112	11	85	21	5.2	1.3	26089	12	24258	39	0.61	528	1200	33	< 42	172	0.9	16	7.1	< 86	1.6	1.1	24	4815	7.9	90	4.8	88	260
PK 150/8	85919	8	745	620	73	7	57	22	4.1	1.0	27380	13	29178	44	0.53	427	1395	27	< 39	177	0.4	14	5.7	< 80	1.2	0.8	18	4035	3.3	69	4.1	82	266
PK 151/1	82101	22	391	1996	113	17	114	27	5.6	1.4	55334	12	17687	53	0.56	1192	3222	40	< 46	206	1.1	16	8.2	< 93	2.0	1.1	23	4690	6.6	121	4.5	111	264
PK 151/2	74324	24	437	1550	99	15	105	28	4.1	1.2	53766	11	17431	53	0.54	1467	3083	40	< 44	215	0.9	14	7.8	< 88	2.0	1.0	22	4088	6.2	107	3.3	100	272
PK 151/3	81158	21	436	2626	106	20	115	25	5.0	1.4	54552	14	20566	51	0.49	1066	3916	40	< 47	192	1.0	15	8.0	< 93	1.9	1.0	23	4428	6.4	119	4.1	129	314
PK 151/4	84753	20	408	2066	119	20	113	24	5.7	1.5	53871	11	21259	52	0.55	1400	3954	40	< 48	202	1.1	17	8.6	< 95	2.0	1.1	22	5159	6.1	123	4.6	121	250
PK 151/5	84540	23	475	905	110	20	114	26	5.8	1.5	55230	11	21847	54	0.62	1096	3507	44	41	201	1.3	17	8.9	< 96	2.0	1.2	25	4713	5.6	129	4.9	117	249
PK 151/6	93720	26	504	2013	124	19	113	27	6.7	1.7	56857	11	19731	54	0.66	911	2642	46	< 50	198	1.3	18	9.4	< 99	2.1	1.5	25	4791	7.5	121	4.9	115	215
PK 151/7	112220	28	522	1384	117	22	117	30	7.6	1.7	59835	11	21346	53	0.69	1132	2006	45	82	183	1.6	21	9.0	< 106	2.2	1.2	25	5539	8.0	147	5.1	109	255
PK 151/8	98096	27	560	724	109	19	116	29	5.7	1.5	58932	12	17139	53	0.64	945	1338	38	< 50	176	1.4	18	8.4	< 100	2.2	1.1	25	5040	7.5	126	5.3	125	279
PK 151/9	86947	27	562	583	128	24	109	31	5.1	1.7	59330	11	15818	58	0.63	1444	1400	47	80	183	1.9	19	9.5	< 103	2.1	1.4	25	4234	6.3	121	4.2	129	249
PK 151/10	94515	23	616	434	123	22	118	25	5.6	1.5	57623	11	19842	54	0.65	955	1435	47	< 50	195	1.3	18	8.6	< 99	2.1	1.2	25	5251	8.7	132	4.1	106	277
PK 151/11	91526	18	566	696	121	18	111	25	6.6	1.5	48155	13	21050	52	0.64	1083	1448	36	40	177	1.4	18	8.8	< 98	2.6	1.2	26	5151	7.1	124	4.7	102	330
PK 151/12	99329	9	526	< 503	90	15	90	24	5.4	1.1	47714	11	25084	34	0.62	722	1988	34	< 48	151	0.9	18	6.6	< 95	1.8	1.0	21	4945	6.0	95	4.5	81	213

Appendix 2 (continued)

sample	Al	As	Ba	Ca	Ce	Co	Cr	Cs	Dy	Eu	Fe	Hf	K	La	Lu	Mn	Na	Nd	Ni	Rb	Sb	Sc	Sm	Sr	Ta	Tb	Th	Ti	U	V	Yb	Zn	Zr
	[ppm]																																
PK 152/1	69431	13	507	2042	95	14	88	32	4.5	1.3	53126	16	17995	47	0.52	1228	1799	35	< 44	168	0.5	14	7.3	< 89	1.6	1.0	21	5246	6.6	101	4.3	102	353
PK 152/2	71355	16	587	1723	100	13	89	32	4.6	1.3	54182	16	16670	45	0.48	904	1782	41	< 45	165	0.5	14	7.1	< 90	2.0	1.1	21	5651	5.7	122	3.4	86	345
PK 152/3	70080	13	482	1824	98	13	89	30	4.7	1.3	53538	16	17311	45	0.56	882	1692	34	< 44	152	0.6	14	7.0	< 89	1.6	0.9	21	5112	4.6	109	3.8	79	380
PK 152/4	74226	18	574	504	104	19	96	20	4.8	1.4	48827	13	17407	46	0.57	888	1763	43	< 45	160	1.2	15	8.0	< 89	1.7	1.1	22	4646	6.7	108	3.5	81	294
PK 152/5	85268	20	530	493	106	22	100	20	4.7	1.3	50590	12	18630	48	0.56	831	1674	37	< 47	164	1.3	17	7.4	< 95	1.7	0.9	23	5352	6.3	126	3.9	71	281
PK 152/6	71103	20	566	364	103	22	93	19	4.1	1.2	49912	12	14770	46	0.48	1037	1269	33	< 46	144	1.3	15	7.0	< 91	1.5	1.0	21	3631	5.9	99	2.9	89	256
PK 152/7	70406	10	490	1329	119	21	88	36	4.9	1.5	54764	14	20695	47	0.52	1116	1262	34	< 47	161	0.6	16	7.5	< 95	1.6	1.0	21	5641	5.6	111	4.2	64	326
PK 152/8	74890	19	623	3621	115	16	89	45	5.8	1.8	50885	12	23558	49	0.60	1164	1679	38	< 47	169	0.5	16	9.0	< 96	1.5	1.2	20	5458	4.1	113	4.6	90	270
PK 154/6	68489	23	208	1758	121	4	88	17	6.7	1.2	57101	18	9476	63	0.68	142	3167	46	< 39	84	1.1	10	8.6	< 77	3.1	1.2	24	8073	7.8	184	5.1	44	449
PK 154/7	116691	27	199	1500	119	23	126	15	7.8	1.7	61773	12	10744	53	0.57	131	3626	45	57	80	1.1	17	9.3	< 96	2.1	1.3	24	6218	6.7	158	4.6	52	266
PK 155/1	141798	33	173	1762	134	22	143	16	9.1	2.4	83072	10	11430	59	0.71	181	3563	57	115	85	1.1	22	12.1	< 111	2.2	1.6	27	5273	8.7	160	5.3	58	176
PK 155/2	108850	20	382	2384	100	23	111	36	6.1	1.4	51296	11	20405	48	0.56	227	5240	33	< 48	179	1.0	16	7.7	98	2.3	1.0	22	5150	4.7	126	4.7	66	247
PK 155/3	95442	18	340	971	72	13	82	50	4.5	1.2	46713	11	26596	36	0.47	572	7248	27	49	274	0.8	13	6.6	< 89	3.3	0.9	19	2834	6.6	89	2.8	70	264
PK 155/4	99414	15	320	1874	56	8	63	62	4.6	1.1	35478	11	28590	28	0.44	496	8835	21	< 41	337	0.6	12	6.6	< 86	4.4	0.9	17	2484	8.2	59	3.5	67	289
PK 155/5	85696	6	245	301	37	6	27	76	2.6	0.6	15297	9	36084	18	0.21	319	11038	14	< 31	423	0.3	7	3.9	< 73	5.0	0.5	11	1436	8.5	22	1.4	51	183

sample	Al	As	Ba	Ca	Ce	Co	Cr	Cs	Dy	Eu	Fe	Hf	K	La	Lu	Mn	Na	Nd	Ni	Rb	Sb	Sc	Sm	Sr	Ta	Tb	Th	Ti	U	V	Yb	Zn	Zr
	[ppm]																																
PK 153/1	66638	5	503	3051	158	14	76	17	7.4	2.0	39906	13	21185	77	0.64	822	4829	52	< 43	166	0.2	14	11.8	< 86	1.7	1.6	24	5026	6.1	87	5.2	96	328
PK 153/2	61786	4	559	2700	116	13	69	16	5.9	1.7	37592	15	18663	60	0.54	709	4481	45	< 40	158	0.3	12	9.9	< 82	1.6	1.2	22	4397	3.8	77	4.7	79	362
PK 153/3	75994	20	539	2771	110	13	100	19	4.4	1.3	54377	12	13954	55	0.53	1069	3516	41	< 44	146	0.8	13	8.1	< 87	1.8	1.1	22	4884	5.3	105	4.9	96	285
PK 153/4	89317	19	391	2199	115	17	111	19	5.2	1.4	57935	11	19304	52	0.58	836	4061	40	< 46	157	1.0	15	8.2	< 92	1.7	1.0	22	5730	6.4	142	4.0	78	234
PK 153/5	89748	26	407	761	111	24	108	20	5.7	1.4	55622	12	18722	52	0.54	813	3934	40	< 47	162	1.1	15	8.2	< 93	1.8	1.0	22	4888	5.1	128	3.5	115	294
PK 153/6	85022	24	424	1568	125	22	115	19	5.4	1.4	49518	12	18302	50	0.57	851	3191	43	63	158	1.1	15	8.6	< 92	1.7	1.3	24	4645	6.6	114	4.4	107	288
PK 153/7	70608	26	429	< 541	115	25	96	17	5.2	1.1	41337	15	16689	47	0.65	931	1059	39	< 46	137	1.5	16	7.5	< 92	1.8	1.0	24	4374	8.1	105	4.5	57	310
PK 156/1	77747	15	289	1611	82	3	64	31	4.2	0.9	42168	12	21033	41	0.54	174	5109	40	< 36	184	0.6	8	6.4	< 73	3.3	0.8	19	4527	5.9	102	3.4	41	271
PK 156/2	109204	22	232	1642	90	4	102	26	5.7	1.3	64680	12	16574	44	0.49	158	4447	41	< 44	146	0.8	12	7.7	87	3.0	1.0	25	4992	8.3	142	3.2	40	286
PK 156/3	117710	25	219	1243	92	8	103	35	6.0	1.5	54854	10	20163	41	0.46	221	4533	41	< 46	198	0.8	15	8.4	< 93	3.2	1.1	23	4047	7.2	110	2.7	65	244
PK 156/4	98584	4	184	454	37	5	27	59	2.6	0.4	14147	7	37022	14	0.21	297	4411	13	< 29	386	0.3	5	3.5	< 60	4.1	0.5	10	798	6.5	22	1.2	56	192
PK 156/5	95918	< 1	153	945	23	5	6	61	1.8	0.3	6976	7	43172	9	0.10	485	5074	9	< 24	420	0.1	3	2.6	< 54	4.8	0.4	7	< 468	6.6	< 6	0.8	70	189

Appendix 2 (continued)

sample	Al	As	Ba	Ca	Ce	Co	Cr	Cs	Dy	Eu	Fe	Hf	K	La	Lu	Mn	Na	Nd	Ni	Rb	Sb	Sc	Sm	Sr	Ta	Tb	Th	Ti	U	V	Yb	Zn	Zr
	[ppm]																																
PK 157/1	58377	3	321	1120	75	9	49	7	4.1	1.0	32739	13	26929	36	0.38	712	868	35	< 36	114	1.7	9	6.1	< 62	1.0	0.8	15	3055	4.3	57	2.6	< 3	329
PK 157/2	57745	4	298	352	79	8	50	8	4.3	1.1	36307	11	27049	38	0.39	611	605	38	< 37	110	1.8	9	5.7	< 63	1.0	0.9	16	2924	4.6	46	2.7	< 3	307
PK 157/3	55572	2	261	< 266	80	8	48	8	4.3	1.0	35914	9	26925	37	0.38	579	445	34	< 36	100	1.6	9	5.5	< 62	1.1	0.9	16	2868	3.9	42	2.8	< 2	256
PK 157/4	59514	2	314	308	83	8	51	8	5.1	1.2	38097	11	28559	39	0.41	645	454	36	< 38	105	1.7	10	6.1	< 65	1.1	0.9	16	3146	3.8	46	3.0	< 3	301
PK 157/5	52431	< 1	244	< 249	68	8	40	6	3.6	0.8	28991	12	24686	33	0.33	405	378	31	< 33	87	1.3	8	4.7	< 57	1.0	0.6	13	2611	3.7	45	2.3	< 2	305
PK 158/1	100042	< 3	< 90	13893	107	53	100	2	7.8	3.2	117690	9	5766	56	0.55	1898	11630	31	< 96	23	0.9	46	12.3	< 165	0.9	3.2	8	13581	1.1	331	4.4	< 11	213
PK 158/2	106545	< 3	< 90	14022	100	51	92	2	8.2	3.0	117540	8	3984	49	0.65	1801	11707	37	< 99	30	< 0.5	49	11.4	< 165	0.8	3.4	7	12730	1.4	368	4.0	< 12	90
PK 158/3	114831	< 3	< 94	15999	86	58	88	1	6.4	2.6	128676	8	< 2412	41	0.50	1968	12243	41	< 105	< 8	< 0.5	52	10.6	< 175	0.6	< 0.3	6	13866	< 1.0	377	3.8	< 13	< 97
PK 158/4	116361	7	< 98	14768	97	59	105	1	7.7	2.9	145376	10	2196	47	0.61	1841	11989	30	< 109	< 8	< 0.6	54	11.2	< 182	0.9	< 0.3	7	12410	< 1.1	426	4.9	< 14	150
PK 158/5	110424	< 4	< 100	10214	54	73	82	< 0.3	9.1	2.7	138354	6	< 2399	44	0.57	1816	16210	20	< 111	< 8	< 0.6	56	10.1	< 186	0.4	< 0.3	4	11536	< 1.1	408	4.9	< 14	< 103
PK 159/1	79381	10	497	3524	98	8	90	14	6.3	1.3	47435	16	22197	52	0.53	808	5064	36	< 45	130	0.7	13	7.8	< 79	1.4	1.2	22	5531	5.6	105	4.4	73	354
PK 159/2	91924	17	479	879	99	16	125	15	6.8	1.5	59655	17	21943	49	0.61	883	3876	30	< 52	131	0.9	17	8.1	< 90	1.4	1.1	22	4410	5.3	147	4.5	97	484
PK 159/3	113302	20	568	< 589	78	22	100	5	4.3	1.8	45064	3	23387	40	0.51	1556	2170	20	< 53	59	4.6	20	6.5	564	0.8	1.2	11	5181	7.2	167	3.8	107	128
PK 159/4	102581	29	481	< 534	109	26	150	20	4.4	1.1	59665	8	24628	41	0.53	1112	2593	22	95	148	1.3	19	6.5	< 98	1.5	1.0	20	5477	4.7	172	4.2	143	163

Appendix 3: Profile colour photographs

This section shows pictures of the profiles which have been more closely discussed within the scope this study. Their location within Bhutan is indicated in *Fig. 8* on page 23.

Unfortunately, all profile pictures from the 2000 Expedition (Bumthang – Bajo – Lame Goempa – Thrumsing La) were lost due to a defective camera. All pictures below are from the 2001 Expedition to Phobjikha Valley – Rukubji – South Bhutan. The exact location of the profiles within this study area is displayed in *Fig. 10* on page 25.

If not stated otherwise, the copyright of the pictures is with the author.

Phobjikha Valley

PK 135

PK 138

PK 139

PK 143, upper part

PK 143, lower part

PK 150, upper part (© Rupert Bäumler)

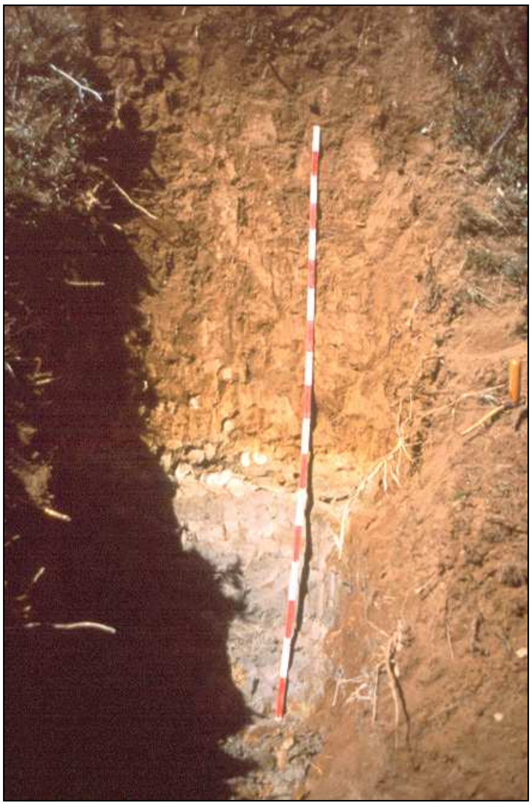

PK 150, lower part (© Rupert Bäumler)

PK 151, upper part

PK 155

Rukubji

PK 156

South-western Bhutan

PK 158, upper part

PK 158, lower part